Programa de Posgrado en Biotecnología, Universidad de la República

Tesis de Doctorado en Biotecnología

Mecanismos moleculares involucrados en la efectividad antitumoral de *Salmonella*: estudios del rol de la inmunidad entrenada y autofagia.

Mag. Sofía Chilibroste Vera

Tutor de Tesis: Dr. José Alejandro Chabalgoity
Co-tutora de Tesis y Asesora Curricular: Dra. María Moreno

TRIBUNAL
Dr. Marcelo Hill
Dr. Álvaro Díaz
Dra. Andrea Villarino

2026

AGRADECIMIENTOS

Quiero agradecer a todas las personas e instituciones que hicieron posible el desarrollo de este trabajo de tesis.

A Marcelo, Álvaro y Andrea, por dedicar su tiempo a la evaluación de esta tesis y por sus aportes. Asimismo, agradezco especialmente a Gustavo y Marcelo por el seguimiento y la orientación brindados durante el desarrollo de este trabajo de tesis, cuyas contribuciones enriquecieron tanto el contenido del trabajo como mi formación académica.

A las instituciones y organismos de financiación (ANII, CAP, CSIC y Posgrado en Biotecnología), cuyo apoyo fue fundamental para el desarrollo de esta investigación y la realización de este proyecto.

Al Posgrado en Biotecnología, por el acompañamiento, las gestiones y el apoyo brindado durante este proceso. Además, agradezco la oportunidad de haber participado como delegada estudiantil en la Comisión de Posgrado, una experiencia enriquecedora que contribuyó a mi formación y crecimiento académico.

A Alejandro y María, por permitirme desarrollar mi doctorado en este proyecto, por la orientación y la dedicación brindada a lo largo de este proceso.

A todos los colaboradores nacionales e internacionales que contribuyeron a este trabajo, por compartir conocimientos, tiempo y herramientas que enriquecieron esta investigación. En especial, a Leo y Jessica, por recibirme tan amablemente en su laboratorio y permitirme vivir una experiencia sumamente formativa y valiosa.

A quienes integran e integraron el laboratorio LVR, por el trabajo compartido, las discusiones, la ayuda cotidiana y también por los momentos que hicieron más llevadero el camino.

A mis amigos y a mi familia, por el apoyo incondicional, la paciencia y el sostén durante estos años.

Finalmente, agradezco a todas las personas que de una forma u otra fueron parte de este recorrido y contribuyeron a hacerlo posible.

“We cannot solve our problems with the same thinking we used when we created them.”

–Albert Einstein

RESUMEN

El uso de bacterias para el tratamiento del cáncer tiene una larga historia. En las últimas décadas ha resurgido el interés en el uso de agentes microbianos para el desarrollo de nuevas inmunoterapias antitumorales. Existe una gran cantidad de trabajos reportando el potencial de *Salmonella* atenuada como inmunoterapia frente al cáncer. Más allá de lo promisorio de los resultados obtenidos, es claro que los efectos inducidos por *Salmonella* en modelos experimentales, en general, son transitorios y, salvo excepciones, no se obtiene una remisión completa. Profundizar en la comprensión de los efectores moleculares y celulares involucrados tanto en la efectividad terapéutica de *Salmonella*, como en la regulación negativa de dichos efectos, permitirá avanzar en el desarrollo de cepas con capacidad de generar efectos más potentes y duraderos. Estudios recientes de nuestro grupo han demostrado que la efectividad terapéutica de la administración intratumoral de *Salmonella* LVR01 es dependiente de macrófagos y células NK. En este trabajo se investigó si *Salmonella* induce inmunidad entrenada en monocitos y células mieloides derivadas de médula ósea, lo que daría fundamento mecanístico a su relevancia en la terapia. Se evaluó si el estímulo de células de la inmunidad innata con LVR01 induce un fenotipo de inmunidad entrenada *in vitro*, y se realizaron ensayos *in vivo* en diversos modelos murinos tumorales. Los resultados fueron duales: comprobamos que LVR01 induce tolerancia en monocitos periféricos humanos y murinos, pero observamos que médulas de animales pretratados con LVR01 intraperitoneal, y reestimuladas *ex vivo* presentaron una respuesta inflamatoria aumentada. Además, en el modelo murino tumoral, la administración profiláctica de LVR01 retrasó el crecimiento de los tumores y aumentó la sobrevida global en los animales tratados. Estos hallazgos nos hacen reflexionar sobre el efecto transitorio que tienen las terapias basadas en *Salmonella* atenuada, y planteamos la hipótesis de que la tolerancia inmunológica periférica podría contribuir a la resistencia a la terapia. Por otro lado, se ha reportado a la inducción de autofagia (o xenofagia) por *Salmonella* como un mecanismo de resistencia al tratamiento, ya que se pierde el fenotipo M1 de los macrófagos infiltrantes de tumor y se controla la replicación bacteriana. Algunos trabajos demuestran que la combinación de *Salmonella* con inhibidores de la autofagia mejora el efecto antitumoral en modelos tumorales murinos. En esta tesis se evaluó el rol de la autofagia en el efecto antitumoral de *Salmonella* LVR01 *in vitro* e *in vivo* en melanoma. Si bien se observó una tendencia a mayor muerte celular cuando se combinó LVR01 con inhibidores de la autofagia *in vitro*, este efecto no se vio reflejado en mayor actividad antitumoral *in vivo*. Los resultados de este trabajo aportan a la comprensión mecanística de la actividad de las inmunoterapias basadas en *Salmonella*, que permitirán avanzar en el diseño de inmunoterapias costo-efectivas para el tratamiento del cáncer.

ÍNDICE

1. ABREVIATURAS 6

2. INTRODUCCIÓN

2.1. CÁNCER

2.1.1. Inmunidad & Cáncer 7

2.1.2. Respuesta inmune antitumoral 8

2.1.3. Inmunoterapias frente al cáncer 10

2.2. INMUNOTERAPIAS ANTITUMORALES BASADAS EN BACTERIAS

2.2.1. Toxinas de Coley 12

2.2.2. BCG 12

2.2.3. *Salmonella* 13

2.2.3.1. *Salmonella* LVR01 14

2.3. MEMORIA DE LA INMUNIDAD INNATA

2.3.1. Inmunidad entrenada

2.3.1.1. Definición 16

2.3.1.2. Implicancias y aplicaciones en la salud 17

2.3.1.3. Inmunidad entrenada, BCG & Cáncer 18

2.3.2. Tolerancia

2.3.2.1. Definición 19

2.3.2.2. Implicancias y aplicaciones en la salud 20

2.4. AUTOFAGIA

2.4.1. Autofagia & Xenofagia 22

2.4.2. Rol de la autofagia en cáncer 22

2.4.3. Modulación de la autofagia por *Salmonella* y sus implicancias en la respuesta antitumoral 23

3. HIPÓTESIS 25

4. OBJETIVOS 25

4.1 Objetivo general

4.2 Objetivos específicos

5. MATERIALES Y MÉTODOS

5.1 INMUNIDAD ENTRENADA

5.1.1. Líneas celulares 26

5.1.2. Cepa bacteriana 26

5.1.3. Parásitos de *Leishmania* 26

5.1.4. Aislamiento de monocitos humanos adherentes 27

5.1.5. Inducción de inmunidad entrenada *in vitro* en monocitos humanos adherentes 27

5.1.6. Animales 28

5.1.7. Inducción de inmunidad entrenada *in vitro* en células mieloides derivadas de médula ósea de ratón 28

5.1.8. Modelos tumorales e inmunización 28

5.1.9. Evaluación *ex vivo* del modelo de inmunidad entrenada *in vivo* 29

5.1.10. ELISA 29

5.1.11. Citometría de flujo 29

5.1.12. Ensayo de lactato 32

5.1.13. Análisis de expresión génica 33

5.1.14. Biodistribución de *Salmonella* LVR01 34

5.2 AUTOFAGIA

5.2.1. Evaluación de inducción de autofagia *in vitro* 35

5.2.1.1. Microscopía confocal 35

5.2.1.2. Western Blot 35

5.2.2. Evaluación de la muerte celular inducida por LVR01 en combinación con inhibidores de la autofagia *in vitro* 36

5.2.3. Evaluación del efecto antitumoral de LVR01 en combinación con inhibidores de la autofagia *in vivo* 36

5.3 ANÁLISIS ESTADÍSTICO 37

6. RESULTADOS

6.1 INMUNIDAD ENTRENADA

6.1.1. Evaluación de la capacidad de *Salmonella* LVR01 para inducir inmunidad entrenada *in vitro* en monocitos humanos adherentes 38

6.1.2. Evaluación de la inducción de inmunidad entrenada por LVR01 *in vitro* en células mieloides derivadas de médula ósea de ratón 42

6.1.3. Evaluación del modelo de inmunidad entrenada *in vivo* con LVR01 43

6.1.3.1. Cuantificación de citoquinas séricas tras la administración de LVR01 43

6.1.3.2. Análisis *ex vivo* del modelo de inmunidad entrenada con LVR01 44

6.1.3.3. Uso profiláctico de LVR01 en modelos tumorales 48

6.1.3.4. Biodistribución de LVR01 en el modelo de inmunidad entrenada 50

6.1.4. Estudio de la respuesta inmune antitumoral en el modelo murino de inmunidad entrenada 51

6.2 AUTOFAGIA

6.2.1. Evaluación de inducción de autofagia en células tumorales B16F10 por *Salmonella* LVR01 57

6.2.2. Evaluación de la muerte celular inducida por LVR01 en combinación con inhibidores de la autofagia *in vitro* 59

6.2.3. Evaluación del efecto antitumoral de LVR01 en combinación con inhibidores de la autofagia *in vivo* 60

7. DISCUSIÓN Y CONCLUSIONES GENEREALES

7.1 INMUNIDAD ENTRENADA 64

7.2 AUTOFAGIA 69

7.3 GLOBAL 75

7.4 CONCLUSIONES GENERALES Y PERSPECTIVAS 77

8. BIBLIOGRAFÍA 79

9. ANEXO 93

1. ABREVIATURAS

3-MA	3-metiladenina
AcMo	Anticuerpo monoclonal
ADCC	Citotoxicidad dependiente de anticuerpos
ATCC	*American Type Culture Collection*
ATG	Proteínas relacionadas a la autofagia
BCG	Bacilo Calmette-Guérin
CAR	Receptor de antígeno quimérico
CFU	Unidades formadoras de colonias
CRT	Calreticulina
d	Días
DAMPs	Patrones moleculares asociados al daño
DC	Célula dendrítica
DMEM	Medio *Dulbecco's modified Eagle's*
DNMTs	DNA metiltransferesas
Fc	Fracción constante de los anticuerpos
FDA	*Food and Drug Administration*
GSDM-D	Gasdermina D
h	Horas
H3K27Ac	Acetilación de la lisina 27 en la histona 3
H3K4me1	Monometilación de lisina 4 en la histona 3
H3K4me3	Trimetilación de la lisina 4 en la histona 3
HBSS	*Hanks Balanced Salt Solution*
hk	*Heat-killed*
HMGB1	*High Mobility Group Box 1*
i.p.	Vía intraperitoneal
i.t.	Vía intratumoral
IDO	*Indoleamine 2,3-dioxygenase 1*
IFN	Interferón
IL	Interleuquina
LB	Caldo Luria-Bertani
LBA	LB Agar
LL	Lisados de *Leishmania braziliensis*
LPS	Lipopolisacárido
LTC	Linfocitos citotóxicos
Ly6G	Antígeno leucocitario 6 complejo locus G6D
Ly6C	Antígeno leucocitario 6 locus C
M1	Macrófagos activados de forma clásica
M2	Macrófagos activados de forma alternativa
MDSC	Células supresoras derivadas de mieolides
MFI	Intensidad de fluorescencia media
MHC	Complejo mayor de histocompatibilidad
MOI	*Multiplicity of infection*
NHL	Linfoma no Hodgkin
NK	Célula *Natural Killer*
p.i.t.	Post implantación de tumor
PAGE	Electroforesis en geles de poliacrilamida
PAMPs	Patrones moleculares asociados a patógenos
PMBC	Células mononucleares de sangre periférica
PVDF	Difluoruro de polivinilideno
RPMI	Medio *Roswell Park Memorial Institute 1640*
s.c.	Vía subcutánea
SCID	Ratones con inmunodeficiencia combinada severa
SCV	*Salmonella-containing vacuoles*
SDS	Dodecil sulfato de sodio
SFV-IL-12	Semliki Forest virus expresando IL-12
TAM	Macrófagos asociados al tumor
TGFβ	Factor de crecimiento transformador beta
Th	Linfocitos T colaboradores
TILs	Linfocitos infiltrantes de tumor
TLS	Estructuras linfoides terciarias
TME	Microambiente tumoral
TNF	Factor de necrosis tumoral
VEGF	Factor de crecimiento vascular endotelial

2. INTRODUCCIÓN

2.1 CÁNCER

El cáncer representa un conjunto de enfermedades caracterizadas por la producción en exceso de células malignas, consecuencia de mutaciones que alteran el equilibrio de los programas que regulan la proliferación, diferenciación y muerte celular. Estas alteraciones no solo afectan a las células transformadas, sino que también involucran al estroma asociado, el cual desempeña un papel activo en el desarrollo y progresión de los tumores. El microambiente tumoral (TME, del inglés *tumor microenvironment*) favorece la adquisición de características conocidas como "*Hallmarks* del cáncer", que representan capacidades biológicas esenciales para el desarrollo y mantenimiento del fenotipo maligno (Weber, 2007).

Entre estos rasgos distintivos se incluyen: proliferación celular sostenida, evasión de mecanismos supresores del crecimiento, resistencia a la muerte celular, inmortalización, angiogénesis, invasión y metástasis, inflamación promotora de tumores, reprogramación metabólica y evasión de la respuesta inmune. A estos, se suman fenómenos más recientemente descritos como el desbloqueo de la plasticidad fenotípica, la reprogramación epigenética, la influencia de un microbioma polimórfico y la inducción de senescencia celular, todos contribuyen de manera interdependiente a la complejidad biológica y clínica del cáncer (Hanahan, 2022).

2.1.1. INMUNIDAD & CÁNCER

El sistema inmune desempeña un papel fundamental en el control y evolución del cáncer, múltiples evidencias clínicas demuestran esto. Entre las evidencias más relevantes se encuentran: las remisiones espontáneas en pacientes sin tratamiento (Radha and Lopus, 2021); la detección de linfocitos T citotóxicos (LTC) específicos de antígenos tumorales, tanto en los propios tumores como en los ganglios linfáticos drenantes de tumor (Giles et al., 2023; Giraldo et al., 2015); la infiltración de células inmunes como granulocitos y linfocitos en el tejido tumoral (Cipponi et al., 2011; Goubran et al., 2014; Mittal et al., 2014); el aumento en la incidencia de cáncer en individuos inmunosuprimidos (Van Leeuwen et al., 2010); y la existencia de remisiones tumorales inducidas mediante agentes inmunomoduladores (Bergman, 2019; Rotte et al., 2015; Zhang and Zhang, 2020).

Las células malignas acumulan múltiples alteraciones genéticas y pierden los mecanismos normales de control celular, lo cual puede llevar a la expresión de antígenos tumorales o asociados a tumor. Dichas alteraciones pueden ser detectadas por células del sistema inmune involucradas en la vigilancia activa, como las células *Natural Killer* (NK) (Morvan and Lanier, 2016). Asimismo, estos antígenos pueden presentarse en el contexto del complejo mayor de histocompatibilidad (MHC) de clase I, permitiendo su reconocimiento y destrucción por LTC $CD8^+$ (Galluzzi et al., 2018; Giles et al., 2023).

Los tumores comienzan un proceso dinámico de inmunoedición que les permite evadir la respuesta inmune antitumoral a través de diversos mecanismos. Entre ellos se incluyen la reducción de la expresión de antígenos, la interferencia en su presentación por MHC, la variación en el repertorio de antígenos y la modificación del TME para bloquear, modular o inhibir la

actividad de las células inmunes. La comprensión de estos procesos es fundamental para diseñar estrategias que fortalezcan la capacidad del sistema inmune de detectar y eliminar las células malignas (Mittal et al., 2014; O'Donnell et al., 2019).

El concepto de inmunoedición del cáncer reconoce el rol dual del sistema inmune, que por un lado protege al huésped al controlar la proliferación de células malignas, pero por otro favorece la progresión tumoral al generar presión selectiva que conduce al escape inmunitario. Este proceso se describe en tres fases interrelacionadas: eliminación, equilibrio y escape. En la fase de eliminación, las células transformadas son reconocidas y destruidas por una respuesta inmune antitumoral eficaz. Posteriormente, en la fase de equilibrio, se establece un balance entre la proliferación de las células tumorales resistentes y el control ejercido por el sistema inmune. Finalmente, en la fase de escape, los tumores "inmunológicamente esculpidos" evaden la respuesta antitumoral y crecen progresivamente al lograr establecer un TME inmunosupresor (Bui and Schreiber, 2007; Dunn et al., 2004; Mittal et al., 2014; O'Donnell et al., 2019; Tsai et al., 2023).

La inmunoedición en cáncer resalta cómo la interacción entre el sistema inmune y el tumor puede influir en la progresión y evolución de la enfermedad, subrayando la importancia de estrategias terapéuticas que apunten a restaurar o potenciar la respuesta antitumoral.

2.1.2. RESPUESTA INMUNE ANTITUMORAL

Los principales mediadores celulares de la respuesta inmune antitumoral incluyen tanto componentes innatos como adaptativos. Entre los primeros, las células NK desempeñan un rol central al eliminar directamente células tumorales que reducen su expresión de moléculas MHC de clase I (señal inhibitoria para las células NK) y que, a su vez, expresan ligandos de estrés celular reconocidos por receptores NK. Esto conduce a la activación de la NK y a la destrucción de células malignas mediante la liberación de gránulos citotóxicos (perforinas y granzimas) y secreción de citoquinas, particularmente IFN–γ. Además, las células NK expresan receptores Fc en su membrana externa, que les permite reconocer células marcadas con anticuerpos y eliminarlas a través de citotoxicidad celular dependiente de anticuerpos (ADCC, del inglés *antibody–dependent cellular cytotoxicity*) (López–Soto et al., 2017; Morvan and Lanier, 2016; Xia et al., 2021). Otro actor fundamental son los macrófagos que tienen un rol dual dependiendo de su estado de activación (M1 o M2). Los macrófagos M1, activados de manera clásica, poseen actividad antitumoral gracias a su actividad fagocítica, la inducción de un TME inflamatorio antitumoral y la mediación de ADCC. En contraste, los macrófagos M2, activados de forma alternativa, presentes en los tumores contribuyen con la progresión del mismo mediante la secreción de factores solubles como el factor de crecimiento vascular endotelial (VEGF, del inglés *vascular endotelial growth factor*) y el factor de crecimiento transformador beta (TGFβ, del inglés *transforming growth factor beta*), que promueven la angiogénesis y la inmunosupresión local (Anderson et al., 2021; Chen et al., 2018; Y. Chen et al., 2021; Galluzzi et al., 2018; Vesely et al., 2011).

Por su parte, la inmunidad adaptativa tiene un rol clave en la vigilancia y control tumoral al generar respuestas antígeno específicas y memoria inmunológica, lo que contribuye a prevenir recurrencias y controlar metástasis. En este contexto destacamos a los LTC, los linfocitos T

colaboradores perfil Th1 y los linfocitos B. Los LTC destruyen células tumorales mediante la producción y liberación de perforinas y granzimas, así como a través de interacciones Fas:FasL que inducen la muerte celular programada (Enamorado et al., 2017; Giles et al., 2023; Mellman et al., 2023; Tang et al., 2020). Los linfocitos Th1 colaboran potenciando la actividad de los LTC mediante la secreción de citoquinas (IFN-γ, IL-12) y quimioquinas (CXCL9, CXCL10), además de la interacción CD40:CD40L (Cipponi et al., 2011; Ngiow et al., 2011; O'Donnell et al., 2019; Töpfer et al., 2011). El componente humoral también es relevante: los linfocitos B pueden producir anticuerpos dirigidos contra diversos antígenos tumorales o asociados al tumor, que median la destrucción de células malignas a través de la activación de la vía clásica del complemento o mediante ADCC, facilitada por macrófagos y células NK (Downs-Canner et al., 2022; Floros and Tarhini, 2015).

La dinámica de la respuesta inmune antitumoral ha sido conceptualizada como el "ciclo inmune del cáncer", que describe los eventos clave para el establecimiento de una respuesta T citotóxica efectiva (Figura 1). El proceso comienza con la liberación de antígenos tumorales o asociados al tumor, que son captados por células dendríticas (DC, del inglés *dendritic cell*) en un entorno proinflamatorio. Tras procesarlos, estas DC migran a los ganglios linfáticos, donde presentan los antígenos a linfocitos T vírgenes. La activación de los linfocitos T depende del reconocimiento antigénico, de señales coestimuladoras y de un contexto de citoquinas que favorezca su expansión clonal a LTC efectores. Estas células activadas migran al tumor, lo infiltran y eliminan células tumorales, generando a su vez liberación de nuevos antígenos que retroalimentan el ciclo (Chen and Mellman, 2013). Actualmente, se resalta la importancia del TME en este proceso y se describe un sub-ciclo vinculado a la formación de estructuras linfoides terciarias (TLSs, del inglés *tertiary lymphoid structures*). Estos agregados linfoides peri-tumorales funcionan como sitios de activación de células T dentro del propio tumor, amplificando la respuesta antitumoral y mejorando los resultados clínicos. La abundancia y composición de las TLSs emergen como factores clave para determinar la efectividad inmunoterapias frente al cáncer (Mellman et al., 2023). Esto resalta la complejidad del TME y su capacidad para influir en el éxito de las estrategias terapéuticas modernas.

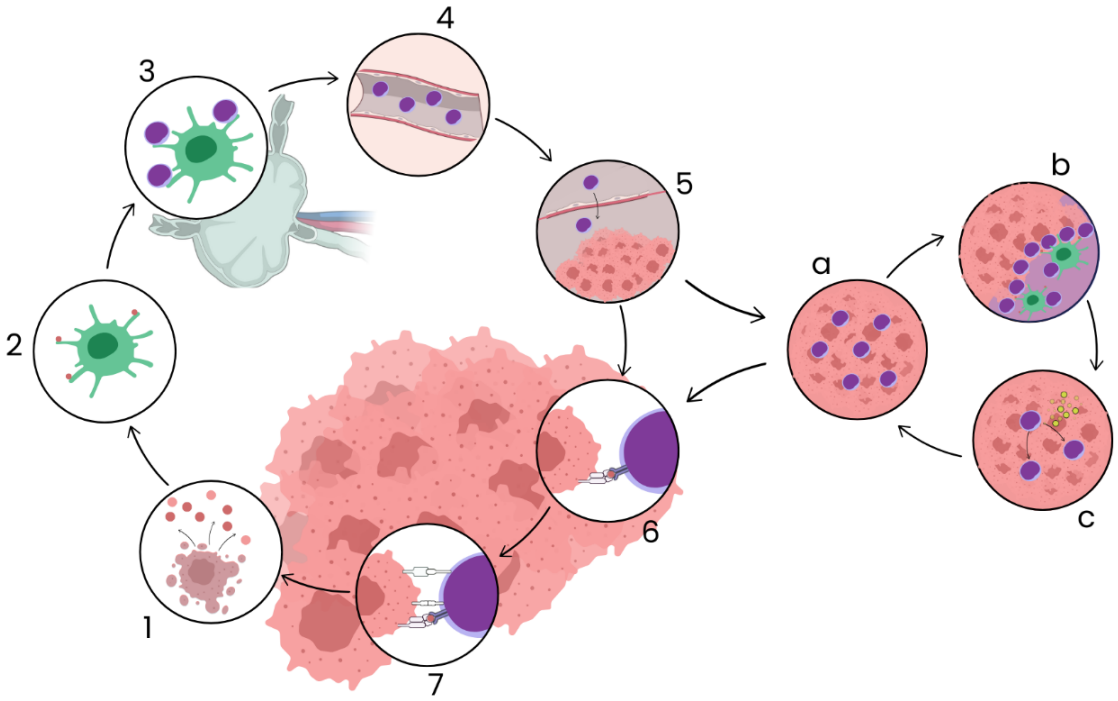


Figura 1 – Respuesta inmune antitumoral. Ilustración de los siete pasos del ciclo inmune del cáncer (Chen and Mellman, 2013): (1) Muerte celular inmunogénica de célula tumoral con liberación de antígenos tumorales al ambiente; (2) Captación y presentación de los antígenos por células presentadoras, principalmente DC; (3) Activación de linfocitos T citotóxicos, LTC, en ganglio; (4) LTC activados en circulación; (5) LTC infiltran el tumor; (6) LTC reconocen célula tumoral; (7) LTC elimina célula tumoral, liberando antígenos y retroalimentando el ciclo. A la derecha de la imagen se ilustra el sub-ciclo inmune del cáncer en el microambiente tumoral (TME) (Mellman et al., 2023): (a) Acumulación de LTC activados en estroma y TME; (b) Interacción con células inmunes del estroma dispersas, agregadas o formando estructuras linfoides terciarias; (c) Mantenimiento del estado efector y funcionamiento de LTC.

2.1.3. INMUNOTERAPIAS FRENTE AL CÁNCER

Las inmunoterapias han transformado el abordaje del cáncer al aprovechar y potenciar la capacidad del sistema inmune para reconocer y eliminar células tumorales. La mayoría de las estrategias aprobadas clínicamente se centran en la acción de linfocitos T, ya sea mediante la modulación endógena de la respuesta T utilizando citoquinas o inhibidores de puntos de control inmunitarios, o a través de terapias celulares en las que las células T modificadas *ex vivo* se convierten en el propio tratamiento (Zhang and Zhang, 2020).

Las citoquinas como la IL-2 y el IFN-α fueron pioneras en la inmunoterapia oncológica, aunque sus efectos adversos han limitado su uso. Más recientemente, moléculas como IL-15, IL-7, IL-12 e IL-21 se encuentran en distintas fases de evaluación clínica, ya sea como agentes individuales o en combinación con otras terapias, con el objetivo de mejorar la activación y persistencia de células inmunes antitumorales efectoras (Floros and Tarhini, 2015; Jiang et al., 2016; Wu, 2013).

Otro grupo de inmunoterapias ampliamente implementado son los anticuerpos monoclonales (AcMo), que actúan bloqueando señales de proliferación tumoral, favoreciendo la eliminación directa de células malignas, inhibiendo la angiogénesis o modulando al sistema inmune para

potenciar la respuesta antitumoral (Dal Bello et al., 2017; Leach et al., 1996; Sharma, 2016; Sharma and Allison, 2015; Singh et al., 2015; Wei et al., 2017). Dentro de estas estrategias, el bloqueo de puntos de control inmunológicos ha representado uno de los mayores avances de la inmunoterapia moderna (Robert, 2020). Uno de los primeros blancos terapéuticos fue CTLA4, un receptor inhibidor que regula etapas tempranas de la activación de las células T. El desarrollo del anticuerpo monoclonal anti-CTLA4 Ipilimumab mostró beneficios clínicos significativos en pacientes con melanoma metastático, aunque asociado a eventos adversos inmunomediados vinculados con la pérdida de mecanismos de tolerancia (Hodi et al., 2010). Posteriormente, el eje PD1/PD-L1 emergió como otro regulador central de la respuesta inmune antitumoral. La interacción entre PD1 y sus ligandos inhibe la proliferación y función efectora de las células T, favoreciendo estados de agotamiento funcional en el microambiente tumoral. Anticuerpos bloqueantes dirigidos contra PD1 o PD-L1, como Pembrolizumab y Nivolumab, demostraron eficacia clínica en distintos tipos de cáncer y actualmente forman parte del tratamiento estándar para múltiples neoplasias . Además, otros puntos de control inhibidores como LAG3 y TIM3 han sido identificados como mediadores relevantes de inmunosupresión tumoral y constituyen blancos prometedores para nuevas estrategias terapéuticas (Farkona et al., 2016).

A estas se suman las terapias celulares adoptivas, que incluyen linfocitos infiltrantes de tumor (TILs, del inglés *tumor infiltrating lymphocytes*), células NK activadas *ex vivo*, vacunas basadas en DCs y, más recientemente, las células T con receptores de antígenos quiméricos (CAR-T, del inglés *chimeric antigen receptor T cell*) (Barnes et al., 2021; Gorabi et al., 2020; Papaioannou et al., 2016; Varadé et al., 2021; Xie et al., 2021; Zhang and Zhang, 2020). Estas últimas han revolucionado el tratamiento de neoplasias hematológicas y continúan expandiéndose hacia tumores sólidos mediante innovaciones en ingeniería genética y combinaciones terapéuticas (De Marco et al., 2023; Uscanga-Palomeque et al., 2023). Las terapias celulares adoptivas requieren un proceso de personalización, ya que las células inmunes se extraen del propio paciente (terapias autólogas) o se seleccionan cuidadosamente en casos alogénicos. Esto tiene implicaciones importantes en términos de costos, logística y tiempo de tratamiento (Lin et al., 2021; Lizana-Vasquez et al., 2023; Martin et al., 2024).

Las vacunas terapéuticas contra el cáncer también son otro tipo de tratamiento personalizado que ha cobrado protagonismo en la actualidad. Consisten en vacunas diseñadas para estimular al sistema inmune a atacar tumores ya establecidos, mediante el uso de antígenos tumorales o asociados al tumor específicos de cada paciente (Fan et al., 2023). Ejemplos de este tipo de aproximación son las vacunas basadas en lisados tumorales y las vacunas de ARNm. Las primeras presentan la ventaja de incorporar un amplio repertorio antigénico tumoral, aunque pueden mostrar menor inmunogenicidad y variabilidad entre preparaciones, mientras que las segundas permiten una mayor precisión y flexibilidad en el diseño antigénico, pero enfrentan desafíos asociados a estabilidad y entrega eficiente. Ambas estrategias han mostrado resultados prometedores en modelos preclínicos y ensayos clínicos, promoviendo respuestas inmunes antitumorales y beneficios clínicos en distintos tipos de cáncer, aunque su eficacia continúa siendo variable según el contexto tumoral y las características de cada plataforma (Chang et al., 2023; Gleisner et al., 2020; Pastor et al., 2018; Pérez-Baños et al., 2023).

Los tratamientos basados en el uso de virus o bacterias modificadas genéticamente han resurgido como estrategias innovadoras dentro de la inmunoterapia del cáncer (Forbes et al.,

2018). Entre ellas, los virus oncolíticos han demostrado un gran potencial al aprovechar la capacidad de ciertos virus para replicarse selectivamente en células tumorales, induciendo su lisis y estimulando la respuesta inmunitaria del huésped (Corrigan et al., 2017; Rothermel and Zager, 2018). La singularidad del TME, caracterizado por vascularización anómala, hipoxia y necrosis, lo convierte en un entorno favorable para la colonización por ciertas bacterias anaerobias obligadas y facultativas, que pueden actuar como agentes terapéuticos directos o como vectores de entrega de moléculas inmunomoduladoras y terapéuticas (Khanduja et al., 2024; Pierce et al., 2021).

2.2. INMUNOTERAPIAS ANTITUMORALES BASADAS EN BACTERIAS

2.2.1. TOXINAS DE COLEY

A fines del siglo XIX, el Dr. William Coley notó que algunos pacientes oncológicos que contraían infecciones bacterianas vivían más tiempo que aquellos que no las presentaban. A partir de esta observación, utilizó una mezcla de bacterias muertas, conocidas como “toxinas de Coley”, para tratar a pacientes con sarcomas (Coley, 1910, 1891). Este procedimiento logró cerca de un 15% de respuestas completas, pero fue abandonado debido a su elevada tasa de fracasos y a importantes efectos secundarios. Pese a ello, el trabajo de Coley sentó las bases para las inmunoterapias inespecíficas frente al cáncer (Bergman, 2019; Carlson et al., 2020; Zhang and Zhang, 2020).

2.2.2. BCG

Una de las inmunoterapias antitumorales más antiguas basadas en microorganismos vivos es el bacilo de *Calmette–Guérin* (BCG), una cepa atenuada de *Mycobacterium bovis* utilizada como tratamiento estándar para el carcinoma superficial de vejiga. Su administración intravesical tras la resección transuretral de pólipos potencia la activación del sistema inmunológico, estimulando células del sistema mononuclear fagocítico y promoviendo la eliminación del tumor (Al–Hilu and Al–Shujairi, 2020; American Cancer Society, 2020).

La respuesta inflamatoria local y la formación de granulomas en las paredes vesicales se consideran mecanismos centrales en la acción antitumoral de BCG. Esta terapia se caracteriza por inducir una fuerte respuesta inmune innata inicial, seguida por la activación de la respuesta adaptativa de perfil Th1. Más recientemente, se ha propuesto un mecanismo adicional basado en la inducción de inmunidad entrenada. Durante las sucesivas instilaciones intravesicales de BCG, las células inmunes innatas son repetidamente estimuladas por diversos ligandos, incluyendo PAMPs (del inglés *pathogen–associated molecular patterns*) y DAMPs (del inglés *damage–associated molecular patterns*). Este entrenamiento incrementa el perfil proinflamatorio del TME, ya que las células entrenadas producen mayores niveles de citoquinas y quimioquinas en el urotelio, amplificando la respuesta inmune y favoreciendo la eliminación de células malignas (van Puffelen et al., 2020). Además de su uso en cáncer de vejiga, en la actualidad se está explorando su uso en otros tipos de cáncer como melanoma (Benitez et al., 2019; Kremenovic et al., 2020).

2.2.3. *SALMONELLA*

Uno de los primeros reportes sobre el uso de *Salmonella* en cáncer mostró, en modelos murinos de melanoma, que cepas atenuadas colonizan preferentemente el tejido tumoral, enlentecen su crecimiento y aumentan la sobrevida global (Pawelek et al., 1997). *Salmonella* presenta ventajas relevantes como agente antitumoral: posee tropismo selectivo hacia el tejido tumoral, puede manipularse genéticamente para generar cepas seguras y, además, utilizarse como vector de moléculas terapéutico (incluyendo neoantígenos, citoquinas o incluso virus oncolíticos) (Aganja et al., 2022; Mi et al., 2019; Singer et al., 2025). No obstante, su elevada inmunogenicidad ha impulsado el desarrollo de cepas atenuadas, capaces de persistir en el tumor y reducir el riesgo de efectos adversos sistémicos (Badie et al., 2021; Dailey et al., 2021; Liang et al., 2021).

Diversos estudios preclínicos han demostrado su eficacia en distintos tipos de cáncer (melanoma, colon, mama, pulmón, renal, hepático, próstata y neoplasias hematológicas). Actualmente se exploran combinaciones con otras terapias como radioterapia (Yoon et al., 2021), quimioterapias (Bascuas et al., 2018; Chilibroste et al., 2021), cirugía (Mónaco & Plata et al., 2022), citoquinas (Agorio et al., 2007; Grille et al., 2013; Kramer et al., 2015), inhibidores de puntos control (Al-Saafeen et al., 2022; L. Wu et al., 2022), agonistas TLR (Vola et al., 2018), virus oncolíticos (Khanduja et al., 2024; Singer et al., 2025) (Figura 2).

La evidencia disponible respalda su uso tanto como vector terapéutico como agente oncolítico, lo que incluso ha dado lugar a ensayos clínicos en varios tipos de cáncer (Aganja et al., 2022; Hernández-Luna and Luria-Pérez, 2018; Moreno et al., 2010; Pangilinan and Lee, 2019).

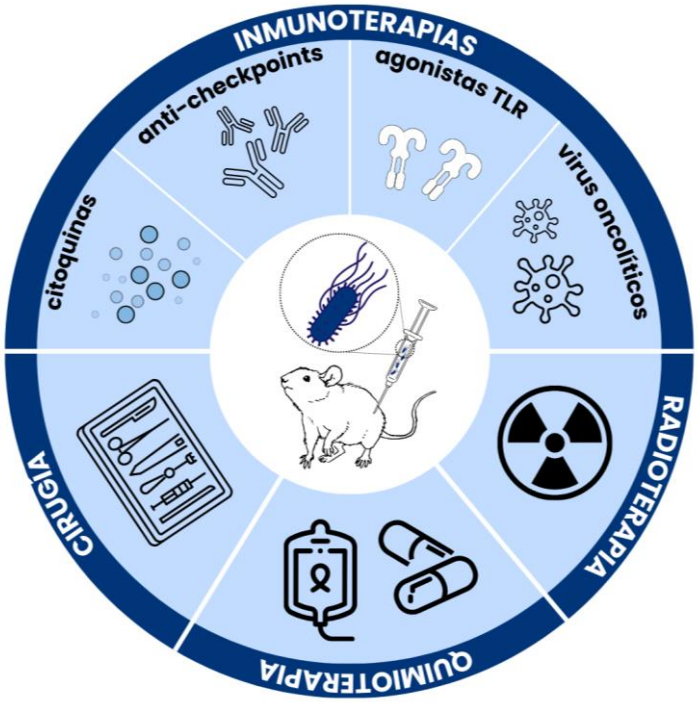


Figura 2 –*Salmonella* atenuada en combinación con otros tratamientos para el cáncer. La combinación de las diversas herramientas terapéuticas (Cirugía, Quimioterapia, Radioterapia, Inmunoterapia) potencia la respuesta antitumoral, prolonga la sobrevida libre de enfermedad y la sobrevida global en modelos preclínicos.

2.2.3.1. *SALMONELLA* LVR01

Nuestro grupo de investigación estudia desde hace varios años el uso de *Salmonella* como estrategia terapéutica contra el cáncer. En este marco, se generó una cepa atenuada de *Salmonella entérica* serovar Typhymurium, denominada LVR01, que presenta una mutación metabólica en el gen *aroC* (Chabalgoity et al., 2000).

Diversos reportes han demostrado que *Salmonella* ejerce efectos antitumorales a través de múltiples mecanismos, que incluyen la inducción directa de muerte celular en células malignas, la colonización selectiva del microambiente tumoral y la activación de respuestas inmunes locales y sistémicas (Hernández-Luna and Luria-Pérez, 2018; Mónaco et al., 2025; Pangilinan and Lee, 2019). Nuestro grupo ha contribuido de manera significativa en este campo, utilizando la cepa atenuada LVR01 en diferentes modelos preclínicos.

En estudios iniciales se observó que la infección con *Salmonella* induce cambios fenotípicos en células de linfoma humano y murino. En particular, se demostró que la cepa LVR01 incrementa significativamente la expresión de moléculas coestimuladoras (CD80, CD86, CD40) y de MHC de clase II en células B de linfoma, lo que potenció su inmunogenicidad y generó una respuesta de tipo Th1 con infiltración de leucocitos y una mayor sobrevida en ratones vacunados terapéuticamente (Grille et al., 2013). Posteriormente, en un modelo murino de linfoma no-Hodgkin a células B (NHL, del inglés *No-Hodgkin lymphoma*) se evidenció que la administración de LVR01 induce muerte celular tumoral, favorece la infiltración leucocitaria, aumenta la expresión de IFN-γ en el tumor y promueve respuestas antígeno-específicas tanto celulares como humorales (Grille et al., 2014).

Investigaciones más recientes demostraron que la infección de células de melanoma con LVR01 activa el inflamasoma NLRP3 y desencadena un tipo de muerte celular inmunogénica, particularmente piroptosis, evidenciada por la exposición en superficie de gasdermina D (GSDM-D) y calreticulina (CRT), así como por la liberación de HMGB1 (Mónaco et al., 2022a). Este efecto depende de la activación del eje caspasa-1/11 y de la presencia de macrófagos, y se asocia a un aumento en la expresión de caspasa-1 en macrófagos de perfil M1, pero no en M2, lo que sugiere un papel central de *Salmonella* en la polarización hacia un fenotipo M1 (Mónaco et al., 2022a).

La versatilidad de LVR01 también se reflejó en terapias combinadas. En un modelo preclínico de melanoma, su administración junto a imiquimod (agonista de TLR7) retrasó el crecimiento tumoral, prolongó de la sobrevida global y redujo la ocurrencia de metástasis, acompañado de una respuesta inflamatoria local y sistémica (Vola et al., 2018). La combinación con quimioterapia potenció el efecto antitumoral de LVR01, retrasando el crecimiento tumoral, disminuyendo la toxicidad del tratamiento y promoviendo la citotoxicidad mediada por células NK (Bascuas et al., 2018; Chilibroste et al., 2021). De manera similar, la administración conjunta de SFV-IL-12 (Semliki Forest virus expresando IL-12) y LVR01 en un modelo agresivo de cáncer de mama inhibió completamente la metástasis pulmonar y aseguró la supervivencia a largo plazo en la mayoría de los animales, con resultados superiores a cada tratamiento por separado (Kramer et al., 2015). Más recientemente, se demostró que la inmunoterapia neoadyuvante con LVR01 mejora los resultados quirúrgicos, induce respuestas inmunes amplias locales y

sistémicas, favorece la participación de células NK y genera memoria antitumoral capaz de controlar desafíos tumorales (Mónaco & Plata et al., 2022).

En conjunto, estos hallazgos evidencian que *Salmonella* LVR01 ejerce efectos antitumorales tanto por acción directa sobre las células malignas como por la reprogramación del microambiente tumoral y la activación coordinada de la inmunidad innata y adaptativa (Figura 3).

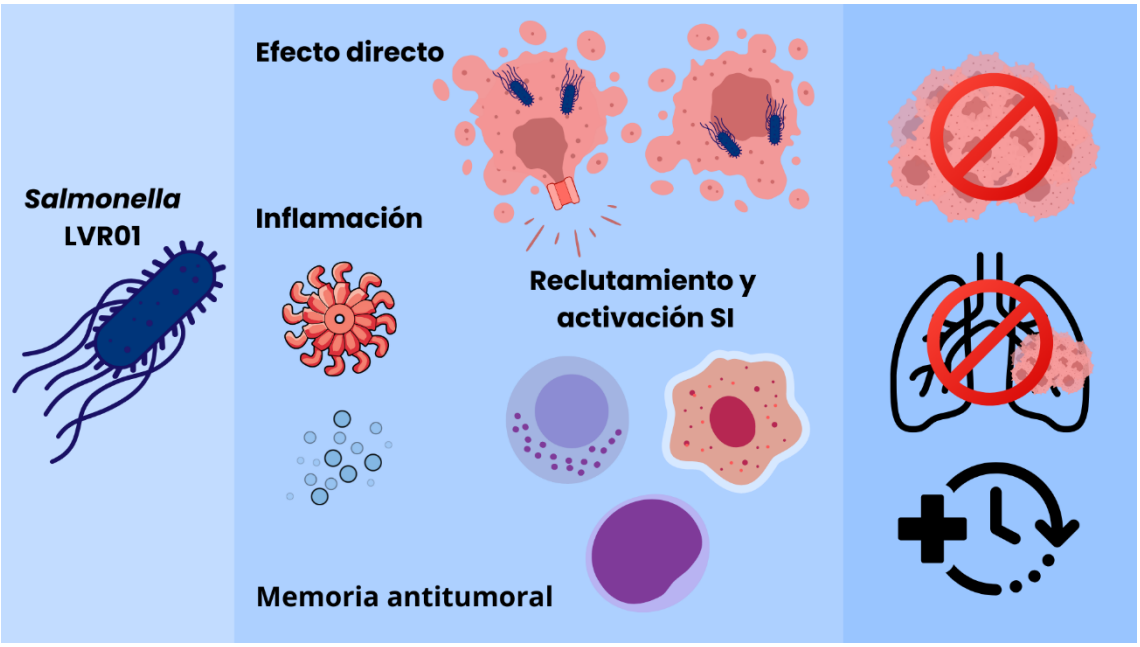


Figura 3 – Mecanismos de acción antitumoral de *Salmonella* LVR01. *Salmonella* LVR01 invade las células tumorales, se replica en ellas e induce su muerte por apoptosis y piroptosis. Genera un TME proinflamatorio con activación del inflamasoma y liberación de citoquinas y quimioquinas al ambiente. Las células efectoras del sistema inmune con perfil antitumoral son reclutadas al TME y, además, se generan células de memoria. Estos mecanismos llevan a una reducción del tamaño tumoral, control de las metástasis y aumento de la sobrevida en modelos preclínicos.

2.3. MEMORIA DE LA INMUNIDAD INNATA

Tradicionalmente, la memoria inmunológica se consideraba una característica exclusiva de la inmunidad adaptativa, mediada por linfocitos. Sin embargo, en los últimos años se ha acumulado evidencia que demuestra que células de la inmunidad innata, como monocitos, macrófagos, células dendríticas y células NK, también pueden experimentar una reprogramación funcional tras la exposición de estímulos inflamatorios, modificando así su respuesta frente a estímulos posteriores. Esta reprogramación, sustentada en cambios epigéneticos y metabólicos, constituye la base de dos fenómenos contrapuestos: la inmunidad entrenada y la tolerancia de la inmunidad innata (Dominguez-Andres & Netea, 2019).

2.3.1. INMUNIDAD ENTRENADA

2.3.1.1. DEFINICIÓN

La inmunidad entrenada se define como una forma de memoria inmunológica no específica, resultado de un proceso biológico que involucra la reprogramación metabólica y epigenética de células de la inmunidad innata. Este proceso se desencadena tras la exposición a estímulos endógenos o exógenos, como β-glucano, lipopolisacárido (LPS) o la vacuna BCG, y se caracteriza por una respuesta más potente frente a un segundo desafío no relacionado, una vez que las células han retornado a un estado basal (Netea et al., 2020) (Figura 4). En este contexto, una respuesta inmune innata más potente refiere principalmente a un aumento tanto en la rapidez como en la magnitud de la producción de citoquinas y quimioquinas proinflamatorias, como TNF, IL-6, IL-1β, IL-8, CXCL1, CXCL2 y CXCL3. Este fenómeno ha sido descrito en monocitos y macrófagos humanos luego de una estimulación secundaria heteróloga (Vuscan et al., 2024).

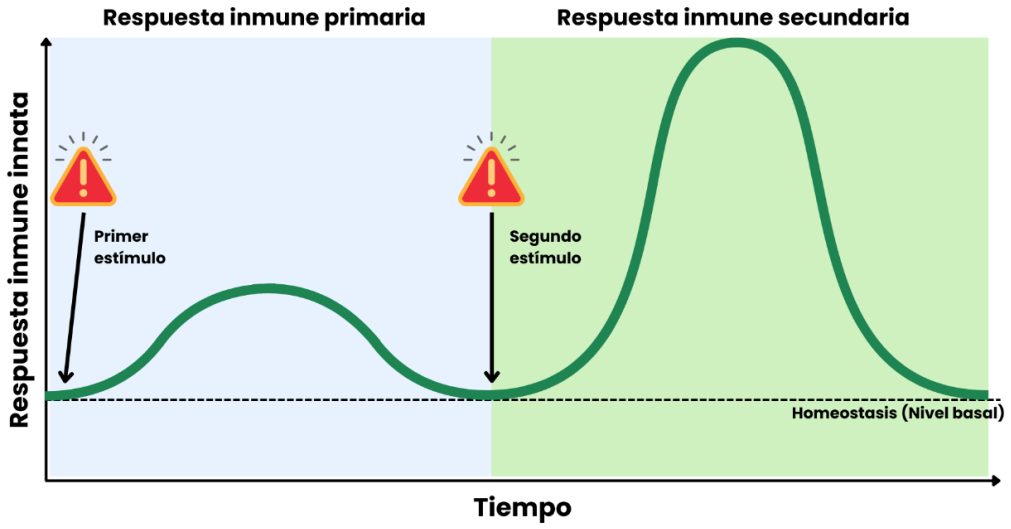


Figura 4 – Inmunidad entrenada. Ilustración gráfica de la intensidad de la respuesta inmune innata primaria y secundaria en células entrenadas. Respuesta secundaria más potente.

Durante el establecimiento del fenotipo de inmunidad entrenada se producen cambios significativos en el metabolismo celular. Entre estos cambios se destaca una fuerte inducción de la glicólisis, incluso en presencia de oxígeno, fenómeno conocido como "efecto Warburg" (Domínguez–Andrés et al., 2023). Estas adaptaciones metabólicas permiten responder al aumento de los requerimientos energéticos y biosintéticos asociados a un estado celular con mayor capacidad funcional y de respuesta (dos Santos et al., 2024). Además, se han identificado distintos metabolitos con capacidad de modular este proceso; entre ellos, el fumarato ha sido descrito como un metabolito clave para la inducción de inmunidad entrenada. Asimismo, las células con un fenotipo entrenado exhiben una mayor producción de lactato (Cai et al., 2025; Domínguez–Andrés et al., 2019a; dos Santos et al., 2024).

A diferencia de la memoria adaptativa, la inmunidad entrenada no depende de la recombinación génica, sino de modificaciones epigenéticas que reconfiguran rutas transcripcionales y funcionales (Netea et al., 2016). Entre los principales mecanismos involucrados se encuentran la metilación del ADN y las modificaciones en la arquitectura de la cromatina. Las ADN metiltransferasas (DNMTs) participan en la represión transcripcional mediante el reconocimiento y metilación de secuencias ricas en CpG. Asimismo, las colas de histonas pueden sufrir distintas modificaciones postraduccionales, como metilación, acetilación, fosforilación y ubiquitinación, regulando la accesibilidad de la cromatina y la expresión génica. Durante la inducción de inmunidad entrenada se han descrito cambios epigenéticos específicos, entre ellos la acetilación de histona 3 lisina 27 (H3K27Ac) y la monometilación de histona 3 lisina 4 (H3K4me1) en regiones *enhancer* distales, así como la trimetilación de histona 3 lisina 4 (H3K4me3) en promotores de genes asociados a la respuesta inmune (Vuscan et al., 2024). El fenotipo entrenado puede persistir durante meses o incluso años, confiriendo protección heteróloga frente a infecciones y otras enfermedades no infecciosas. Inicialmente fue descrita en células mieloides maduras de vida corta, pero estudios posteriores demostraron que la inmunidad entrenada puede establecerse tanto en progenitores hematopoyéticos de médula ósea (inmunidad entrenada central) como en células diferenciadas circulantes y tisulares (inmunidad entrenada periférica), lo que explica su duración prolongada (Netea et al., 2020).

2.3.1.2. IMPLICANCIAS Y APLICACIONES EN LA SALUD

La presencia de rasgos de la inmunidad entrenada ha sido documentada en vertebrados desde hace más de cinco décadas. Un estudio pionero mostró que ratones vacunados con BCG quedaban además protegidos frente a *Listeria monocytogenes* y *Salmonella* Typhimurium (Blanden et al., 1969). Esta protección inespecífica recordaba a los hallazgos de Lloyd Old y colaboradores en 1959, quienes observaron que la infección con BCG retrasaba el crecimiento de tumores trasplantados en ratones (Domínguez–Andrés et al., 2023). Luego se describió que la vacuna BCG protegía frente a candidiasis letal en ratones con inmunodeficiencia combinada severa (SCID, del inglés *Severe Combined Immunodeficient mice*), que carecen de linfocitos T y B funcionales (Bromuro et al., 2002; Polonelli et al., 2003). De igual manera, se observó que la exposición a flagelina protege a animales frente a neumonía inducida por *Streptococcus pneumoniae* (Muñoz et al., 2010).

En humanos se han evidenciado múltiples efectos inespecíficos de las vacunas vivas atenuadas. Estas vacunas inducen respuestas inmunes sistémicas de larga duración que involucran tanto a

la inmunidad innata como la adaptativa (Domínguez–Andrés et al., 2020). La inmunidad entrenada explica por qué algunas vacunas confieren protección frente a patógenos distintos a su blanco específico. Por ejemplo, la vacunación contra sarampión, BCG, viruela y la vacunación oral contra poliomielitis, se asocian con una menor mortalidad infantil, menor riesgo de asma y hospitalizaciones (Aaby et al., 2010; de Bree et al., 2018; Domínguez–Andrés et al., 2023; Netea et al., 2016).

2.3.1.3. INMUNIDAD ENTRENADA, BCG & CÁNCER

Se ha documentado que la vacunación con BCG puede inducir una respuesta inmune antitumoral, pudiendo prevenir y tratar distintos tipos de cáncer, incluidos vejiga, melanoma, leucemia y linfoma (Netea et al., 2020). No obstante, su uso aprobado por la FDA se limita actualmente al tratamiento del cáncer de vejiga, mientras que su aplicación en otras neoplasias continúa en fase de investigación (Singh et al., 2021).

Estudios sugieren que la inducción de inmunidad entrenada por BCG constituye un mecanismo clave para generar una respuesta antitumoral efectiva en el contexto de la inmunoterapia. La respuesta inmune generada por esta bacteria intracelular, con un perfil citotóxico y Th1, se potencia cuando las células entrenadas se enfrentan a nuevos estímulos. Durante las instilaciones intravesicales de BCG en cáncer de vejiga, el TME presenta muchas señales de peligro, PAMPs y DAMPs, que reestimulan a las células previamente entrenadas y amplifican la respuesta inmune (Figura 5). En este sentido, se propone que parámetros terapéuticos como la frecuencia y dosis de las instilaciones de BCG son determinantes para la eficacia clínica del tratamiento. Incluso, se ha planteado la hipótesis de que la vacunación con BCG previa al tratamiento intravesical podría potenciar aún más la magnitud de la respuesta inmune antitumoral (van Puffelen et al., 2020).

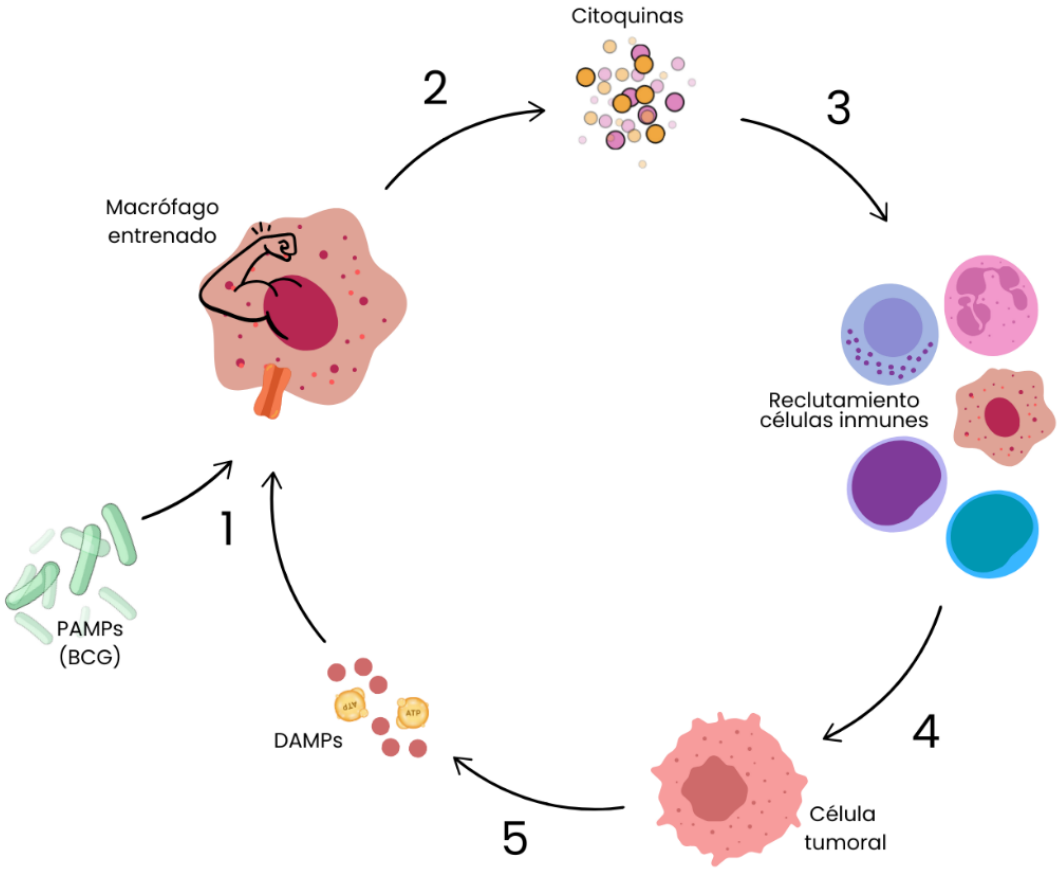


Figura 5 – Mayor capacidad antitumoral de células entrenadas por BCG. Hipótesis planteada por Van Puffelen y colaboradores, describen 5 pasos que explican la respuesta citotóxica más potente: (1) Macrófago entrenado, por tratamiento con BCG, recibe un segundo estímulo relacionado o no (PAMPs de BCG o DAMPs del TME); (2) Intensa respuesta con liberación de citoquinas; (3) Reclutamiento y activación de células inmunes; (4) Eliminación de células tumorales; (5) Liberación de DAMPs que potencian la actividad de las células entrenadas por BCG (van Puffelen et al., 2020).

2.3.2. TOLERANCIA

2.3.2.1. DEFINICIÓN

Lo opuesto a la inmunidad entrenada es la tolerancia de la inmunidad innata, un estado en el que las células no son capaces de activar la transcripción de genes ni de responder frente a reestímulos. Al igual que la inmunidad entrenada, este fenómeno resulta de un proceso biológico que involucra la reprogramación epigenética y metabólica, aunque con un desenlace funcional supresor en lugar de potenciador (Figura 6) (Divangahi et al., 2021).

El ejemplo más estudiado es la tolerancia a la endotoxina (o tolerancia a LPS), en la que monocitos y macrófagos previamente estimulados con LPS reducen su producción de citoquinas proinflamatorias, como TNF, IL-6 e IL-1β, y muestran una capacidad disminuida de respuesta frente a estímulos subsecuentes, relacionados o no con LPS (Li et al., 2023). Este fenómeno ocurre de manera independiente a la participación de los linfocitos; entre los mecanismos descritos se incluyen alteraciones en las vías de señalización *downstream* de TLR4 y NF-κB,

modificaciones epigenéticas en genes inflamatorios y una reprogramación metabólica asociada a una menor glicólisis y mayor oxidación de ácidos grasos. Además, se ha descrito que el LPS induce la producción de itaconato y previene la acumulación de fumarato, un metabolito clave para la inducción de inmunidad entrenada, favoreciendo así el establecimiento de un estado de hiporrespuesta inflamatoria (Butcher et al., 2018; Domínguez-Andrés et al., 2019b).

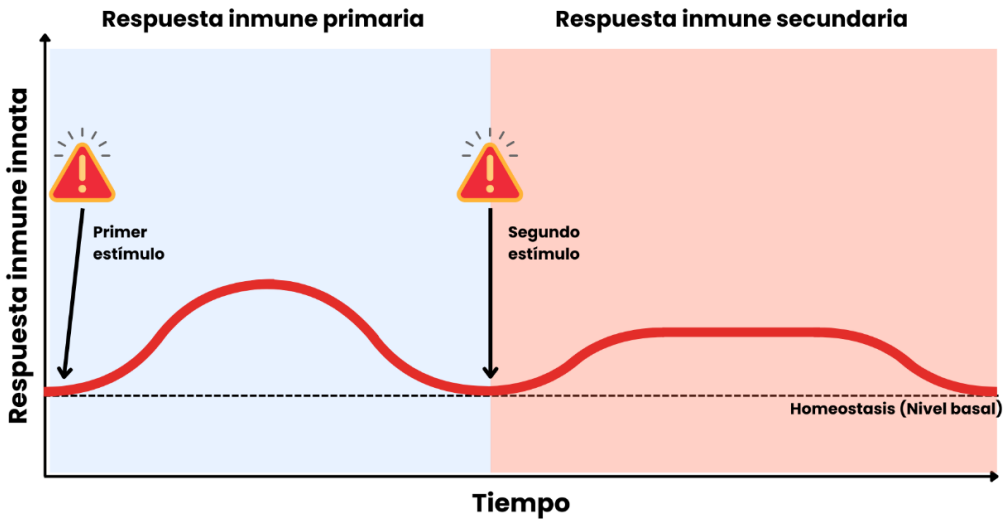


Figura 6 – Tolerancia. Ilustración gráfica de la intensidad de la respuesta inmune innata primaria y secundaria en células en tolerancia. Respuesta secundaria menos potente e incluso inexistente (parálisis inmune).

Además, otros mecanismos también pueden contribuir al establecimiento de estados de tolerancia inmune. Entre ellos se destaca la acumulación de Galectina-1, una lectina β-galactósido-dependiente ampliamente reconocida por su rol inmunomodulador y asociada a la supresión de respuestas inflamatorias. Se ha descrito que esta glicoproteína puede ser producida por células del compartimento mieloide y contribuir al establecimiento de un microambiente antiinflamatorio, promoviendo la inhibición funcional de células efectoras y favoreciendo la resolución de la respuesta inmune (Rabinovich & Croci, 2012; Yu et al., 2023).

2.3.2.2. IMPLICANCIAS Y APLICACIONES EN SALUD

La tolerancia a LPS tiene una relevancia clínica significativa, principalmente en el contexto de la sepsis, donde una respuesta inflamatoria sistémica desregulada frente a una infección diseminada constituye una de las principales causas de mortalidad (Seeley et al., 2018). Este fenómeno contribuye al establecimiento de un estado de inmunoparálisis, término acuñado para describir una disfunción inmune persistente caracterizada por hiporrespuesta funcional, reducción en la producción de citoquinas y mayor susceptibilidad a infecciones secundarias y otras patologías. En pacientes que han cursado sepsis severa, este estado de tolerancia inmune puede persistir durante varias semanas (Biswas & Lopez-Collazo, 2009).

La inmunoparálisis suele aparecer tras una potente respuesta inflamatoria inicial y puede mantenerse incluso cuando el recuento de leucocitos se normaliza, reflejando un cambio en la funcionalidad. Involucra una reprogramación que afecta tanto a células innatas como

adaptativas, con disminución en la producción de citoquinas y respuestas antimicrobianas (Lu et al., 2013; Martin et al., 2020; Silva et al., 2023).

La tolerancia a LPS impacta de forma crítica en la progresión del cáncer mediante la reprogramación de células del TME, favoreciendo un fenotipo inmunosupresor que promueve la viabilidad, proliferación y capacidad metastásica de las células tumorales (Roy et al., 2023; Silva et al., 2023). Se ha demostrado que la inmunoparálisis inducida por sepsis reduce la funcionalidad de LTC específicos de tumor, con menor producción de citoquinas claves. Asimismo, en hospedadores sépticos, las células tumorales presentan menor expresión de MHC I, lo que limita la presentación antigénica y compromete la inmunidad antitumoral. Esta disminución de la capacidad de respuesta inmune puede reducir de manera crítica la eficacia de las inmunoterapias (C. Chen et al., 2021; Danahy et al., 2019; Silva et al., 2023).

Estos antecedentes resultan particularmente relevantes en el contexto de inmunoterapias bacterianas basadas en *Salmonella*, donde la exposición sostenida a componentes bacterianos como el LPS podría influir en el balance entre activación antitumoral y establecimiento de estados tolerogénicos.

2.4. AUTOFAGIA

2.4.1. AUTOFAGIA & XENOFAGIA

La autofagia es un proceso catabólico altamente conservado y esencial para la homeostasis celular, mediante el cual organelos disfuncionales, agregados proteicos y otros componentes citoplasmáticos son degradados y reciclados en autofagolisosomas (Tattoli et al., 2012). Si bien es un proceso que ocurre a un nivel basal en condiciones fisiológicas, su activación se amplifica frente a situaciones de estrés celular, como la deprivación de nutrientes, hipoxia, depleción energética o infecciones (Casanova, 2017). La autofagia implica la formación de vesículas de doble membrana LC3 positivas, llamadas autofagosomas, que secuestran el material a degradar y posteriormente se fusionan con lisosomas, donde el contenido es procesado por hidrolasas lisosomales (Lamark and Johansen, 2021).

La autofagia tiene un rol clave en la inmunidad innata al participar en la eliminación de patógenos intracelulares, proceso llamado como xenofagia (Tattoli et al., 2012; Wu et al., 2020). S*almonella* es capaz de inducir autofagia por varios mecanismos, tras la invasión activa la bacteria puede ser reconocida directamente en el citosol o se pueden detectar vacuolas dañadas conteniendo *Salmonella* (SCV, del inglés *Salmonella–containing vacuoles*). *Salmonella* invade la célula en SCVs y la integridad de esas vacuolas se puede ver comprometida por la acción del sistema de secreción de tipo III (Birmingham et al., 2006). Cuando los componentes bacterianos quedan expuestos en el citosol, son rápidamente ubiquitinados, lo que favorece el reclutamiento de proteínas adaptadoras de la autofagia, como p62, NDP52 y OPTN. Estas proteínas reconocen los componentes bacterianos ubiquitinados y, simultáneamente, interactúan con LC3 presente en la membrana del autofagosoma, promoviendo el secuestro selectivo del material bacteriano y su posterior degradación mediante la vía autofágica (Zheng et al., 2009).

La xenofagia tiene un rol clave en el control de la proliferación bacteriana y mantenimiento de la integridad del citosol de las células. Esto queda evidenciado en estudios realizados con células *Atg5*$^{-/-}$, deficientes en autofagia, donde la replicación intracelular de *Salmonella* aumenta en comparación con células *wild type* (Birmingham et al., 2006; Wu et al., 2020).

2.4.2. ROL DE LA AUTOFAGIA EN CÁNCER

La autofagia tiene un rol dual en el desarrollo de tumores, puede promover la progresión o regresión de los mismos dependiendo de diferentes parámetros como el tipo de cáncer, el estadío de la enfermedad, el *background* genético, el TME, entre otros (Dikic and Elazar, 2018; Gao et al., 2022; Towers et al., 2019). Estudios realizados en modelos animales, donde se implantaron células tumorales *Atg5*$^{-/-}$ y se compararon con células tumorales *wild type*, demostraron que la ausencia de autofagia aceleró el crecimiento inicial de los tumores pero redujo la progresión de adenomas a adenocarcinomas (Rao et al., 2014). Por tanto, el estadío del desarrollo del tumor parece ser crítico en el rol de la autofagia en cáncer (Figura 7). Es necesaria para el proceso de inmunovigilancia en etapas tempranas, pero favorece el crecimiento y sobrevida de las células tumorales una vez que se encuentra establecido el tumor (Amaravadi et al., 2016; Galluzzi et al., 2015; Mónaco et al., 2025; White, 2012).

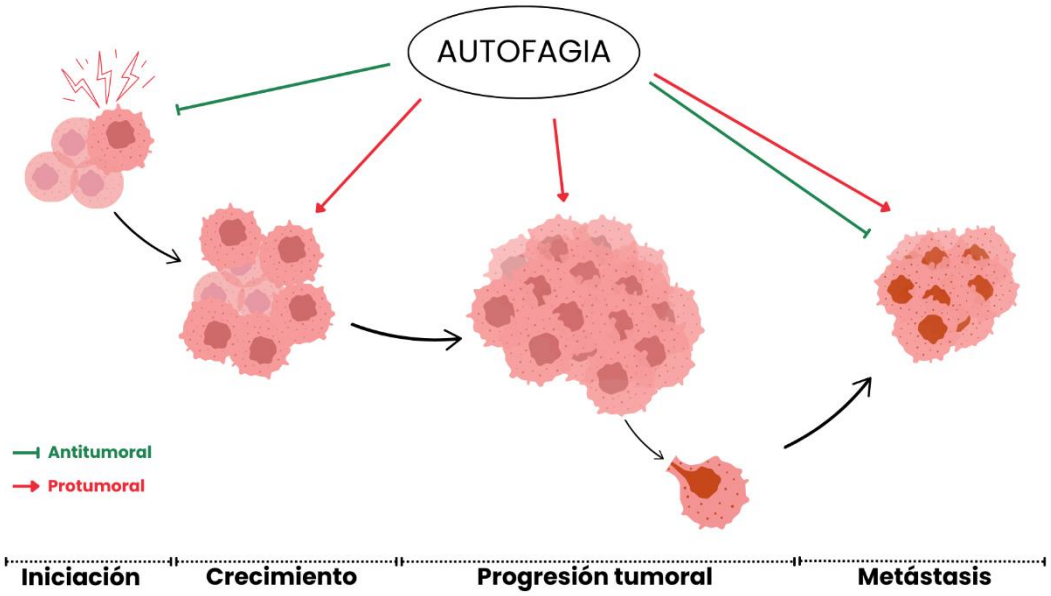


Figura 7 – Rol de la autofagia en el desarrollo de tumores. La autofagia puede ejercer efectos antitumorales (líneas verdes) o protumorales (flechas rojas) en distintas etapas de la carcinogénesis, influyendo en la iniciación, crecimiento, progresión y metástasis.

Además del rol directo de la autofagia en las células tumorales, este proceso es crucial también en la influencia de la actividad de las células inmunes y en moldear el TME. La autofagia tiene una acción moduladora de la respuesta inflamatoria; estímulos inflamatorios desencadenan autofagia y esta limita la producción de IL-1β mediante la degradación en autofagolisosomas de componentes del inflamasoma que son ubiquitinados en el citosol (Shi et al., 2012). Estudios preclínicos utilizando inhibidores farmacológicos de la autofagia demostraron un cambio en el fenotipo de los macrófagos asociados al tumor de un perfil M2 inmunosupresor a un perfil tipo M1 proinflamatorio. Este cambio condujo a un aumento de LTC en el TME y una reducción en el tamaño tumoral (Chen et al., 2018). De manera similar, la inhibición de la autofagia en linfocitos T CD8+ potenció la respuesta antitumoral, aumentando la producción de TNF e IFN-γ y eliminando células tumorales (DeVorkin et al., 2019).

2.4.3. MODULACIÓN DE LA AUTOFAGIA POR *SALMONELLA* Y SUS IMPLICANCIAS EN LA RESPUESTA ANTITUMORAL

La relación entre la progresión tumoral y el proceso de autofagia en los diferentes tipos celulares evidencian el potencial terapéutico de la inhibición o promoción de la autofagia con el fin de modular la respuesta inmune antitumoral. En este contexto, se ha demostrado que *Salmonella* es capaz de inducir autofagia en células tumorales mediante la baja en la regulación de la vía AKT/mTOR (Lee et al., 2014; L.-H. Wu et al., 2022). Además, esto contribuye a la supresión de IDO (del inglés, *indoleamine 2,3-dioxygenase 1*), un inmunosupresor presente en el TME, potenciando la activación de una respuesta antitumoral (Kuan and Lee, 2016).

El uso combinado de terapias contra el cáncer basadas en *Salmonella* con inhibidores farmacológicos de la autofagia como cloroquina han demostrado potenciar el efecto antitumoral en modelos murinos. Esta combinación refuerza la respuesta inmune frente a los

tumores al aumentar la cantidad de bacterias invadiendo las células tumorales, incrementando la muerte de las células tumorales y modulando el TME (Liu et al., 2016; Morinaga et al., 2025; Zhang et al., 2016).

En conjunto, la compleja interacción entre autofagia, modulación inmune y progresión tumoral resalta el potencial terapéutico de modular estratégicamente la autofagia en el marco de aproximaciones basadas en *Salmonella* para potenciar la inmunidad antitumoral (Mónaco et al., 2025).

3. HIPÓTESIS

Trabajamos bajo la hipótesis de que el tratamiento con *Salmonella* LVR01 es capaz de inducir inmunidad entrenada y esto explica parte del efecto antitumoral de la bacteria. Además, consideramos que la inhibición de la autofagia en combinación con el tratamiento con LVR01 potencia el efecto antitumoral del tratamiento.

4. OBJETIVOS

4.1. OBJETIVO GENERAL

Avanzar en el diseño de inmunoterapias costo-efectivas para el tratamiento del cáncer basadas en el uso de *Salmonella* atenuada con actividad antitumoral e investigar la inducción de inmunidad entrenada y el rol de la autofagia en la actividad antitumoral de *Salmonella*.

4.2. OBJETIVOS ESPECÍFICOS

1. Evaluar si *Salmonella* LVR01 induce inmunidad entrenada en células mieloides o monocitos adherentes.
2. Determinar si *Salmonella* LVR01 induce inmunidad entrenada en los modelos experimentales de melanoma y NHL.
3. Caracterizar la respuesta inmune antitumoral en el modelo murino de inmunidad entrenada.
4. Determinar si *Salmonella* LVR01 induce autofagia en células tumorales.
5. Evaluar la muerte de células tumorales inducida por *Salmonella* LVR01 *in vitro,* en presencia de inhibidores o promotores farmacológicos de la autofagia.
6. Elucidar el rol de la autofagia, mediante inhibidores de la misma, en la actividad antitumoral de *Salmonella* en modelos murinos tumorales.

5. MATERIALES Y MÉTODOS

5.1 INMUNIDAD ENTRENADA

5.1.1 Líneas celulares

Melanoma

Se utilizó la línea celular de melanoma de ratón B16F10, obtenida de American Type Culture Collection (ATCC, N° de línea CRL-6475). La línea fue cultivada en medio Dulbecco's modified Eagle's (Capricorn Scientific) enriquecido con suero fetal bovino al 10% (Capricorn Scientific), a 37°C y atmósfera de CO_2 al 5%, siguiendo recomendaciones de ATCC.

Linfoma No-Hodgkin

Se utilizó la línea celular de linfoma de ratón A20, obtenida de American Type Culture Collection (ATCC, N° de línea TIB-208). La línea fue cultivada en medio Roswell Park Memorial Institute 1640 (Capricorn Scientific) enriquecido con suero fetal bovino al 10% (Capricorn Scientific), 0,05 mM 2-mercaptoetanol (Sigma-Aldrich), 1 mM piruvato de sodio (Sigma-Aldrich) y 2,5 g/L D-glucosa adicional (Sigma-Aldrich), a 37°C y atmósfera de CO_2 al 5%, siguiendo recomendaciones de ATCC.

5.1.2 Cepa bacteriana

Se utilizó una cepa de *Salmonella enterica* serovar Typhimurium atenuada, con una mutación en el gen *aroC* (*aroC*$^-$) de la vía de los compuestos aromáticos, sin resistencia antibiótica, llamada LVR01 (Chabalgoity et al., 2000). Para la preparación de los inóculos se cultivó la cepa bacteriana en caldo Luria-Bertani (LB, Sigma) a 37°C y con agitación (200 rpm) durante 16 horas (ON). Se prepararon alícuotas del mismo, y se almacenaron -80°C en el mismo medio de cultivo con 15% de glicerol en una concentración conocida.

Al momento de su utilización, se descongeló una alícuota a temperatura ambiente y se resuspendieron las bacterias en suero fisiológico estéril a una concentración final de $1x10^7$ CFU/mL (CFU, del inglés *colony-forming unit*). En todas las ocasiones, se chequeó el inóculo utilizado por conteo de diluciones seriadas apropiadas en placa de LB agar (LBA, Sigma).

Para los ensayos realizados con LVR01 inactivada por calor, las bacterias fueron incubadas a 70 °C durante 10 minutos. Posteriormente, se prepararon alícuotas y se almacenaron a -80 °C hasta su utilización. La ausencia de bacterias viables fue confirmada mediante incubación en caldo LB durante 16 horas a 37 °C con agitación (200 rpm), verificando ausencia de crecimiento bacteriano.

5.1.3 Parásitos de *Leishmania*

Los lisados de *Leishamania braziliensis* utilizados en este trabajo fueron obtenidos mediante colaboración con el grupo del Prof. Leo Joosten. La generación y caracterización de los lisados fue realizada según la metodología descrita en Dos Santos et al., 2024. Brevemente,

las cepas fueron obtenidas del Leishbank IPTSP/UFG (Goia´s, Brazil). Las formas promastigotas fueron cultivadas en medio Grace's insect (Gibco, Life Technologies, USA) suplementado con 20% de suero fetal bovino inactivado por calor (FBS, Gibco, Life Technologies, USA) y 100 U/mL de penicilina/estreptomicina (Sigma–Aldrich) a 26°C. La fase estacionaria de los parásitos se obtuvo al sexto día de crecimiento en cultivo, se lavó tres veces con PBS (1000xg, 10 min 10°C). Luego, fueron resuspendidos en PBS y cuantificados utilizando un hemocitómetro después de la fijación con PBS al 0,4% de formaldehído. Los lisados de parásitos se obtuvieron mediante 5 ciclos de congelación y descongelación de promastigotes en presencia de inhibidores de proteasas (cocktail de inhibidores de proteasas, Sigma–Aldrich), utilizando nitrógeno líquido para la congelación y un baño de agua a 37 °C para la descongelación. La cuantificación de proteínas se realizó utilizando el kit de ensayo de proteínas Pierce BCA (ThermoFisher Scientific, USA).

5.1.4 Aislamiento de monocitos humanos adherentes

Los monocitos se aislaron a partir de la capa leucocitaria (*buffy coat*) de sangre obtenida de donantes sanos (Sanquin Blood Bank, Nijmegen, Países Bajos). Las células mononucleares de sangre periférica (PMBCs) se obtuvieron por centrifugación en gradiente de densidad con Ficoll–Paque (GE Healthcare), a partir de sangre diluida al medio en PBS. Las células se lavaron tres veces con PBS y se cuantificaron. Las PMBCs se colocaron sobre una solución hiperosmótica de Percoll (48,5% Percoll (Sigma–Aldrich), 41,5% de agua estéril, 0,16 M de NaCl filtrado y esterilizado) y se centrifugaron durante 15 minutos a 580 x g, 4 °C. Se aisló la capa de interfase, las células se lavaron una vez con PBS frío, se resuspendieron en medio de cultivo RPMI 1640 (Invitrogen), suplementado con 5 µg/mL de gentamicina (Centraform), 2 mM de Glutamax (Gibco) y 1 mM de piruvato (Gibco), y se contaron. Finalmente, los monocitos adherentes se aislaron permitiendo que los monocitos aislados con Percoll se adhirieran a placas de fondo plano de poliestireno (Corning) durante 1 hora a 37 °C; luego, las células se lavaron con PBS tibio para obtener la mayor pureza posible. La obtención de muestras de sangre humana fue aprobada por el Comité de Ética de la Universidad Radboud de Nijmegen, Países Bajos. Los estudios fueron realizados de acuerdo con la normativa local y los requerimientos institucionales correspondientes. Todos los participantes proporcionaron consentimiento informado escrito previo a su inclusión en el estudio.

5.1.5 Inducción de inmunidad entrenada *in vitro* en monocitos humanos adherentes

Los monocitos humanos se incubaron en RPMI 1640 (Invitrogen), suplementado con 2 mM de Glutamax (Gibco) y 1 mM de piruvato (Gibco), y 10% de un pool de suero humano, junto con diferentes estímulos: medio suplementado como control negativo, 25 µg/mL de lisados de *L. braziliensis* como control positivo (Dos Santos et al., 2024), diferentes MOI (del inglés, *multiplicity of infection*) de LVR01:células (1:1, 1:2, 1:4, 1:8, 1:16, 1:32) y LVR01 inactivado por calor. Tras 1 hora, las células se lavaron con PBS tibio y se agregó medio de cultivo suplementado con 5 µg/mL de gentamicina (Centraform). Luego de 24 horas, se recolectaron los sobrenadantes, se almacenaron a –20 °C hasta su posterior uso y se renovó el medio de cultivo. A los 3 días, se renovó el medio de cultivo nuevamente. En el día 6, las células se reestimularon con medio de cultivo sin suero, 10 ng/mL de LPS de *Escherichia coli* (Sigma–

Aldrich) o 10 µg/mL de Pam3Cys, lipopéptido sintético que actúa como un potente agonista del receptor tipo Toll 2, (EMC Microcollections). Tras 24 horas, se recolectaron nuevamente los sobrenadantes y se almacenaron a −20 °C hasta su posterior uso.

5.1.6 Animales

Para los experimentos *in vivo* se utilizaron ratones C57BL/6 y BALB/c (Dilave, Uruguay), hembras de 6 a 8 semanas de edad. Los animales se mantuvieron en ciclos de luz/oscuridad de 12:12 horas, con temperatura controlada (22 ± 2 °C) y humedad del 60%, con acceso libre a agua y alimento (*ad libitum*). Todos los protocolos de experimentación con animales fueron aprobados por el Comité de Ética en Experimentación Animal de la Universidad, Uruguay (número de protocolo 1329).

5.1.7 Inducción de inmunidad entrenada *in vitro* en células mieloides derivadas de médula ósea de ratón

Se aislaron células frescas de médula ósea a partir de los fémures de ratones C57BL/6 y BALB/c. La médula ósea fue extraída asépticamente, incubada con Buffer de Lisis (155 mM de NH_4Cl, 10 mM de $KHCO_3$ en H_2O estéril), filtrada a través de un filtro celular de 40 µm (Corning 431750, Sigma–Aldrich) y resuspendida en RPMI (Capricorn Scientific) suplementado con 10% de suero fetal bovino (Capricorn Scientific), penicilina–estreptomicina (Capricorn Scientific) y 1 mM de piruvato de sodio (Sigma–Aldrich). Las células se contaron y se sembraron en placas de 96 pocillos de fondo plano (1×10^6 células/pocillo). Durante las primeras 24 horas, las células fueron estimuladas con 50 µg/mL de lisados de *L. braziliensis* (control positivo), 1×10^6 CFU de *Salmonella* LVR01 inactivada por calor o medio suplementado (control negativo). Posteriormente, las células se lavaron con 200 µL de PBS tibio para eliminar los estímulos y las células no adherentes, y se añadió medio fresco. Luego de seis días de reposo, las células fueron reestimuladas con medio de cultivo sin suero, 10 ng/mL de LPS (Invivogen) o 100 µg/mL de Poly IC (Sigma–Aldrich). Tras 24 horas, se recolectaron los sobrenadantes y se almacenaron a −80 °C hasta su posterior uso.

5.1.8 Modelos tumorales e inmunización

Para el enfoque profiláctico en ratones, se administraron 1×10^6 CFU de *Salmonella* LVR01 por vía intraperitoneal (i.p.) una semana o un mes antes de la implantación tumoral.

Implantación tumoral: Las líneas celulares B16F10 y A20 se cultivaron y se recolectaron en fase logarítmica. Luego, las células se lavaron y se resuspendieron en solución salina, obteniéndose concentraciones finales de $2{,}5 \times 10^6$ células/mL o 5×10^6 células/mL, respectivamente. Los ratones fueron inyectados por vía subcutánea (s.c.) en el flanco derecho con 0,1 mL o 0,2 mL, respectivamente. Las mediciones tumorales se realizaron día por medio con un calibrador digital, y los volúmenes tumorales se calcularon utilizando la fórmula: largo × ancho × profundidad × $\pi/6$. La eutanasia se realizó por dislocación cervical

cuando los tumores alcanzaron los 4000 mm^3 o antes si los animales mostraban signos de sufrimiento.

5.1.9 Evaluación *ex vivo* del modelo de inmunidad entrenada *in vivo*

Para los experimentos de inmunidad entrenada *in vivo*, se inocularon ratones por vía i.p. con solución salina o 1×10^6 CFU de *Salmonella* LVR01, y 7 días después se administraron 35 µg/dosis de LPS de *Escherichia* coli (Invivogen) también por vía i.p. Veinticuatro horas antes del segundo estímulo y 90 minutos después, se colectó sangre y se centrifugó a 6000 rpm durante 10 minutos para obtener el suero destinado a la detección de niveles de citoquinas.

Para investigar el efecto de la inducción de inmunidad entrenada en la médula ósea y en las células derivadas de médula ósea, se inocularon ratones por vía i.p. con solución salina o LVR01, como se describió anteriormente. A los 6 días, se extrajo la médula ósea y se procesó como se describió en sección 5.1.7 de M&M. Se cultivaron 1×10^5 células de médula ósea por pocillo de cada ratón en dos placas diferentes. En una de las placas, las células fueron reestimuladas *ex vivo* de forma inmediata con LPS (10 ng/mL), y 24 horas después se recolectó el sobrenadante para la detección de citoquinas. En la otra placa, se cultivaron células adherentes derivadas de médula ósea durante 6 días y luego se reestimularon con LPS (10 ng/mL); 24 horas después, se recolectó el sobrenadante.

5.1.10 ELISA

La producción de TNF, IL-6, IL-1β, IL-8 e IL-1Ra en humanos o TNF, IL-6 e IL-1β en ratones se midió en los sobrenadantes de cultivo celular o en sueros de ratón utilizando kits comerciales de ELISA para humanos o ratones (R&D Systems y Biolegend, respectivamente), siguiendo las instrucciones del fabricante.

La producción de Galectina-1 se midió en los sobrenadantes de cultivo celular utilizando el kit comercial de ELISA para ratones (Sigma), siguiendo las instrucciones del fabricante.

5.1.11 Citometría de flujo

Inmunofenotipificación y detección de citoquinas intracelulares en células de médula ósea

La médula ósea fue extraída como se describió anteriormente y las células reestimuladas *ex vivo* con LPS (10 ng/mL). Después de 1 hora, las células fueron tratadas con GolgiPlug, y cuatro horas más tarde se realizó la tinción intracelular según las instrucciones del fabricante. Las células se tiñeron con anticuerpos contra CD11b-FITC, Ly6G-BV510, CD49b-APC, TNF-PE e IL-6-PE (BD Pharmingen y Biolegend).

TNF e IL-6 fueron evaluados en ensayos independientes, y el análisis de los marcadores de superficie se realizó dentro de las poblaciones positivas para PE correspondientes a cada citoquina.

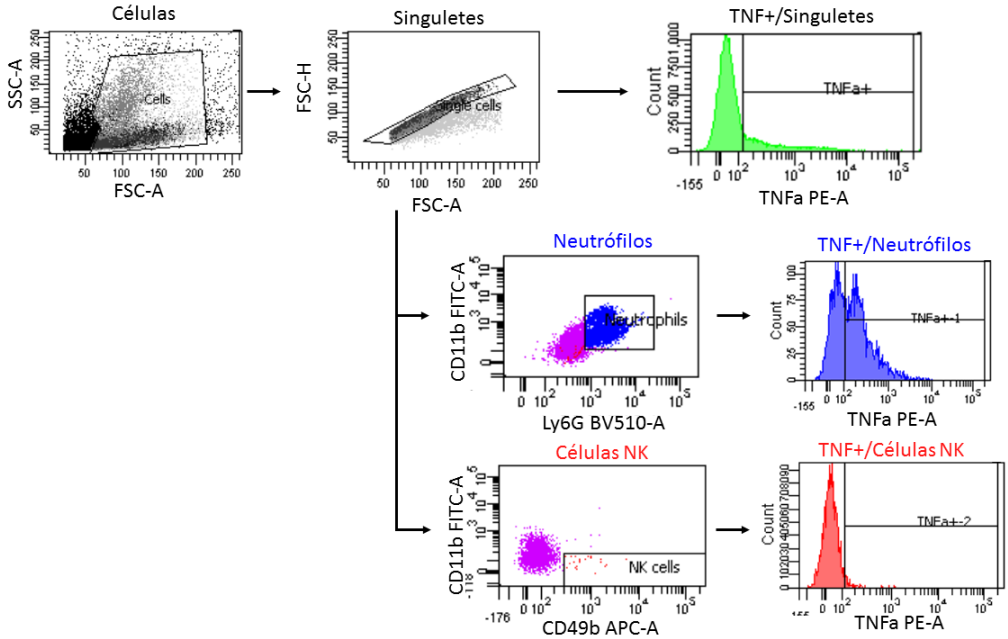


Figura 8 – Estrategia de gating utilizada para el análisis por citometría de flujo. Se seleccionaron células, se excluyeron dobletes y se identificaron poblaciones de neutrófilos ($CD11b^{+}Ly6G^{+}$) y células NK ($CD11b^{-}CD49b^{+}$). Posteriormente, se determinó la producción intracelular de TNF en la población total y en cada subpoblación celular.

Inmunofenotipificación de TME

En los días 14 o 17 posteriores a la implantación tumoral, se sacrificaron los ratones y se extrajeron los tumores. Se obtuvo una suspensión celular mediante disgregación mecánica y las células se tiñeron con anticuerpos contra CD45–BV510, CD11b–APC.Cy7, NK1.1–FITC o CD49b–PE, CD3–FITC y CD8–PE.Cy7 (BD Pharmingen y Biolegend). Los marcadores utilizados variaron según la cepa murina empleada, de acuerdo con la expresión diferencial de marcadores de superficie entre BALB/c y C57BL/6, así como con la disponibilidad de reactivos.

Marcador de superficie	BALB/C	C57BL/6
CD45	−	+
CD11b	+	+
NK1.1	−	+
CD49b	+	−
CD3	+	−
CD8	+	+

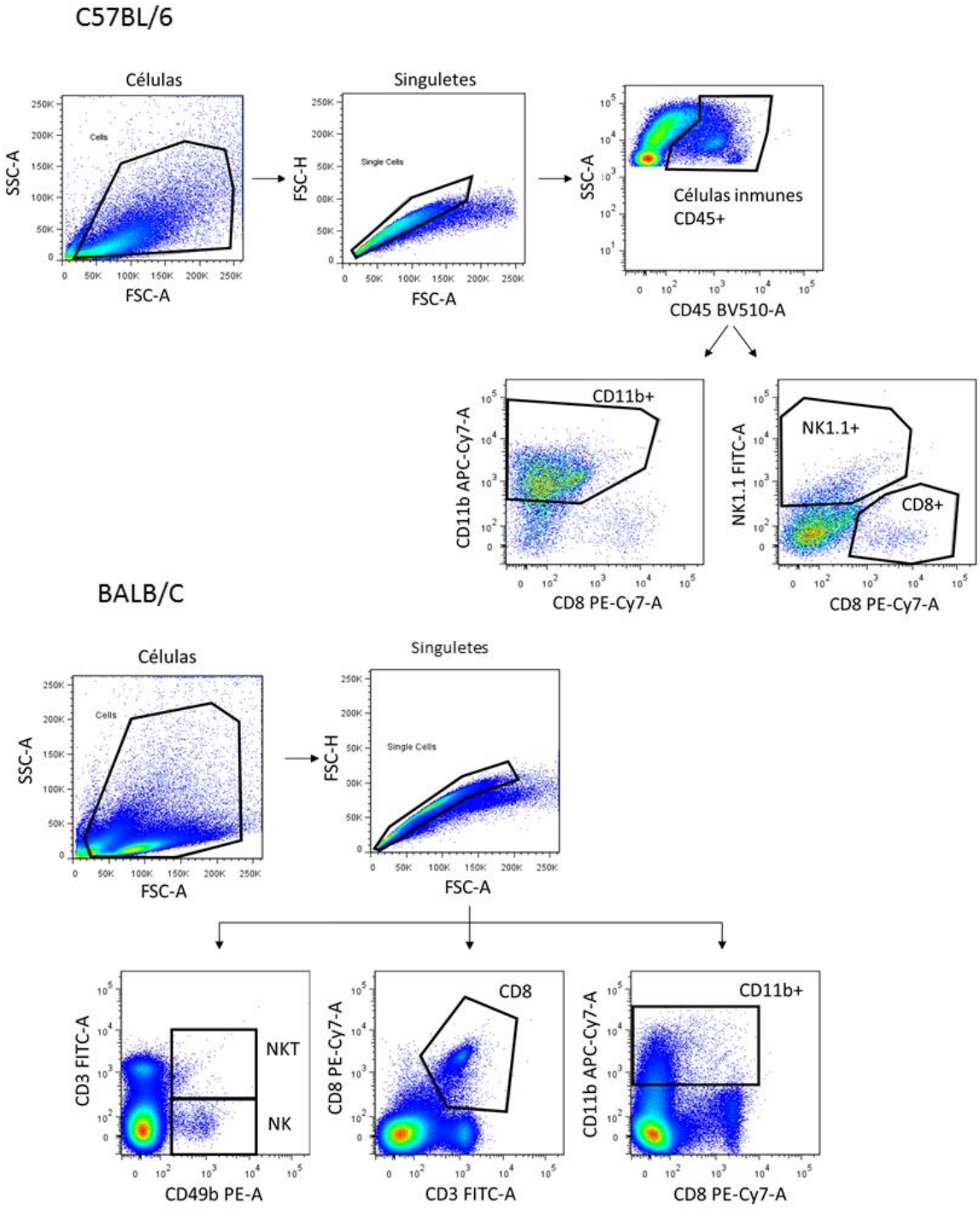


Figura 9 – Estrategia de gating utilizada para la inmunofenotipificación del TME mediante citometría de flujo en muestras de ratones C57BL/6 y BALB/c. Tras la selección de células y exclusión de dobletes, se identificaron poblaciones inmunes y subpoblaciones celulares según la expresión de marcadores específicos.

Cinética de poblaciones inmunes en diversos órganos post–LVR01

Los ratones fueron sacrificados en los días 3, 6, 9, 22 y 27 tras el tratamiento con LVR01; se extrajeron sangre, médula ósea y tejido tumoral (en los días 22 y 27). Siguiendo las recomendaciones del fabricante, las células se prepararon y tiñeron con anticuerpos contra

CD45–PE, CD11b–FITC, Ly6G–BV510, CD49b–APC y F4/80–PB (BD Pharmingen y Biolegend). Los marcadores utilizados variaron según el órgano analizado.

Marcador de superficie	Médula ósea	Sangre	Tumor
CD45	+	+	+
CD49b	+	+	+
CD11b	+	+	+
Ly6G	+	+	+
F4/80	−	+	+

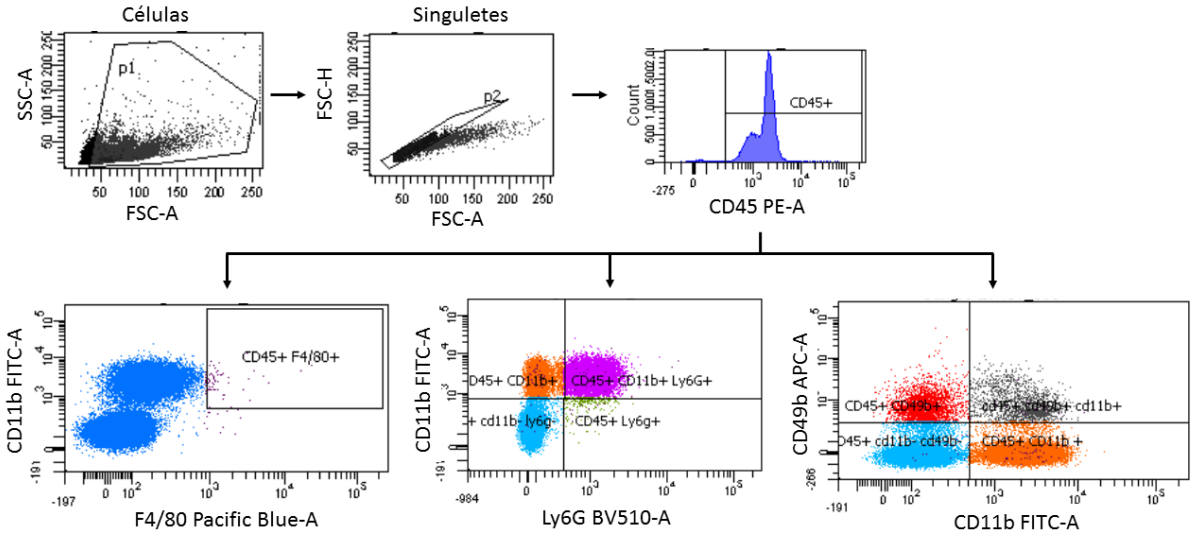


Figura 10 – Estrategia de gating empleada para el análisis cinético de poblaciones inmunes en distintos órganos mediante citometría de flujo tras el tratamiento con LVR01. Se seleccionaron células, se excluyeron dobletes y se identificaron poblaciones $CD45^+$ y subpoblaciones celulares según la expresión de marcadores específicos

Los datos de citometría de flujo se adquirieron en un citómetro FACS Canto II. El análisis se realizó utilizando el software FACS Diva y FlowJo 10.10 (BD Biosciences).

El análisis de datos de alta dimensión se llevó a cabo utilizando t–SNE (del inglés, *t–distributed Stochastic Neighbor Embedding*) para la reducción de dimensionalidad, X–Shift para el agrupamiento (clustering), Cluster Explorer y Euclid para el control de calidad del agrupamiento.

5.1.12 Ensayo de lactato

Las concentraciones de lactato se midieron en los sobrenadantes de cultivo celular en los días 1 y 7 del protocolo de entrenamiento de monocitos adherentes humanos, utilizando un

ensayo enzimático acoplado en el cual el lactato fue oxidado. El H_2O_2 resultante se acopló a la conversión del reactivo Amplex Red (Life Technologies) en resorufina fluorescente mediante HRP (peroxidasa de rábano picante, Thermo Scientific).

5.1.13 Análisis de expresión génica

En experimentos independientes, los ratones fueron sacrificados en el día 14 posterior a la implantación tumoral, y los tumores fueron extraídos, recolectados en reactivo TRIzol (Invitrogen) y almacenados a −80 °C hasta su procesamiento, como se describió previamente (Vola et al., 2018). Luego de la retrotranscripción, se realizó RT−PCR cuantitativa para los ARN mensajeros de *Tnf, Il6, Ifng, Il12, Cxcl1, Cxcl2, Cxcl9, Cxcl10, Il1a, Il1b, Ccl2, Ccl3, Ccl4, Ccl5, Ccl20* y *Tlr4* utilizando el kit QuantiTect® SYBR® Green PCR (Qiagen) en un Rotor−Gene 6000 (Corbett) (Tabla 1). Este panel se basó en trabajos previos del grupo, con algunas modificaciones (Mónaco & Plata et al., 2022). El gen que codifica para β−actina se utilizó como gen de referencia (*housekeeping*). La cantidad relativa de ARNm en cada muestra se calculó mediante el método 2^−ΔΔCt, como se describió previamente (Livak and Schmittgen, 2001), donde ΔCt = Ct_gen de interés − Ct_gen de referencia, y se expresó como niveles relativos de ARNm en los grupos experimentales en comparación con el grupo control.

Tabla 1 − Secuencias nucleotídicas de *primers* murinos utilizados para estudiar la expresión diferencial de genes por PCR en tiempo real.

Gen		Secuencia
Tnf	F	5´−CATCTTCTCAAAATTCGAGTGACAA−3´
	R	5´−CCTCCACTTGGTGGTTTGCT−3´
Il6	F	5´−GTTCTCTGGGAAATCGTGGAAA−3´
	R	5´−AAGTGCATCATCGTTGTTCATACA−3
Ifng	F	5´−TCAGCAACAGCAAGGCGAAA−3´
	R	5´−CCGCTTCCTGAGGCTGGAT−3´
Il12	F	5´−ATCACACGGGACCAAACCA−3´
	R	5´−CAGGCAACTCTCGTTCTTGTGTAGT−3´
Cxcl1	F	5´−CTTGGTTCAGAAAATTGTCCAAAA−3´
	R	5´−ACGGTGCCATCAGAGCAGTCT−3´
Cxcl2	F	5´−CCCTCAACGGAAGAACCAAA−3´
	R	5´−CACATCAGGTACGATCCAGGC−3´
Cxcl9	F	5´−TGGAGCAGTGTGGAGTTCGA
	R	5´−CCTCGGCTGGTGCTGATG
Cxcl10	F	5´−GCCGTCATTTTCTGCCTCAT−3´
	R	5´−GCTTCCCTATGGCCCTCATT−3´
Il1a	F	5´−CAGGGCAGAGAGGGAGTCAA−3´
	R	5´−GTCAGGAACTTTGGCCATCTTG−3´
	F	5´−CAACCAACAAGTGATATTCTCCATG−3´

Il1b	R	5´–GATCCACACTCTCCAGCTGCA–3´
Ccl2	F	5´–AGCTCTCTCTTCCTCCACCAC–3´
	R	5´–CGTTAACTGCATCTGGCTGA–3´
Ccl3	F	5´–AACATCATGAAGGTCTCCAC–3´
	R	5´–CCAAGACTCTCAGGCATTCA–3´
Ccl4	F	5´–GCCCTCTCTCTCCTCTTGCT–3´
	R	5´–GTCTGCCTCTTTTGGTCAGG–3´
Ccl5	F	5´–GGTACCATGAAGATCTCTGCA–3´
	R	5´–AAACCCTCTATCCTAGCTCAT–3´
Ccl20	F	5´–TTTTGGGATGGAATTGGACAC–3´
	R	5´–TGCAGGTGAAGCCTTCAACC–3´
Tlr4	F	5´–AGCTTCTCCAATTTTTCAGAACTTC–3´
	R	5´–TGAGAGGTGGTGTAAGCCATGC–3´

5.1.14 Biodistribución de *Salmonella* LVR01

Con el objetivo de evaluar la biodistribución de *Salmonella* LVR01 en el modelo de inmunidad entrenada, ratones C57BL/6 fueron inoculados por vía i.p. con 1×10^6 CFU de LVR01. Los animales fueron sacrificados en los días 1, 3, 8, 19 y 27 post–administración (n = 3 por tiempo experimental). Se recolectaron muestras de médula ósea y bazo para la determinación de carga bacteriana.

Los órganos fueron extraídos en condiciones estériles y procesados para la cuantificación de CFU. Brevemente, los tejidos fueron homogeneizados en condiciones asépticas, se realizaron diluciones seriadas y las muestras fueron sembradas en placas de agar Luria–Bertani (LBA). Las placas fueron incubadas en las condiciones apropiadas para el crecimiento bacteriano y posteriormente se realizó el recuento de colonias. Los resultados fueron expresados como $\log_{10}$ CFU por tejido.

5.2 AUTOFAGIA

5.2.1 Evaluación de inducción de autofagia *in vitro*

Para los experimentos de evaluación de la autofagia *in vitro*, las células B16F10 se cultivaron en medio DMEM (Capricorn Scientific) suplementado con 10% de suero fetal bovino (Capricorn Scientific) hasta alcanzar confluencia. Posteriormente, se resuspendieron a una densidad de 5×10^5 células/mL y se sembraron $2{,}5 \times 10^5$ células por pocillo, dejándolas adherir durante 2 h a 37 °C y 5% de CO_2. Las células se incubaron durante 3 horas con moduladores de la autofagia: rapamicina (1 µM, inductor, Sigma–Aldrich), cloroquina (10 µM, inhibidor, Sigma–Aldrich), 3–metiladenina (3 µM, inhibidor, Sigma–Aldrich) o con medio (control sin modulador). Posteriormente, se infectaron con LVR01 a una MOI de 100:1 durante 1 hora. En las condiciones sin infección se adicionó un volumen equivalente de medio. Finalizada la incubación, las células fueron procesadas de acuerdo con los protocolos específicos de cada ensayo.

5.2.1.1 Microscopía confocal

Para los ensayos de microscopía confocal, las células B16F10 se cultivaron en cámaras de vidrio de cuatro compartimientos (Cellvis). Tras 1 hora de infección con LVR01, se descartó el sobrenadante y las células fueron incubadas con una solución de tinción compuesta por la sonda *Autophagy Detection Probe Green* (1:500, BioLegend) y Hoechst 33342 (Molecular Probes, ThermoFisher Scientific) en HBSS (*Hanks Balanced Salt Solution*). La incubación se realizó durante 30 minutos a 37 °C, protegidas de la luz. Finalizado este período, la solución de tinción fue retirada y las células se lavaron dos veces con HBSS. La adquisición de imágenes se realizó en el microscopio confocal de la Unidad de Microscopía Confocal, Facultad de Medicina, Universidad de la República. El análisis de la fluorescencia se efectuó con el software Fiji ImageJ.

5.2.1.2 Western Blot

Para los ensayos de Western blot, las células B16F10 se cultivaron en placas de 6 pocillos a una densidad de 1×10^6 células por pocillo. Tras los tratamientos correspondientes, las células fueron lisadas con Tritón X–100 0,1% (Sigma–Aldrich). Los lisados de cada condición se poolearon y transfirieron a tubos de 1,5 mL. Las muestras se centrifugaron a 13000 × g durante 15 minutos a 4 °C, separándose la fracción soluble y fracción insoluble, que ambas se conservaron para análisis posteriores. La concentración de proteínas se determinó mediante el método de Bradford (Sigma–Aldrich). Las muestras fueron mezcladas con buffer de carga reductor y calentadas durante 5 min a 95 °C previo a la electroforesis. Las proteínas se separaron por electroforesis en geles de poliacrilamida con dodecil sulfato de sodio (SDS–PAGE) y posteriormente se transfirieron a membranas PVDF (*Immobilon Membrane* – P, Sigma–Aldrich) mediante el método de transferencia húmeda. El análisis de Western blot se realizó utilizando anticuerpos específicos frente a LC3 (BioLegend) y ATG5 (BioLegend). Para el revelado se utilizó el anticuerpo secundario anti–*mouse*–IgGTotales–PO (Sigma) y kit para detección por quimioluminiscencia (GE–Healthcare). Las imágenes de los geles y membranas se

obtuvieron con el sistema de documentación G:BOX (Syngene) y el análisis densitométrico de las bandas se realizó con el software Fiji ImageJ.

5.2.2 Evaluación de la muerte celular inducida por LVR01 en combinación con inhibidores de la autofagia *in vitro*

Para los experimentos de evaluación de la muerte celular las células B16F10 se cultivaron DMEM suplementado hasta alcanzar confluencia. Luego, se resuspendieron a una densidad de 5×10^5 células/mL y se sembraron $2,5 \times 10^5$ células por pocillo en placas de 24 wells, dejándolas adherir durante 2 h a 37 °C y 5% de CO_2. Las células se incubaron durante 3 horas con moduladores de la autofagia: rapamicina (1 µM, inductor, Sigma–Aldrich), cloroquina (10 µM, inhibidor, Sigma–Aldrich), 3– metiladenina (3 µM, inhibidor, Sigma–Aldrich) o con medio (control sin modulador). Se infectaron con LVR01 a una MOI de 100:1 durante 1 hora o 20 horas (agregando gentamicina al medio a la hora de infección). Se recuperó el sobrenadante de las células en tubos de citometría y las células fueron recuperadas mediante tripsinización (100 µL por pocillo, 3 minutos a 37 °C) y transferidas a tubos de citometría. Las muestras se centrifugaron a 1800 rpm durante 3 minutos y se resuspendieron en buffer FACS. Se tiñieron con PI (ioduro de propidio, Sigma–Aldrich). La adquisición de eventos se realizó en un citómetro de flujo CytoFLEX (Beckman Coulter), utilizando el canal PE (Ex/Em 488/~585 nm) para la detección del marcador. Los datos obtenidos fueron analizados con el software CytExpert correspondiente al equipo.

5.2.3 Evaluación del efecto antitumoral de LVR01 en combinación con inhibidores de la autofagia *in vivo*

Para la evaluación *in vivo* se implantaron tumores B16F10 vía s.c. en el flanco derecho de ratones C57BL/6 como se explicó anteriormente. A partir del día 6 y hasta el día 15 post implantación del tumor (p.i.t.), se administró cloroquina (60 mg/kg) diariamente vía i.p. Además, al día 8 p.i.t., cuando el tumor es palpable, se administró vía intratumoral (i.t.) 1×10^6 CFU de *Salmonella* LVR01 o PBS. Las mediciones tumorales se realizaron día por medio con un calibrador digital, y los volúmenes tumorales se calcularon utilizando la fórmula: largo × ancho × profundidad × $\pi/6$. La eutanasia se realizó por dislocación cervical cuando los tumores alcanzaron los 4000 mm^3 o antes si los animales mostraban signos de sufrimiento.

Además, se evaluó el impacto del uso de inhibidores en el modelo *in vivo* de inmunidad entrenada. Para ello, se administró cloroquina (60 mg/kg) diariamente vía i.p por una semana, al segundo día se administró vía i.p. 1×10^6 CFU de *Salmonella* LVR01 o PBS y al octavo día post inicio del tratamiento con cloroquina se implantaron tumores B16F10 vía s.c. en el flanco derecho de los animales. El seguimiento de los animales se realizó como se describió anteriormente.

5.3 ANÁLISIS ESTADÍSTICO

Las diferencias en los tiempos de supervivencia se determinaron mediante análisis de Kaplan–Meier y pruebas de log-rank, utilizando el software GraphPad Prism 8. La significancia estadística de las diferencias entre los grupos de estudio se analizó utilizando la prueba t de Student. En todos los casos, se consideró estadísticamente significativo un valor de $p < 0,05$.

6. RESULTADOS

6.1 INMUNIDAD ENTRENADA

6.1.1. Evaluación de la capacidad de *Salmonella* LVR01 para inducir inmunidad entrenada *in vitro* en monocitos humanos adherentes.

Como primera aproximación a este trabajo, se propuso evaluar el potencial de *Salmonella* LVR01 para inducir inmunidad entrenada *in vitro*. Para ello, se siguieron protocolos experimentales previamente establecidos para el estudio de la inmunidad entrenada, los cuales consisten en la exposición secuencial de las células a dos estímulos: un estímulo primario o de entrenamiento, destinado a inducir la reprogramación funcional, seguido de un período de reposo y un segundo estímulo o reestímulo. En este tipo de ensayos, la respuesta celular se evalúa tanto a las 24 horas del estímulo inicial, con el fin de caracterizar la activación primaria inducida por el agente de entrenamiento, como a las 24 horas tras el reestímulo, para determinar la presencia de una respuesta funcional modificada compatible con inmunidad entrenada.

Se infectaron monocitos adherentes humanos obtenidos de sangre periférica con diferentes MOI de LVR01 durante una hora. Posteriormente, se adicionó gentamicina al medio de cultivo para eliminar las bacterias extracelulares. Como control positivo de inmunidad entrenada, se estimularon las células con lisados de *Leishmania braziliensis* (LL), mientras que el medio RPMI se utilizó como control negativo. Las concentraciones de citoquinas proinflamatorias se determinaron en los sobrenadantes de los cultivos celulares a las 24 horas luego del estímulo inicial. Se observó una respuesta primaria con un aumento significativo en los niveles de IL-6, TNF, IL-1β e IL-8 en las células infectadas con LVR01 en comparación con las condiciones tratadas con LL o RPMI (Figura 11 a-d). Además, se midió la producción de IL-1Ra en los sobrenadantes y se observó un aumento significativo en las células estimuladas con LL respecto a las demás condiciones (Figura 11 e).

Las células se mantuvieron en cultivo durante 6 días sin recibir estímulos adicionales. Tras el período de reposo, se evaluó el metabolismo celular mediante la cuantificación de lactato en el sobrenadante, observándose niveles significativamente más altos en las células entrenadas con LL que en las estimuladas con LVR01 o las no entrenadas (RPMI) (Figura 11 f). En ese momento, las células fueron reestimuladas con LPS, Pam3Cys o RPMI por 24 horas, y se cuantificaron las citoquinas proinflamatorias IL-6 y TNF en los sobrenadantes. Como era esperado, las células entrenadas con LL mostraron un incremento significativo en la producción de citoquinas ante la reestimulación, consistente con un fenotipo de inmunidad entrenada. En contraste, las células previamente expuestas a LVR01 exhibieron una disminución significativa en la producción de IL-6 y TNF tras la reestimulación, lo que sugiere la inducción de un estado de tolerancia (Figura 11 g-h, Figura 12). Mientras que en la Figura 11 se muestran los valores promedio obtenidos a partir de los distintos donantes analizados, la Figura 12 presenta los resultados individualizados correspondientes a cada donante.

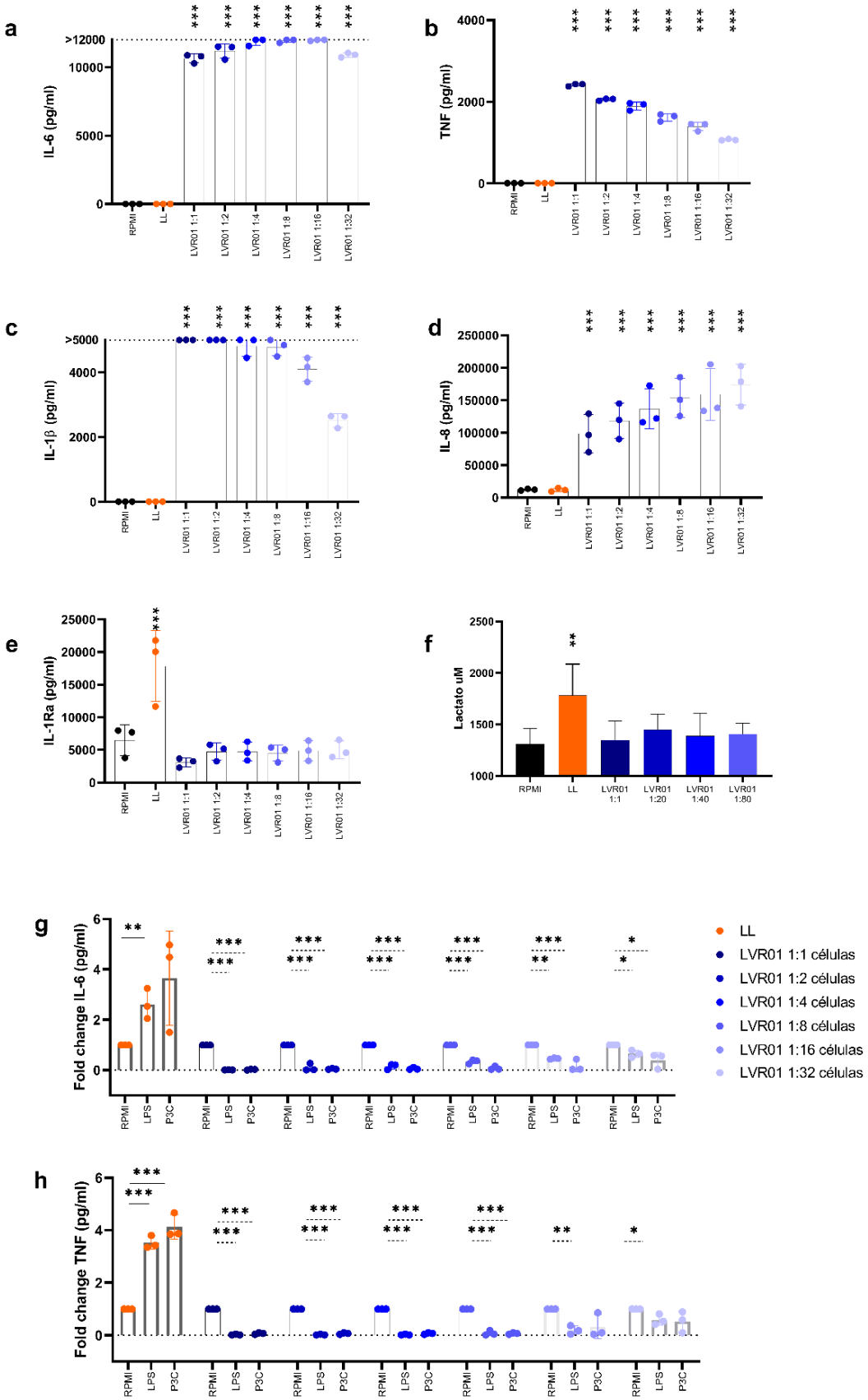


Figura 11 – *Salmonella* induce tolerancia *in vitro* en monocitos periféricos humanos.

Figura 11 – *Salmonella* induce tolerancia *in vitro* en monocitos periféricos humanos. (a) IL-6, (b) TNF, (c) IL-1b, (d) IL-8 y (e) IL-1Ra secretados por monocitos humanos estimulados con RPMI, lisados de *L. braziliensis* (LL, 25 μg/ml) y diversas MOI de *Salmonella* LVR01:células (1:1, 1:2, 1:4, 1:8, 1:16, 1:32) por 1 hora, luego de 24 horas, medidos por ELISA. (f) Producción de lactato medida por un ensayo fluorométrico en sobrenadantes de monocitos entrenados al día 6. Datos presentados como media ± SD de 3 réplicas biológicas (*p < 0,05, **p < 0,01, ***p < 0,001, t test). (g) IL-6 y (h) TNF secretado por monocitos entrenados, y reestimulados al día 6 con LPS (10 ng/ml) o Pam3Cys (10 μg/ml) por 24 horas, medido por ELISA. Se muestra un experimento representativo de un total de siete experimentos independientes realizados con monocitos de tres donantes sanos. Cada punto representa un donante. Cada sobrenadante fue analizado por ELISA en triplicado técnico para cada condición. Datos representados como cambio relativo (*fold change*) normalizado con RPMI (células no entrenadas) y mostrado como media ± SD de 3 réplicas biológicas (*p < 0,05, **p < 0,01, ***p < 0,001, t test).

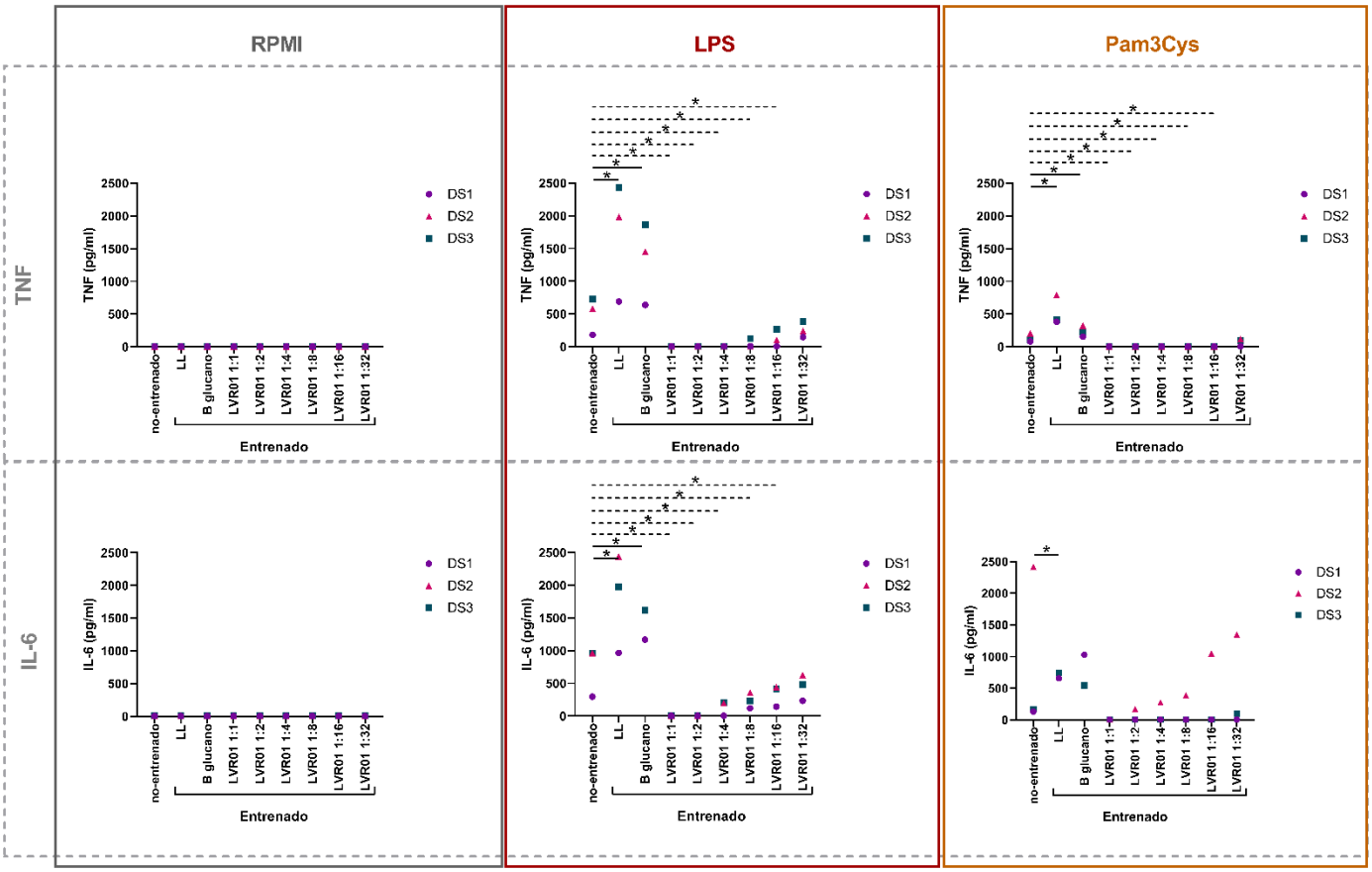


Figura 12 – *Salmonella* induce tolerancia *in vitro* en monocitos periféricos humanos (valores individuales). TNF e IL-6 secretados por monocitos humanos de donantes sanos (DS) estimulados con RPMI (no-entrenados), lisados de *L. braziliensis* (LL, 25 μg/ml) y diversas MOI de *Salmonella* LVR01:células (1:1, 1:2, 1:4, 1:8, 1:16, 1:32) por 1 hora, y reestimulados al día 6 con LPS (10 ng/ml) o Pam3Cys (10 μg/ml) por 24 horas, medido por ELISA. Resultados representativos de 7 experimentos independientes realizados con monocitos de 3 donantes sanos y triplicados técnicos por condición. Datos representados como concentración pg/ml y mostrado como valores individuales (*p < 0,05, **p < 0,01, ***p < 0,001, t test).

Finalmente, para evaluar si la viabilidad bacteriana era necesaria para inducir este efecto tolerante, se realizó la misma aproximación *in vitro* utilizando *Salmonella* LVR01 inactivada por calor (LVR01hk, del inglés *heat-killed* LVR01) en cantidades equivalentes a diferentes MOI. De manera consistente con los resultados previos, la estimulación con LVR01hk también indujo un fenotipo tolerante en los monocitos humanos (Figura 13).

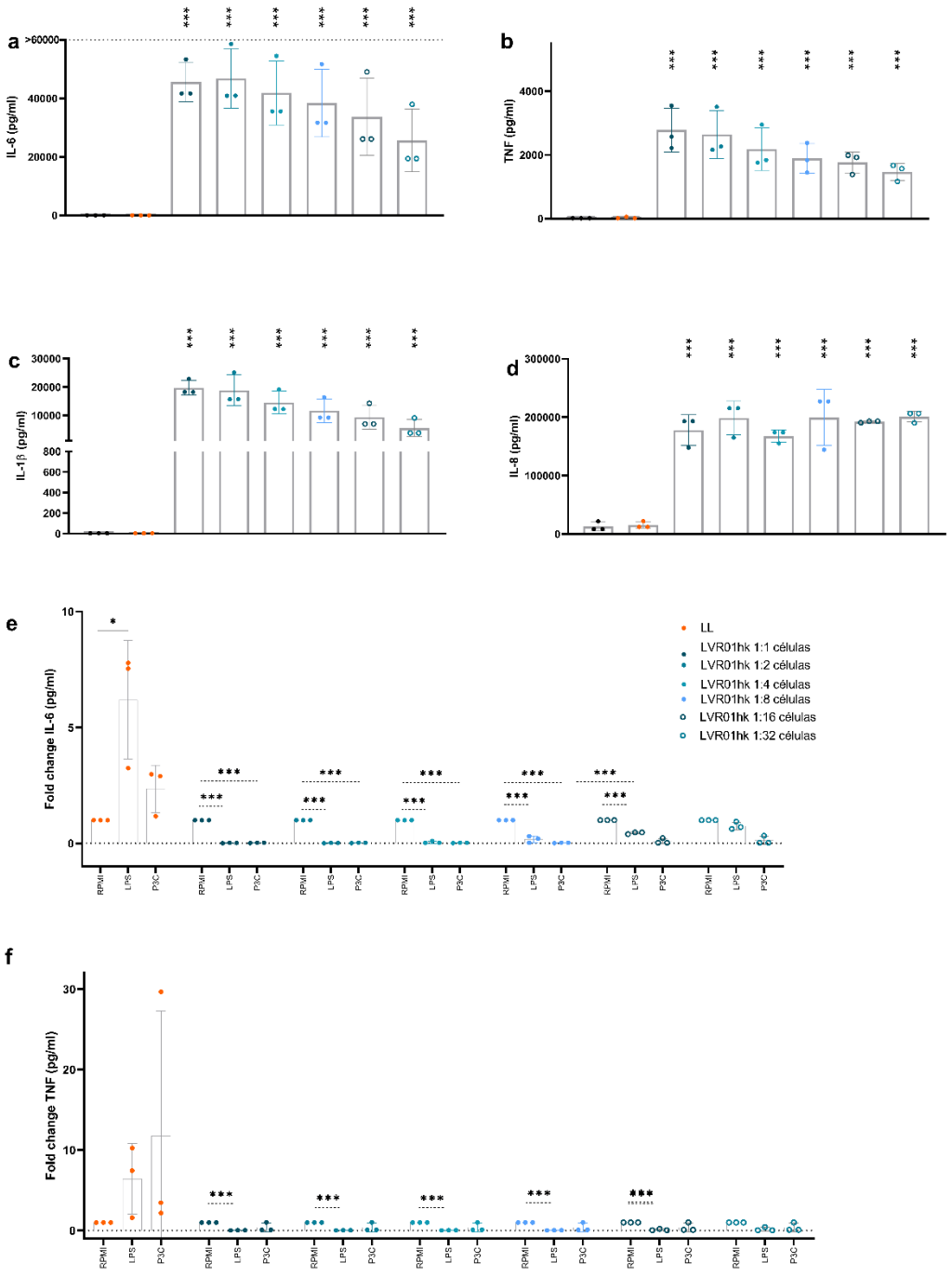


Figura 13 – *Salmonella* inactivada por calor induce tolerancia *in vitro* en monocitos periféricos humanos. (a) IL-6, (b) TNF, (c) IL-1b y (d) IL-8 secretados por monocitos humanos estimulados con RPMI, lisados de *L. braziliensis* (LL, 25 μg/ml) y diversas MOI de *Salmonella* inactivada por calor (LVR01hk, *heat-killed* LVR01) LVR01hk:células (1:1, 1:2, 1:4, 1:8, 1:16, 1:32) por 1 hora luego de 24 horas, medidos por ELISA. Datos presentados como media ± SD de 3 réplicas biológicas (*p < 0,05, **p < 0,01, ***p < 0,001, t test). (e) IL-6 y (f) TNF secretado por monocitos entrenados con RPMI, lisados de *L. braziliensis* y diversas MOI de LVR01hk:células (1:1, 1:2, 1:4, 1:8, 1:16, 1:32) y reestimulados al día 6 con LPS (10 ng/ml) o Pam3Cys (10 μg/ml) por 24 horas, medido por ELISA. Resultados representativos de 3 experimentos independientes realizados con monocitos de 3 donantes sanos y triplicados técnicos por condición. Datos representados como cambio relativo (*fold change*) normalizado con RPMI (células no entrenadas) y mostrado como media ± SD de 3 réplicas biológicas (*p < 0,05, **p < 0,01, ***p < 0,001, t test).

En conjunto, estos resultados indican que la exposición a *Salmonella* LVR01, viva o inactivada, no induce un perfil de inmunidad entrenada en monocitos humanos derivados de sangre periférica, sino que promueve un estado de tolerancia de la inmunidad innata, caracterizado por una menor respuesta inflamatoria frente a estímulos secundarios.

6.1.2 Evaluación de la inducción de inmunidad entrenada por LVR01 *in vitro* en células mieloides derivadas de médula ósea de ratón.

Dado que nuestros estudios preclínicos se basan en modelos murinos y que previamente demostramos el efecto antitumoral de LVR01 en estos animales, decidimos determinar si LVR01 inducía inmunidad entrenada en células mieloides derivadas de médula ósea. Para ello, se obtuvieron las células de médula ósea, se cultivaron y se sometieron al protocolo clásico de inmunidad entrenada *in vitro.* Las células fueron inicialmente estimuladas con RPMI, LL o LVR01hk (*Salmonella* inactivada por calor). Tras 6 días de reposo en cultivo, las células fueron reestimuladas durante 24 horas con RPMI, LPS o PolyIC, y luego se cuantificaron citoquinas proinflamatorias en los sobrenadantes.

De manera coherente con lo observado en monocitos humanos, la estimulación con LVR01hk resultó en una disminución significativa de la producción de citoquinas ante los estímulos secundarios, evidenciando un fenotipo tolerante en estas células (Figura 14).

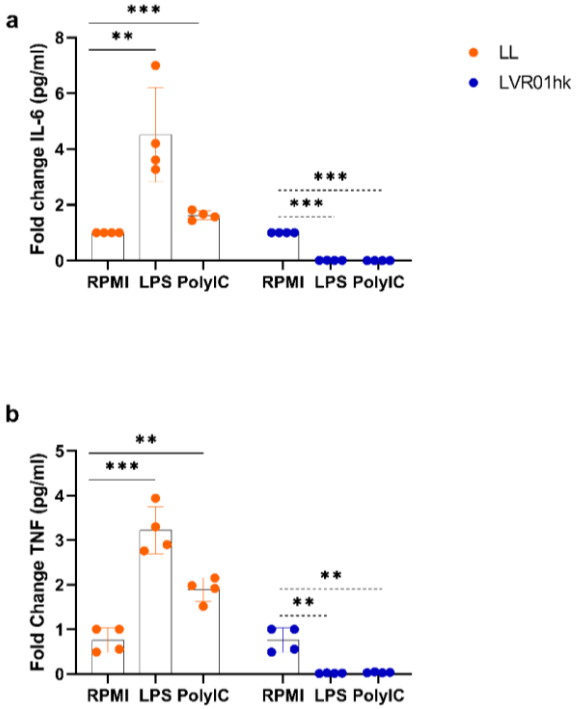


Figura 14 – *Salmonella* inactivada por calor induce tolerancia *in vitro* en células mieloides de médula ósea de ratón. (a) IL-6 y (b) TNF secretados por células mieloides murinas derivadas de médula ósea estimuladas con RPMI, lisados de *L. braziliensis* (LL, 25 µg/ml) y 1x10^6 CFU de *Salmonella* inactivada por calor (LVR01hk, *heat-killed* LVR01) por 24 horas, y reestimuladas al día 6 con LPS (10 ng/ml) o PolyIC (100 µg/ml) por 24 horas, medido por ELISA. Resultados representativos de 2 experimentos independientes realizados con células de médula ósea obtenidas a partir de pools de 3 ratones sanos y cuatriplicados técnicos por condición. Datos representados como cambio relativo (*fold change*) normalizado con RPMI (células no entrenadas) y mostrado como media ± SD (**p < 0,01, ***p < 0,001, t test).

6.1.3 Evaluación del modelo de inmunidad entrenada *in vivo* con LVR01.

Si bien los ensayos *in vitro* demostraron que LVR01 induce un fenotipo tolerante en monocitos humanos periféricos y en células mieloides derivadas de médula ósea de ratón, consideramos fundamental evaluar su efecto *in vivo*, donde la complejidad del organismo, los mecanismos compensatorios y la interacción entre múltiples poblaciones de la inmunidad innata pueden modificar sustancialmente la respuesta.

En este contexto, resulta particularmente relevante determinar si la exposición a LVR01 modula de manera diferente la respuesta sistémica, dado que otras células innatas no contempladas en los modelos *in vitro* podrían contribuir a un fenotipo inmunológico distinto. Además, consideramos que el abordaje *in vivo* constituye la aproximación más completa para evaluar el efecto de LVR01 en un contexto fisiológico.

6.1.3.1 Cuantificación de citoquinas séricas tras la administración de LVR01.

Con el objetivo de evaluar el potencial de *Salmonella* LVR01 para inducir inmunidad entrenada *in vivo*, se trataron ratones con una dosis única i.p. de LVR01 o con PBS. Siete días después, los animales fueron reestimulados por vía i.p. con LPS. Se obtuvieron muestras de sangre 24 horas antes y 90 minutos después de la reestimulación (Figura 15 a). Los ratones pretratados con LVR01 mostraron niveles séricos significativamente aumentados de IL-6 y TNF tras la administración de LPS en comparación con el grupo control tratado con PBS (Figura 15 b–c). Estos resultados sugieren que la exposición previa a LVR01 potencia la respuesta inflamatoria sistémica frente a un reestímulo, característica compatible con un fenotipo de inmunidad entrenada.

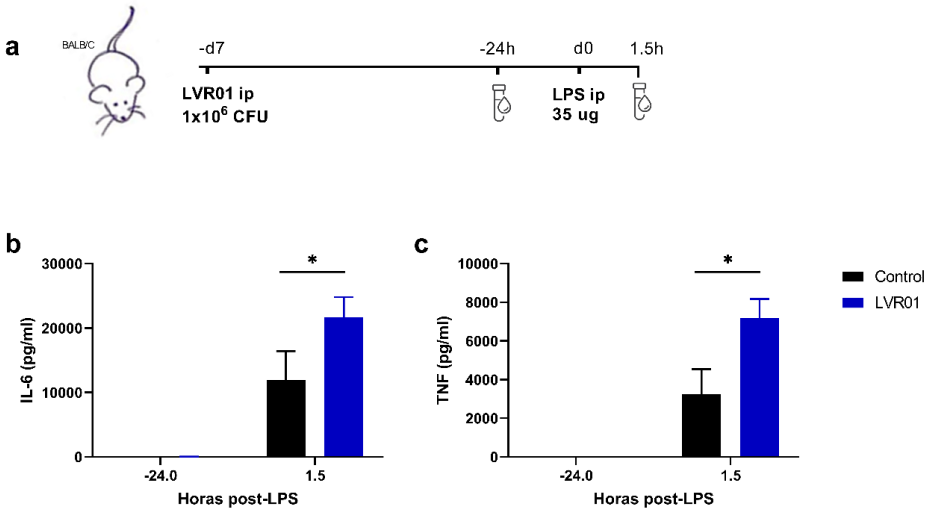


Figura 15 – La reestimulación *in vivo* incrementa los niveles séricos de citoquinas proinflamatorias de animales pretratados con *Salmonella*. (a) Diseño experimental, "d" son días y "h" son horas. (b) IL-6 y (c) TNF en suero de ratones entrenados *in vivo* con PBS (Control) o $1x10^6$ CFU de LVR01 i.p. y reestimulados con LPS (35 ug, i.p.) al séptimo día. Citoquinas medidas por ELISA 24 horas antes y 90 minutos después del estímulo con LPS. Resultados representativos de 2 experimentos independientes, n=3/grupo. Datos representados como media ± SD (*p < 0,05, t test).

6.1.3.2 Análisis *ex vivo* del modelo de inmunidad entrenada con LVR01.

Se pretrataron ratones con LVR01 o PBS como control de forma i.p. y, seis días después, se extrajeron las células de médula ósea. Las células fueron reestimuladas *ex vivo* con LPS durante 24 horas, y se cuantificaron los niveles de IL-6 y TNF en los sobrenadantes. En concordancia con los resultados *in vivo*, ambos mediadores se encontraron aumentados en el grupo pretratado con LVR01 respecto al control (Figura 16 a–c).

Para caracterizar mejor las poblaciones celulares responsables de esta producción aumentada de citoquinas, se realizó tinción intracelular de las células de médula ósea luego de 4 horas de reestimulación en presencia de GolgiPlug (Figura 16 d). Se observó un mayor porcentaje de células productoras de TNF en la médula ósea de animales tratados con LVR01, en comparación con animales control (Figura 16 e). Antecedentes del grupo han demostrado que neutrófilos y células NK tienen un importante rol en el efecto antitumoral de LVR01, es por esto que se evaluó específicamente la contribución de estas poblaciones, junto a los monocitos, incorporando marcadores al estudio por citometría de flujo (Mónaco & Plata et al., 2022). Se observó que las células productoras de TNF no corresponden a la población NK (Figura 16 f). En cambio, se identificaron como $CD11b^+$ mieloides, principalmente células $Ly6C^+Ly6G^+$ —probablemente neutrófilos, y no MDSCs debido a su capacidad proinflamatoria— y monocitos $Ly6C^{high}$ (Figura 16 e–f).

Además, se realizó un análisis no supervisado mediante t-SNE que confirmó estos resultados. La concatenación de eventos individuales, el análisis de clusters y su representación en mapas de calor basados en la intensidad de expresión de los marcadores analizados mostró que las células productoras de TNF ante reestimulación pertenecen exclusivamente a poblaciones mieloides $CD11b^+$ (Figura 16 g).

Cuando las células de médula ósea fueron cultivadas *ex vivo* y se seleccionaron las células adherentes, se obtuvo una población predominantemente mieloide (Figura 17). Tras 6 días de reposo, estas células, predominantemente monocitos, fueron reestimuladas (Figura 16 h), y en este esquema el patrón observado cambió de manera notable. En este contexto, las células provenientes de animales tratados con LVR01 mostraron una reducción en la producción de IL-6 frente al segundo estímulo, alcanzando niveles comparables a los del grupo control (Figura 16 i–j). Estos resultados indican que la respuesta proinflamatoria inicial no se sostiene en estas poblaciones mieloides enriquecidas, sino que progresa hacia un fenotipo tolerante en los animales pretratados con LVR01.

De manera acorde, se observó una marcada disminución en la producción de TNF, correlacionada con la pérdida de monocitos $Ly6C^{high}$ productores de esta citoquina, reforzando su papel central en la respuesta proinflamatoria temprana (Figura 16 k–l).

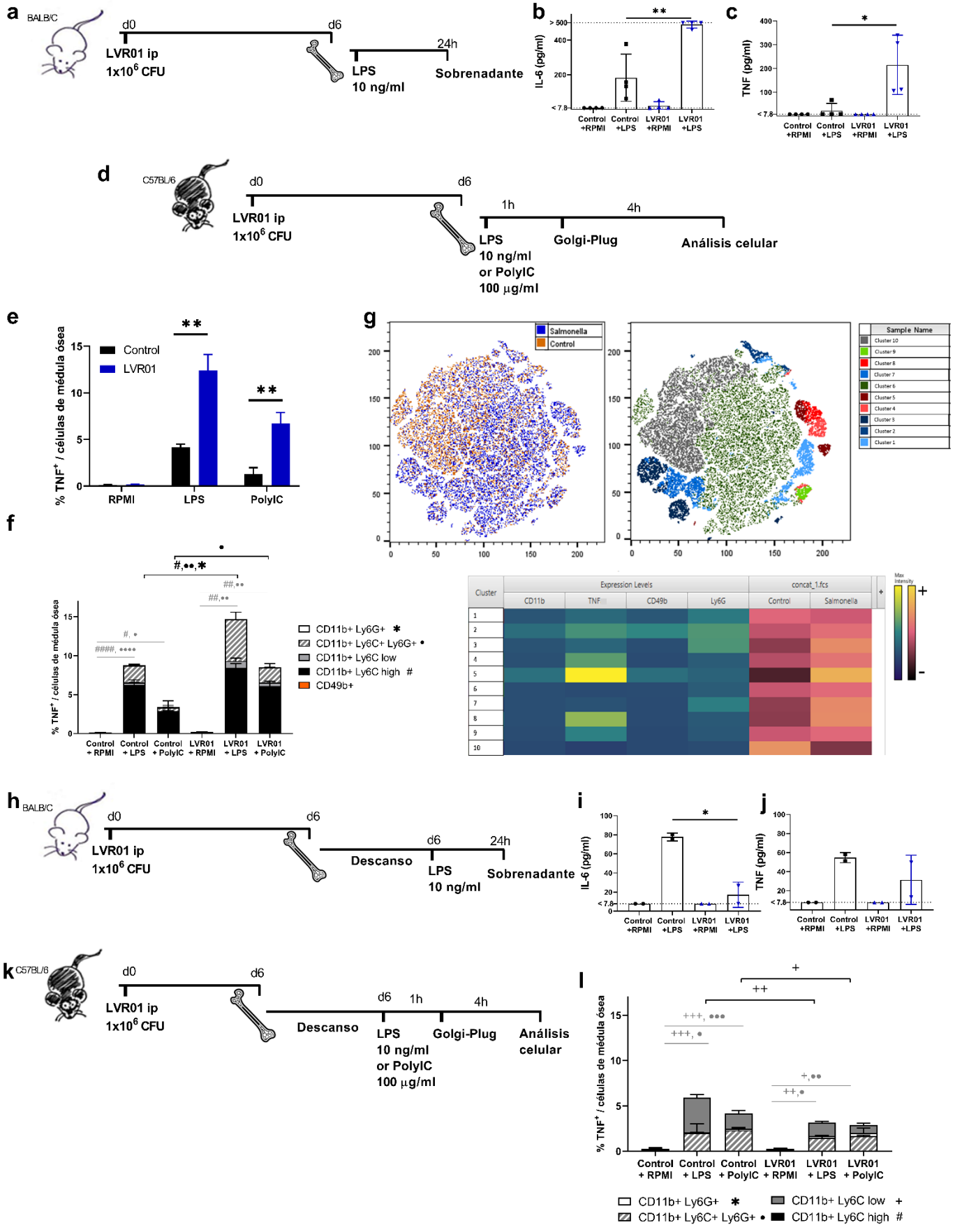


Figura 16 – *Salmonella* incrementa los niveles de citoquinas proinflamatorias en células de médula ósea reestimuladas *ex vivo*.

Figura 16 – *Salmonella* incrementa los niveles de citoquinas proinflamatorias en células de médula ósea reestimuladas *ex vivo*. (a, d, h, k) Diseños experimentales, "d" son días y "h" son horas. (b) IL–6 y (c) TNF secretadas por células de médula ósea entrenadas *in vivo* con PBS o LVR01 (1x10^6 CFU) y reestimuladas *ex vivo* con LPS (10 ng/ml), medido por ELISA. Análisis por citometría de flujo de (e) células TNF$^+$ totales y (f) de las poblaciones celulares productoras de TNF dentro de las células de médula ósea de ratones entrenados, reestimuladas *ex vivo* con LPS o Poly I:C y luego tratadas con GolgiPlug. (g) Análisis no supervisado de eventos individuales obtenidos del set de citometría de flujo de médula ósea mediante el algoritmo t–SNE. Se muestra el gráfico t–SNE de las condiciones concatenadas Control+LPS y LVR01+LPS. El mapa de calor representa los niveles de expresión de los marcadores seleccionados sobre los gráficos t–SNE concatenados. Secreción de (i) IL–6 y (j) TNF de células de médula ósea provenientes de ratones entrenados con LVR01 o controles (PBS), mantenidas en reposo durante 6 días antes de la reestimulación *ex vivo* con LPS, cuantificada por ELISA. (l) Análisis por citometría de flujo de las poblaciones celulares productoras de TNF en médula ósea de ratones entrenados con LVR01 y controles (PBS), mantenidas en reposo antes de la reestimulación *ex vivo* con LPS y posteriormente tratadas con GolgiPlug. Resultados representativos de 2 experimentos independientes, n=3/grupo. Datos presentados como media ± SD (*p < 0,05, **p < 0,01, ***p < 0,001, t test).

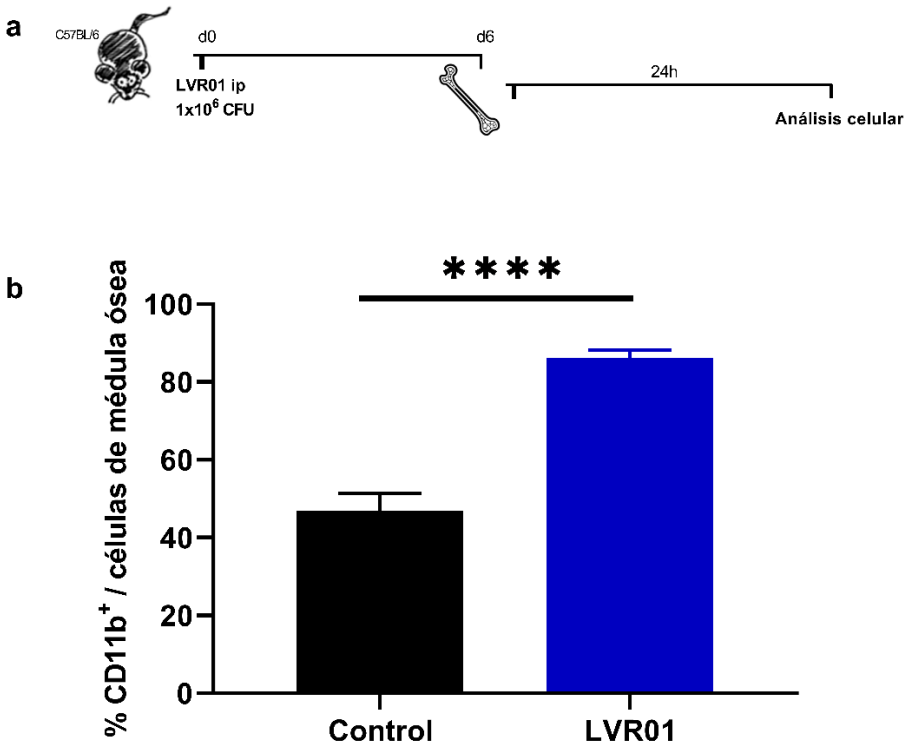


Figura 17 – Caracterización de células CD11b$^+$ derivadas de médula ósea a las 24 horas. (a) Diseño experimental; "d" son días y "h" horas. (b) Porcentaje de células CD11b$^+$ en cultivos derivados de médula ósea a las 24 h post–siembra. Resultados de 1 experimento, n=3/grupo. Datos presentados como media ± SD (****p < 0,0001, t test).

Además, se evaluaron los niveles de Galectina–1 en los sobrenadantes de estas células, observándose concentraciones mayores en el grupo pretratado con LVR01 en comparación con el control. Este aumento podría contribuir, al menos en parte, a los mecanismos que conducen a la adquisición posterior del fenotipo tolerante (Figura 18).

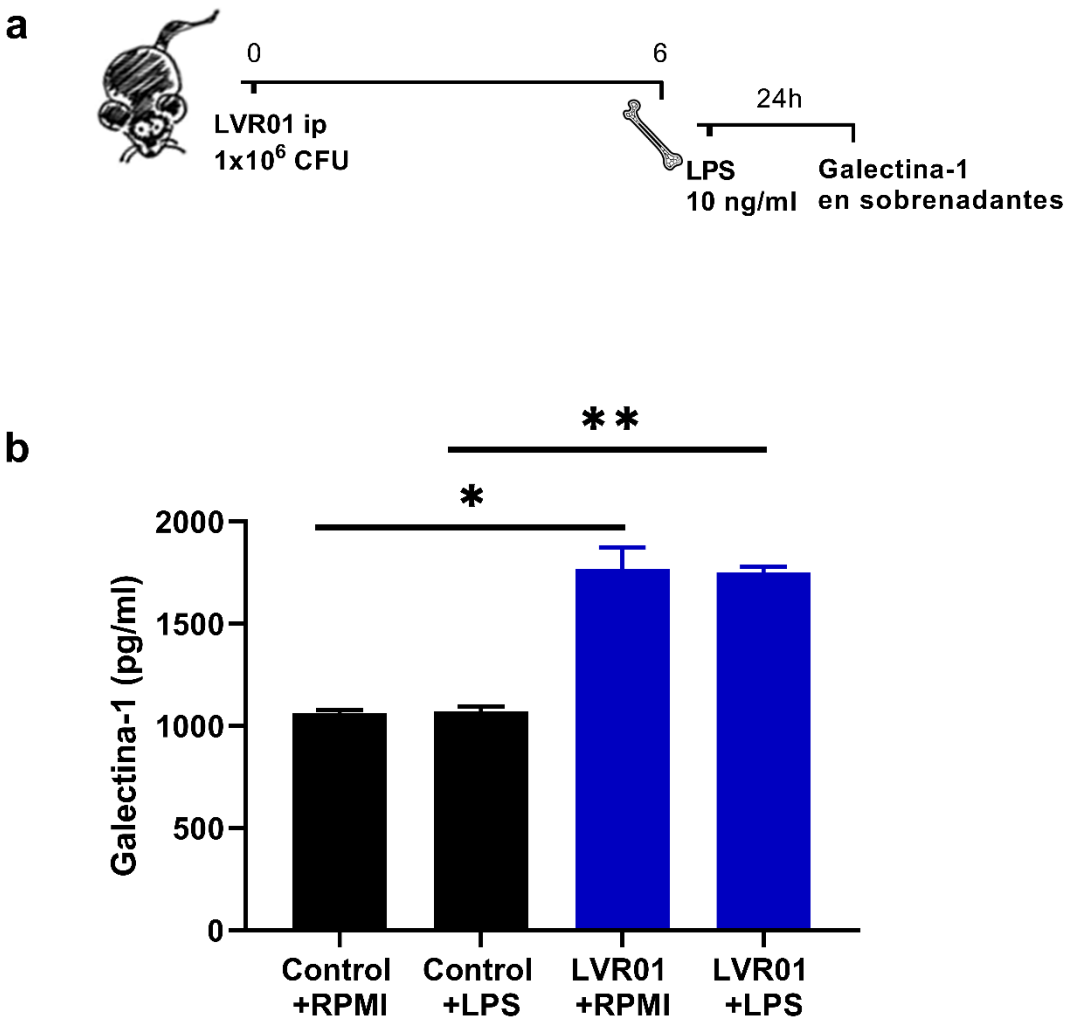


Figura 18 – *Salmonella* incrementa los niveles de Galectina-1 en células de médula ósea. (a) Diseño experimental. (b) Concentración de Galectina-1 en cultivos derivados de médula ósea, proveniente de animales pretratados con LVR01 o PBS, a las 24 h post-estimulación con LPS. Resultados representativos de 2 experimentos independientes, n=3/grupo. Datos presentados como media ± SD (****p < 0,0001, t test).

6.1.3.3 Uso profiláctico de LVR01 en modelos tumorales.

Primero se evaluó el impacto del pretratamiento con LVR01 en el desarrollo tumoral utilizando un modelo murino de melanoma. Se implantaron células B16F10 vía s.c. en ratones una semana después de la administración i.p. de *Salmonella* (Figura 19 a). Los animales pretratados con LVR01 presentaron una reducción significativa en el volumen tumoral en comparación con el grupo control (Figura 19 b), acompañada de una mejora en la sobrevida global (Figura 19 c).

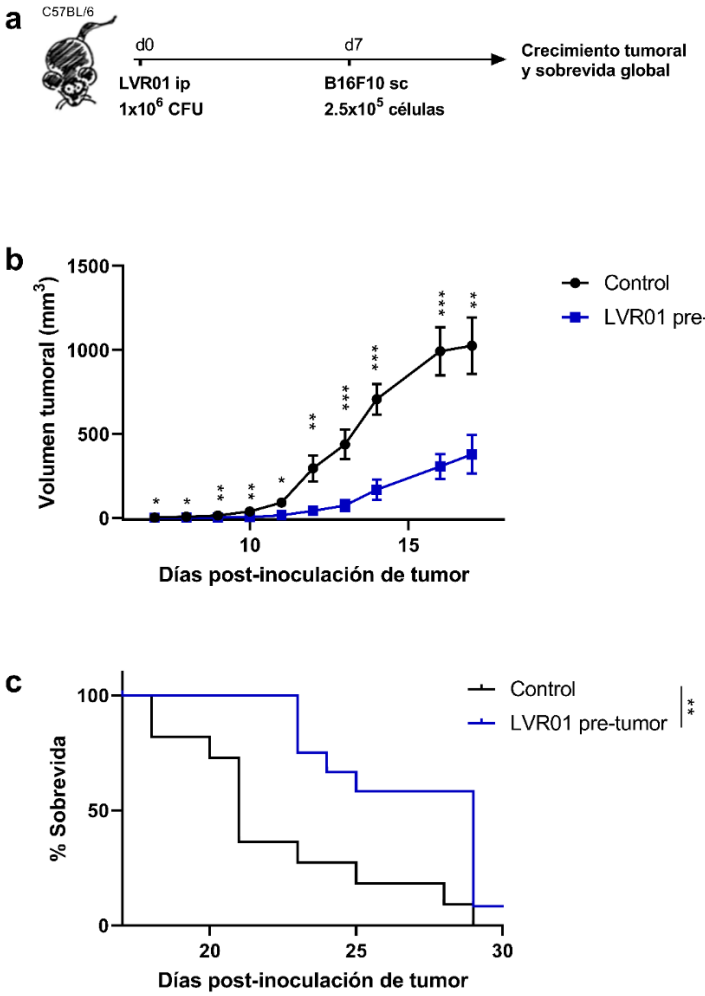


Figura 19 – Uso profiláctico de *Salmonella* retrasa el crecimiento tumoral y prolonga la sobrevida global de ratones portadores de tumores B16F10. (a) Diseño experimental, "d" son días. (b) Curva de seguimiento del volumen tumoral y (c) sobrevida global de ratones C57BL/6 que fueron inoculados con $1x10^6$ CFU de *Salmonella* LVR01 o PBS (Control) vía intraperitoneal, una semana antes de la implantación de tumor subcutáneo B16F10 ($2,5x10^5$ células). La sobrevida global se siguió hasta el día 30 post–inoculación del tumor (n=12). Resultados representativos de 3 experimentos independientes. El análisis estadístico se realizó entre los 2 grupos (*p < 0,05, ** p < 0,01, *** p < 0,001, t test y log rank, respectivamente).

Para determinar la duración potencial del efecto, se implementó un esquema de pretratamiento con LVR01 administrado un mes antes de la implantación tumoral, observándose un enlentecimiento del crecimiento tumoral en los animales que fueron tratados con LVR01 (Figura 20).

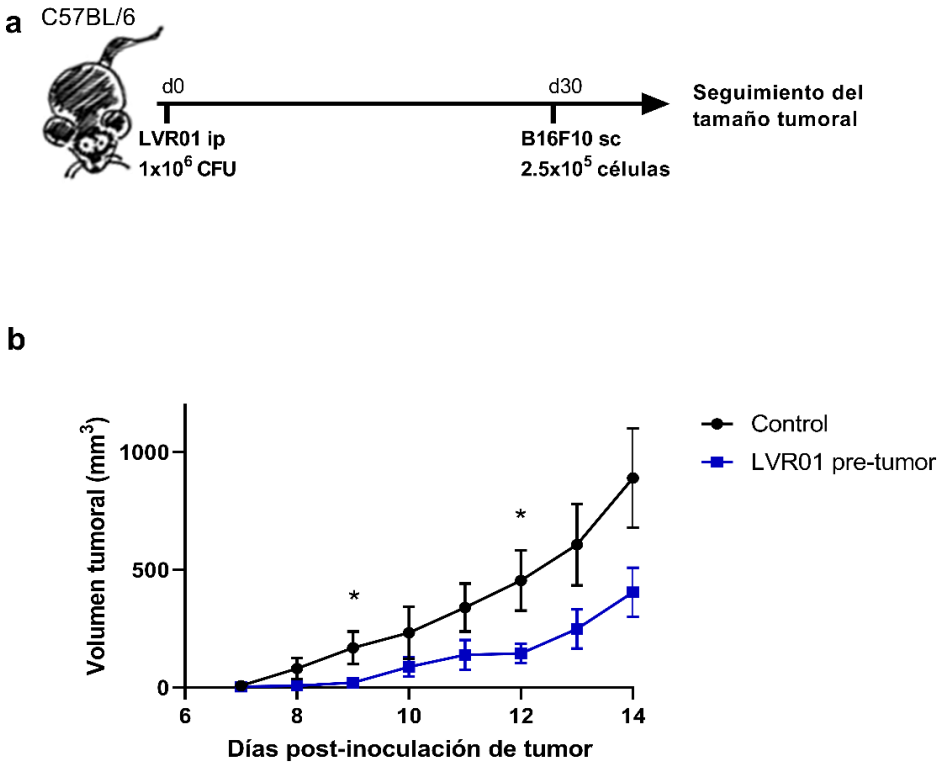


Figura 20 – Uso profiláctico de *Salmonella* retrasa el crecimiento tumoral de ratones portadores de tumores B16F10. (a) Diseño experimental, "d" son días. (b) Curva de seguimiento del volumen tumoral de ratones C57BL/6 que fueron inoculados con $1x10^6$ CFU de *Salmonella* LVR01 o PBS (Control) vía intraperitoneal, un mes antes de la implantación de tumor subcutáneo B16F10 ($2,5x10^5$ células) (n=12). Resultados representativos de 3 experimentos independientes. El análisis estadístico se realizó entre los 2 grupos (*p < 0,05, ** p < 0,01, *** p < 0,001, t test).

Posteriormente, se replicó el protocolo de pretratamiento con *Salmonella* 7 días antes de la implantación de tumor en un modelo de linfoma no Hodgkin (A20). De manera consistente con lo observado en melanoma, los ratones tratados con LVR01 mostraron un retraso en el crecimiento tumoral y una prolongación de la sobrevida (Figura 21).

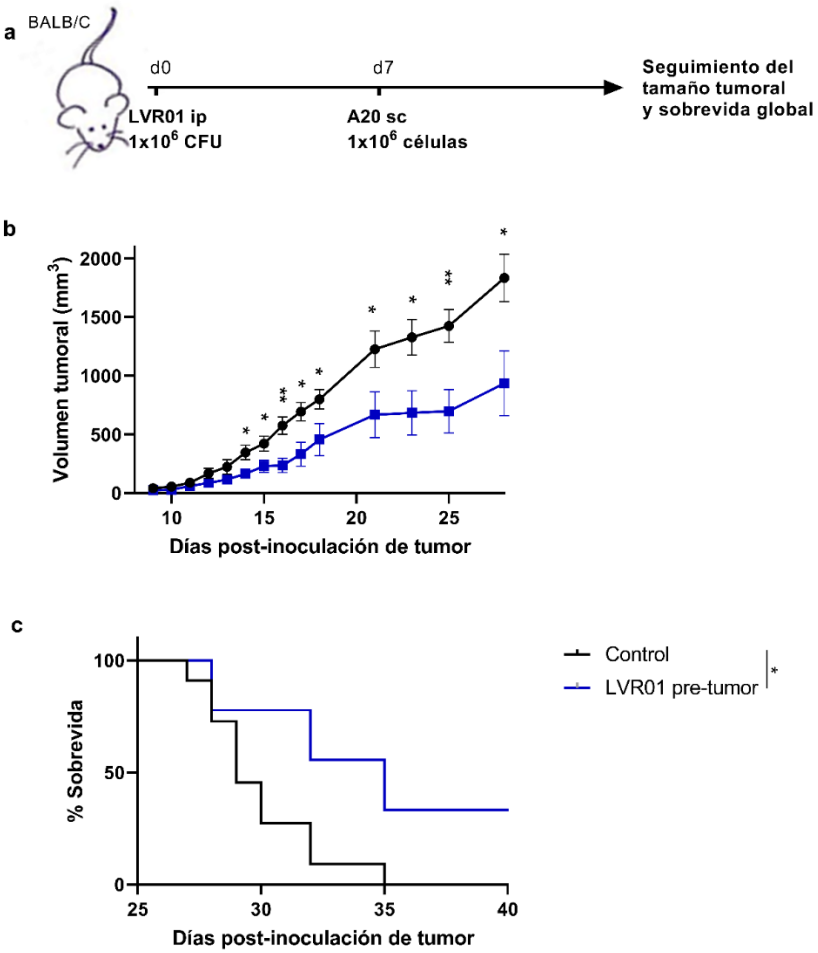


Figura 21 – Uso profiláctico de *Salmonella* retrasa el crecimiento tumoral y prolonga la sobrevida global de ratones portadores de tumores A20. (a) Diseño experimental, "d" son días. (b) Curva de seguimiento del volumen tumoral y (c) sobrevida global de ratones BALB/C que fueron inoculados con 1x10^6 CFU de *Salmonella* LVR01 o PBS (Control) vía intraperitoneal, una semana antes de la implantación de tumor subcutáneo A20 (1x10^6 células). La sobrevida global se siguió hasta el día 40 post-inoculación del tumor (n=12). Resultados representativos de 3 experimentos independientes. El análisis estadístico se realizó entre los 2 grupos (*p < 0,05, ** p < 0,01, *** p < 0,001, t test y log rank, respectivamente).

6.1.3.4 Biodistribución de LVR01 en el modelo de inmunidad entrenada.

Con el objetivo de evaluar la biodistribución de LVR01 en el modelo de inmunidad entrenada, se cuantificó la carga bacteriana en médula ósea y bazo en distintos tiempos post-administración i.p. de LVR01 (Figura 22).

Los resultados mostraron que LVR01 fue detectable tanto en médula ósea como en bazo desde tiempos tempranos post-administración. En médula ósea, la carga bacteriana fue baja en comparación con el bazo y disminuyó progresivamente con el tiempo, hasta resultar indetectable al día 27 post-inoculación. En contraste, el bazo presentó una mayor carga bacteriana a lo largo del ensayo, manteniéndose detectable incluso en los

tiempos más tardíos evaluados, aunque con una disminución progresiva hacia el final del seguimiento.

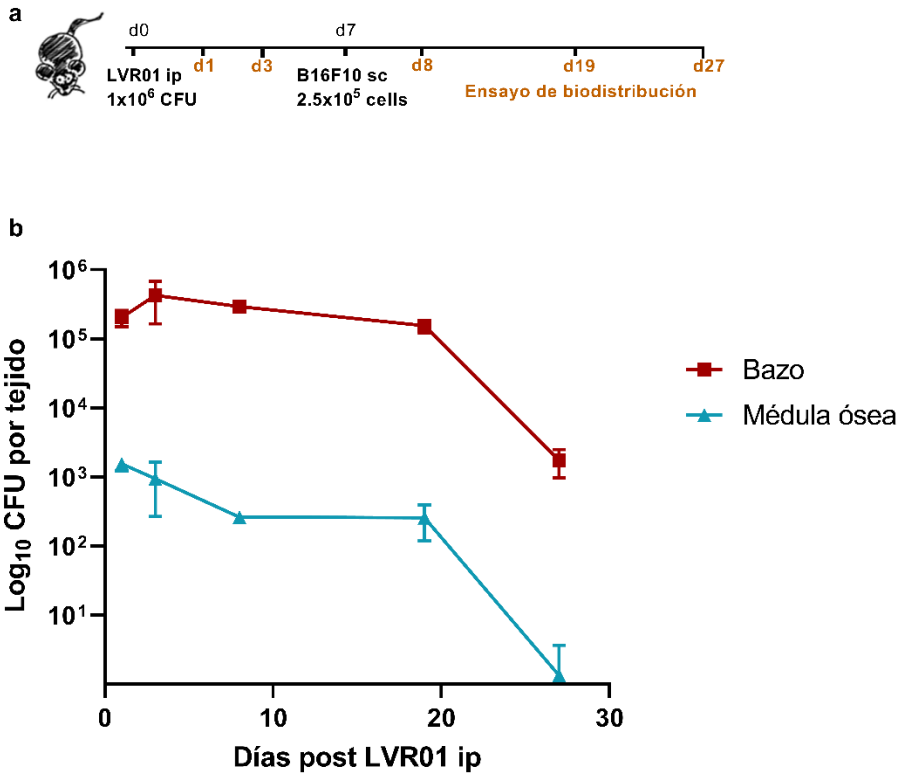


Figura 22 – Biodistribución de *Salmonella* LVR01 en el modelo de inmunidad entrenada. (a) Diseño experimental (b) Cuantificación de *Salmonella* LVR01 en bazo y médula ósea a los días 1, 3, 8, 19 y 27 post-administración (n = 3/grupo/tiempo experimental). La carga bacteriana se determinó mediante recuento de CFU y se expresó como $\log_{10}$ CFU por tejido. Los datos se presentan como media ± SD. Resultados representativos de 2 experimentos independientes.

Estos resultados indican que LVR01 se distribuye a médula ósea y bazo, luego de 27 días resulta indetectable en la médula y en bazo se detecta en menor cantidad. Dado que la médula ósea constituye un compartimento central para procesos asociados a reprogramación hematopoyética y memoria inmune innata, estos hallazgos resultan consistentes con la posibilidad de que la exposición transitoria a LVR01 contribuya al establecimiento de mecanismos asociados a inmunidad entrenada.

6.1.4 Estudio de la respuesta inmune antitumoral en el modelo murino de inmunidad entrenada.

Salmonella LVR01 ha sido ampliamente estudiada como estrategia terapéutica contra el cáncer. Su efecto antitumoral se ha vinculado clásicamente a una fuerte respuesta inflamatoria en el microambiente tumoral (TME), caracterizada por un incremento de citoquinas y quimioquinas proinflamatorias, y por una marcada infiltración de células inmunes, principalmente neutrófilos, macrófagos y células NK, siendo las dos últimas esenciales para el efecto antitumoral (Mónaco & Plata et al., 2022).

Con el fin de determinar si el efecto profiláctico observado en este trabajo está asociado a un mecanismo similar, se evaluó el reclutamiento de células inmunes al tumor. Para

ello, se analizaron tumores de melanoma cuando alcanzaron un tamaño adecuado para su resección (aproximadamente 14 días después de la implantación). El análisis por citometría reveló que no existían diferencias significativas en los porcentajes de células infiltrantes $CD45^+$, $CD11b^+$, $NK1.1^+$ o $CD8^+$ entre el grupo pretratado con LVR01 y el grupo control (Figura 23).

Asimismo, se analizó el perfil transcripcional del TME en el modelo profiláctico (LVR01 pretumor) y se lo comparó con el modelo terapéutico (LVR01 intratumoral). Aunque el pretratamiento con LVR01 indujo la expresión de algunos genes proinflamatorios, la firma inflamatoria fue considerablemente menos marcada que la observada en el tratamiento intratumoral (Figura 23 f). Un comportamiento similar se observó en el modelo de linfoma no Hodgkin A20 evaluado 17 días después de la implantación tumoral (Figura 24).

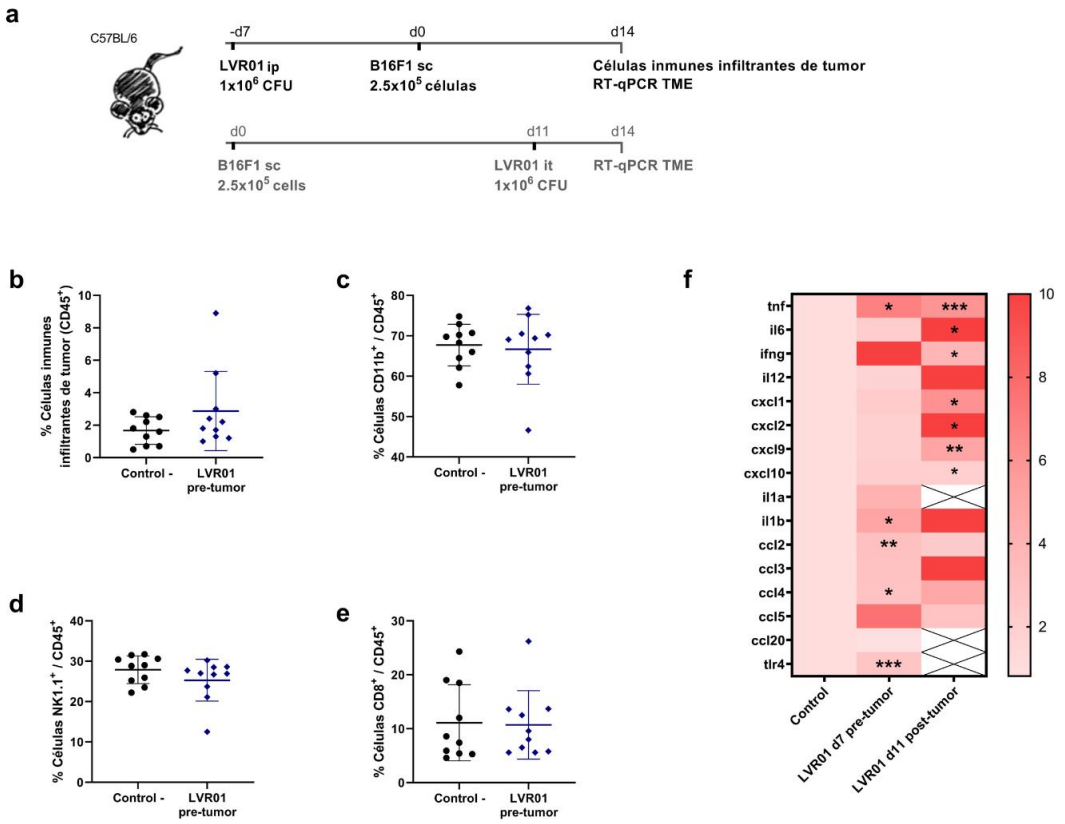


Figura 23 – Microambiente tumoral en ratones pretratados con *Salmonella*. (a) Diseño experimental ("d" indica días). Porcentaje de células (b) CD45+, (c) CD45+CD11b+, (d) CD45+NK1.1+ y (e) CD45+CD8+ presentes en el microambiente tumoral 14 días después de la implantación tumoral, en ratones pretratados con LVR01 o PBS una semana antes de la implantación (n=10). (f) Heatmap que representa el perfil de citoquinas/quimioquinas en ratones pretratados con Salmonella (LVR01 pre-tumor, 7 días antes de la implantación) y tratados (LVR01 intratumoral, 11 días después de la implantación, datos tomados de Mónaco & Plata et al., 2022), normalizado respecto al grupo control sin tratamiento y expresado como Log_2 promedio. La significancia estadística se calculó entre grupos (*p < 0,05, **p < 0,01, ***p < 0,001, t test).

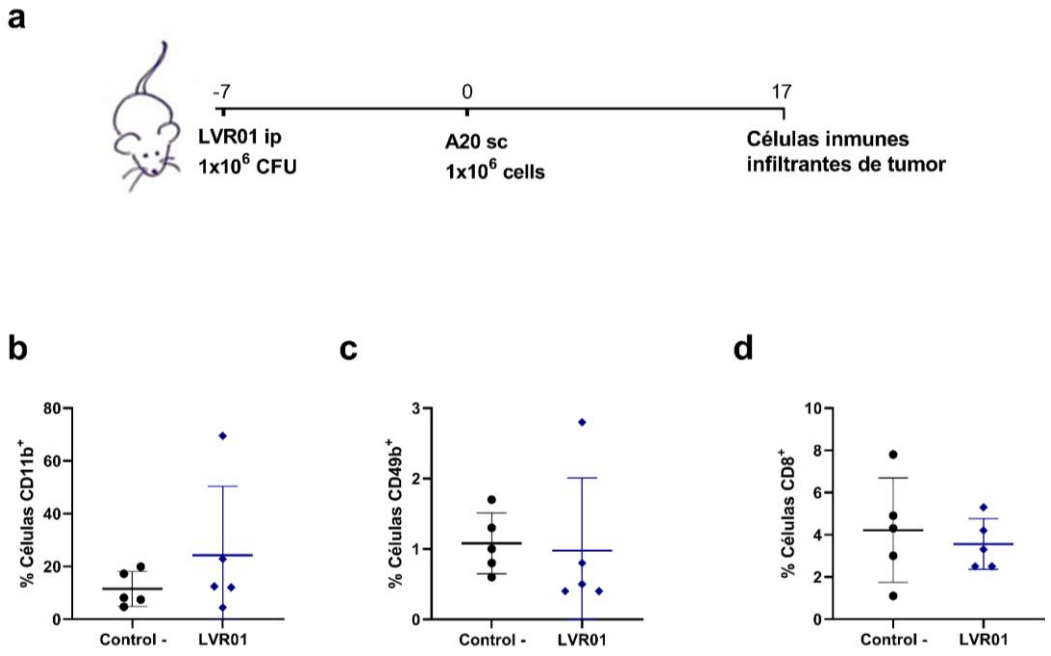


Figura 24 – Células inmunes infiltrantes de tumor en ratones pretratados con *Salmonella*. (a) Esquema experimental ("d" indica días). Porcentaje de células $CD11b^+$ (b), $CD49b^+$ (c) y $CD8^+$ (d) en el microambiente tumoral, 17 días después de la implantación tumoral, evaluado por citometría de flujo en ratones pretratados con LVR01 o PBS una semana antes de la implantación (n = 5). La significancia estadística se calculó entre grupos mediante t test.

Posteriormente, se analizó la cinética de distintas poblaciones celulares en médula ósea y sangre, a posterior del tratamiento con LVR01 y de la implantación de células tumorales. Los ratones fueron tratados i.p. con LVR01 o PBS y, una semana más tarde (d=7), se implantaron células de melanoma B16F10 por vía s.c. Se recolectaron muestras de sangre y médula ósea en los días 3, 6, 9, 22 y 27 posteriores al tratamiento con LVR01 (Figura 25 a).

En la médula ósea, los animales tratados con LVR01 mostraron un rápido aumento en el porcentaje de células $CD45^+$ y, en particular, de células $CD11b^+$ mieloides (Figura 25 b–c). En sangre periférica, el porcentaje total de células $CD45^+$ se mantuvo estable (Figura 25 f), pero las células $CD11b^+$ aumentaron de manera marcada luego del tratamiento con LVR01 (Figura 25 g).

En particular, se registró un incremento sostenido en sangre de células $CD11b^+Ly6G^+$ dentro de la fracción $CD45^+$ después del tratamiento, el cual disminuyó gradualmente con el tiempo (Figura 25 h). Esta misma población también aumentó en la médula ósea, aunque únicamente después de la implantación tumoral (Figura 25 d). En contraste, no se observaron diferencias significativas en la proporción de células $CD49b^+$, tanto en médula como en sangre (Figura 25 e,i).

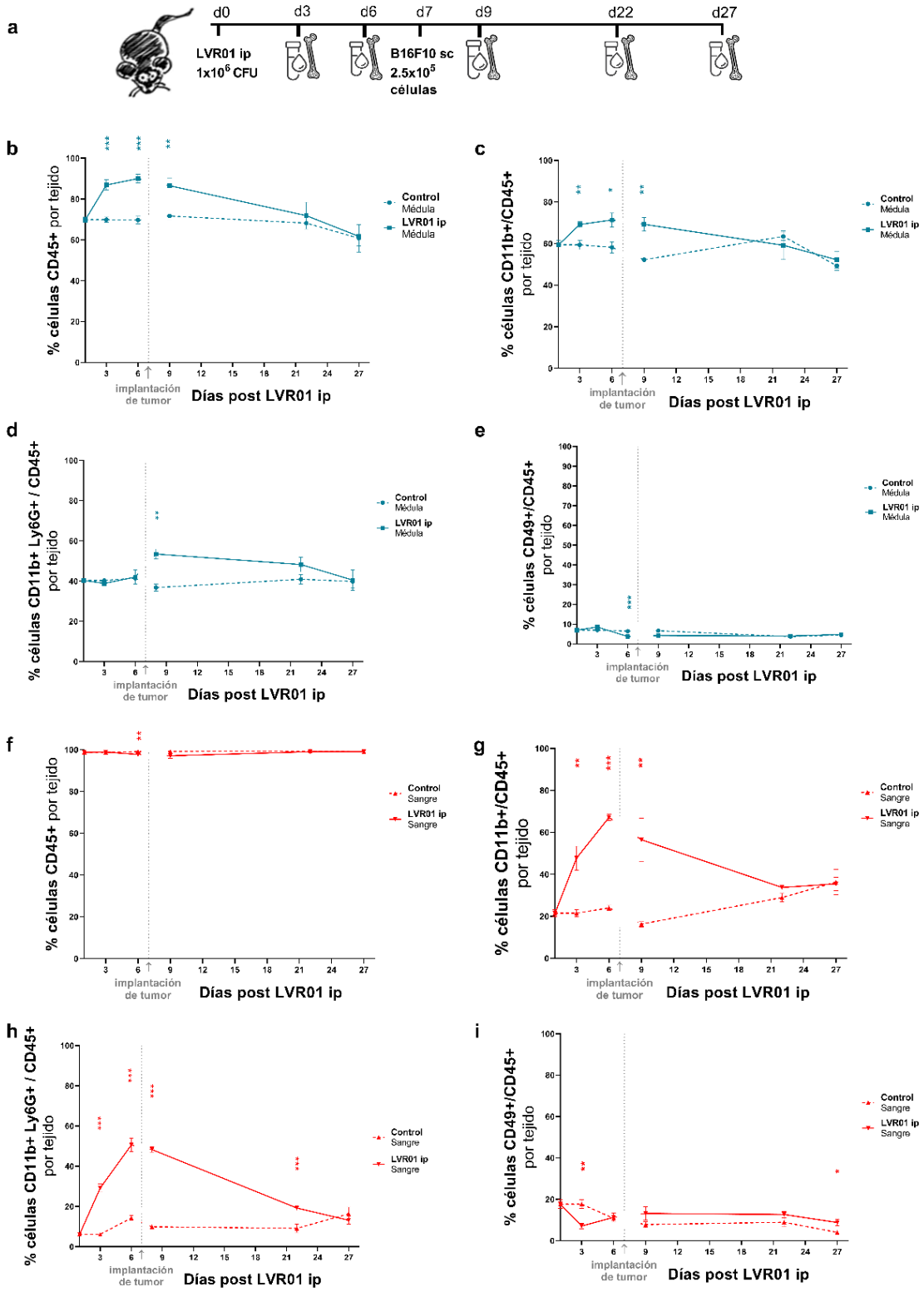


Figura 25 – Cinética de células efectoras inmunes tras la administración de *Salmonella*. (a) Esquema experimental ("d" indica días). Cinética de células $CD45^+$ (b), $CD45^+CD11b^+$ (c), $CD45^+CD11b^+Ly6G^+$ (d) y $CD45^+CD49b^+$ (e) en muestras de médula ósea de ratones pretratados con LVR01 una semana antes de la implantación del tumor B16F10. Cinética de células $CD45^+$ (f), $CD45^+CD11b^+$ (g), $CD45^+CD11b^+Ly6G^+$ (h) y $CD45^+CD49b^+$ (i) en muestras de sangre de ratones pretratados con LVR01 una semana antes de la implantación del tumor B16F10. Resultados representativos de 2 experimentos independientes, n=5/grupo/día. Los datos se presentan como media ± SEM (*p < 0,05, **p < 0,01, ***p < 0,001; t test).

Para profundizar en la caracterización de estas poblaciones, se llevó a cabo un análisis no supervisado mediante t-SNE. Los eventos celulares individuales se exportaron, concatenaron y visualizaron en mapas de calor por condición (Control vs. LVR01) y por tiempo (Figura 26). El análisis permitió identificar distintos clústeres definidos por sus niveles de expresión de marcadores y visualizar cambios temporales en su distribución y representación relativa entre condiciones, evidenciando una dinámica diferencial de las poblaciones inmunes tras el tratamiento con LVR01.

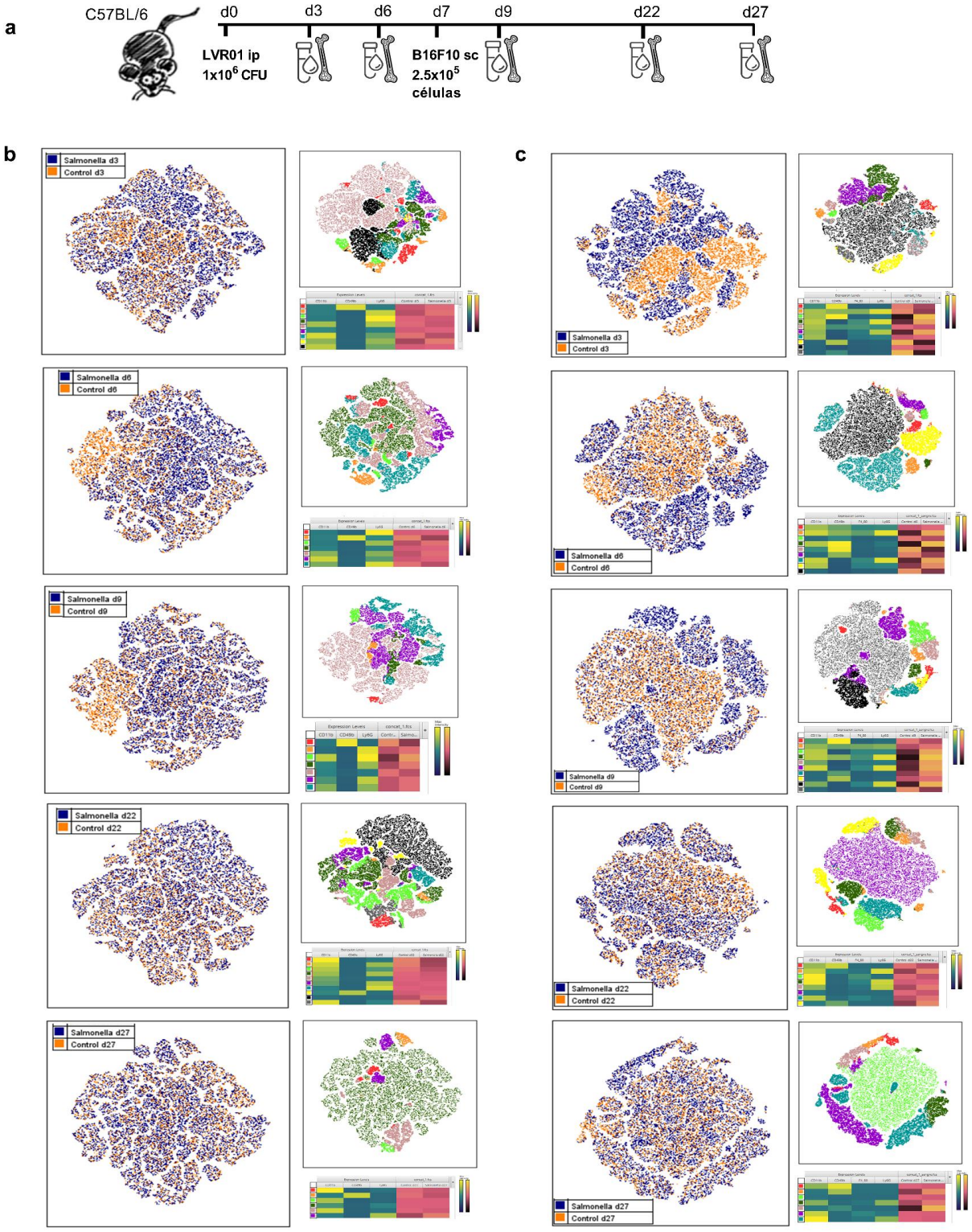


Figura 26 – Cinética de células efectoras inmunes tras la administración de *Salmonella*.

Figura 26 – Cinética de células efectoras inmunes tras la administración de *Salmonella*. (a) Esquema experimental ("d" indica días). Análisis no supervisado de eventos individuales provenientes de los datos de citometría de flujo de (b) médula ósea o (c) sangre, utilizando el algoritmo t-SNE. Se muestran los mapas t-SNE concatenados de médula Control y médula LVR01, o de sangre Control y sangre LVR01, en los diferentes puntos temporales. Los mapas de calor exhiben los niveles de expresión de los marcadores seleccionados sobre los gráficos t-SNE concatenados.

Finalmente, cuando fue posible, se evaluó el porcentaje de células inmunes infiltrantes en tumores (días 22 y 27 post-LVR01). En concordancia con los resultados previos, no se detectaron diferencias entre los grupos tratados con LVR01 y los controles (Figura 27).

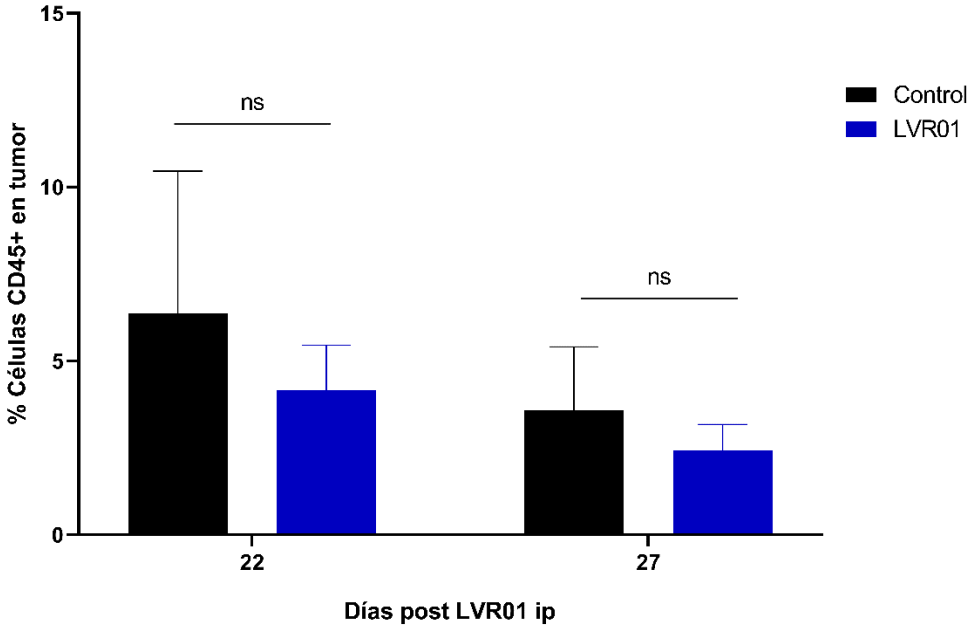


Figura 27 – Células inmunes infiltrantes de tumor en ratones pretratados con *Salmonella*. Porcentaje de células $CD45^+$ en el microambiente tumoral, 15 y 20 días después de la implantación tumoral (d22 y 27, respectivamente), evaluado por citometría de flujo en ratones pretratados con LVR01 una semana antes de la implantación (n = 5). La significancia estadística se calculó entre grupos mediante t test.

6.2 AUTOFAGIA

6.2.1 Evaluación de inducción de autofagia en células tumorales B16F10 por *Salmonella* LVR01.

A continuación, se abordó el segundo aspecto planteado en esta tesis: el estudio de la autofagia en el contexto del efecto antitumoral inducido por *Salmonella* LVR01. Primeramente, se evaluó si *Salmonella* es capaz de inducir autofagia en células tumorales. Para ello, se cultivaron células de melanoma murino B16F10 y se las sometió a distintos tratamientos, como se detalla en Materiales y Métodos: rapamicina durante 3 horas, como control positivo de inducción de autofagia; LVR01 a una MOI 100:1 durante 1 hora; o se mantuvieron sin tratamiento como condición basal. El diseño experimental se basó en antecedentes publicados que describen la capacidad de cepas atenuadas de *Salmonella* para modular la autofagia en células tumorales, y en particular el trabajo de Zhang et al., quienes analizaron este fenómeno utilizando la cepa VNP20009 en células B16F10 (Zhang et al., 2016).

Para evidenciar la inducción de autofagia, se utilizó una sonda fluorescente verde que marca autofagosomas, y se realizó su análisis mediante microscopía confocal y citometría de flujo. En la Figura 28 se muestran las imágenes obtenidas de los cultivos celulares en las diferentes condiciones experimentales: en verde se observan los autofagosomas y en azul los núcleos celulares. Se realizaron 2 réplicas por condición y se tomaron 4 tomas de 4 campos distintos en cada una. Mediante el uso del software Fiji ImageJ se compararon las intensidades de fluorescencia entre las diferentes condiciones, comprobándose que tanto la condición tratada con rapamicina como la condición tratada con LVR01 presentan una tendencia a un aumento de la intensidad de fluorescencia verde en comparación con la condición basal (Figura 29). No se observaron estas tendencias entre las condiciones rapamicina y LVR01. En conjunto, estos resultados sugieren que *Salmonella* LVR01 tiene la capacidad de inducir autofagia en las células B16F10.

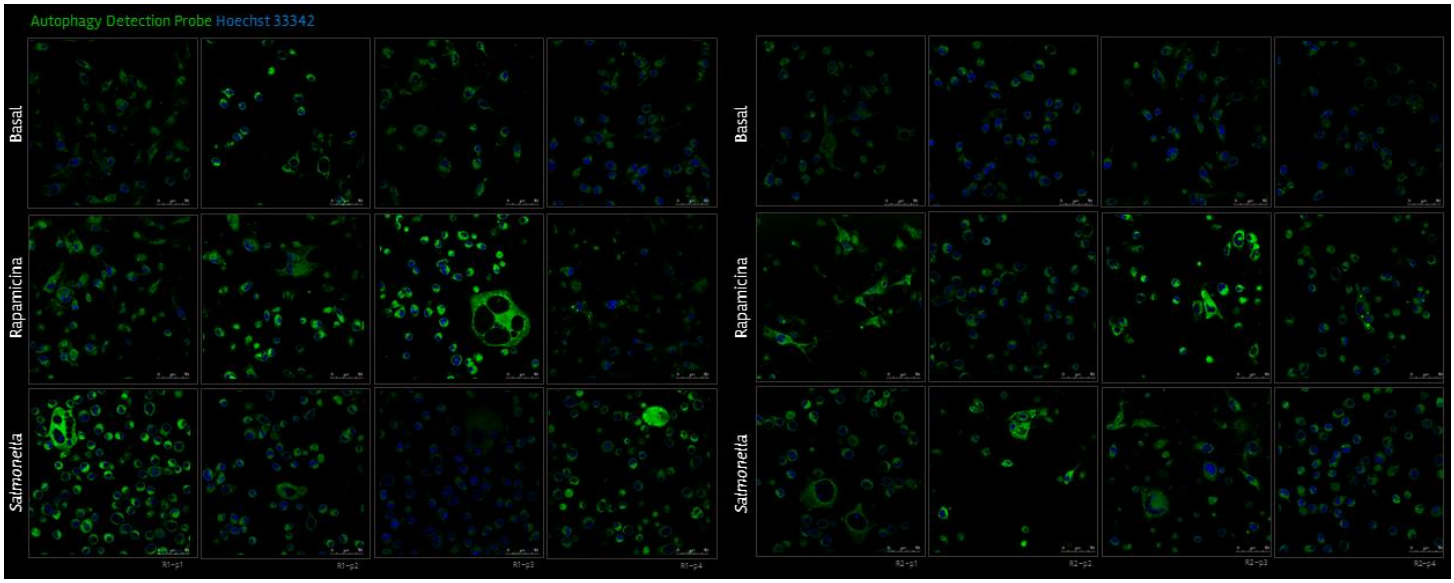


Figura 28 – Inducción de autofagia en células B16F10 evaluada por microscopía confocal. Imágenes representativas de cultivos celulares de melanoma murino B16F10 en distintas condiciones

experimentales (basal, rapamicina y *Salmonella* LVR01). En verde se visualizan los autofagosomas (Autophagy Detection Probe), mientras que en azul se observan los núcleos celulares (Hoechst 33342).

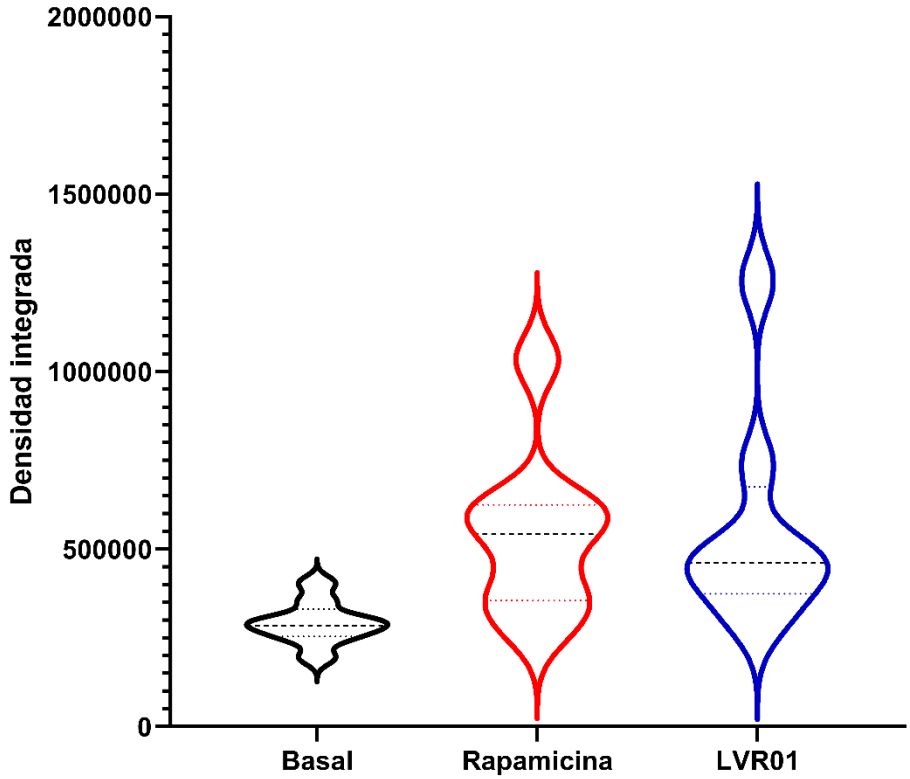


Figura 29 – Cuantificación de la señal autofágica por microscopía confocal. Análisis de la densidad integrada de fluorescencia verde correspondiente a los autofagosomas en células B16F10 para las distintas condiciones experimentales (basal, rapamicina y *Salmonella* LVR01), realizado a partir de las imágenes obtenidas por microscopía confocal y analizadas con el software Fiji ImageJ. Se realizaron 2 réplicas por condición y se tomaron 4 tomas de 4 campos distintos en cada una.

Posteriormente, se realizó un ensayo de Western blot, en condiciones reductoras y desnaturalizantes, utilizando anticuerpos anti-LC3 (ATG8) y anti-ATG5 con el objetivo de evaluar la presencia de autofagia en células B16F10 bajo distintas condiciones experimentales (basal, rapamicina, LVR01, LVR01 + cloroquina, y LVR01 + 3-MA). Pese a los intentos realizados, no se pudieron observar bandas correspondientes a LC3 ni en la fracción soluble ni en la fracción insoluble en ninguna de las condiciones analizadas. En cuanto a ATG5, se detectó una banda correspondiente al complejo ATG5–ATG12, en concordancia con lo descrito en la hoja de datos del anticuerpo utilizado (Figura 30). Se desestimó el uso de estos datos para evaluar la inducción de autofagia, dado que está descrito que la expresión del complejo ATG5–ATG12 no varía en condiciones de presencia o ausencia de autofagia.

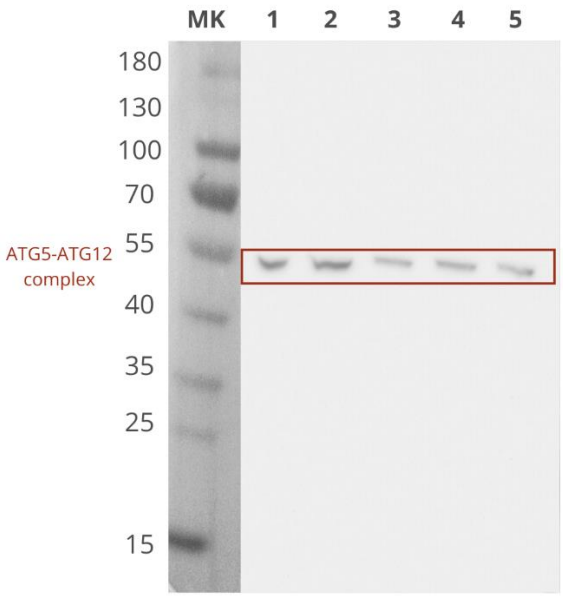


Figura 30 – Análisis de ATG5 por Western blot en células B16F10. Western blot revelado con anticuerpo anti-ATG5 en cultivos celulares de melanoma murino B16F10 bajo las distintas condiciones experimentales. En todos los carriles se observa una banda correspondiente al complejo ATG5–ATG12, indicada en la imagen. De izquierda a derecha se muestran: MK (marcador de peso molecular), 1 (basal), 2 (rapamicina), 3 (LVR01), 4 (LVR01 + cloroquina) y 5 (LVR01 + 3-MA).

6.2.2 Evaluación de la muerte celular inducida por LVR01 en combinación con inhibidores de la autofagia *in vitro*

Para evaluar el efecto que tiene la combinación de inhibidores de autofagia con *Salmonella* LVR01 se pretrataron células B16F10 con inhibidores de la autofagia, cloroquina y 3-MA, y luego se infectaron a una MOI 100:1. Reportes previos de otros grupos indican que la combinación de *Salmonella* atenuada con cloroquina incrementa la capacidad de eliminar células tumorales de la bacteria *in vitro* (Zhang et al 2016). En estos ensayos el readout se realiza por citometría de flujo, basándonos en estos estudios es que nos propusimos evaluar este efecto con la misma técnica. Luego de 1 hora o 20 horas post infección se evaluó utilizando ioduro de propidio el porcentaje de células muertas en las condiciones evaluadas y se analizó el cambio relativo normalizado con la condición basal. A la hora post infección con LVR01 no se observa una diferencia en la inducción de muerte celular entre las condiciones. Luego de 20 horas post infección se observa que los grupos que contienen *Salmonella* presentan una mayor muerte celular, pero no se observan diferencias significativas entre ellas. En las células tratadas con cloroquina y *Salmonella*, se puede observar una tendencia a una mayor muerte celular que en el resto de los grupos (Figura 31).

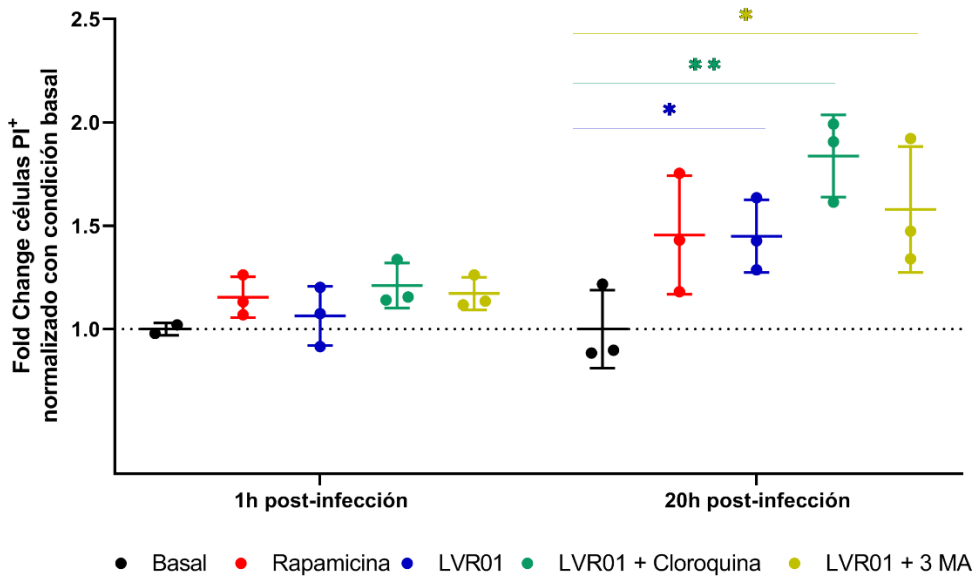


Figura 31 – Muerte celular inducida por LVR01 en combinación con inhibidores de la autofagia *in vitro*. Células B16F10 se cultivaron e incubaron por 3 horas con moduladores de la autofagia: rapamicina (1 µM), cloroquina (10 µM), 3-MA (3 µM) o con medio (control sin modulador). Se infectaron con LVR01 a una MOI de 100:1 durante 1 hora o 20 horas (agregando gentamicina al medio a la hora de infección). Se recuperaron células y sobrenadante de las muestras (n=3), se tiñieron con PI (ioduro de propidio) y se adquirieron eventos en citómetro de flujo. Datos representados como cambio relativo (*fold change*) normalizado con condición basal (control sin modulador) y mostrado como media ± SD (*p < 0,05, **p < 0,01, t test).

6.2.3 Evaluación del efecto antitumoral de LVR01 en combinación con inhibidores de la autofagia *in vivo*.

Con el objetivo de evaluar el impacto de la inhibición de la autofagia sobre el efecto antitumoral de *Salmonella* LVR01, se analizaron dos aproximaciones experimentales *in vivo*: el clásico tratamiento intratumoral con LVR01 en tumores establecidos y el esquema utilizado en esta tesis de pretratamiento con LVR01 previo a la implantación tumoral (inmunidad entrenada), en presencia o ausencia de cloroquina.

En el primer enfoque experimental, se implantaron tumores B16F10 por vía s.c. en ratones C57BL/6 y se administró cloroquina diariamente desde el día 6 hasta el día 15 post implantación tumoral. Al día 8 post implantación, los animales recibieron una única administración i.t. de LVR01 o PBS. El crecimiento tumoral fue monitoreado mediante mediciones periódicas del volumen tumoral. El análisis de las curvas de crecimiento tumoral mostró que los grupos tratados únicamente con cloroquina presentaron un comportamiento similar al del grupo control, sin observarse diferencias significativas en el crecimiento tumoral. En contraste, los animales tratados con LVR01 evidenciaron un efecto antitumoral en comparación con los grupos control y cloroquina. Sin embargo, la combinación de LVR01 con cloroquina no mostró diferencias en el control tumoral respecto al grupo tratado únicamente con LVR01 (Figura 32).

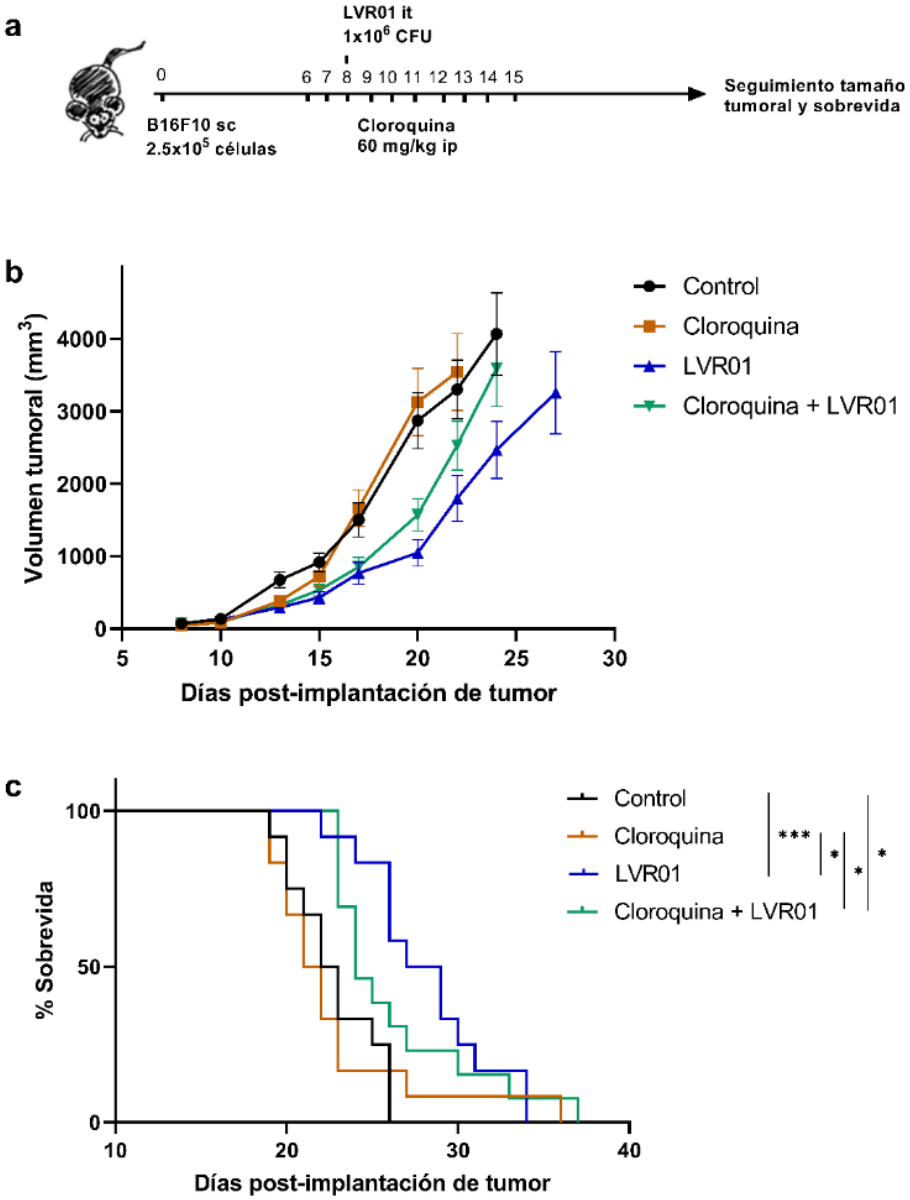


Figura 32 – Tratamiento con *Salmonella* en combinación con cloroquina en ratones portadores de tumores B16F10. (a) Diseño experimental. (b) Curva de seguimiento del volumen tumoral y (c) sobrevida global de ratones C57BL/6. La sobrevida global se siguió hasta el día 37 post-inoculación del tumor (n=12). El análisis estadístico se realizó entre los grupos (*p < 0,05, *** p < 0,001 log rank).

En el segundo enfoque experimental, orientado a evaluar el impacto de la inhibición de la autofagia en un modelo *in vivo* de inmunidad entrenada, los animales fueron tratados con cloroquina durante una semana y recibieron *Salmonella* LVR01 o PBS por vía intraperitoneal al segundo día de tratamiento. Posteriormente, al octavo día post inicio del tratamiento con cloroquina, se implantaron tumores B16F10 y se realizó el seguimiento tumoral según el esquema previamente descrito. De manera similar a lo observado en el modelo de tratamiento intratumoral, los grupos tratados con cloroquina no mostraron diferencias en el crecimiento tumoral en comparación con el grupo control. El grupo pretratado con LVR01 presentó un efecto antitumoral, mientras

que la combinación de LVR01 con cloroquina no modificó dicho efecto en relación con el tratamiento con LVR01 solo (Figura 33).

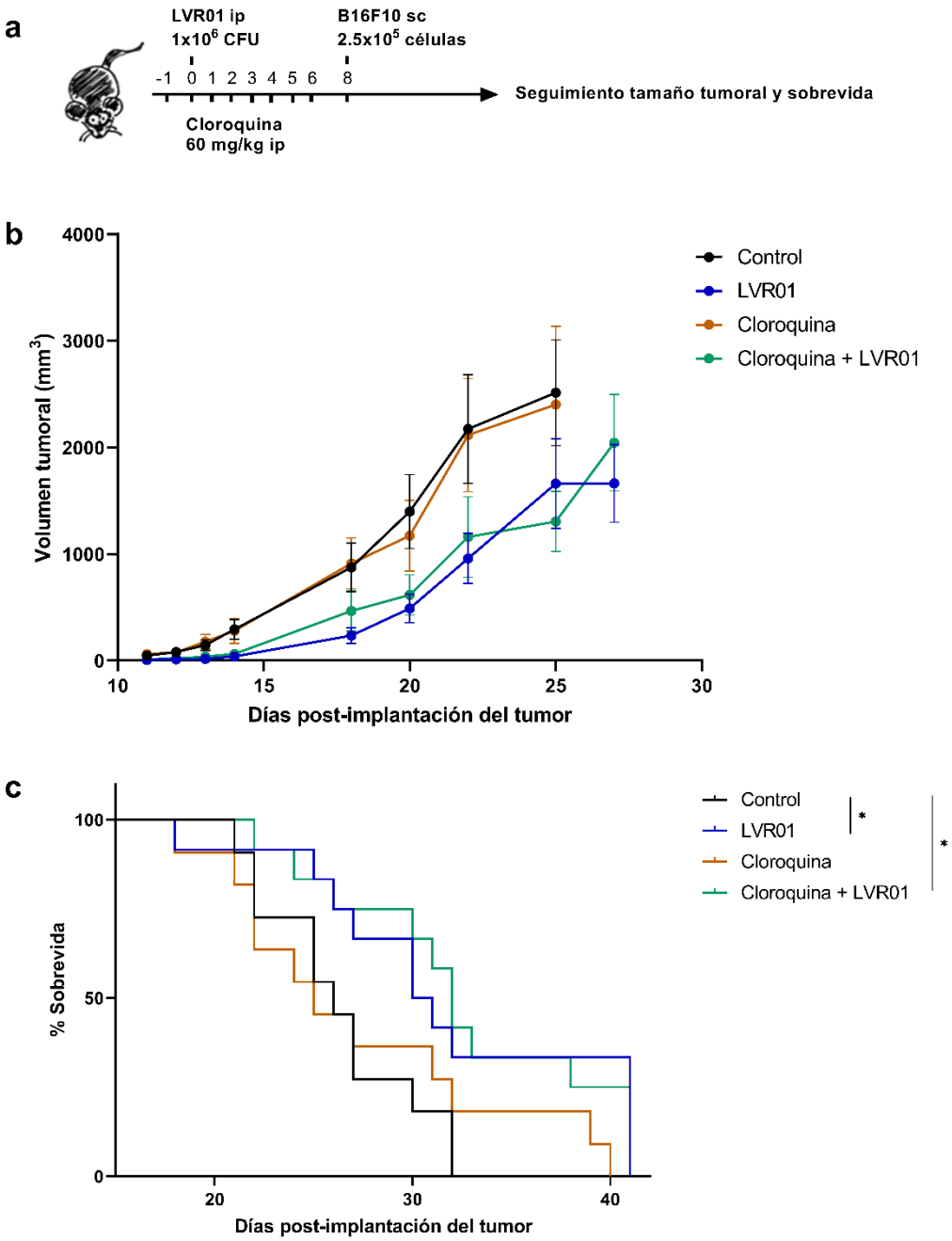


Figura 33 – Uso profiláctico de *Salmonella* en combinación con cloroquina en ratones portadores de tumores B16F10. (a) Diseño experimental. (b) Curva de seguimiento del volumen tumoral y (c) sobrevida global de ratones C57BL/6. La sobrevida global se siguió hasta el día 41 post-inoculación del tumor (n=12). El análisis estadístico se realizó entre los grupos (*p < 0,05, ** p < 0,01 log rank).

En conjunto, estos resultados indican que el efecto antitumoral observado en ambos modelos experimentales se asocia a la acción de *Salmonella* LVR01, sin evidenciarse un claro impacto adicional de la inhibición de la autofagia mediante cloroquina en las condiciones evaluadas.

Cabe destacar que ambos modelos experimentales evalúan contextos biológicos diferentes. Mientras que en el modelo profiláctico la inhibición de la autofagia ocurre durante la etapa de inducción de memoria inmune innata previa al desafío tumoral y no modifica el efecto protector inducido por LVR01, en el modelo de tratamiento intratumoral se observa una tendencia a una disminución del efecto antitumoral de *Salmonella* en presencia de cloroquina.

7. DISCUSIÓN Y CONCLUSIONES GENERALES

7.1 INMUNIDAD ENTRENADA

La hipótesis de este trabajo planteó que *Salmonella* LVR01 podría inducir fenómenos de memoria inmune innata, particularmente inmunidad entrenada, y que esta reprogramación funcional contribuiría al efecto antitumoral previamente descrito para esta bacteria atenuada. Con este objetivo, se investigó la capacidad de LVR01 de modular respuestas de memoria innata en distintos compartimentos inmunológicos humanos y murinos. Nuestros resultados muestran que LVR01 ejerce efectos diferenciales dependiendo del contexto experimental y del compartimento inmune evaluado. En primer lugar, se observó un efecto tolerogénico, dependiente de la dosis, al tratar monocitos humanos adherentes derivados de sangre periférica con LVR01 (Figuras 11–13). Grandes cantidades de LPS inducen parálisis inmune o tolerancia a la endotoxina en células inmunes (Li et al., 2023; Novakovic et al., 2016). Algunos de los mecanismos subyacentes a este efecto tolerante en monocitos humanos incluyen la reprogramación metabólica y modificaciones epigenéticas caracterizadas por el silenciamiento selectivo y transitorio de genes proinflamatorios (Domínguez–Andrés et al., 2019a). Encontramos que LVR01 induce fuertemente a los monocitos a producir citoquinas proinflamatorias durante las primeras 24 horas posteriores a la estimulación (Figura 11 a–e; Figura 13 a–d). Sin embargo, tras un período de reposo, estas células desarrollaron una respuesta inmune tolerante sin capacidad de responder tras un reestímulo (Figura 11 g–h; Figura 12; Figura 13 e–f). En contraste, el lisado de *Leishmania*, descritos como promotor de inmunidad entrenada, indujo un aumento en la producción de citoquinas proinflamatorias tras la reestimulación con LPS.

La inmunidad entrenada se asocia a una profunda reprogramación metabólica que permite sostener el incremento de los requerimientos energéticos y biosintéticos de células con mayor capacidad funcional y de respuesta (dos Santos et al., 2024). Asimismo, metabolitos como fumarato e itaconato cumplen un rol central en la regulación de este proceso; mientras el fumarato ha sido vinculado a la inducción de inmunidad entrenada, el itaconato se asocia a mecanismos regulatorios capaces de limitar este fenotipo (Cai et al., 2025; Domínguez–Andrés et al., 2019a; dos Santos et al., 2024). Además, células con un perfil entrenado exhiben una mayor producción de lactato, reflejando esta reprogramación metabólica. En este trabajo evaluamos este parámetro mediante la cuantificación de lactacto en sobrenadante seis días después del estímulo inicial y observamos que, en el grupo entrenado, tratado con lisados de *Leishmania*, hay un aumento de la producción de lactato en comparación con los grupos tratados con *Salmonella* y el grupo control (Figura 11f). Cuando evaluamos la capacidad de LVR01 de inducir inmunidad entrenada *in vitro* en células mieloides derivadas de médula ósea de ratón, observamos el mismo efecto tolerante que describimos anteriormente (Figura 14).

La tolerancia inmune innata probablemente haya evolucionado como un mecanismo protector destinado a limitar la inflamación excesiva y prevenir el daño tisular asociado. Esta respuesta adaptativa restringe la exposición del hospedador a señales inflamatorias prolongadas, contribuyendo al mantenimiento de la integridad tisular y a la homeostasis (Butcher et al., 2018; Cavaillon & Adib–Conquy, 2006). Desde el punto de vista fisiológico, la tolerancia innata cumple un rol central en el control de la respuesta inflamatoria, disminuyendo el riesgo de daño tisular provocado por la producción sostenida de citoquinas proinflamatorias (Butcher et al., 2018). La exposición repetida a PAMPs, como el LPS,

conduce al establecimiento de macrófagos con un fenotipo tolerante, caracterizado por una menor secreción de citoquinas proinflamatorias y una mayor producción de mediadores antiinflamatorios (Biswas & Lopez-Collazo, 2009).

La tolerancia a endotoxinas puede impactar de manera crítica en la progresión del cáncer mediante la reprogramación de las células del microambiente tumoral, conduciendo al desarrollo de un fenotipo inmunosupresor que favorece el crecimiento tumoral. Estas células tolerizadas contribuyen de forma significativa a la generación de un microambiente tumoral permisivo, caracterizado por una mayor viabilidad, proliferación y capacidad metastásica de las células tumorales (Roy et al., 2023; Silva et al., 2023). Hay evidencia de que el estado de parálisis inmune inducido por LPS en las células puede ser revertido con el uso de β-glucano, inductor de inmunidad entrenada. En estos trabajos se identifica al itaconato como regulador central entre el estado de tolerancia e inmunidad entrenada, lo que lo convierte en un blanco terapéutico prometedor (Domínguez-Andrés et al., 2019b). Es necesario profundizar en futuros estudios sobre la reprogramación metabólica que provoca *Salmonella* en las células inmunes, para evaluar si esta estrategia funcionara para revertir el estado de tolerancia. También sería interesante generar mutantes de *Salmonella* con baja o nula expresión de LPS y evaluar si este efecto se mantiene o se pierde.

En nuestro estudio observamos la inducción de tolerancia en monocitos periféricos de individuos o animales sin tumor, por lo que no evaluamos directamente la reprogramación a nivel del microambiente tumoral. Sin embargo, es razonable hipotetizar que procesos similares podrían estar ocurriendo, dado que el efecto de *Salmonella* como inmunoterapia es transitorio. Estudios previos han demostrado que el tratamiento con LVR01 induce un rápido reclutamiento de macrófagos M1 al microambiente tumoral, pero posteriormente los macrófagos asociados a tumor (TAM, del inglés *tumor associated macrophages*) van cambiando paulatinamente el fenotipo desde un estado M1 hacia un perfil M2 (Mónaco et al., 2022).

Una limitación de nuestro estudio *in vitro* es que nos enfocamos en una única población de la inmunidad innata. Sin embargo, se ha reportado que la inmunidad entrenada puede inducirse en múltiples tipos de células mieloides mononucleares, incluyendo monocitos, macrófagos, células dendríticas y neutrófilos, así como también en células linfoides, tales como las células NK y otras células linfoides innatas (Li et al., 2025; Vuscan et al., 2024). Por esto, consideramos fundamental evaluar el efecto de la exposición a *Salmonella* LVR01 *in vivo*, donde la complejidad del organismo, los mecanismos compensatorios y la interacción entre múltiples poblaciones de la inmunidad innata pueden modificar sustancialmente la respuesta.

En este contexto, demostramos que los ratones tratados con LVR01 presentan un aumento significativo en la producción de citoquinas proinflamatorias en suero tras la exposición a LPS en comparación a ratones control (Figura 15). Este mismo efecto lo observamos en las células de médula ósea de animales pretratados *in vivo* tras la exposición a LPS *ex vivo* (Figura 16). Además, identificamos que los principales productores de TNF fueron células derivadas del linaje mieloide $CD11b^{+}$ $Ly6C^{high}$ (Figura 16 f). Estos resultados sugieren que LVR01 podría modificar la respuesta inmune central frente a un estímulo secundario, mostrando características compatibles con una respuesta de inmunidad entrenada. Sin embargo, luego de permitir que los cultivos celulares reposaran durante seis días y posteriormente exponer a LPS a la población adherente enriquecida en monocitos, estas células exhibieron una

respuesta tolerante, concomitantemente con la desaparición de la población CD11b^{+}Ly6C^{high} ya no está (Figura 16 h–l).

Las células CD11b^{+}Ly6C^{high} corresponden principalmente a monocitos inflamatorios, una subpoblación del compartimento mieloide caracterizada por una alta expresión de Ly6C, elevada producción de citoquinas proinflamatorias y un rol clave en la respuesta inmune innata temprana y en procesos inflamatorios sistémicos (Shi & Pamer, 2011). Sin embargo, estudios recientes han demostrado que la población CD11b^{+}Ly6C^{high} es altamente heterogénea y sufre una profunda reprogramación funcional tras estímulos infecciosos sistémicos, incluyendo la adquisición de estados inmunosupresores y metabólicamente adaptados a largo plazo. En este contexto, las diferencias en la capacidad de respuesta proinflamatoria observadas en nuestro modelo *ex vivo* podrían reflejar dinámicas de reprogramación funcional compatibles con lo descrito para poblaciones mieloides expuestas a estímulos infecciosos sistémicos (Watanabe et al., 2024).

Estudios preliminares de biodistribución muestran que *Salmonella* LVR01 alcanza la médula ósea en bajas cantidades (Figura 22). Considerando esto, es posible hipotetizar que la bacteria podría inducir algún grado de remodelación central del sistema inmune, potencialmente a través de la reprogramación de células madre y progenitoras hematopoyéticas, dando lugar a la generación de células mieloides con un fenotipo funcionalmente modificado. Esta hipótesis se apoya en evidencia previa obtenida con otros modelos de inmunoterapia basados en inmunidad entrenada, en particular el modelo de BCG, en el cual estímulos microbianos han sido asociados a cambios duraderos a nivel del compartimento hematopoyético central (Chronopoulos et al., 2025).

Otro hallazgo relevante en el modelo de reestimulación *ex vivo* fue el aumento de Galectina–1 en los sobrenadantes de cultivos celulares derivados de animales tratados con *Salmonella* LVR01, independientemente de la reestimulación con LPS o RPMI (Figura 18). Dado el rol inmunomodulador previamente descrito para Galectina–1 y su asociación con mecanismos de regulación de la respuesta inflamatoria y tolerancia inmune (Rabinovich & Croci, 2012; Yu et al., 2023), el aumento de Galectina–1 observado en nuestro modelo podría contribuir, al menos en parte, al fenotipo tolerante detectado en etapas tardías en células mieloides derivadas de médula ósea tras el tratamiento con LVR01.

Trabajos previos demostraron que la inmunidad entrenada inducida por β–glucano promueve actividad antitumoral en modelos preclínicos (Kalafati et al., 2020). En línea con estos resultados, cuando los animales fueron pretratados con *Salmonella* LVR01, se observó un retraso en el crecimiento tumoral y una mayor sobrevida global, en dos modelos tumorales diferentes (Figura 19, 21). Este efecto también se mantuvo incluso cuando los ratones fueron pretratados con LVR01 un mes antes de la implantación tumoral (Figura 20).

Llamativamente, el efecto antitumoral observado en este modelo no estuvo acompañado por los cambios típicamente descritos para la administración terapéutica intratumoral de *Salmonella* LVR01, particularmente un marcado aumento de la infiltración de células inmunes o un perfil inflamatorio exacerbado en el microambiente tumoral al momento evaluado (Figura 23–24, 27). Hasta el momento, el efecto antitumoral de las terapias basadas en *Salmonella* LVR01 se ha relacionado principalmente con la capacidad de la bacteria de inducir una fuerte respuesta inflamatoria en el microambiente tumoral, caracterizada por un aumento significativo de citoquinas y quimioquinas proinflamatorias, acompañado por la infiltración de células inmunes, en particular neutrófilos, macrófagos y

células NK (Grille et al., 2014; Mónaco et al., 2022; Mónaco & Plata et al., 2022). Sin embargo, debe considerarse que las determinaciones realizadas en el modelo profiláctico corresponden a tiempos alejados del estímulo inicial, por lo que cambios tempranos relevantes podrían no haber sido detectados. Además, al tratarse de modelos terapéuticos diferentes podrían involucrar mecanismos distintos en el efecto antitumoral observado.

En el contexto de la inmunidad entrenada y de la respuesta antitumoral, se ha demostrado que los neutrófilos y los progenitores granulopoyéticos, más que los monocitos, constituyen los principales efectores celulares (Kalafati et al., 2022, 2020). Análogamente, tras el tratamiento con LVR01 observamos un aumento de células mieloides en sangre y médula ósea, lo cual es razonable dado que se administran bacterias atenuadas que causan una infección controlada en los animales (Figura 25–26). En este análisis, el comportamiento de la población $CD11b^{+}Ly6G^{+}$ en médula ósea llamó particularmente nuestra atención, ya que su frecuencia aumentó significativamente tras el estímulo de la implantación tumoral.

Estos resultados son consistentes con la hipótesis de que las células entrenadas podrían potenciar respuestas citotóxicas leucocitarias: luego de la muerte de células tumorales, se liberan DAMPs que pueden actuar como un segundo estímulo para las células entrenadas, amplificando el efecto antitumoral (van Puffelen et al., 2020). En este sentido, la implantación tumoral podría constituir una señal adicional capaz de modular la granulopoyesis en médula ósea, reflejada en un aumento del porcentaje de neutrófilos y de sus progenitores. No obstante, el rol específico de los neutrófilos en nuestro modelo tumoral utilizando LVR01 como inmunoterapia no pudo ser demostrado directamente debido a limitaciones experimentales, incluyendo la dificultad de depletar selectivamente neutrófilos sin afectar otras células inmunes, y la imposibilidad de mantener dicha depleción en el tiempo, dado su rápido recambio y la expansión compensatoria tras la depleción (Mónaco & Plata et al., 2022).

En conjunto, nuestros resultados muestran que la administración de *Salmonella* viva atenuada induce una impronta inmunológica caracterizada por dos comportamientos contrapuestos que, no obstante, culminan en una actividad antitumoral detectable y sostenida al menos durante un mes tras la administración. De manera notable, esta actividad antitumoral se desarrolla en ausencia de una marcada infiltración de células inmunes y de inflamación en el microambiente tumoral, lo que sugiere la existencia de un mecanismo alternativo, hasta ahora no descrito, para el efecto antitumoral de *Salmonella*. El hecho de que el efecto antitumoral de *Salmonella* persista incluso cuando los tumores se implantan un mes después del tratamiento respalda la hipótesis de la inducción de alteraciones inmunológicas de larga duración y sugiere que el efecto antitumoral observado no depende del efecto directo de *Salmonella* en el TME.

Durante la inducción de inmunidad entrenada central vías metabólicas importantes de los progenitores hematopoyéticos aumentan su actividad, mientras se dan modificaciones epigenéticas y se remodela la cromatina dejando disponibles para expresarse genes involucrados en la inflamación y diferenciación de células mieloides (Vuscan et al., 2025). Por ejemplo en el trabajo de Kalafati demuestran que la administración de β-glucano modifica los progenitores de granulocitos y macrófagos a un perfil que expresa más IFN I, que promueve un aumento en la actividad antitumoral de los neutrófilos entrenados (Kalafati et al., 2020).

Con los ensayos realizados en este trabajo no contamos con evidencia suficiente para confirmar de manera directa estos mecanismos, por lo que nos mantenemos en un marco estrictamente hipotético. Para evaluar de forma concluyente un posible efecto de remodelación central inducido por *Salmonella* y su contribución a la respuesta antitumoral, sería necesario implementar abordajes experimentales adicionales, como ensayos de trasplante de médula ósea, que permitan determinar si los progenitores hematopoyéticos condicionados confieren al hospedador una mayor capacidad antitumoral. En este sentido, Priem y colaboradores desarrollaron un tratamiento frente al cáncer basado en un nanobiológico con capacidad de inducir inmunidad entrenada central, y demostraron mediante un trasplante de médula ósea que la actividad antitumoral se podía transferir a animales naive portadores de tumores (Priem et al., 2020). Más recientemente, se demostró que la inmunoterapia con BCG induce inmunidad entrenada central y que la reprogramación de los progenitores hematopoyéticos inducida por esta terapia es suficiente para conferir una mayor capacidad antitumoral. Mediante ensayos de trasplante de médula ósea, los autores demostraron que esta programación en los progenitores puede transferirse a animales receptores, lo que se traduce en una remodelación del TME caracterizada por un incremento en la producción e infiltración de neutrófilos, monocitos y células dendríticas (Daman et al., 2025). Esta remodelación central puede deberse tanto al efecto directo del estímulo sobre las células de la médula ósea como al efecto indirecto mediado por moduladores proinflamatorios producidos durante la respuesta inflamatoria sistémica desencadenada por dicho estímulo (Chavakis et al., 2019).

En este marco, hipotetizamos que *Salmonella* LVR01 es capaz de inducir cambios centrales beneficiosos para la respuesta inmune antitumoral, al tiempo que promueve mecanismos de tolerancia periférica, lo cual podría contribuir a explicar el carácter transitorio del efecto terapéutico observado en modelos preclínicos (Figura 34).

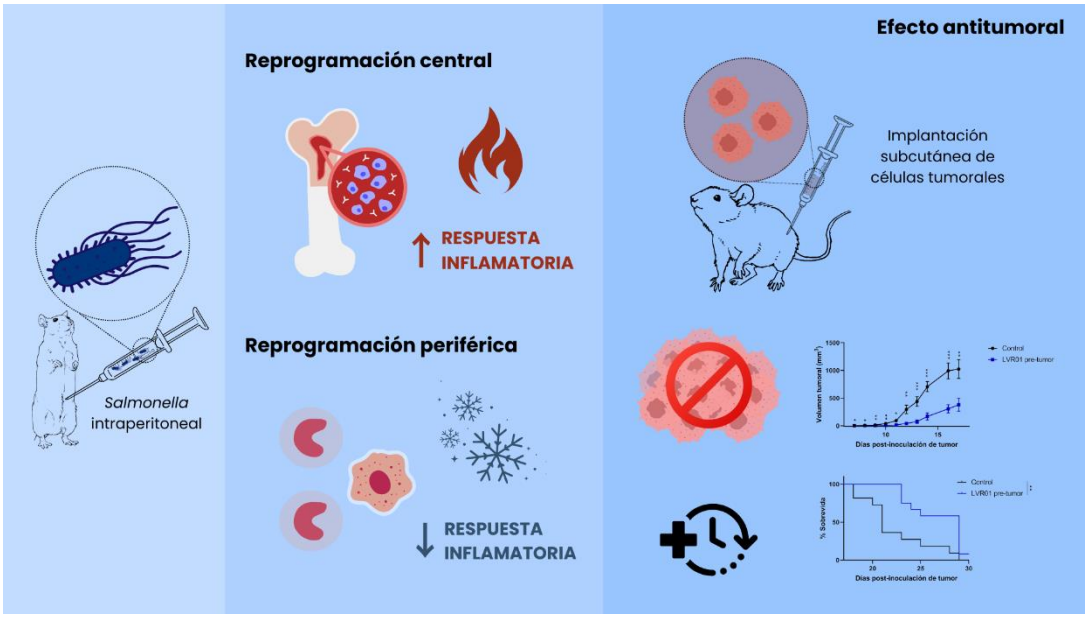


Figura 34 – Modelo conceptual de la reprogramación central y periférica inducida por *Salmonella* y su impacto en la respuesta antitumoral. La administración intraperitoneal de *Salmonella* LVR01 induce una reprogramación central del sistema inmune, asociada a una mayor capacidad de respuesta frente a estímulos secundarios, y una reprogramación periférica caracterizada por un estado tolerante con disminución de la respuesta inflamatoria. Esta respuesta se asocia a un efecto antitumoral *in vivo*, evidenciado por un retraso en el crecimiento tumoral y una mayor sobrevida, aun en ausencia de una inflamación marcada en el microambiente tumoral.

7.2 AUTOFAGIA

En esta tesis también nos propusimos elucidar el rol de la autofagia en el efecto antitumoral inducido por *Salmonella* LVR01. Se ha reportado que *Salmonella* es capaz de inducir autofagia, o xenofagia, en las células que infecta como parte de un mecanismo celular destinado al control de la infección y a la adaptación frente al estrés asociado a la deprivación de nutrientes (Casanova, 2017; Wu et al., 2020). Asimismo, Zhang y colaboradores demostraron que la cepa atenuada *Salmonella* VNP20009, ampliamente utilizada como inmunoterapia experimental frente al cáncer, induce autofagia en células tumorales murinas B16F10 (Zhang et al., 2016). En base a estos antecedentes, evaluamos si la cepa *Salmonella* LVR01 presentaba una capacidad similar.

Mediante una sonda fluorescente específica para la detección de autofagosomas se detectó un aumento en estructuras autofágicas en células B16F10 tras la infección con LVR01 (Figuras 28–29), lo que indica que la bacteria es capaz de activar etapas tempranas del proceso autofágico en esta línea celular. Múltiples intentos por corroborar la inducción de autofagia mediante análisis por western blot de proteínas asociadas a esta vía, como ATG5 y LC3 no fueron exitosos. Diversos factores podrían explicar este resultado, no puede descartarse que el uso de un buffer de lisis con Triton X–100 al 0,1%, en lugar de un buffer RIPA, haya limitado la extracción de proteínas asociadas a membrana como LC3 y, en consecuencia, su detección por western blot. Si bien fue posible detectar el complejo ATG5–ATG12 (Figura 30), no hubo diferencias entre condiciones. Esta aproximación no permite determinar variaciones en el flujo autofágico. Tal como se establece en las guías para el monitoreo de autofagia, la conjugación ATG5–ATG12 no constituye un marcador dinámico adecuado de inducción de autofagia, dado que en muchos tipos celulares la mayoría de estas proteínas se encuentran constitutivamente en forma conjugada y sus niveles no varían significativamente durante la activación de esta vía (Klionsky et al., 2021). En este contexto, la detección del complejo ATG5–ATG12 por sí sola no permite inferir un aumento en el flujo autofágico. Por otra parte, no se observaron bandas detectables correspondientes a LC3, otro de los marcadores comúnmente utilizados para el estudio de la autofagia (Murugan & Amaravadi, 2016). Está descrito que, durante la inducción de autofagia, la forma citosólica LC3–I es procesada a la forma lipídica LC3–II, la cual se asocia a la membrana del autofagosoma. Sin embargo, la relación entre LC3–I y LC3–II es altamente dependiente del tipo celular y del estímulo utilizado para inducir autofagia, y no siempre existe una correlación directa entre el aumento del flujo autofágico y la acumulación detectable de LC3–II. Además, la estabilidad diferencial de ambas formas, así como su sensibilidad en condiciones de procesamiento de las muestras pueden dificultar su detección (Klionsky et al., 2021; Murugan & Amaravadi, 2016). En este sentido, resulta fundamental considerar que la autofagia es un proceso dinámico y continuo que culmina en la degradación proteica; por lo tanto, su caracterización mediante la marcación de una única proteína o estructura puede resultar parcial o incluso sesgada. Proteínas de la familia ATG8 (como LC3), utilizadas como marcadores de estructuras autofágicas, son herramientas valiosas para visualizar autofagosomas. Sin embargo, existen múltiples isoformas con funciones potencialmente diferenciales, aspecto que debe considerar al diseñar una estrategia e interpretar los resultados. El uso de marcadores debe complementarse con ensayos que permitan estimar

el flujo autofágico global para lograr una interpretación adecuada de los resultados (Klionsky et al., 2021).

El concepto de flujo autofágico refiere al proceso completo que abarca la selección y el secuestro del cargo, la fusión con lisosomas y su posterior degradación y reciclado (Mizushima, 2025). La evaluación del flujo puede abordarse mediante estrategias que bloqueen transitoriamente la degradación lisosomal y permitan analizar la acumulación dependiente del tiempo de marcadores autofágicos, o mediante el seguimiento de la degradación de proteínas sensibles a autofagia tras inhibición de la síntesis proteica, considerando las posibles interferencias de otras vías proteolíticas o de señalización metabólica (Klionsky et al., 2021). Asimismo, se han desarrollado reporteros fluorescentes que permiten discriminar entre autofagosomas y autolisosomas, y estimar de manera más precisa el flujo autofágico en células vivas. Entre ellos, el sistema tándem mRFP–EGFP fusionado a ATG8/LC3 actúa como un sensor sensible al pH: en los autofagosomas ambas señales fluorescentes coexisten, mientras que tras la fusión con lisosomas la acidificación del compartimento apaga la señal verde (EGFP) y predomina la fluorescencia roja (mRFP), permitiendo diferenciar estructuras en etapas tempranas y tardías del proceso (Figura 35) (Al Outa et al., 2023).

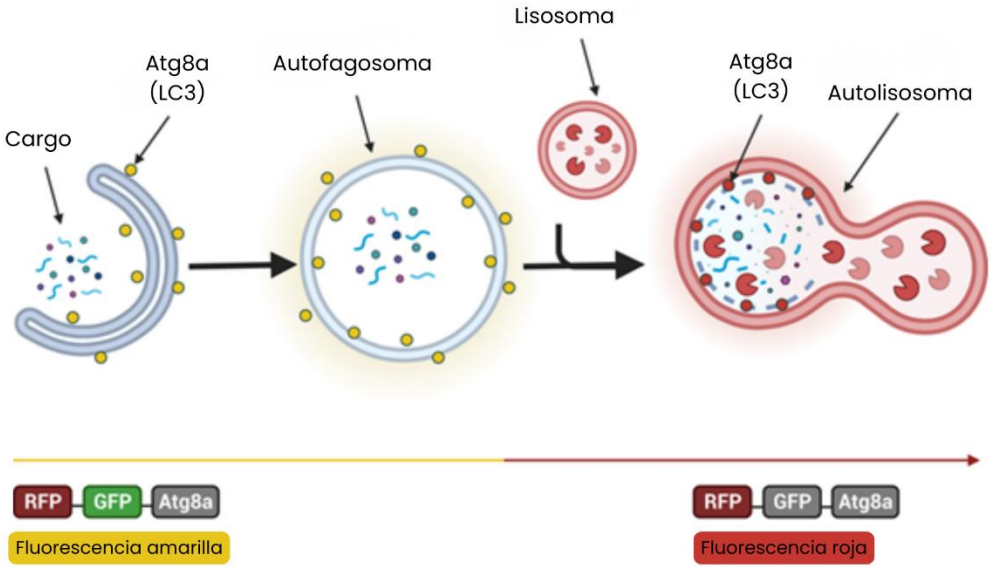


Figura 35 – Representación esquemática de ensayo para evaluar flujo autofágico *in vivo*. Adaptado de Al Outa et al., 2023.

En conjunto, estos abordajes permiten interpretar con mayor precisión si el aumento de estructuras autofágicas refleja una verdadera activación del flujo autofágico o, alternativamente, una alteración en su maduración o degradación final. Estos aspectos metodológicos adquieren particular relevancia en el contexto tumoral, donde la autofagia se encuentra estrechamente vinculada al estado metabólico celular y a las demandas energéticas (Klionsky et al., 2021). En este escenario, aproximaciones integrativas como el análisis proteómico emergen como herramientas especialmente valiosas, ya que permiten caracterizar con mayor profundidad modificaciones globales asociadas a la activación o modulación de la maquinaria autofágica (Cudjoe et al., 2017). Si bien estas aproximaciones

no fueron exploradas en el contexto de esta tesis, su implementación en estudios futuros permitirá profundizar en el análisis del rol de la autofagia inducida por *Salmonella* LVR01.

Habiendo observado que LVR01 es capaz de inducir autofagia en la línea celular B16F10, continuamos evaluando el impacto que tenía el uso de moduladores de la autofagia en la acción citotóxica de *Salmonella*. Por otro lado, los reportes de Zhang y colaboradores demostraron que la combinación de *Salmonella* con cloroquina incrementa la capacidad de la bacteria de eliminar células tumorales B16F10 *in vitro* en comparación con el tratamiento sólo con la bacteria (Zhang et al., 2016).

La cloroquina es un agente lisosomotrópico que se acumula en compartimentos ácidos e interfiere con la función lisosomal, inhibiendo la autofagia. Su uso induce fosfolipidosis y la formación de cuerpos multilamelares característicos de lisosomas disfuncionales, que contienen fosfolípidos y colesterol no degradados. En el contexto de la autofagia, incrementa el número de autofagosomas al inhibir la degradación lisosomal del contenido secuestrado y bloquear predominantemente la fusión entre autofagosomas y lisosomas. En consecuencia, el aumento de estructuras autofágicas observado en presencia de cloroquina no refleja necesariamente una mayor inducción del proceso, sino la interrupción de etapas tardías del flujo autofágico (Klionsky et al., 2021; Yang et al., 2013). Por su parte, la 3-metiladenina es un inhibidor ampliamente utilizado de la autofagia debido a su efecto sobre la fosfatidilinositol 3-quinasa de clase III (PtdIns3K), enzima esencial para la nucleación del autofagosoma. Sin embargo, 3-metiladenina también inhibe la PI3K de clase I, lo que introduce un grado adicional de complejidad en la interpretación de sus efectos biológicos. En términos funcionales, la inhibición de la PtdIns3K de clase III resulta en la supresión de etapas tempranas de la formación del autofagosoma, bloqueando la iniciación del proceso autofágico (Dai et al., 2016; Klionsky et al., 2021; Yang et al., 2013).

LVR01 promueve la muerte de células tumorales B16F10, en comparación con las células sin tratar. Sin embargo, no se observaron diferencias estadísticamente significativas entre las células tratadas con LVR01 solo y aquellas en combinación con inhibidores de la autofagia, como cloroquina y 3-metiladenina. Las células tratadas con cloroquina y LVR01 muestran una tendencia hacia una mayor muerte celular a las 20 horas, aunque sin respaldo estadístico (Figura 31). Una limitación de este análisis radica en que la evaluación de muerte celular se realizó exclusivamente mediante marcación con ioduro de propidio (PI), lo que permite detectar pérdida de integridad de la membrana pero no discrimina entre distintos mecanismos de muerte celular ni etapas tempranas del proceso (Crowley et al., 2016). Esto podría haber condicionado la sensibilidad del ensayo para detectar diferencias sutiles entre los tratamientos. Inicialmente se planificó evaluar viabilidad celular mediante el ensayo de MTT; sin embargo, debido a que LVR01 es capaz de metabolizar este compuesto y a las dificultades para eliminar completamente las bacterias intracelulares mediante tratamiento antibiótico, se optó por el análisis por citometría de flujo, estrategia metodológica similar a la utilizada por Zhang y colaboradores. En el trabajo mencionado se propone que el aumento de la capacidad citotóxica observado al combinar *Salmonella* con cloroquina se debe, al menos en parte, a la inhibición de la autofagia como mecanismo de control de la replicación bacteriana intracelular. En este contexto, la autofagia actuaría limitando la carga bacteriana dentro de las células infectadas; por lo tanto, su inhibición

favorecería una mayor acumulación intracelular de bacterias, con el consecuente aumento del daño celular (Zhang et al., 2016).

El uso de inhibidores químicos de la autofagia puede generar dificultades asociadas a sus efectos fuera de blanco, particularmente en células del sistema inmune (Schroeder et al., 2017). Por este motivo, su aplicación requiere un análisis cuidadoso de las condiciones experimentales y la inclusión de controles adecuados que permitan discriminar efectos específicos sobre la maquinaria autofágica de aquellos derivados de la modulación de otras vías celulares. En este contexto, suele considerarse preferible el empleo de modelos genéticos de pérdida de función de genes Atg para evaluar de manera más específica el rol de la autofagia. Sin embargo, incluso esta aproximación presenta limitaciones, ya que varios productos génicos asociados clásicamente a la autofagia desempeñan funciones independientes de este proceso. Por ejemplo, ATG5 ha sido implicado en mecanismos de muerte celular, mientras que complejos que contienen PIK3C3/VPS34 y BECN1 participan en apoptosis, tráfico endosomal y homeostasis de proteínas. Asimismo, algunas proteínas relacionadas con autofagia pueden ser dispensables en contextos no canónicos del proceso. En consecuencia, tanto las estrategias farmacológicas, como las genéticas, deben interpretarse considerando la complejidad funcional de estas moléculas (Klionsky et al., 2021).

En la presente tesis nos enfocamos en estudiar el efecto de la modulación de la autofagia sobre células tumorales. No obstante, se encuentra reportado que *Salmonella* es capaz de inducir autofagia en células de la inmunidad innata, modulando su fenotipo funcional (Hos et al., 2025). En macrófagos, por ejemplo, la inhibición de la autofagia se ha asociado con el mantenimiento prolongado de un fenotipo proinflamatorio tipo M1, lo que podría potenciar sus funciones microbicidas y antitumorales (Chen et al., 2018). Estos antecedentes sugieren que la modulación de la autofagia en el contexto de la terapia con *Salmonella* podría tener efectos adicionales a nivel del microambiente tumoral, más allá del impacto directo sobre la viabilidad de las células tumorales. En este contexto, la modulación farmacológica de la autofagia puede afectar tanto a las células tumorales como a los distintos componentes del microambiente tumoral.

A diferencia de los reportado por Zhang y colaboradores, la combinación de tratamiento terapéutico de LVR01 con cloroquina en modelo de melanoma B16F10 no presentó un efecto sinérgico (Figura 32). Por el contrario, el grupo de animales que recibieron a la terapia combinada presentó un comportamiento similar al grupo control, sugiriendo que el tratamiento con cloroquina inhibe parcialmente el efecto antitumoral de *Salmonella*. Sumado a ello, la inhibición farmacológica con cloroquina al momento de inducción de inmunidad entrenada con LVR01 tampoco tuvo un impacto en el efecto antitumoral de LVR01 (Figura 33). Las diferencias observadas respecto al trabajo de Zhang podrían explicarse, al menos en parte, por variaciones en los esquemas terapéuticos empleados. Mientras en nuestro modelo la cloroquina fue administrada diariamente, en dicho estudio se utilizó un esquema de administración día por medio. Estas diferencias metodológicas podrían modificar la magnitud o dinámica de la modulación inmunológica inducida por el tratamiento y contribuir a las discrepancias observadas entre ambos estudios.

Es importante considerar que la modulación farmacológica de la autofagia en animales introduce un nivel adicional de complejidad biológica. La cloroquina no solo interfiere con etapas tardías del proceso autofágico, sino que también ejerce efectos inmunomoduladores. Se ha descrito que puede alterar la expresión de citoquinas inducidas por LPS y afectar procesos de presentación antigénica mediante la modificación del pH endosomal (Klionsky et al., 2021). Dado que el efecto antitumoral de *Salmonella* LVR01 depende en gran medida de la activación de la respuesta inmune, la administración sistémica de cloroquina podría modular componentes del microambiente tumoral de manera compleja, potencialmente contrarrestando cualquier efecto derivado de la inhibición de la autofagia en las células tumorales. En este sentido, la evaluación de otros inhibidores de la autofagia podría aportar información complementaria en futuros estudios. Por ejemplo, la leupeptina ha sido utilizada como inhibidor de proteasas lisosomales para el análisis del flujo autofágico *in vivo*, permitiendo una inhibición transitoria de la degradación lisosomal con menor interferencia sobre vías de señalización aguas arriba o sobre la activación inmune sistémica. A diferencia de la cloroquina, su uso en esquemas de corta duración (por ejemplo, aproximadamente 4 horas) minimiza efectos pleiotrópicos y modulaciones inmunológicas indirectas, lo que la convierte en una herramienta útil para la evaluación puntual del flujo autofágico. Por el contrario, la 3-metiladenina presenta efectos pleiotrópicos sobre la señalización PI3K y diversas vías inmunes, lo que limita su aplicabilidad en modelos *in vivo* y dificulta la interpretación específica de sus efectos sobre la autofagia. En este contexto, su utilización se considera más apropiada para estudios *in vitro* que para la evaluación sistémica en animales completos (Klionsky et al., 2021). No obstante, dado que el objetivo de los experimentos realizados en esta tesis no fue medir el flujo autofágico agudo sino analizar el impacto de la modulación sostenida de la autofagia sobre el efecto antitumoral de LVR01, la implementación de inhibidores de acción corta como la leupeptina no se ajustaría directamente al diseño experimental planteado. En consecuencia, la exploración de herramientas farmacológicas o genéticas más específicas constituye una perspectiva futura para profundizar en el rol de la autofagia en este modelo.

Además, debe considerarse que el rol de la autofagia en el desarrollo tumoral es altamente dependiente del estadio de la enfermedad. La autofagia puede ejercer funciones duales en cáncer, actuando como mecanismo supresor tumoral en etapas tempranas y favoreciendo la adaptación metabólica y la supervivencia en etapas avanzadas (Towers et al., 2019). Esta naturaleza contextual complejiza la búsqueda de un efecto sinérgico mediante su inhibición, ya que bloquear la autofagia no necesariamente conduce a un beneficio terapéutico uniforme. En los modelos tumorales empleados en esta tesis, caracterizados por un crecimiento rápido y una progresión acelerada, la ventana temporal para modular procesos biológicos como la autofagia es limitada. En consecuencia, la posibilidad de explorar distintos esquemas de tratamiento en función del estadio tumoral resulta restringida. Desde una perspectiva futura, podría ser relevante evaluar esta estrategia en modelos tumorales de progresión más lenta, que permitan una caracterización más detallada de las distintas fases del desarrollo tumoral y de la contribución diferencial de la autofagia en cada una de ellas. Asimismo, el uso exclusivo de inhibidores farmacológicos no es suficiente para establecer conclusiones mecanísticas robustas, particularmente en modelos oncológicos. Las aproximaciones químicas deberían complementarse con estrategias genéticas de

modulación de genes Atg y con análisis basados en flujo autofágico, junto con lecturas funcionales relevantes para la biología tumoral (Klionsky et al., 2021). En este sentido, la integración de herramientas farmacológicas, genéticas y funcionales constituye una vía necesaria para profundizar en la comprensión del rol de la autofagia en la terapia antitumoral mediada por *Salmonella*.

La Figura 36 resume el modelo conceptual derivado de estos resultados: aunque nuestros resultados preliminares sugieren que LVR01 induce autofagia en células tumorales *in vitro*, la modulación farmacológica de este proceso no potencia su efecto antitumoral en el contexto *in vivo*. Este escenario sugiere que el impacto de la autofagia en la terapia mediada por *Salmonella* debe interpretarse dentro de la complejidad del microambiente tumoral y de sus interacciones inmunológicas.

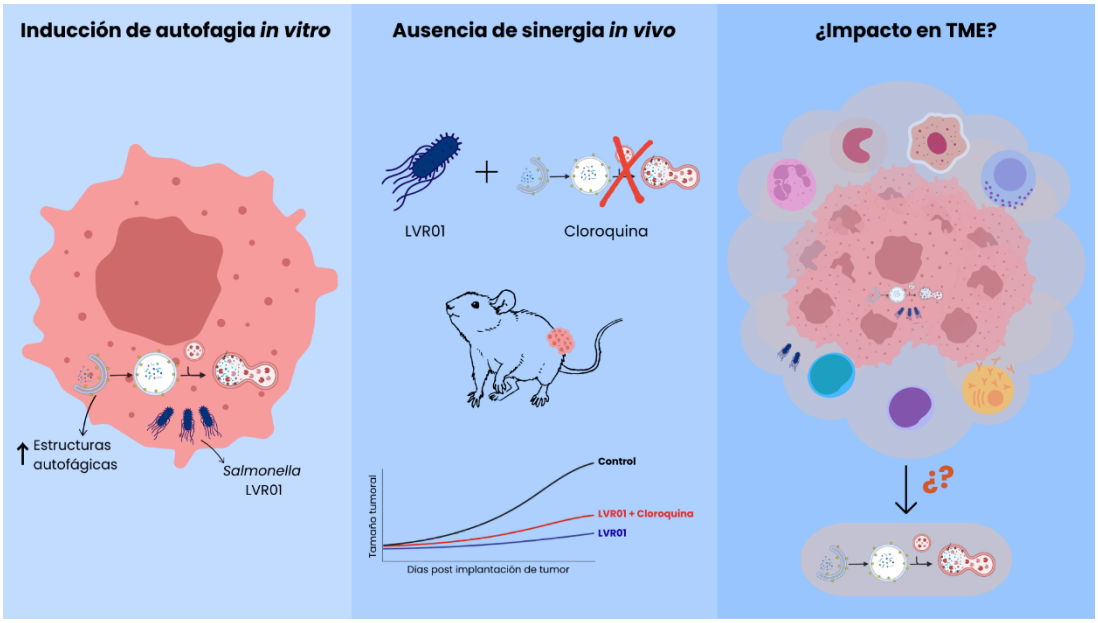


Figura 36 – Rol de la autofagia en la terapia antitumoral mediada por *Salmonella* LVR01. En células tumorales B16F10 *in vitro*, la infección con LVR01 induce un aumento de estructuras autofágicas, evidenciando activación de etapas tempranas del proceso autofágico. En modelos *in vivo*, la combinación de LVR01 con inhibición farmacológica de la autofagia mediante cloroquina no mostró un efecto sinérgico sobre el crecimiento tumoral, siendo el efecto antitumoral atribuible principalmente a la bacteria. Estos resultados plantean la interrogante sobre cómo la modulación de la autofagia impacta en el microambiente tumoral (TME), donde múltiples poblaciones celulares inmunes y tumorales interactúan dinámicamente y podrían condicionar la respuesta terapéutica.

7.3 GLOBAL

Los resultados de esta tesis permiten proponer un modelo integrador sobre el efecto antitumoral de *Salmonella* LVR01 en distintos contextos de administración. En primer lugar, la administración profiláctica de la bacteria atenuada demostró ejercer un efecto antitumoral significativo. Este efecto no se asoció a un aumento evidente en la infiltración de células inmunes en el microambiente tumoral ni a una exacerbada respuesta inflamatoria local, lo que sugiere que los mecanismos subyacentes difieren de aquellos descritos para la administración intratumoral (Chilibroste et al., 2021; Mónaco et al., 2022; Mónaco & Plata et al., 2022; Vola et al., 2018). En este escenario, proponemos como hipótesis que la bacteria podría inducir modificaciones a nivel de progenitores hematopoyéticos, generando un estado de inmunidad entrenada central que se traduzca en una mayor capacidad citotóxica funcional sin necesidad de un incremento cuantitativo en el reclutamiento celular. Si bien esta hipótesis no fue confirmada experimentalmente en el marco de esta tesis, los resultados obtenidos son consistentes con este modelo y justifican su exploración futura. En contraste, a nivel periférico se observó que la exposición a LVR01 induce un estado de tolerancia en monocitos circulantes. Este hallazgo introduce una dimensión adicional al modelo propuesto, ya que sugiere que la misma intervención bacteriana puede generar efectos divergentes según el compartimento inmunológico analizado. Proponemos que este estado tolerogénico periférico podría contribuir al carácter transitorio del efecto terapéutico observado, favoreciendo con el tiempo un TME protumoral que limite la eficacia sostenida del tratamiento.

En relación con la autofagia, se observó que LVR01 es capaz de inducir la formación de estructuras autofágicas en células tumorales B16F10 *in vitro*. Sin embargo, la inhibición farmacológica de la autofagia no potenció el efecto antitumoral *in vivo*, lo que sugiere que la modulación directa de este proceso en células tumorales no constituye un determinante principal de la respuesta terapéutica en el sistema integrado. Además, la inhibición farmacológica impacta no solo sobre células tumorales sino también sobre múltiples componentes del microambiente tumoral, introduciendo un nivel adicional de complejidad interpretativa.

Antecedentes del grupo habían demostrado que el efecto antitumoral de LVR01 administrada por vía intratumoral depende del reclutamiento de células inmunes, de una fuerte respuesta inflamatoria local y de la presencia de macrófagos con perfil M1, fenotipo que posteriormente se pierde (Mónaco et al., 2022). Sumado a esto, estudios previos de otros grupos indican que la inhibición de la autofagia puede favorecer la transición de macrófagos M2 hacia un perfil M1 (Chen et al., 2018). A partir de estos reportes se planteó inicialmente la hipótesis de que la autofagia inducida por *Salmonella* podría participar en la pérdida de la polarización M1 y, en consecuencia, en el desarrollo de resistencia al tratamiento. No obstante, nuestros resultados y la dinámica temporal del modelo sugieren que esta hipótesis pierde peso. La inducción de autofagia ocurre en las primeras horas post infección, período en el cual el inflamasoma se encuentra activamente inducido en el microambiente tumoral. Dado que existe una relación inversa entre activación del inflamasoma y autofagia, y siendo la activación del inflamasoma un mecanismo esencial en el efecto antitumoral

inducido por LVR01 (Mónaco et al., 2022), resulta poco probable que la autofagia temprana sea el principal determinante de la pérdida posterior del perfil M1 (Hos et al., 2025).

En conjunto, los resultados apoyan un modelo en el cual *Salmonella* LVR01 actúa como un modulador inmunometabólico capaz de inducir simultáneamente programas de activación y de regulación. La eficacia y duración del efecto antitumoral dependerían del balance entre estos dos ejes: un componente entrenado con potencial citotóxico aumentado y un componente tolerogénico. En este contexto, adquiere mayor relevancia la posibilidad de que la resistencia al tratamiento esté asociada al estado tolerogénico periférico inducido por la bacteria, el cual podría reprogramar el microambiente tumoral hacia un estado protumoral (Figura 37).

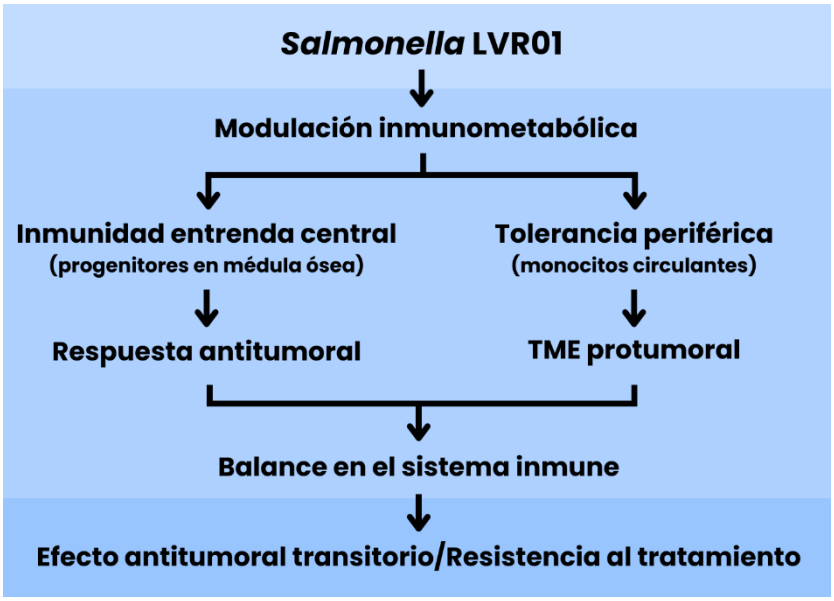


Figura 37 – Modelo conceptual del efecto inmunológico inducido por *Salmonella* LVR01. La bacteria actúa como modulador inmunometabólico capaz de inducir simultáneamente programas de inmunidad entrenada central y tolerancia periférica. El balance entre ambos procesos podría determinar la duración del efecto antitumoral y el desarrollo de resistencia al tratamiento.

7.4 CONCLUSIONES GENERALES Y PERSPECTIVAS

Los resultados de esta tesis contribuyen a ampliar la comprensión de los mecanismos involucrados en el uso de bacterias atenuadas como inmunoterapia antitumoral. Tradicionalmente, el efecto de *Salmonella* en modelos tumorales ha sido interpretado principalmente en términos de inflamación local, reclutamiento celular, invasión bacteriana y citotoxicidad directa. Sin embargo, los hallazgos presentados aquí sugieren que su impacto trasciende el microambiente tumoral inmediato y puede involucrar reprogramaciones inmunológicas sistémicas con consecuencias divergentes. La evidencia de un posible componente de inmunidad entrenada central, junto con la inducción concomitante de tolerancia periférica, plantea la necesidad de considerar estas terapias dentro del marco conceptual de la memoria de la inmunidad innata. Este doble eje introduce una dimensión temporal crítica: la eficacia inicial podría depender de mecanismos de activación entrenada, mientras que la pérdida progresiva de respuesta podría estar asociada a circuitos reguladores inducidos en paralelo. En este contexto, la autofagia emerge no como un mecanismo aislado determinante del efecto terapéutico, sino como un componente más dentro de una red inmunometabólica compleja cuya contribución depende del equilibrio sistémico global. Estos hallazgos refuerzan la idea de que la modulación de procesos celulares debe interpretarse en el contexto de la biología integrada del huésped.

En definitiva, esta tesis sugiere que la terapia bacteriana con *Salmonella* atenuada no puede entenderse únicamente como un estímulo inflamatorio antitumoral, sino como una intervención que reconfigura el sistema inmune en múltiples niveles. Comprender la dinámica temporal y compartimental de los diversos estados —entrenamiento y tolerancia— será clave para optimizar futuras estrategias terapéuticas basadas en bacterias atenuadas.

En función de los hallazgos presentados, una primera línea de trabajo futuro consiste en el desarrollo de nuevas construcciones de la cepa atenuada de *Salmonella* con una menor carga o actividad de LPS, uno de los principales estímulos implicados en la inducción de tolerancia en células de la inmunidad innata. La modulación racional de este componente podría permitir preservar el efecto antitumoral inicial de la bacteria, minimizando simultáneamente los mecanismos regulatorios que limitan la duración de la respuesta terapéutica. Sin embargo, dado que el LPS constituye además uno de los principales PAMPs responsables de la activación inmune inducida por *Salmonella*, futuras estrategias deberán considerar cuidadosamente el balance entre reducir mecanismos tolerogénicos y mantener una adecuada capacidad inmunoestimuladora. Este enfoque abriría la posibilidad de optimizar el balance entre activación e inducción de tolerancia, eje central del modelo propuesto en esta tesis. Por otra parte, será importante evaluar en trabajos futuros si el tratamiento con LVR01 induce fenómenos de tolerancia inmune a nivel del TME, mediante abordajes funcionales que permitan caracterizar la capacidad de respuesta de las poblaciones inmunes infiltrantes y determinar si mecanismos regulatorios similares a los observados sistémicamente también ocurren a nivel local.

En segundo lugar, resulta fundamental avanzar en la validación experimental del modelo de inmunidad entrenada central sugerido por los resultados obtenidos. Estudios de trasplante

de médula ósea, junto con análisis funcionales de progenitores hematopoyéticos, permitirían determinar si la administración profiláctica de LVR01 induce reprogramaciones persistentes a nivel medular. Complementariamente, abordajes metabólicos y epigenéticos —incluyendo análisis transcriptómicos, epigenómicos y proteómicos— contribuirían a caracterizar de manera integral los cambios asociados a este estado funcional.

En relación con la autofagia, los resultados obtenidos señalan la necesidad de estrategias más integrales para esclarecer su rol en la terapia bacteriana antitumoral. La combinación de inhibidores farmacológicos con modelos genéticamente modificados en genes Atg permitiría superar las limitaciones asociadas a los efectos pleiotrópicos de los compuestos químicos. Asimismo, la implementación de ensayos específicos de flujo autofágico y la utilización de modelos tumorales de progresión más lenta podrían facilitar la evaluación temporal de este proceso en un contexto más representativo del desarrollo tumoral.

En conjunto, estas perspectivas apuntan a profundizar en la comprensión de los mecanismos inmunometabólicos que regulan la eficacia y la duración de la respuesta antitumoral inducida por *Salmonella*, con el objetivo de avanzar hacia estrategias terapéuticas más precisas y sostenidas en el tiempo.

8. BIBLIOGRAFÍA

Aaby, P., Martins, C.L., Garly, M.-L., Bale, C., Andersen, A., Rodrigues, A., Ravn, H., Lisse, I.M., Benn, C.S., Whittle, H.C., 2010. Non-specific effects of standard measles vaccine at 4.5 and 9 months of age on childhood mortality: randomised controlled trial. BMJ 341, c6495–c6495. https://doi.org/10.1136/bmj.c6495

Aganja, R.P., Sivasankar, C., Senevirathne, A., Lee, J.H., 2022. Salmonella as a Promising Curative Tool against Cancer. Pharmaceutics 14, 2100. https://doi.org/10.3390/pharmaceutics14102100

Agorio, C., Schreiber, F., Sheppard, M., Mastroeni, P., Fernandez, M., Martinez, M.A., Chabalgoity, J.A., 2007. Live attenuated Salmonella as a vector for oral cytokine gene therapy in melanoma. J. Gene Med. 9, 416–423. https://doi.org/10.1002/jgm.1023

Al-Hilu, S.A., Al-Shujairi, W.H., 2020. Dual Role of Bacteria in Carcinoma: Stimulation and Inhibition. Int. J. Microbiol. 2020, 1–15. https://doi.org/10.1155/2020/4639761

Al Outa, A., Hicks, S., Thambawita, V., Andresen, S., Enserink, J.M., Halvorsen, P., Riegler, M.A., Knævelsrud, H., 2023. CELLULAR, A Cell Autophagy Imaging Dataset. Sci. Data 10, 806. https://doi.org/10.1038/s41597-023-02687-x

Al-Saafeen, B.H., Al-Sbiei, A., Bashir, G., Mohamed, Y.A., Masad, R.J., Fernandez-Cabezudo, M.J., Al-Ramadi, B.K., 2022. Attenuated Salmonella potentiate PD-L1 blockade immunotherapy in a preclinical model of colorectal cancer. Front. Immunol. 13, 1–24. https://doi.org/10.3389/fimmu.2022.1017780

Amaravadi, R., Kimmelman, A.C., White, E., 2016. Recent insights into the function of autophagy in cancer. Genes Dev. 30, 1913–1930. https://doi.org/10.1101/gad.287524.116

American Cancer Society, 2020. Treating Bladder Cancer [WWW Document]. URL https://www.cancer.org/cancer/bladder-cancer/treating.html

Anderson, N.R., Minutolo, N.G., Gill, S., Klichinsky, M., 2021. Macrophage-Based Approaches for Cancer Immunotherapy. Cancer Res. 81, 1201–1208. https://doi.org/10.1158/0008-5472.CAN-20-2990

Badie, F., Ghandali, M., Tabatabaei, S.A., Safari, M., Khorshidi, A., Shayestehpour, M., Mahjoubin-Tehran, M., Morshedi, K., Jalili, A., Tajiknia, V., Hamblin, M.R., Mirzaei, H., 2021. Use of Salmonella Bacteria in Cancer Therapy: Direct, Drug Delivery and Combination Approaches. Front. Oncol. 11. https://doi.org/10.3389/fonc.2021.624759

Barnes, S.A., Trew, I., de Jong, E., Foley, B., 2021. Making a Killer: Selecting the Optimal Natural Killer Cells for Improved Immunotherapies. Front. Immunol. 12, 1–17. https://doi.org/10.3389/fimmu.2021.765705

Bascuas, T., Moreno, M., Grille, S., Chabalgoity, J.A., 2018. Salmonella immunotherapy improves the outcome of CHOP chemotherapy in non-Hodgkin lymphoma-bearing mice. Front. Immunol. 9, 1–15. https://doi.org/10.3389/fimmu.2018.00007

Benitez, M.L.R., Bender, C.B., Oliveira, T.L., Schachtschneider, K.M., Collares, T., Seixas, F.K., 2019. Mycobacterium bovis BCG in metastatic melanoma therapy. Appl. Microbiol.

Biotechnol. 103, 7903–7916. https://doi.org/10.1007/s00253-019-10057-0

Bergman, P.J., 2019. Cancer Immunotherapies. Vet. Clin. North Am. Small Anim. Pract. 49, 881–902. https://doi.org/10.1016/j.cvsm.2019.04.010

Birmingham, C.L., Smith, A.C., Bakowski, M.A., Yoshimori, T., Brumell, J.H., 2006. Autophagy Controls Salmonella Infection in Response to Damage to the Salmonella-containing Vacuole. J. Biol. Chem. 281, 11374–11383. https://doi.org/10.1074/jbc.M509157200

Biswas, S.K., Lopez-Collazo, E., 2009. Endotoxin tolerance: new mechanisms, molecules and clinical significance. Trends Immunol. https://doi.org/10.1016/j.it.2009.07.009

Blanden, R.V., Lefford, M.J., Mackaness, G.B., 1969. The host response to Calmette-Guérin bacillus infection in mice. J. Exp. Med. 129, 1079–1107. https://doi.org/10.1084/jem.129.5.1079

Bromuro, C., Torosantucci, A., Chiani, P., Conti, S., Polonelli, L., Cassone, A., 2002. Interplay between Protective and Inhibitory Antibodies Dictates the Outcome of Experimentally Disseminated Candidiasis in Recipients of a Candida albicans Vaccine. Infect. Immun. 70, 5462–5470. https://doi.org/10.1128/IAI.70.10.5462-5470.2002

Bui, J.D., Schreiber, R.D., 2007. Cancer immunosurveillance, immunoediting and inflammation: independent or interdependent processes? Curr. Opin. Immunol. https://doi.org/10.1016/j.coi.2007.02.001

Butcher, S.K., O'Carroll, C.E., Wells, C.A., Carmody, R.J., 2018. Toll-Like Receptors Drive Specific Patterns of Tolerance and Training on Restimulation of Macrophages. Front. Immunol. 9. https://doi.org/10.3389/fimmu.2018.00933

Cai, H., Chen, Xueyuan, Liu, Y., Chen, Y., Zhong, G., Chen, Xiaoyu, Rong, S., Zeng, H., Zhang, L., Li, Z., Liao, A., Zeng, X., Xiong, W., Guo, C., Zhu, Y., Deng, K.-Q., Ren, H., Yan, H., Cai, Z., Xu, K., Zhou, L., Lu, Z., Wang, F., Liu, S., 2025. Lactate activates trained immunity by fueling the tricarboxylic acid cycle and regulating histone lactylation. Nat. Commun. 16, 3230. https://doi.org/10.1038/s41467-025-58563-2

Carlson, R.D., Flickinger, J.C., Snook, A.E., 2020. Talkin' Toxins: From Coley's to Modern Cancer Immunotherapy. Toxins (Basel). 12, 241. https://doi.org/10.3390/toxins12040241

Casanova, J.E., 2017. Bacterial Autophagy: Offense and Defense at the Host–Pathogen Interface. Cell. Mol. Gastroenterol. Hepatol. 4, 237–243. https://doi.org/10.1016/j.jcmgh.2017.05.002

Cavaillon, J.-M., Adib-Conquy, M., 2006. Bench-to-bedside review: endotoxin tolerance as a model of leukocyte reprogramming in sepsis. Crit. Care 10, 233. https://doi.org/10.1186/cc5055

Chabalgoity, J.A., Moreno, M., Carol, H., Dougan, G., Hormaeche, C.E., 2000. Salmonella typhimurium as a basis for a live oral Echinococcus granulosus vaccine. Vaccine 19, 460–469. https://doi.org/10.1016/S0264-410X(00)00197-3

Chang, R., Gulley, J.L., Fong, L., 2023. Vaccinating against cancer: getting to prime time. J. Immunother. Cancer 11, e006628. https://doi.org/10.1136/jitc-2022-006628

Chavakis T, Mitroulis I, Hajishengallis G. Hematopoietic progenitor cells as integrative hubs for adaptation to and fine-tuning of inflammation. Nat Immunol. 2019;20(7):802–811. doi:10.1038/s41590-019-0402-5

Chen, C., Bennion, K.B., Swift, D.A., Morrow, K.N., Zhang, W., Oami, T., Coopersmith, C.M., Ford, M.L., 2021. Tumor-Specific T Cells Exacerbate Mortality and Immune Dysregulation during Sepsis. J. Immunol. 206, 2412–2419. https://doi.org/10.4049/jimmunol.2000865

Chen, D., Xie, J., Fiskesund, R., Dong, W., Liang, X., Lv, J., Jin, X., Liu, J., Mo, S., Zhang, T., Cheng, F., Zhou, Y., Zhang, H., Tang, K., Ma, J., Liu, Y., Huang, B., 2018. Chloroquine modulates antitumor immune response by resetting tumor-associated macrophages toward M1 phenotype. Nat. Commun. 9, 873. https://doi.org/10.1038/s41467-018-03225-9

Chen, D.S., Mellman, I., 2013. Oncology Meets Immunology: The Cancer-Immunity Cycle. Immunity 39, 1–10. https://doi.org/10.1016/j.immuni.2013.07.012

Chen, Y., Jin, H., Song, Y., Huang, T., Cao, J., Tang, Q., Zou, Z., 2021. Targeting tumor-associated macrophages: A potential treatment for solid tumors. J. Cell. Physiol. 236, 3445–3465. https://doi.org/10.1002/jcp.30139

Chilibroste, S., Mónaco, A., Plata, M.C., Vola, M., Agorio, C.I., Chabalgoity, J.A., Moreno, M., 2021. Preclinical Evaluation of LVR01 Attenuated Salmonella as Neoadjuvant Intralesional Therapy in Combination with Chemotherapy for Melanoma Treatment. J. Invest. Dermatol. https://doi.org/10.1016/j.jid.2021.08.442

Chronopoulos, J., Crespo, M., Chavakis, T., 2025. Central trained immunity in the context of bladder cancer immunotherapy. Cancer Cell 43, 1394–1396. https://doi.org/10.1016/j.ccell.2025.06.010

Cipponi, A., Wieers, G., Van Baren, N., Coulie, P.G., 2011. Tumor-infiltrating lymphocytes: Apparently good for melanoma patients. but why? Cancer Immunol. Immunother. 60, 1153–1160. https://doi.org/10.1007/s00262-011-1026-2

Coley, W.B., 1910. The Treatment of Inoperable Sarcoma by Bacterial Toxins (the Mixed Toxins of the Streptococcus erysipelas and the Bacillus prodigiosus). Proc. R. Soc. Med. 3, 1–48.

Coley, W.B., 1891. Contribution To the Knowledge of Sarcoma. Ann Surg 14, 199–220.

Corrigan, P.A., Beaulieu, C., Patel, R.B., Lowe, D.K., 2017. Talimogene Laherparepvec: An Oncolytic Virus Therapy for Melanoma. Ann. Pharmacother. 51, 675–681. https://doi.org/10.1177/1060028017702654

Crowley, L.C., Scott, A.P., Marfell, B.J., Boughaba, J.A., Chojnowski, G., Waterhouse, N.J., 2016. Measuring Cell Death by Propidium Iodide Uptake and Flow Cytometry. Cold Spring Harb. Protoc. 2016, pdb.prot087163. https://doi.org/10.1101/pdb.prot087163

Cudjoe, E.K., Saleh, T., Hawkridge, A.M., Gewirtz, D.A., 2017. Proteomics Insights into Autophagy. Proteomics 17. https://doi.org/10.1002/pmic.201700022

Dai, S., Wang, B., Li, W., Wang, L., Song, X., Guo, C., Li, Y., Liu, F., Zhu, F., Wang, Q., Wang, X., Shi, Y., Wang, J., Zhao, W., Zhang, L., 2016. Systemic application of 3-methyladenine markedly inhibited atherosclerotic lesion in ApoE-/- mice by modulating autophagy, foam cell formation and immune-negative molecules. Cell Death Dis. 7, e2498–e2498.

https://doi.org/10.1038/cddis.2016.376

Dailey, K.M., Allgood, J.E., Johnson, P.R., Ostlie, M.A., Schaner, K.C., Brooks, B.D., Brooks, A.E., 2021. The next frontier of oncotherapy: accomplishing clinical translation of oncolytic bacteria through genetic engineering. Future Microbiol. 16, 341–368. https://doi.org/10.2217/fmb-2020-0245

Dal Bello, M.G., Alama, A., Coco, S., Vanni, I., Grossi, F., 2017. Understanding the checkpoint blockade in lung cancer immunotherapy. Drug Discov. Today 22, 1266–1273. https://doi.org/10.1016/j.drudis.2017.05.016

Daman, A.W., Antonelli, A.C., Redelman-Sidi, G., Paddock, L., Khayat, S., Ketavarapu, M., Cheong, J.G., Jurado, L.F., Benjamin, A., Jiang, S., Ahimovic, D., Lawless, V.R., Bale, M.J., Loutochin, O., McPherson, V.A., Divangahi, M., Niec, R.E., Pe'er, D., Pietzak, E., Josefowicz, S.Z., Glickman, M.S., 2025. Microbial cancer immunotherapy reprograms hematopoiesis to enhance myeloid-driven anti-tumor immunity. Cancer Cell 43, 1442–1459.e10. https://doi.org/10.1016/j.ccell.2025.05.002

Danahy, D.B., Kurup, S.P., Winborn, C.S., Jensen, I.J., Harty, J.T., Griffith, T.S., Badovinac, V.P., 2019. Sepsis-Induced State of Immunoparalysis Is Defined by Diminished CD8 T Cell–Mediated Antitumor Immunity. J. Immunol. 203, 725–735. https://doi.org/10.4049/jimmunol.1900435

De Bree, L.C.J., Koeken, V.A.C.M., Joosten, L.A.B., Aaby, P., Benn, C.S., van Crevel, R., Netea, M.G., 2018. Non-specific effects of vaccines: Current evidence and potential implications. Semin. Immunol. 39, 35–43. https://doi.org/10.1016/j.smim.2018.06.002

De Marco, R.C., Monzo, H.J., Ojala, P.M., 2023. CAR T Cell Therapy: A Versatile Living Drug. Int. J. Mol. Sci. 24, 6300. https://doi.org/10.3390/ijms24076300

DeVorkin, L., Pavey, N., Carleton, G., Comber, A., Ho, C., Lim, J., McNamara, E., Huang, H., Kim, P., Zacharias, L.G., Mizushima, N., Saitoh, T., Akira, S., Beckham, W., Lorzadeh, A., Moksa, M., Cao, Q., Murthy, A., Hirst, M., DeBerardinis, R.J., Lum, J.J., 2019. Autophagy Regulation of Metabolism Is Required for CD8+ T Cell Anti-tumor Immunity. Cell Rep. 27, 502–513.e5. https://doi.org/10.1016/j.celrep.2019.03.037

Dikic, I., Elazar, Z., 2018. Mechanism and medical implications of mammalian autophagy. Nat. Rev. Mol. Cell Biol. 19, 349–364. https://doi.org/10.1038/s41580-018-0003-4

Divangahi, M., Aaby, P., Khader, S.A., Barreiro, L.B., Bekkering, S., Chavakis, T., van Crevel, R., Curtis, N., DiNardo, A.R., Dominguez-Andres, J., Duivenwoorden, R., Fanucchi, S., Fayad, Z., Fuchs, E., Hamon, M., Jeffrey, K.L., Khan, N., Joosten, L.A.B., Kaufmann, E., Latz, E., Matarese, G., van der Meer, J.W.M., Mhlanga, M., Moorlag, S.J.C.F.M., Mulder, W.J.M., Naik, S., Novakovic, B., O'Neill, L., Ochando, J., Ozato, K., Riksen, N.P., Sauerwein, R., Sherwood, E.R., Schlitzer, A., Schultze, J.L., Sieweke, M.H., Benn, C.S., Stunnenberg, H., Sun, J., van de Veerdonk, F.L., Weis, S., Williams, D.L., Xavier, R., Netea, M.G., 2021. Trained immunity, tolerance, priming and differentiation: distinct immunological processes. Nat. Immunol. 22, 2–6. https://doi.org/10.1038/s41590-020-00845-6

Domínguez-Andrés, J., dos Santos, J.C., Bekkering, S., Mulder, W.J.M., van der Meer, J.W.M., Riksen, N.P., Joosten, L.A.B., Netea, M.G., 2023. Trained immunity: adaptation within innate immune mechanisms. Physiol. Rev. 103, 313–346. https://doi.org/10.1152/physrev.00031.2021

Domínguez-Andrés, J., Fanucchi, S., Joosten, L.A.B., Mhlanga, M.M., Netea, M.G., 2020. Advances in understanding molecular regulation of innate immune memory. Curr. Opin. Cell Biol. 63, 68–75. https://doi.org/10.1016/j.ceb.2019.12.006

Dominguez-Andres, J., Netea, M.G., 2019. Long-term reprogramming of the innate immune system. J. Leukoc. Biol. 105, 329–338. https://doi.org/10.1002/JLB.MR0318-104R

Domínguez-Andrés, J., Novakovic, B., Li, Y., Scicluna, B.P., Gresnigt, M.S., Arts, R.J.W., Oosting, M., Moorlag, S.J.C.F.M., Groh, L.A., Zwaag, J., Koch, R.M., ter Horst, R., Joosten, L.A.B., Wijmenga, C., Michelucci, A., van der Poll, T., Kox, M., Pickkers, P., Kumar, V., Stunnenberg, H., Netea, M.G., 2019b. The Itaconate Pathway Is a Central Regulatory Node Linking Innate Immune Tolerance and Trained Immunity. Cell Metab. 29, 211–220.e5. https://doi.org/10.1016/j.cmet.2018.09.003

Dos Santos, J.C., Moreno, M., Teufel, L.U., Chilibroste, S., Keating, S.T., Groh, L., Domínguez-Andrés, J., Williams, D.L., Ma, Z., Lowman, D.W., Ensley, H.E., Novakovic, B., Ribeiro-Dias, F., Netea, M.G., Chabalgoity, J.A., Joosten, L.A.B., 2024. Leishmania braziliensis enhances monocyte responses to promote anti-tumor activity. Cell Rep. 43, 113932. https://doi.org/10.1016/j.celrep.2024.113932

Downs-Canner, S.M., Meier, J., Vincent, B.G., Serody, J.S., 2022. B Cell Function in the Tumor Microenvironment. Annu. Rev. Immunol. 40, 169–193. https://doi.org/10.1146/annurev-immunol-101220-015603

Dunn, G.P., Old, L.J., Schreiber, R.D., 2004. The Three Es of Cancer Immunoediting. Annu. Rev. Immunol. https://doi.org/10.1146/annurev.immunol.22.012703.104803

Enamorado, M., Iborra, S., Priego, E., Cueto, F.J., Quintana, J.A., Martýnez-Cano, S., Mejyás-Perez, E., Esteban, M., Melero, I., Hidalgo, A., Sancho, D., 2017. Enhanced anti-tumour immunity requires the interplay between resident and circulating memory CD8+ T cells. Nat. Commun. 8, 1–11. https://doi.org/10.1038/ncomms16073

Fan, T., Zhang, M., Yang, J., Zhu, Z., Cao, W., Dong, C., 2023. Therapeutic cancer vaccines: advancements, challenges, and prospects. Signal Transduct. Target. Ther. 8. https://doi.org/10.1038/s41392-023-01674-3

Farkona, S., Diamandis, E.P. and Blasutig, I.M. (2016) Cancer Immunotherapy: The Beginning of the End of Cancer? BMC Medicine, BMC Medicine, 14, 1–18. https://doi.org/10.1186/s12916-016-0623-5.

Floros, T., Tarhini, A.A., 2015. Anticancer Cytokines: Biology and Clinical Effects of Interferon-α2, Interleukin (IL)-2, IL-15, IL-21, and IL-12. Semin. Oncol. 42, 539–548. https://doi.org/10.1053/j.seminoncol.2015.05.015

Forbes, N.S., Coffin, R.S., Deng, L., Evgin, L., Fiering, S., Giacalone, M., Gravekamp, C., Gulley, J.L., Gunn, H., Hoffman, R.M., Kaur, B., Liu, K., Lyerly, H.K., Marciscano, A.E., Moradian, E., Ruppel, S., Saltzman, D.A., Tattersall, P.J., Thorne, S., Vile, R.G., Zhang, H.H., Zhou, S., McFadden, G., 2018. White paper on microbial anti-cancer therapy and prevention. J. Immunother. Cancer 6, 1–24. https://doi.org/10.1186/s40425-018-0381-3

Galluzzi, L., Chan, T.A., Kroemer, G., Wolchok, J.D., López-Soto, A., 2018. The hallmarks of successful anticancer immunotherapy. Sci. Transl. Med. 10, 1–15. https://doi.org/10.1126/scitranslmed.aat7807

Galluzzi, L., Pietrocola, F., Bravo-San Pedro, J.M., Amaravadi, R.K., Baehrecke, E.H., Cecconi, F., Codogno, P., Debnath, J., Gewirtz, D.A., Karantza, V., Kimmelman, A., Kumar, S., Levine, B., Maiuri, M.C., Martin, S.J., Penninger, J., Piacentini, M., Rubinsztein, D.C., Simon, H., Simonsen, A., Thorburn, A.M., Velasco, G., Ryan, K.M., Kroemer, G., 2015. Autophagy in malignant transformation and cancer progression. EMBO J. 34, 856–880. https://doi.org/10.15252/embj.201490784

Gao, W., Wang, Xueying, Zhou, Y., Wang, Xueqian, Yu, Y., 2022. Autophagy, ferroptosis, pyroptosis, and necroptosis in tumor immunotherapy. Signal Transduct. Target. Ther. 7, 196. https://doi.org/10.1038/s41392-022-01046-3

Giles, J.R., Globig, A.-M., Kaech, S.M., Wherry, E.J., 2023. CD8+ T cells in the cancer-immunity cycle. Immunity 56, 2231–2253. https://doi.org/10.1016/j.immuni.2023.09.005

Giraldo, N.A., Becht, E., Vano, Y., Sautès-Fridman, C., Fridman, W.H., 2015. The immune response in cancer: from immunology to pathology to immunotherapy. Virchows Arch. 467, 127–135. https://doi.org/10.1007/s00428-015-1787-7

Gleisner, M.A., Pereda, C., Tittarelli, A., Navarrete, M., Fuentes, C., Ávalos, I., Tempio, F., Araya, J.P., Becker, M.I., González, F.E., López, M.N., Salazar-Onfray, F., 2020. A heat-shocked melanoma cell lysate vaccine enhances tumor infiltration by prototypic effector T cells inhibiting tumor growth. J. Immunother. Cancer 8. https://doi.org/10.1136/jitc-2020-000999

Gorabi, A.M., Hajighasemi, S., Sathyapalan, T., Sahebkar, A., 2020. Cell transfer-based immunotherapies in cancer: A review. IUBMB Life 72, 790–800. https://doi.org/10.1002/iub.2180

Goubran, H.A., Kotb, R.R., Stakiw, J., Emara, M.E., Burnouf, T., 2014. Regulation of Tumor Growth and Metastasis: The Role of Tumor Microenvironment. Cancer Growth Metastasis 7, CGM.S11285. https://doi.org/10.4137/CGM.S11285

Grille, S., Moreno, M., Bascuas, T., Marqués, J.M., Muñoz, N., Lens, D., Chabalgoity, J.A., 2014. Salmonella enterica serovar Typhimurium immunotherapy for B-cell lymphoma induces broad anti-tumour immunity with therapeutic effect. Immunology 143, 428–437. https://doi.org/10.1111/imm.12320

Grille, S., Moreno, M., Brugnini, A., Lens, D., Chabalgoity, J.A., 2013. A therapeutic vaccine using Salmonella-modified tumor cells combined with interleukin-2 induces enhanced antitumor immunity in B-cell lymphoma. Leuk. Res. 37, 341–348. https://doi.org/10.1016/j.leukres.2012.10.003

Hanahan, D., 2022. Hallmarks of Cancer: New Dimensions. Cancer Discov. 12, 31–46. https://doi.org/10.1158/2159-8290.CD-21-1059

Hernández-Luna, M.A., Luria-Pérez, R., 2018. Cancer Immunotherapy: Priming the Host Immune Response with Live Attenuated Salmonella enterica. J. Immunol. Res. 2018, 1–15. https://doi.org/10.1155/2018/2984247

Hodi, F.S., O'Day, S.J., McDermott, D.F., Weber, R.W., Sosman, J.A., Haanen, J.B., Gonzalez, R., Robert, C., Schadendorf, D., Hassel, J.C., Akerley, W., van den Eertwegh, A.J.M., Lutzky, J., Lorigan, P., Vaubel, J.M., Linette, G.P., Hogg, D., Ottensmeier, C.H., Lebbé, C., Peschel, C., Quirt, I., Clark, J.I., Wolchok, J.D., Weber, J.S., Tian, J., Yellin, M.J., Nichol, G.M., Hoos, A. and

Urba, W.J. (2010) Improved Survival with Ipilimumab in Patients with Metastatic Melanoma. New England Journal of Medicine, 363, 711–723. https://doi.org/10.1056/NEJMoa1003466.

Hos, N.J., Fischer, J., Murthy, A.M. V., Hejazi, Z., Krönke, M., Hos, D., Robinson, N., 2025. P62 inhibits IL-1β release during Salmonella Typhimurium infection of macrophages. Front. Cell. Infect. Microbiol. 15, 1–8. https://doi.org/10.3389/fcimb.2025.1495567

Jiang, T., Zhou, C., Ren, S., 2016. Role of IL-2 in cancer immunotherapy. Oncoimmunology 5, e1163462. https://doi.org/10.1080/2162402X.2016.1163462

Kalafati, L., Hatzioannou, A., Hajishengallis, G., Chavakis, T., 2022. The role of neutrophils in trained immunity. Immunol. Rev. https://doi.org/10.1111/imr.13142

Kalafati, L., Kourtzelis, I., Schulte-Schrepping, J., Li, X., Hatzioannou, A., Grinenko, T., Hagag, E., Sinha, A., Has, C., Dietz, S., de Jesus Domingues, A.M., Nati, M., Sormendi, S., Neuwirth, A., Chatzigeorgiou, A., Ziogas, A., Lesche, M., Dahl, A., Henry, I., Subramanian, P., Wielockx, B., Murray, P., Mirtschink, P., Chung, K.-J., Schultze, J.L., Netea, M.G., Hajishengallis, G., Verginis, P., Mitroulis, I., Chavakis, T., 2020. Innate Immune Training of Granulopoiesis Promotes Anti-tumor Activity. Cell 183, 771–785.e12. https://doi.org/10.1016/j.cell.2020.09.058

Khanduja, S., Bloom, S.M.K., Raman, V., Deshpande, C.P., Hall, C.L., Forbes, N.S., 2024. Intracellular delivery of oncolytic viruses with engineered Salmonella causes viral replication and cell death. iScience 27, 109813. https://doi.org/10.1016/j.isci.2024.109813

Klionsky, D.J., Abdel-Aziz, A.K., Abdelfatah, S., Abdellatif, M., Abdoli, A., Abel, S., Abeliovich, H., Abildgaard, M.H., Abudu, Y.P., Acevedo-Arozena, A., ..., Tong, C.K., 2021. Guidelines for the use and interpretation of assays for monitoring autophagy (4th edition)1. Autophagy 17, 1–382. https://doi.org/10.1080/15548627.2020.1797280

Kramer, M.G., Masner, M., Casales, E., Moreno, M., Smerdou, C., Chabalgoity, J.A., 2015. Neoadjuvant administration of Semliki Forest virus expressing interleukin-12 combined with attenuated Salmonella eradicates breast cancer metastasis and achieves long-term survival in immunocompetent mice. BMC Cancer 15, 1–15. https://doi.org/10.1186/s12885-015-1618-x

Kremenovic, M., Schenk, M., Lee, D.J., 2020. Clinical and molecular insights into BCG immunotherapy for melanoma. J. Intern. Med. 288, 625–640. https://doi.org/10.1111/joim.13037

Kuan, Y.D., Lee, C.H., 2016. Salmonella overcomes tumor immune tolerance by inhibition of tumor indoleamine 2, 3-dioxygenase 1 expression. Oncotarget 7, 374–385. https://doi.org/10.18632/ONCOTARGET.6258

Lamark, T., Johansen, T., 2021. Mechanisms of Selective Autophagy. Annu. Rev. Cell Dev. Biol. 37, 143–169. https://doi.org/10.1146/annurev-cellbio-120219-035530

Leach, D.R., Krummel, M.F., Allison, J.P., 1996. Enhancement of Antitumor Immunity by CTLA-4 Blockade. Science (80-.). 271, 1734–1736. https://doi.org/10.1126/science.271.5256.1734

Lee, C.-H., Lin, S.-T., Liu, J.-J., Chang, W.-W., Hsieh, J.-L., Wang, W.-K., 2014. Salmonella induce autophagy in melanoma by the downregulation of AKT/mTOR pathway. Gene Ther. 21,

309–316. https://doi.org/10.1038/gt.2013.86

Li, H., Breedijk, A., Dietrich, N., Nitschke, K., Jarczyk, J., Nuhn, P., Krämer, B.K., Yard, B.A., Leipe, J., Hauske, S., 2023. Lipopolysaccharide Tolerance in Human Primary Monocytes and Polarized Macrophages. Int. J. Mol. Sci. 24, 12196. https://doi.org/10.3390/ijms241512196

Li, S., Zou, Y., McMasters, A., Chen, F., Yan, J., 2025. Trained immunity: A new player in cancer immunotherapy. Elife 14, 1–20. https://doi.org/10.7554/elife.104920

Liang, K., Zhang, R., Luo, H., Zhang, J., Tian, Z., Zhang, X., Zhang, Y., Ali, M.K., Kong, Q., 2021. Optimized Attenuated Salmonella Typhimurium Suppressed Tumor Growth and Improved Survival in Mice. Front. Microbiol. 12. https://doi.org/10.3389/fmicb.2021.774490

Lin, H., Cheng, J., Mu, W., Zhou, J., Zhu, L., 2021. Advances in Universal CAR-T Cell Therapy. Front. Immunol. 12, 1–12. https://doi.org/10.3389/fimmu.2021.744823

Liu, B., Jiang, Y., Dong, T., Zhao, M., Wu, J., Li, L., Chu, Y., She, S., Zhao, H., Hoffman, R.M., Jia, L., 2016. Blockage of autophagy pathway enhances Salmonella tumor-targeting. Oncotarget 7, 22873–22882. https://doi.org/10.18632/oncotarget.8251

Livak, K.J., Schmittgen, T.D., 2001. Analysis of relative gene expression data using real-time quantitative PCR and the 2-ΔΔCT method. Methods 25, 402–408. https://doi.org/10.1006/meth.2001.1262

Lizana-Vasquez, G.D., Torres-Lugo, M., Dixon, R.B., Powderly, J.D., Warin, R.F., 2023. The application of autologous cancer immunotherapies in the age of memory-NK cells. Front. Immunol. 14, 1–20. https://doi.org/10.3389/fimmu.2023.1167666

López-Soto, A., Gonzalez, S., Smyth, M.J., Galluzzi, L., 2017. Control of Metastasis by NK Cells. Cancer Cell 32, 135–154. https://doi.org/10.1016/j.ccell.2017.06.009

Lu, M., Varley, A.W., Munford, R.S., 2013. Persistently Active Microbial Molecules Prolong Innate Immune Tolerance In Vivo. PLoS Pathog. 9, e1003339. https://doi.org/10.1371/journal.ppat.1003339

Martin, K.E., Hammer, Q., Perica, K., Sadelain, M., Malmberg, K.-J., 2024. Engineering immune-evasive allogeneic cellular immunotherapies. Nat. Rev. Immunol. 24, 680–693. https://doi.org/10.1038/s41577-024-01022-8

Martin, M.D., Badovinac, V.P., Griffith, T.S., 2020. CD4 T Cell Responses and the Sepsis-Induced Immunoparalysis State. Front. Immunol. 11, 1–11. https://doi.org/10.3389/fimmu.2020.01364

Mellman, I., Chen, D.S., Powles, T., Turley, S.J., 2023. The cancer-immunity cycle: Indication, genotype, and immunotype. Immunity 56, 2188–2205. https://doi.org/10.1016/j.immuni.2023.09.011

Mi, Z., Feng, Z.-C., Li, C., Yang, X., Ma, M.-T., Rong, P.-F., 2019. Salmonella -Mediated Cancer Therapy: An Innovative Therapeutic Strategy. J. Cancer 10, 4765–4776. https://doi.org/10.7150/jca.32650

Mittal, D., Gubin, M.M., Schreiber, R.D., Smyth, M.J., 2014. New insights into cancer immunoediting and its three component phases—elimination, equilibrium and escape.

Current opinion in immunology. 2014 Apr 1;27:16–25. Curr Opin Immunol 27, 16–25. https://doi.org/10.1016/j.coi.2014.01.004.

Mizushima, N., 2025. Autophagic flux measurement: Cargo degradation versus generation of degradation products. Curr. Opin. Cell Biol. 93, 102463. https://doi.org/10.1016/j.ceb.2025.102463

Mónaco, A., Chilibroste, S., Plata, M.C., Chabalgoity, J.A., Moreno, M., 2025. Salmonella–Induced Cell Death in Cancer Immunotherapy: What Lies Beneath? Biomedicines 14, 12. https://doi.org/10.3390/biomedicines14010012

Mónaco, A., Chilibroste, S., Yim, L., Chabalgoity, J.A., Moreno, M., 2022a. Inflammasome activation, NLRP3 engagement and macrophage recruitment to tumor microenvironment are all required for Salmonella antitumor effect. Cancer Immunol. Immunother. https://doi.org/10.1007/s00262–022–03148–x

Mónaco, A., Plata, M.C., Chilibroste, S., Vola, M., Chabalgoity, J.A., Moreno, M., 2022b. Salmonella–induced immune response reduces recurrence and tumor dissemination in preclinical melanoma model. Curr. Res. Immunol. 3, 159–166. https://doi.org/10.1016/j.crimmu.2022.08.001

Moreno, M., Kramer, M., Yim, L., Chabalgoity, J., 2010. Salmonella as Live Trojan Horse for Vaccine Development and Cancer Gene Therapy. Curr. Gene Ther. 10, 56–76. https://doi.org/10.2174/156652310790945566

Morinaga, S., Zhao, M., MIZUTA, K., KANG, B.M., BOUVET, M., YAMAMOTO, N., HAYASHI, K., KIMURA, H., MIWA, S., IGARASHI, K., HIGUCHI, T., TSUCHIYA, H., DEMURA, S., HOFFMAN, R.M., 2025. The Combination of Tumor–targeting Salmonella typhimurium A1–R Plus the Autophagy–inhibitor Chloroquine Synergistically Eradicates HT1080 Fibrosarcoma Cells In Vitro and In Vivo. In Vivo (Brooklyn). 39, 102–109. https://doi.org/10.21873/invivo.13807

Morvan, M.G., Lanier, L.L., 2016. NK cells and cancer: you can teach innate cells new tricks. Nat. Rev. Cancer 16, 7–19. https://doi.org/10.1038/nrc.2015.5

Muñoz, N., Van Maele, L., Marqués, J.M., Rial, A., Sirard, J.–C., Chabalgoity, J.A., 2010. Mucosal Administration of Flagellin Protects Mice from Streptococcus pneumoniae Lung Infection. Infect. Immun. 78, 4226–4233. https://doi.org/10.1128/IAI.00224–10

Murugan, S., Amaravadi, R.K., 2016. Methods for studying autophagy within the tumor microenvironment. Adv. Exp. Med. Biol. 899, 145–166. https://doi.org/10.1007/978–3–319–26666–4_9

Netea, M.G., Domínguez–Andrés, J., Barreiro, L.B., Chavakis, T., Divangahi, M., Fuchs, E., Joosten, L.A.B., van der Meer, J.W.M., Mhlanga, M.M., Mulder, W.J.M., Riksen, N.P., Schlitzer, A., Schultze, J.L., Stabell Benn, C., Sun, J.C., Xavier, R.J., Latz, E., 2020. Defining trained immunity and its role in health and disease. Nat. Rev. Immunol. 20, 375–388. https://doi.org/10.1038/s41577–020–0285–6

Netea, M.G., Joosten, L.A.B., Latz, E., Mills, K.H.G., Natoli, G., Stunnenberg, H.G., O'Neill, L.A.J., Xavier, R.J., 2016. Trained immunity: A program of innate immune memory in health and disease. Science (80–.). 352, 1–23. https://doi.org/10.1126/science.aaf1098

Ngiow, S.F., Von Scheidt, B., Akiba, H., Yagita, H., Teng, M.W.L., Smyth, M.J., 2011. Anti–TIM3

antibody promotes T cell IFN-γ-mediated antitumor immunity and suppresses established tumors. Cancer Res. 71, 3540–3551. https://doi.org/10.1158/0008-5472.CAN-11-0096

Novakovic, B., Habibi, E., Wang, S.Y., Arts, R.J.W., Davar, R., Megchelenbrink, W., Kim, B., Kuznetsova, T., Kox, M., Zwaag, J., Matarese, F., van Heeringen, S.J., Janssen-Megens, E.M., Sharifi, N., Wang, C., Keramati, F., Schoonenberg, V., Flicek, P., Clarke, L., Pickkers, P., Heath, S., Gut, I., Netea, M.G., Martens, J.H.A., Logie, C., Stunnenberg, H.G., 2016. β-Glucan Reverses the Epigenetic State of LPS-Induced Immunological Tolerance. Cell 167, 1354–1368.e14. https://doi.org/10.1016/j.cell.2016.09.034

O'Donnell, J.S., Teng, M.W.L., Smyth, M.J., 2019. Cancer immunoediting and resistance to T cell-based immunotherapy. Nat. Rev. Clin. Oncol. 16, 151–167. https://doi.org/10.1038/s41571-018-0142-8

Pangilinan, C.R., Lee, C.-H., 2019. Salmonella-Based Targeted Cancer Therapy: Updates on A Promising and Innovative Tumor Immunotherapeutic Strategy. Biomedicines 7, 36. https://doi.org/10.3390/biomedicines7020036

Papaioannou, N.E., Beniata, O. V., Vitsos, P., Tsitsilonis, O., Samara, P., 2016. Harnessing the immune system to improve cancer therapy. Ann. Transl. Med. 4, 261–261. https://doi.org/10.21037/atm.2016.04.01

Pastor, F., Gilboa, E., Frederick, J., Melero, I., Berraondo, P., Etxeberria, I., Sahin, U., 2018. An RNA toolbox for cancer immunotherapy. Nat. Rev. Drug Discov. 17, 751–767. https://doi.org/10.1038/nrd.2018.132

Pawelek, J.M., Low, K.B., Bermudes, D., 1997. Tumor-targeted salmonella as a novel anti-melanoma vector. Melanoma Res. 7, S141. https://doi.org/10.1097/00008390-199706001-00491

Pérez-Baños, A., Gleisner, M.A., Flores, I., Pereda, C., Navarrete, M., Araya, J.P., Navarro, G., Quezada-Monrás, C., Tittarelli, A., Salazar-Onfray, F., 2023. Whole tumour cell-based vaccines: tuning the instruments to orchestrate an optimal antitumour immune response. Br. J. Cancer 129, 572–585. https://doi.org/10.1038/s41416-023-02327-6

Pierce, K.M., Miklavcic, W.R., Cook, K.P., Hennen, M.S., Bayles, K.W., Hollingsworth, M.A., Brooks, A.E., Pullan, J.E., Dailey, K.M., 2021. The Evolution and Future of Targeted Cancer Therapy: From Nanoparticles, Oncolytic Viruses, and Oncolytic Bacteria to the Treatment of Solid Tumors. Nanomaterials 11, 3018. https://doi.org/10.3390/nano11113018

Polonelli, L., Magliani, W., Conti, S., Bracci, L., Lozzi, L., Neri, P., Adriani, D., De Bernardis, F., Cassone, A., 2003. Therapeutic Activity of an Engineered Synthetic Killer Antiidiotypic Antibody Fragment against Experimental Mucosal and Systemic Candidiasis. Infect. Immun. 71, 6205–6212. https://doi.org/10.1128/IAI.71.11.6205-6212.2003

Priem, B., van Leent, M.M.T., Teunissen, A.J.P., Sofias, A.M., Mourits, V.P., Willemsen, L., Klein, E.D., Oosterwijk, R.S., Meerwaldt, A.E., Munitz, J., Prévot, G., Vera Verschuur, A., Nauta, S.A., van Leeuwen, E.M., Fisher, E.L., de Jong, K.A.M., Zhao, Y., Toner, Y.C., Soultanidis, G., Calcagno, C., Bomans, P.H.H., Friedrich, H., Sommerdijk, N., Reiner, T., Duivenvoorden, R., Zupančič, E., Di Martino, J.S., Kluza, E., Rashidian, M., Ploegh, H.L., Dijkhuizen, R.M., Hak, S., Pérez-Medina, C., Bravo-Cordero, J.J., de Winther, M.P.J., Joosten, L.A.B., van Elsas, A., Fayad, Z.A., Rialdi, A., Torre, D., Guccione, E., Ochando, J., Netea, M.G., Griffioen, A.W.,

Mulder, W.J.M., 2020. Trained Immunity–Promoting Nanobiologic Therapy Suppresses Tumor Growth and Potentiates Checkpoint Inhibition. Cell 183, 786–801.e19. https://doi.org/10.1016/j.cell.2020.09.059

Rabinovich, G.A., Croci, D.O., 2012. Regulatory Circuits Mediated by Lectin–Glycan Interactions in Autoimmunity and Cancer. Immunity 36, 322–335. https://doi.org/10.1016/j.immuni.2012.03.004

Radha, G., Lopus, M., 2021. The spontaneous remission of cancer: Current insights and therapeutic significance. Transl. Oncol. 14, 101166. https://doi.org/10.1016/j.tranon.2021.101166

Rao, S., Tortola, L., Perlot, T., Wirnsberger, G., Novatchkova, M., Nitsch, R., Sykacek, P., Frank, L., Schramek, D., Komnenovic, V., Sigl, V., Aumayr, K., Schmauss, G., Fellner, N., Handschuh, S., Glösmann, M., Pasierbek, P., Schlederer, M., Resch, G.P., Ma, Y., Yang, H., Popper, H., Kenner, L., Kroemer, G., Penninger, J.M., 2014. A dual role for autophagy in a murine model of lung cancer. Nat. Commun. 5, 3056. https://doi.org/10.1038/ncomms4056

Robert, C. (2020) A Decade of Immune–Checkpoint Inhibitors in Cancer Therapy. Nature Communications, Springer US, 11, 3801. https://doi.org/10.1038/s41467–020–17670–y.

Rothermel, L.D., Zager, J.S., 2018. Engineered oncolytic viruses to treat melanoma: where are we now and what comes next? Expert Opin. Biol. Ther. 18, 1199–1207. https://doi.org/10.1080/14712598.2018.1544614

Rotte, A., Bhandaru, M., Zhou, Y., McElwee, K.J., 2015. Immunotherapy of melanoma: Present options and future promises. Cancer Metastasis Rev. 34, 115–128. https://doi.org/10.1007/s10555–014–9542–0

Roy, K., Kozłowski, H.M., Jędrzejewski, T., Sobocińska, J., Maciejewski, B., Dzialuk, A., Wrotek, S., 2023. Endotoxin Tolerance Creates Favourable Conditions for Cancer Development. Cancers (Basel). 15, 5113. https://doi.org/10.3390/cancers15205113

Schroeder, M.E., Russo, S., Costa, C., Hori, J., Tiscornia, I., Bollati–Fogolín, M., Zamboni, D.S., Ferreira, G., Cairoli, E., Hill, M., 2017. Pro–inflammatory Ca++–activated K+ channels are inhibited by hydroxychloroquine. Sci. Rep. 7, 1892. https://doi.org/10.1038/s41598–017–01836–8

Seeley, J.J., Baker, R.G., Mohamed, G., Bruns, T., Hayden, M.S., Deshmukh, S.D., Freedberg, D.E., Ghosh, S., 2018. Induction of innate immune memory via microRNA targeting of chromatin remodelling factors. Nature 559, 114–119. https://doi.org/10.1038/s41586–018–0253–5

Sharma, P., 2016. Immune checkpoint therapy and the search for predictive biomarkers. Cancer J. (United States) 22, 68–72. https://doi.org/10.1097/PPO.0000000000000185

Sharma, P., Allison, J.P., 2015. Immune Checkpoint Targeting in Cancer Therapy: Toward Combination Strategies with Curative Potential. Cell 161, 205–214. https://doi.org/10.1016/j.cell.2015.03.030

Shi, C.–S., Shenderov, K., Huang, N.–N., Kabat, J., Abu–Asab, M., Fitzgerald, K.A., Sher, A., Kehrl, J.H., 2012. Activation of autophagy by inflammatory signals limits IL–1β production by targeting ubiquitinated inflammasomes for destruction. Nat. Immunol. 13, 255–263.

https://doi.org/10.1038/ni.2215

Shi, C., Pamer, E.G., 2011. Monocyte recruitment during infection and inflammation. Nat. Rev. Immunol. 11, 762–774. https://doi.org/10.1038/nri3070

Silva, E.E., Skon-Hegg, C., Badovinac, V.P., Griffith, T.S., 2023. The Calm after the Storm: Implications of Sepsis Immunoparalysis on Host Immunity. J. Immunol. 211, 711–719. https://doi.org/10.4049/jimmunol.2300171

Singer, Z.S., Pabón, J., Huang, H., Sun, W., Luo, H., Grant, K.R., Obi, I., Coker, C., Rice, C.M., Danino, T., 2025. Engineered bacteria launch and control an oncolytic virus. Nat. Biomed. Eng. 84, 6906–6906. https://doi.org/10.1038/s41551-025-01476-8

Singh, A.K., Netea, M.G., Bishai, W.R., 2021. BCG turns 100: its nontraditional uses against viruses, cancer, and immunologic diseases. J. Clin. Invest. 131, 1–11. https://doi.org/10.1172/JCI148291

Singh, P.P., Sharma, P.K., Krishnan, G., Lockhart, A.C., 2015. Immune checkpoints and immunotherapy for colorectal cancer. Gastroenterol. Rep. 3, 289–297. https://doi.org/10.1093/gastro/gov053

Tang, R., Xu, J., Zhang, B., Liu, J., Liang, C., Hua, J., Meng, Q., Yu, X., Shi, S., 2020. Ferroptosis, necroptosis, and pyroptosis in anticancer immunity. J. Hematol. Oncol. 13, 110. https://doi.org/10.1186/s13045-020-00946-7

Tattoli, I., Sorbara, M.T., Philpott, D.J., Girardin, S.E., 2012. Bacterial autophagy. Autophagy 8, 1848–1850. https://doi.org/10.4161/auto.21863

Töpfer, K., Kempe, S., Müller, N., Schmitz, M., Bachmann, M., Cartellieri, M., Schackert, G., Temme, A., 2011. Tumor evasion from T cell surveillance. J. Biomed. Biotechnol. 2011. https://doi.org/10.1155/2011/918471

Towers, C.G., Wodetzki, D., Thorburn, A., 2019. Autophagy and cancer: Modulation of cell death pathways and cancer cell adaptations. J. Cell Biol. 219, jcb.201909033. https://doi.org/10.1083/jcb.201909033

Tsai, C.-H., Chuang, Y.-M., Li, X., Yu, Y.-R., Tzeng, S.-F., Teoh, S.T., Lindblad, K.E., Di Matteo, M., Cheng, W.-C., Hsueh, P.-C., Kao, K.-C., Imrichova, H., Duan, L., Gallart-Ayala, H., Hsiao, P.-W., Mazzone, M., Ivanesevic, J., Liu, X., de Visser, K.E., Lujambio, A., Lunt, S.Y., Kaech, S.M., Ho, P.-C., 2023. Immunoediting instructs tumor metabolic reprogramming to support immune evasion. Cell Metab. 35, 118–133.e7. https://doi.org/10.1016/j.cmet.2022.12.003

Uscanga-Palomeque, A.C., Chávez-Escamilla, A.K., Alvizo-Báez, C.A., Saavedra-Alonso, S., Terrazas-Armendáriz, L.D., Tamez-Guerra, R.S., Rodríguez-Padilla, C., Alcocer-González, J.M., 2023. CAR-T Cell Therapy: From the Shop to Cancer Therapy. Int. J. Mol. Sci. 24, 15688. https://doi.org/10.3390/ijms242115688

Van Leeuwen, M.T., Webster, A.C., McCredie, M.R.E., Stewart, J.H., McDonald, S.P., Amin, J., Kaldor, J.M., Chapman, J.R., Vajdic, C., Grulich, A.E., 2010. Effect of reduced immunosuppression after kidney transplant failure on risk of cancer: Population based retrospective cohort study. BMJ 340, 463. https://doi.org/10.1136/bmj.c570

Van Puffelen, J.H., Keating, S.T., Oosterwijk, E., van der Heijden, A.G., Netea, M.G., Joosten, L.A.B.,

Vermeulen, S.H., 2020. Trained immunity as a molecular mechanism for BCG immunotherapy in bladder cancer. Nat. Rev. Urol. 17, 513–525. https://doi.org/10.1038/s41585-020-0346-4

Varadé, J., Magadán, S., González-Fernández, Á., 2021. Human immunology and immunotherapy: main achievements and challenges. Cell. Mol. Immunol. 18, 805–828. https://doi.org/10.1038/s41423-020-00530-6

Vesely, M.D., Kershaw, M.H., Schreiber, R.D., Smyth, M.J., 2011. Natural innate and adaptive immunity to cancer. Annu. Rev. Immunol. 29, 235–271. https://doi.org/10.1146/annurev-immunol-031210-101324

Vola, M., Mónaco, A., Bascuas, T., Rimsky, G., Agorio, C.I., Chabalgoity, J.A., Moreno, M., 2018. TLR7 agonist in combination with Salmonella as an effective antimelanoma immunotherapy. Immunotherapy 10, 665–679. https://doi.org/10.2217/imt-2017-0188

Vuscan, P., Kischkel, B., Joosten, L.A.B., Netea, M.G., 2025. Microbial-induced trained immunity for cancer immunotherapy. Pharmacol. Rev. 77, 100074. https://doi.org/10.1016/j.pharmr.2025.100074

Vuscan, P., Kischkel, B., Joosten, L.A.B., Netea, M.G., 2024. Trained immunity: General and emerging concepts. Immunol. Rev. 164–185. https://doi.org/10.1111/imr.13326

Watanabe, H., Rana, M., Son, M., Chiu, P.Y., Fei-Bloom, Y., Choi, K., Diamond, B., Sherry, B., 2024. Single cell RNA-seq reveals cellular and transcriptional heterogeneity in the splenic CD11b+Ly6Chigh monocyte population expanded in sepsis-surviving mice. Mol. Med. 30, 202. https://doi.org/10.1186/s10020-024-00970-0

Weber, G.F., 2007. Molecular Mechanisms of Cancer, Springer. Dordrecht, The Netherlands : Springer c2007.

Wei, S.C., Levine, J.H., Cogdill, A.P., Zhao, Y., Anang, N.-A.A.S., Andrews, M.C., Sharma, P., Wang, J., Wargo, J.A., Pe'er, D., Allison, J.P., 2017. Distinct Cellular Mechanisms Underlie Anti-CTLA-4 and Anti-PD-1 Checkpoint Blockade. Cell 170, 1120–1133.e17. https://doi.org/10.1016/j.cell.2017.07.024

White, E., 2012. Deconvoluting the context-dependent role for autophagy in cancer. Nat. Rev. Cancer 12, 401–410. https://doi.org/10.1038/nrc3262

Wu, J., 2013. IL-15 Agonists: The Cancer Cure Cytokine. J. Mol. Genet. Med. 07, 1–6. https://doi.org/10.4172/1747-0862.1000085

Wu, L.-H., Pangilinan, C.R., Lee, C.-H., 2022. Downregulation of AKT/mTOR signaling pathway for Salmonella -mediated autophagy in human anaplastic thyroid cancer. J. Cancer 13, 3268–3279. https://doi.org/10.7150/jca.75163

Wu, L., Li, L., Li, S., Liu, L., Xin, W., Li, C., Yin, X., Xu, X., Bao, F., Hua, Z., 2022. Macrophage-mediated tumor-targeted delivery of engineered Salmonella typhimurium VNP20009 in anti-PD1 therapy against melanoma. Acta Pharm. Sin. B 12, 3952–3971. https://doi.org/10.1016/j.apsb.2022.05.006

Wu, S., Shen, Y., Zhang, S., Xiao, Y., Shi, S., 2020. Salmonella Interacts With Autophagy to Offense or Defense. Front. Microbiol. 11, 1–13. https://doi.org/10.3389/fmicb.2020.00721

Xia, M., Wang, B., Wang, Z., Zhang, X., Wang, X., 2021. Epigenetic Regulation of NK Cell–Mediated Antitumor Immunity. Front. Immunol. 12, 1–13. https://doi.org/10.3389/fimmu.2021.672328

Xie, Y., Xie, F., Zhang, Lei, Zhou, X., Huang, J., Wang, F., Jin, J., Zhang, Long, Zeng, L., Zhou, F., 2021. Targeted Anti-Tumor Immunotherapy Using Tumor Infiltrating Cells. Adv. Sci. 8, 2101672. https://doi.org/10.1002/advs.202101672

Yang, Y., Hu, L., Zheng, H., Mao, C., Hu, W., Xiong, K., Wang, F., Liu, C., 2013. Application and interpretation of current autophagy inhibitors and activators. Acta Pharmacol. Sin. 34, 625–635. https://doi.org/10.1038/aps.2013.5

Yoon, W., Park, Yongsung, Kim, S., Park, Yongkeun, Kim, C.Y., 2021. Combined Therapy with microRNA–Expressing Salmonella and Irradiation in Melanoma. Microorganisms 9, 2408. https://doi.org/10.3390/microorganisms9112408

Yu, X., Qian, J., Ding, L., Yin, S., Zhou, L., Zheng, S., 2023. Galectin–1: A Traditionally Immunosuppressive Protein Displays Context–Dependent Capacities. Int. J. Mol. Sci. 24, 6501. https://doi.org/10.3390/ijms24076501

Zhang, X., Xu, Q., Zhang, Z., Cheng, W., Cao, W., Jiang, C., Han, C., Li, J., Hua, Z., 2016. Chloroquine enhanced the anticancer capacity of VNP20009 by inhibiting autophagy. Sci. Rep. 6, 29774. https://doi.org/10.1038/srep29774

Zhang, Y., Zhang, Z., 2020. The history and advances in cancer immunotherapy: understanding the characteristics of tumor–infiltrating immune cells and their therapeutic implications. Cell. Mol. Immunol. 17, 807–821. https://doi.org/10.1038/s41423–020–0488–6

Zheng, Y.T., Shahnazari, S., Brech, A., Lamark, T., Johansen, T., Brumell, J.H., 2009. The Adaptor Protein p62/SQSTM1 Targets Invading Bacteria to the Autophagy Pathway. J. Immunol. 183, 5909–5916. https://doi.org/10.4049/jimmunol.0900441

9. ANEXO

Lista de artículos publicados en revistas arbitradas en el período del doctorado

PRIMERA AUTORA:

1 – Chilibroste, S., dos Santos, J.C., Mónaco, A., Joosten, L.A.B., Moreno, M., Chabalgoity, J.A., 2025. *Salmonella* LVR01 triggers antagonistic two-armed innate immune memory that impacts on antitumor efficacy. Front. Immunol. 16, 1–13. https://doi.org/10.3389/fimmu.2025.1535131

CO-AUTORA:

1 – Mónaco, A., Chilibroste, S., Plata, M.C., Chabalgoity, J.A., Moreno, M., 2025. *Salmonella*-Induced Cell Death in Cancer Immunotherapy: What Lies Beneath? Biomedicines 14, 12. https://doi.org/10.3390/biomedicines14010012

2 – Dos Santos, J.C., Moreno, M., Teufel, L.U., Chilibroste, S., Keating, S.T., Groh, L., Domínguez-Andrés, J., Williams, D.L., Ma, Z., Lowman, D.W., Ensley, H.E., Novakovic, B., Ribeiro-Dias, F., Netea, M.G., Chabalgoity, J.A., Joosten, L.A.B., 2024. *Leishmania braziliensis* enhances monocyte responses to promote anti-tumor activity. Cell Rep. 43, 113932. https://doi.org/10.1016/j.celrep.2024.113932

3 – Mónaco, A., Plata, M.C., Chilibroste, S., Vola, M., Chabalgoity, J.A., Moreno, M., 2022. *Salmonella*-induced immune response reduces recurrence and tumor dissemination in preclinical melanoma model. Curr. Res. Immunol. 3, 159–166. https://doi.org/10.1016/j.crimmu.2022.08.001

frontiers | Frontiers in Immunology

TYPE Original Research
PUBLISHED 30 April 2025
DOI 10.3389/fimmu.2025.1535131

Check for updates

OPEN ACCESS

EDITED BY
Ana Carolina Martinez-Torres,
Autonomous University of Nuevo León, Mexico

REVIEWED BY
Paola Italiani,
National Research Council (CNR), Italy
Trim Lajqi,
Heidelberg University Hospital, Germany
Kenny Calvillo,
Autonomous University of Nuevo León, Mexico

*CORRESPONDENCE
José A. Chabalgoity
jachabal@higiene.edu.uy
María Moreno
mmoreno@higiene.edu.uy

RECEIVED 26 November 2024
ACCEPTED 08 April 2025
PUBLISHED 30 April 2025

CITATION
Chilibroste S, dos Santos JC, Mónaco A, Joosten LAB, Moreno M and Chabalgoity JA (2025) *Salmonella* LVR01 triggers antagonistic two-armed innate immune memory that impacts on antitumor efficacy. *Front. Immunol.* 16:1535131. doi: 10.3389/fimmu.2025.1535131

COPYRIGHT
© 2025 Chilibroste, dos Santos, Mónaco, Joosten, Moreno and Chabalgoity. This is an open-access article distributed under the terms of the Creative Commons Attribution License (CC BY). The use, distribution or reproduction in other forums is permitted, provided the original author(s) and the copyright owner(s) are credited and that the original publication in this journal is cited, in accordance with accepted academic practice. No use, distribution or reproduction is permitted which does not comply with these terms.

Salmonella LVR01 triggers antagonistic two-armed innate immune memory that impacts on antitumor efficacy

Sofía Chilibroste[1], Jéssica C. dos Santos[2], Amy Mónaco[1], Leo A. B. Joosten[2,3], María Moreno[1*] and José A. Chabalgoity[1*]

[1]Departamento de Desarrollo Biotecnológico, Instituto de Higiene, Facultad de Medicina, Universidad de la República, Montevideo, Uruguay, [2]Department of Internal Medicine, Radboud University Medical Center, Nijmegen, Netherlands, [3]Department of Medical Genetics, Iuliu Hatieganu University of Medicine and Pharmacy, Cluj-Napoca, Romania

The current understanding of innate immune memory encompasses both trained immunity and immune tolerance, where cells can exhibit enhanced responsiveness or immune paralysis upon subsequent stimuli, respectively. Various agents induce either of these responses, including β-glucan, *Leishmania*, BCG and LPS. BCG is a clinically approved immunotherapy for bladder cancer and BCG-induced trained immunity is important in driving anti-tumor adaptive immunity. *Salmonella* also shows promise in cancer treatment, eliciting potent anti-tumor immune responses, but with transitory effects. This led us to investigate whether *Salmonella* LVR01, like BCG, triggers trained immunity and its impact on anti-tumor responses. Herein, we report that *Salmonella* induces an enhanced response in bone marrow cells, characterized by a robust cytokine response upon a second stimulus, in a fashion that resembles trained immunity. Coherently with that, *Salmonella* administration induces enhanced responsiveness to a tumor implanted later in time, resulting in slow tumor growth and extended survival. However, *in vitro* stimulation of human monocytes and murine bone-marrow derived myeloid-enriched cells with *Salmonella* results in decreased production of cytokines resembling immune paralysis. Overall, our results suggest that *Salmonella* LVR01 induces enhanced responses of innate immune memory, as well as paralysis on monocytes. These two antagonistic effects could be the basis of the transitory effect of *Salmonella* treatment and suggest that further investigation on these phenomena could shed light on how to improve *Salmonella*-based immunotherapies for cancer.

KEYWORDS

***Salmonella*, innate immune memory, trained immunity, tolerance, cancer immunotherapies, anti-tumor Immunity**

1 Introduction

Innate immune memory has been thoroughly explored in the context of diseases, revealing various underlying mechanisms. Innate immune cells exhibit the capability for epigenetic reprogramming in response to a stimulus, resulting in increased responsiveness to subsequent stimuli, known as trained immunity, or a shift towards a state of tolerance characterized by a diminished response and immune paralysis (1–3). Lipopolysaccharide (LPS) has been established as a key inducer of tolerance, while agents like *Candida albicans*, β-glucan, *Leishmania* species lysates, and Bacillus Calmette-Guérin (BCG) have been recognized for their role in promoting trained immunity (4–6). Our interest lies in BCG because it is a live attenuated vaccine with diverse applications, serving both as an anti-tuberculosis vaccine and an immunotherapeutic agent for cancer treatment (7, 8). In our research, we employ an attenuated strain of *Salmonella* Typhimurium for cancer immunotherapy and have noted significant similarities between the application of BCG and *Salmonella* in cancer treatment scenarios. Both bacteria share the characteristic of being capable of eliciting an immune response against neoplastic cells (9–12). Initially, they activate the innate immune system by signaling through microbial-associated molecular patterns (MAMPs) and damage-associated molecular patterns (DAMPs), ensuing from the controlled initial infection (13, 14). Subsequently, they elicit an adaptive immune response directed against tumor cells, with the induction of immunogenic cell death, which provides antigens and signaling, facilitating T and B cell response (14, 15). The presence of LPS on the surface of *Salmonella*, as a difference from BCG, cannot be overlooked, given its well-established role as a potent inducer of innate immune tolerance (16). Moreover, LPS significantly contributes to the anti-tumor response by triggering the initial immune response (17). Hence, we are motivated to investigate whether *Salmonella*, analogously to BCG, can induce trained immunity and if this mechanism contributes to the anti-tumor response. *In vitro* experiments demonstrated that *Salmonella* induces immune tolerance in adherent monocytes, but not in other bone marrow-derived cells, likely attributable to robust initial stimuli. However, intriguingly, our *in vivo* investigations revealed that prophylactic administration of *Salmonella* in mice elicits a strong cytokine response throughout the bone marrow cells and confers protection against cancer upon pre-treatment. These results suggest that *Salmonella* could promote heterologous immunomodulation useful in the prevention of cancer through the modulation of the innate immune environment.

2 Materials and methods

2.1 Cell lines

B16F10 melanoma cells were purchased from ATCC (CRL-6475) and maintained in DMEM medium (Capricorn Scientific, cat. DMEM-HPSTA) supplemented with 10% fetal bovine serum (Capricorn Scientific, cat. FBS-11A) at 37 °C in 5% CO_2 atmosphere.

A20 lymphoma cells were purchased from ATCC (TIB-208) and maintained in RPMI-1640 medium (Capricorn Scientific, cat. RPMI-STA) supplemented with 10% fetal bovine serum (Capricorn Scientific, cat. FBS-11A), 0.05 mM 2-mercaptoethanol (Sigma-Aldrich), 1 mM sodium pyruvate (Sigma-Aldrich), and additional 2.5 g/L D-glucose (Sigma-Aldrich) at 37 °C in 5% CO_2 atmosphere.

2.2 Bacterial strain

Salmonella enterica serovar Typhimurium LVR01, an attenuated strain constructed by introducing a null deletion into the *aroC* gene of the parental canine *S.* Typhimurium isolate P228067 (18), was employed in the present study. Bacteria were routinely cultured at 37 °C in LB broth (Difco), shaken at 200 rpm overnight and stored at -80 °C in 15% glycerol stocks until needed. For *in vivo* experiments, bacteria were thawed and resuspended in saline solution to a final concentration of 1 x 10^7 CFU/ml. The bacterial inoculum was verified through serial dilution and plating in LB agar (LBA, Difco).

2.3 *Leishmania* parasites

Leishmania braziliensis strains were obtained from Leishbank IPTSP/UFG (Goia´s, Brazil). Promastigote forms were cultured in Grace's insect medium (Gibco, Life Technologies, USA) supplemented with 20% of heat-inactivated fetal bovine serum (FBS, Gibco, Life Technologies, USA) and 100 U/mL of penicillin/streptomycin (Sigma-Aldrich) at 26 °C. Stationary-phase parasites were obtained on the 6th day of growth and washed three times with PBS (1000 xg, 10 min 10°C). After, they were suspended in PBS and quantified by using hemocytometer after fixation with PBS/0.4% formaldehyde. Parasite lysates were obtained by 5 freeze-thaw cycles of promastigotes in the presence of protease inhibitors (Protease inhibitor cocktail, Sigma-Aldrich) in liquid nitrogen followed by thawing in a water bath at 37 °C. Protein quantification was performed by using Pierce BCA protein assay kit (ThermoFisher Scientific, USA).

2.4 Adherent human monocyte isolation

Monocytes were isolated from buffy coats obtained from healthy donors (Sanquin Blood Bank, Nijmegen, the Netherlands). Peripheral blood mononuclear cells (PMBCs) were isolated by differential density centrifugation over Ficoll-Paque (GE Healthcare) of blood diluted in PBS. Cells were washed three times with PBS and quantified. PMBCs were put on a hyperosmotic Percoll solution (48.5% Percoll (Sigma-Aldrich), 41.5% sterile H_2O, 0.16 M filter-sterilized NaCl) and centrifuged for 15 min at 580 xg, 4 °C. The interphase layer was isolated, and cells were washed once with cold PBS and suspended in Dutch-modified RPMI 1640 culture medium (Invitrogen) supplemented with 5 µg/mL gentamicin (Centraform), 2 mM Glutamax (Gibco) and 1 mM

pyruvate (Gibco) and counted. Finally, adherent monocytes were isolated by allowing Percoll-isolated monocytes to adhere to polystyrene flat-bottom plates (Corning) for 1 h at 37°C; the cells were washed with warm PBS to obtain maximal purity (7).

2.5 *In vitro* induction of trained immunity in human adherent monocytes

Cells were incubated with culture medium supplemented with 10% human pooled serum together with different stimuli: supplemented medium as a negative control, 25 µg/ml of *L. braziliensis* lysates as a positive control (5), different MOI (multiplicity of infection) of LVR01:cells (1:1, 1:2, 1:4, 1:8, 1:16, 1:32) and heat-killed (hk) LVR01. After 1 h, cells were washed with warm PBS and culture medium with gentamicin was added. After 24 h, supernatants were collected and stored at -20°C until further use. After 3 days, culture medium was refreshed. On day 6, cells were restimulated with culture medium without serum, 10 ng/mL LPS (Sigma-Aldrich) or 10 µg/mL Pam_3Cys (Sigma-Aldrich). After 24 h, supernatants were collected and stored at -20°C until further use.

2.6 Mice

Female C57BL/6 and BALB/C mice (Dilave, Uruguay), 6–8 weeks old, were used for *in vivo* experiments. Animals were housed on 12:12 h light/dark cycles with controlled temperature (22 ± 2°C) and humidity (60%), with water and food *ad libitum*. All animal experimentation protocols were approved by the University's Ethical Committee for Animal Experimentation, Uruguay (protocol number 1329).

2.7 *In vitro* induction of trained immunity in murine bone marrow-derived enriched myeloid cells

Fresh bone marrow cells were isolated from the femurs of C57BL/6 and BALB/C mice. Bone marrow was aseptically removed, and cells were incubated with Lysis Buffer (155 mM NH_4Cl, 10 mM $KHCO_3$ in sterile H_20), filtered through a 40 µm cell strainer (Corning 431750, Sigma-Aldrich), and resuspended in RPMI (Capricorn Scientific, cat. RPMI-STA) supplemented with 10% fetal bovine serum (Capricorn Scientific, cat. FBS-11A), Penicillin-Streptomycin (Capricorn Scientific, cat. PS-B) and 1 mM sodium pyruvate (Sigma-Aldrich). Cells were counted and plated in a 96 well flat bottom plate (1 x 10^6 cells/well). During the first 24 h cells were stimulated with 50 µg/ml of L. *braziliensis* lysates (positive control), 1 x 10^6 CFU of hk *Salmonella* LVR01, or supplemented medium (negative control). Subsequently, cells were washed with 200 µl of warm PBS to wash away the stimuli and non-adherent cells, and fresh medium was added. After 3 days, culture medium was refreshed. After six days of total rest, cells were restimulated with culture medium without serum, 10 ng/ml LPS (Invivogen) or 100 µg/ml Poly I:C (Sigma-Aldrich). After 24 h, supernatants were collected and stored at -80°C until further use.

2.8 *Ex vivo* evaluation of *in vivo* trained immunity model

To investigate the effect of inducing trained immunity on the bone marrow, mice were inoculated intraperitoneally (i.p) with saline or 1x10^6 CFU of Salmonella LVR01. After 6 days, bone marrow was removed. 1 x 10^5 bone marrow cells were cultured per well in two different plates One plate was immediately restimulated *ex vivo* with LPS (10 ng/ml), and 24 hours later, the supernatant was collected to detect cytokine levels. Besides, adherent cells were characterized by flow cytometry (Supplementary Figure 1). On the other plate, adherent cells derived from bone marrow were allowed to rest for 6 days and then restimulated with LPS (10 ng/ml), 24 hours after, the supernatant was collected.

For *in vivo* trained immunity immunization experiments, mice were inoculated with saline or LVR01 i.p, and 7 days later, 35 µg/dose LPS from *E. coli* (Invivogen) was administered i.p. 24 hours before the second stimulus and 90 minutes after, blood was collected and centrifuged at 6000 rpm for 10 minutes to obtain the serum for detection of cytokine levels.

2.8.1 Flow cytometry

Bone marrow was removed as described above and cells were restimulated *ex vivo* with LPS (10 ng/ml) or allowed to rest for 6 days and then restimulated with LPS (10 ng/ml) or PolyIC (100 µg/ml), as described above (section 2.8). After 1 h of LPS or PolyIC stimulation, cells were treated with GolgiPlug, and four hours later, the cells were stained for surface marker, and then fixed, permeabilized and intracellularly stained for cytokines following the manufacturer's instructions. Cells were stained with antibodies against CD11b, Ly6G, Ly6C, CD49b, TNF and IL-6 (BD Pharmingen and Biolegend).

Flow cytometry data were acquired on a FACS Canto II cytometer (BD Biosciences). Data was analyzed using FACS Diva software and FlowJo10.10 (BD Biosciences). High dimensional data analysis was performed using tSNE for dimensionality reduction, X-Shift for clustering, Cluster Explorer and Euclid for clustering quality control.

2.9 Tumor models and immunization

For the prophylactic approach in mice, 1 x 10^6 CFU of *Salmonella* LVR01 were i.p administered one week or one month before tumor implantation.

Tumor implantation: B16F10 and A20 cell lines were grown in culture and harvested in log phase. Then, cells were washed and resuspended in saline, resulting in final concentrations of 2.5 x 10^6 cells/ml or 5 x 10^6 cells/ml, respectively. Mice were injected subcutaneously (s.c.) into the right flank with 0.1 ml or 0.2 ml,

respectively. Tumor measurements were taken every other day with a microcaliper, and tumor volumes were calculated using the formula length x width x depth x π/6. Euthanasia was carried out by cervical dislocation when tumors reached 2000 mm^3 or earlier if animals displayed signs of distress.

2.9.1 Flow cytometry

On day 14 or 17 post tumor implantation, mice were sacrificed and tumors were removed. Single cell suspensions were obtained by mechanical disaggregation. Cells were stained with antibodies against CD45, CD11b, NK1.1 or CD49b and CD8 (BD Pharmingen and Biolegend).

Mice were sacrificed at day 3, 6, 9, 22 and 27 post LVR01-treatment; blood, bone marrow and tumor tissue when available (at days 22 and 27) were removed. Red blood cells were then lysed using the Qiagen Erythrocyte Lysis Buffer (Cat No 79217). Following the manufacturer's suggestions, cells were prepared as described above and stained with antibodies against CD45, CD11b, Ly6G, CD49b and F4/80 (BD Pharmingen and Biolegend).

Data acquisition and analysis were performed as described above.

2.9.2 Gene expression analysis

In independent experiments, mice were sacrificed at day 14 post-tumor implantation, and tumors were removed, collected in TRizol reagent (Invitrogen) and stored at -80°C until processed as previously described (19). Following retrotranscription, quantitative RT-PCR for *Tnf, Il6, Ifng, Il12, Cxcl1, Cxcl2, Cxcl9, Cxcl10, Il1a, Il1b, Ccl2, Ccl3, Ccl4, Ccl5, Ccl20* and *Tlr4* mRNA were conducted using QuantiTect® SYBR® Green PCR Kit (Qiagen) in a Rotor-Gene 6000 (Corbett), primer sequences are available under request. This panel was based on our previous work with modifications (15). β-actin encoding gene was used as the housekeeping gene. The relative mRNA amount in each sample was calculated using the $2^{-\Delta\Delta Ct}$ method as previously described (20) where $\Delta Ct = Ct_{\text{gene of interest}} - Ct_{\text{housekeeping}}$, and expressed as relative mRNA levels in the test groups compared to the control group.

2.10 ELISA

Cytokine production was measured in cell culture supernatants or mouse sera using commercial ELISA kits for humans or mice (R&D Systems and Biolegend, respectively), following the manufacturer's instructions.

2.11 Lactate assay

Lactate concentrations were measured in cell culture supernatants on days 1 and 6 of the training protocol using a coupled enzymatic assay in which lactate was oxidized. The resulting H_2O_2 was coupled to the conversion of Amplex Red (Life Technologies) reagent to fluorescent resorufin by HRP (horseradish peroxidase, Thermo Scientific) (21).

2.12 Statistical analysis

Differences in survival times were determined using Kaplan–Meier and log-rank tests using GraphPad Prism 8 software. The statistical significance of differences between study groups was analyzed using the Student T-test. In every case, $p < 0.05$ was considered statistically significant.

3 Results

3.1 *Salmonella* induces trained immunity-like response in whole bone marrow cells but immune tolerance in bone marrow-derived myeloid-enriched cells

To evaluate the capability of *Salmonella* LVR01 to promote a stronger response upon a second stimulus, mice underwent pre-treatment with *Salmonella* or PBS as control, and after 6 days, bone marrow cells were extracted. The entire bone marrow samples were subsequently restimulated *ex vivo* with LPS. Following a 24-hour incubation period, levels of IL-6 and TNF were measured in supernatants. Both cytokines were increased in the LVR01-treated group in comparison with the PBS-control group (Figures 1a–c). Additionally, after 4 hours of stimulation, cells were treated with GolgiPlug for intracellular staining to ascertain which bone marrow cells were responsible for the production of these cytokines (Figure 1d). In agreement with cytokine concentration, we found that LVR01-trained mice presented a greater percentage of TNF-producing cells in BM than in unprimed mice upon a second stimulus (Figure 1e). Given the important role of neutrophils and NK cells in the anti-tumoral effect of *Salmonella* LVR01 (15) and that both cell types can be trained, we investigated whether these cells were responsible for the production of proinflammatory cytokines and found that TNF-producing cells were not NK cells (Figure 1f). However, we found that the source of TNF was $CD11b^+$ myeloid cells, mainly double-positive $Ly6C^+$ $Ly6G^+$ population (probably neutrophils, and not myeloid-derived suppressor cells (MDSC), due to its potential to produce pro-inflammatory cytokines), and Ly6C high monocytes. A similar scenario was observed upon a different second stimulus, i.e. Poly I:C (Figures 1e, f). We next used t-distributed stochastic neighbor embedding (tSNE) to perform an unsupervised analysis of the flow cytometry dataset generated from different conditions (Control+LPS and LVR01+LPS). Single-cell events were exported, concatenated, and displayed in a single tSNE heatmap plot for each condition. Heatmap representations of the expression levels of different markers defined clusters of cells (Figure 1g). A comparison of the different conditions showed that all cells producing TNF in the bone marrow are myeloid cell types that express CD11b markers. Intracellular IL-6 production could not be detected under these conditions.

However, when bone marrow cells were allowed to adhere (and non-adherent cells were removed) to obtained a myeloid-enriched cell population (Supplementary Figure 1), and then to rest in culture

10.3389/fimmu.2025.1535131

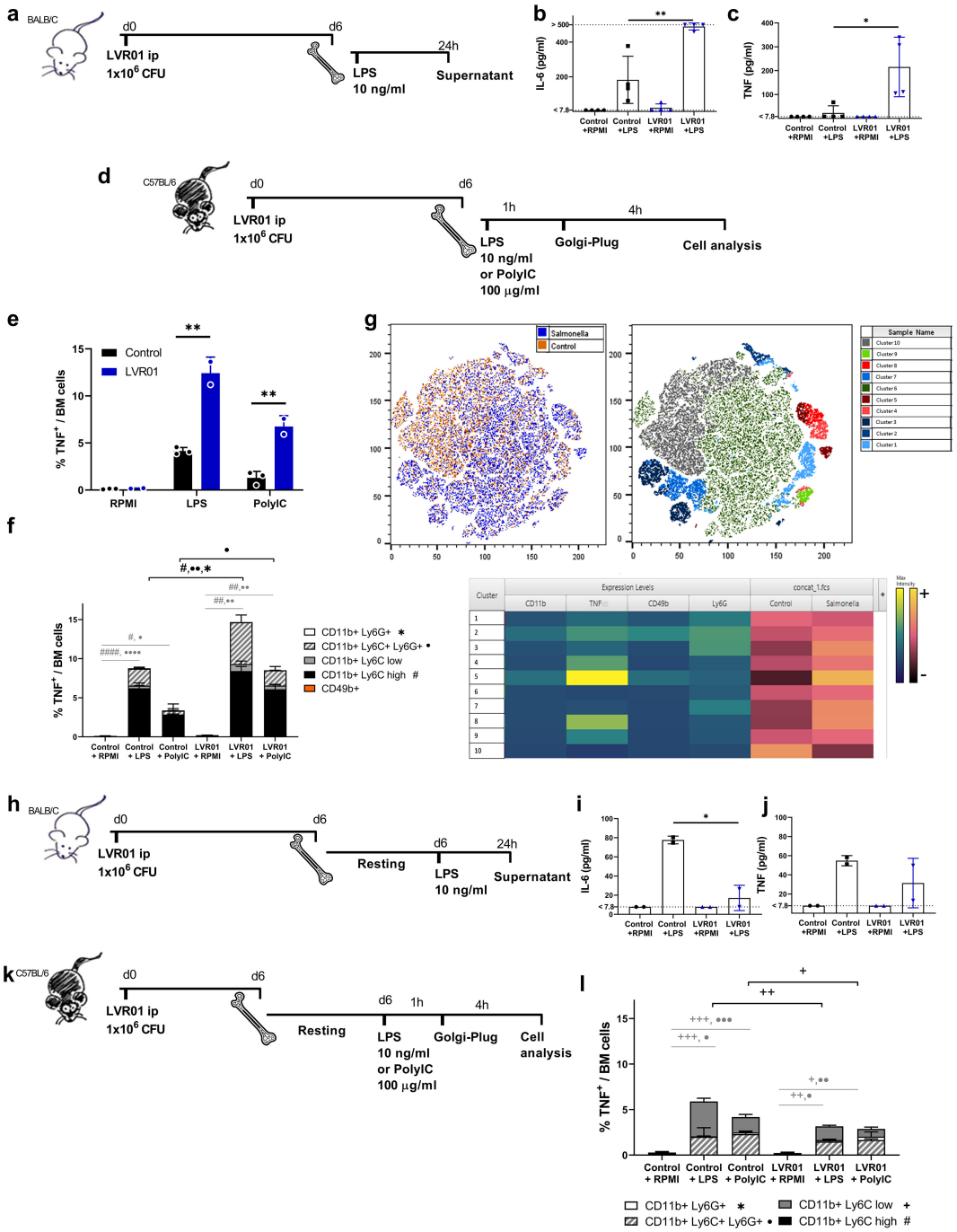


FIGURE 1
Salmonella increases pro-inflammatory cytokines in bone marrow cells upon *ex vivo* restimulation. **(a,d,h and k)** Experimental setups, "d" for days and "h" for hours. **(b)** IL-6 and **(c)** TNF release from bone marrow cells trained with PBS or LVR01 (1 x 10^6 CFU) *in vivo* after LPS (10 ng/ml) restimulation *ex vivo* at day 6, measured by ELISA. Flow cytometry analysis of **(e)** total TNF+ and **(f)** cell populations producing TNF within bone marrow cells from trained-mice, *ex vivo* restimulated with LPS or Poly I:C at day 6 and then treated with GolgiPlug. **(g)** Unsupervised analysis of single-cell events from the flow cytometry data of bone marrow using the t-SNE algorithm. The t-SNE plot of concatenated BM Control+LPS and BM LVR01+LPS is shown. The heatmap displays the expression levels of the selected markers on the concatenated t-SNE plots. **(i)** IL-6 and **(j)** TNF release from bone marrow cells from LVR-trained mice and control ones (PBS), allowed to rest for 6 days before *ex vivo* restimulation with LPS, measured by ELISA. **(l)** Flow cytometry analysis of TNF-producing cell populations within bone marrow cells from LVR- trained mice and control ones (PBS), allowed to rest before *ex vivo* restimulation with LPS and then treated with GolgiPlug. Data are presented as mean ± SD (*p < 0.05, **p < 0.01, ***p < 0.001 by t test).

10.3389/fimmu.2025.1535131

for 6 days prior to restimulation (Figure 1h), cells from the LVR01-treated group exhibited a reduction in IL-6 production upon restimulation, reaching levels comparable to those of the control group (Figures 1i, j). This suggests that the initially enhanced cytokine production was not sustained by these myeloid-enriched cells, but instead became tolerized in *Salmonella*-treated animals. In line with this, we observed a marked decrease in TNF production, which correlated with the disappearance of TNF-expressing Ly6C high monocytes—further supporting their central role in the proinflammatory response (Figures 1k, l).

3.2 *Salmonella* increases concentrations of pro-inflammatory cytokines in serum upon *in vivo* restimulation with LPS

To study the potential of *Salmonella* in inducing trained immunity *in vivo*, mice were treated with either LVR01 or PBS. After 7 days, they were restimulated with LPS i.p. Blood samples were collected 24 hours before and 90 minutes after LPS administration (Figure 2a). Mice pre-treated with LVR01 exhibited increased levels of IL-6 and TNF compared to the control group (Figures 2b, c).

3.3 *Salmonella* induces immune tolerance in human adherent monocytes *in vitro*

To investigate the potential of *Salmonella* LVR01 to induce trained immunity *in vitro*, human adherent monocytes were stimulated by infection with varying multiplicities of infection (MOI) of *Salmonella* for one hour, and then gentamicin was added. In addition, monocytes were stimulated with *Leishmania braziliensis* lysates (LL) or remained without stimuli (RPMI). Cytokine levels were assessed in the supernatant 24 hours after the initial stimulus. Significantly elevated concentrations of IL-6, TNF, IL-1β, and IL-8 (in a MOI-dependent manner) were observed in cells infected with *Salmonella* compared to the RPMI and LL groups (Figures 3a–d). Instead, IL-1Ra production was heightened in the LL group compared to the other experimental groups (Figure 3e).

Alternatively, cells were allowed to rest for six days after the initial stimulus, and then they were restimulated with LPS or Pam_3Cys for 24 hours, and proinflammatory cytokines in the supernatant were quantified. LL served as a positive control for trained immunity induction, while RPMI medium was a negative control. Despite the great initial cytokine response induced by *Salmonella*, a reduction in the production of IL-6 and TNF was observed upon restimulation (Figures 3g, h, Supplementary Figure 2A), confirming the tolerant effect induced by *Salmonella* in mouse monocytes. Additionally, lactate production was measured upon the second stimulus. Cells treated with LL maintained high lactate levels, whereas in *Salmonella*-treated cells lactate production is similar to RPMI non-trained cells (Figure 3f).

Next, we conducted the same trained immunity *in vitro* experiments using heat-killed *Salmonella* instead of live attenuated bacteria. Consistently, we observed the induction of human monocyte tolerance (Supplementary Figure 2B). The same effect was corroborated in mice, when bone marrow-derived murine cells were trained *in vitro* with LL or heat-killed LVR01, and 6 days later, myeloid-enriched cells were restimulated with LPS or PolyIC for 24 hours. The results revealed a reduction in proinflammatory cytokines in cells treated with heat-killed LVR01, as observed with human monocytes (Supplementary Figure 2C).

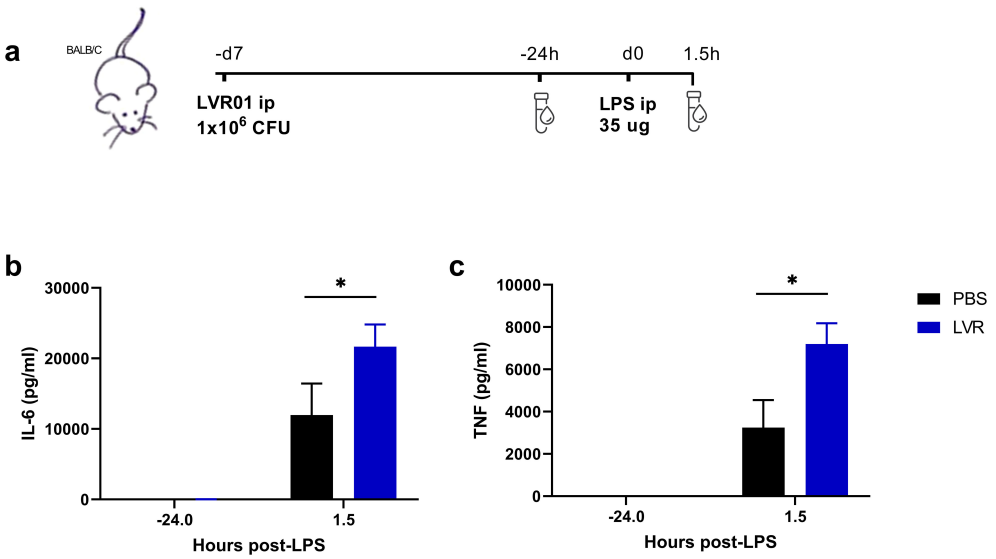


FIGURE 2
Salmonella increases pro-inflammatory cytokines in serum upon *in vivo* restimulation. **(a)** Experimental setup, "d" for days and "h" for hours. **(b)** IL-6 and **(c)** TNF production levels from serum of mice trained with PBS or LVR01 (1 x 10^6 CFU) *in vivo* after LPS (35 ug) restimulation at day 7, measured 24 hours before and 90 minutes after LPS challenge, measured by ELISA. Data are presented as mean ± SD (*p < 0.05 by t test).

10.3389/fimmu.2025.1535131

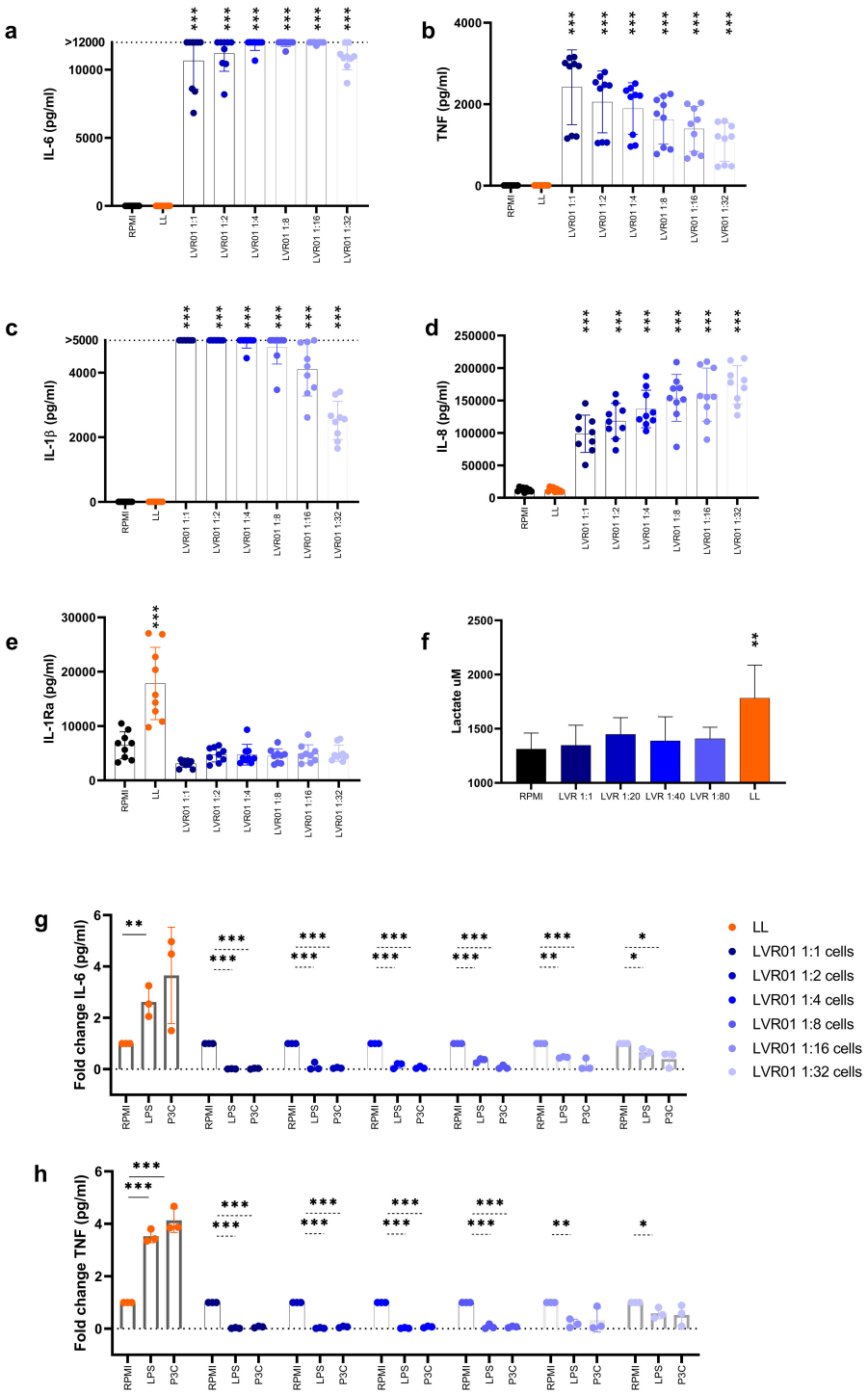


FIGURE 3
Salmonella induces immune tolerance *in vitro*. **(a)** IL-6, **(b)** TNF, **(c)** IL-1β, **(d)** IL-8 and **(e)** IL-1Ra release from monocytes-trained with RPMI, *L. braziliensis* lysates (25 µg/ml) and different MOI of *Salmonella* LVR01:cells (1:1, 1:2, 1:4, 1:8, 1:16, 1:32) for 1 hour, and measured after 24 hours by ELISA. **(f)** Lactate production assessed in the supernatants of trained monocytes upon second stimulus by fluorometric assay. Data are presented as mean ± SD (*p < 0.05, **p < 0.01, ***p < 0.001 by t test) **(g)** IL-6 and **(h)** TNF release from monocytes-trained with RPMI, *L. braziliensis* lysates and different MOI of *Salmonella* LVR01:cells (1:1, 1:2, 1:4, 1:8, 1:16, 1:32) for 1 hour, and restimulated with LPS (10 ng/ml) or Pam_3Cys (10 µg/ml) at day 7, measured by ELISA. Data are represented as fold increase normalized to RPMI (non-trained cells) and shown as mean ± SD (*p < 0.05, **p < 0.01, ***p < 0.001 by t test).

3.4 Pre-treatment with LVR01 inhibits tumor growth and extends animal survival

Given the differing results from whole bone marrow cells and monocytes, we consider that the *in vivo* approach is the most comprehensive model for further investigation. Hence, we evaluated the effect of LVR01 pre-treatment on the development of a melanoma tumor implanted one week later (Figure 4a). Significantly reduced tumor volume was observed in mice receiving *Salmonella* compared to control mice (Figure 4b), a trend reflected in the overall survival of the animals (Figure 4c). Additionally, we examined the effects of pre-treatment with *Salmonella* one month before tumor implantation, which resulted in similar outcomes (Supplementary Figure 3a, b). Subsequently, we repeated the one-week pre-treatment protocol in a non-Hodgkin lymphoma model. As observed in melanoma-bearing mice, LVR01-treated mice exhibited a delay in A20-tumor growth and prolonged overall survival too (Supplementary Figure 3c-e).

3.5 LVR01 pre-treatment anti-tumor effect is not the result of an increased inflammatory response in the tumor microenvironment

Salmonella LVR01 has been extensively studied as cancer therapeutic approach. Its anti-tumor effect is due to a strong inflammatory response in the tumor microenvironment (TME) characterized by a great increase in pro-inflammatory cytokines and chemokines, accompanied by the infiltration of immune cells, primary neutrophils, macrophages, and NK cells (13, 15). To explore whether the hereby observed prophylactic anti-tumor effect was also related to a local inflammatory immune response, we assessed the recruitment of immune cells into the tumor. When melanoma tumors reached a reasonable size and can be excised (approx. 14 days after implantation, see M&M section), the percentage of tumor-infiltrating immune cells was assessed. The results revealed no discernible difference in the percentage of CD45+, CD11b+, NK1.1+, or CD8+ tumor-infiltrating immune cells between LVR01 and control group (Figure 5). Moreover, when we analyze the transcriptional profile of the TME 14 days after tumor implantation in the prophylactic model (LVR01 pre-tumor) and in the therapeutic model (LVR01 intratumoral), we observed differences in the expression of pro-inflammatory cytokines and chemokines. Although pre-treatment with *Salmonella* induces mRNA expression of certain cytokines, the pro-inflammatory signature in the TME is not so noticeable as in LVR01 intratumoral treatment (Figure 5g). Furthermore, similar outcomes were observed in the A20 non-Hodgkin lymphomas, 17 days after tumor implantation (Supplementary Figure 4).

3.6 Kinetics of immune effector cells over time after *Salmonella* administration

To evaluate the role of immune effector cells in the prophylactic anti-tumor effect of *Salmonella* LVR01, we studied the kinetics of specific cell populations over time. Mice were treated with LVR01 or PBS intraperitoneally, and one week later, B16F10 melanoma cells were implanted subcutaneously. Blood and bone marrow samples were collected on days 3, 6, 9, 22 and 27 post-LVR01 treatment (Figure 6a). Animals treated with *Salmonella* rapidly exhibited an increased percentage of CD45+ and specifically CD45+CD11b+ myeloid cells in bone marrow (Figures 6b, c). In blood, the percentage of CD45+ cells remained unchanged during the experiment (Figure 6f), while CD45+CD11b+ myeloid cells markedly increased after LVR01 treatment (Figure 6g). In particular, there is an increased percentage of CD45+CD11b +Ly6G+ cell population in the blood post-LVR01 treatment, which is sustained for days and then decreases over time (Figure 6h). This cell population also increased in bone marrow, but only after tumor implantation (Figure 6d). No significant differences were observed between the percentage of CD45 +CD49b+ cells, neither in bone marrow or blood (Figures 6e, i). We used t-distributed stochastic neighbor embedding (tSNE) to perform an unsupervised analysis of the flow cytometry dataset generated from different conditions (Control and *Salmonella*) at different bone marrow and blood time points. Single-cell events were exported, concatenated, and displayed in a single tSNE heatmap plot for each condition. Heatmap representations of the expression levels of different markers defined clusters of cells (Supplementary Figure 5). Additionally, we studied the percentage of tumor-infiltrating immune cells at days 22 and 27 post-LVR01, and the results revealed no discernible difference between the LVR01 and control groups (data not shown).

4 Discussion

In this study, we investigated the innate immune response induced by *Salmonella* and its effect on subsequently implanted tumors.

First, we demonstrate that mice pre-treated with LVR01 have a significant increased production of pro-inflammatory cytokines by bone marrow cells upon exposure to LPS. Additionally, our study identified that the primary producers of TNF were cells derived from the myeloid lineage (Figure 1). These results suggest that LVR01 modifies the central immune response to a secondary stimulus, resembling the trained immunity response (22). However, after allowing cell cultures to rest for 6 days and then exposing the adherent monocyte-enriched cell population to LPS, these cells exhibited a tolerant response (Figure 1). A dose-dependent tolerogenic effect was observed when priming human monocytes with different MOI of LVR01 (Figure 3). It is well known that large amounts of LPS induce immune paralysis or LPS tolerance in monocytes (23). Some mechanisms underlying the LPS-tolerant effect involve metabolic reprogramming and epigenetic modifications characterized by selective and transient silencing of pro-inflammatory genes (2). LPS triggers the production of itaconate and prevents the accumulation of fumarate, a crucial metabolite for the induction of trained immunity. As a consequence, these cells maintain stable lactate

10.3389/fimmu.2025.1535131

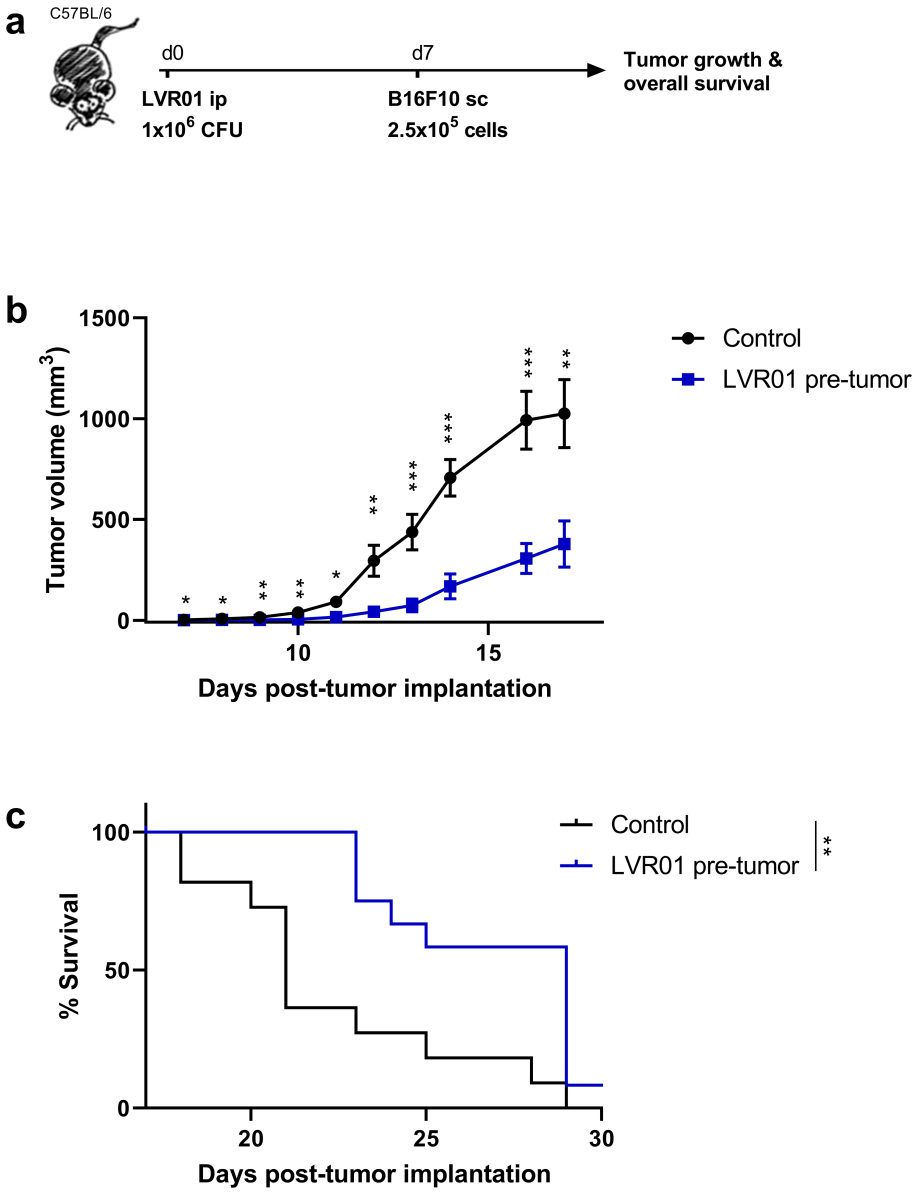


FIGURE 4
Pre-treatment with *Salmonella* inhibits tumor growth and prolongs survival of B16F10-bearing mice. **(a)** Experimental setup, "d" for days. *In vivo* **(b)** tumor growth and **(c)** survival curves of C57BL/6 mice were inoculated with 1 x 10^6 CFU of *Salmonella* LVR01 or PBS intraperitoneally one week before B16F10 (2.5 x 10^5 cells) implantation. Overall survival was followed up for 35 days (n=12). Significance was calculated between the groups (*p < 0.05, ** p < 0.01, *** p < 0.01 by t test and log rank, respectively).

levels, whereas trained cells exhibit increased lactate production (1). We observed this behavior in our *in vitro* studies using human adherent monocytes. We found that LVR01 strongly induced monocytes to produce proinflammatory cytokines during the first 24 hours after stimulation. However, after a resting period, those cells developed an immune-tolerant response (Figure 3). Interestingly, our findings contrast with previous reports describing a biphasic, dose-dependent response to LPS stimulation, where low doses of LPS induce trained immunity, whereas high doses promote tolerance (24, 25). These studies, however, used experimental designs that differ from ours, particularly in two aspects: the studied cell population and timing of restimulation. For example, Lajqi et al. observed a dose-dependent response in a short-term experimental setup of neutrophils, where restimulation occurred within 24–48 hours. In contrast, our study focuses on a longer time frame, with bone-marrow cells resting for six days before the second stimulus. These differences in cell population and experimental conditions may be crucial in shaping the outcome of innate immune memory. In contrast, our positive control using *Leishmania* lysates induced trained immunity, as was previously reported (5), characterized by an enhancement in the production of pro-inflammatory cytokines after restimulation with LPS, and an increase in lactate production six days after the initial stimulus (Figure 3). It has already been

10.3389/fimmu.2025.1535131

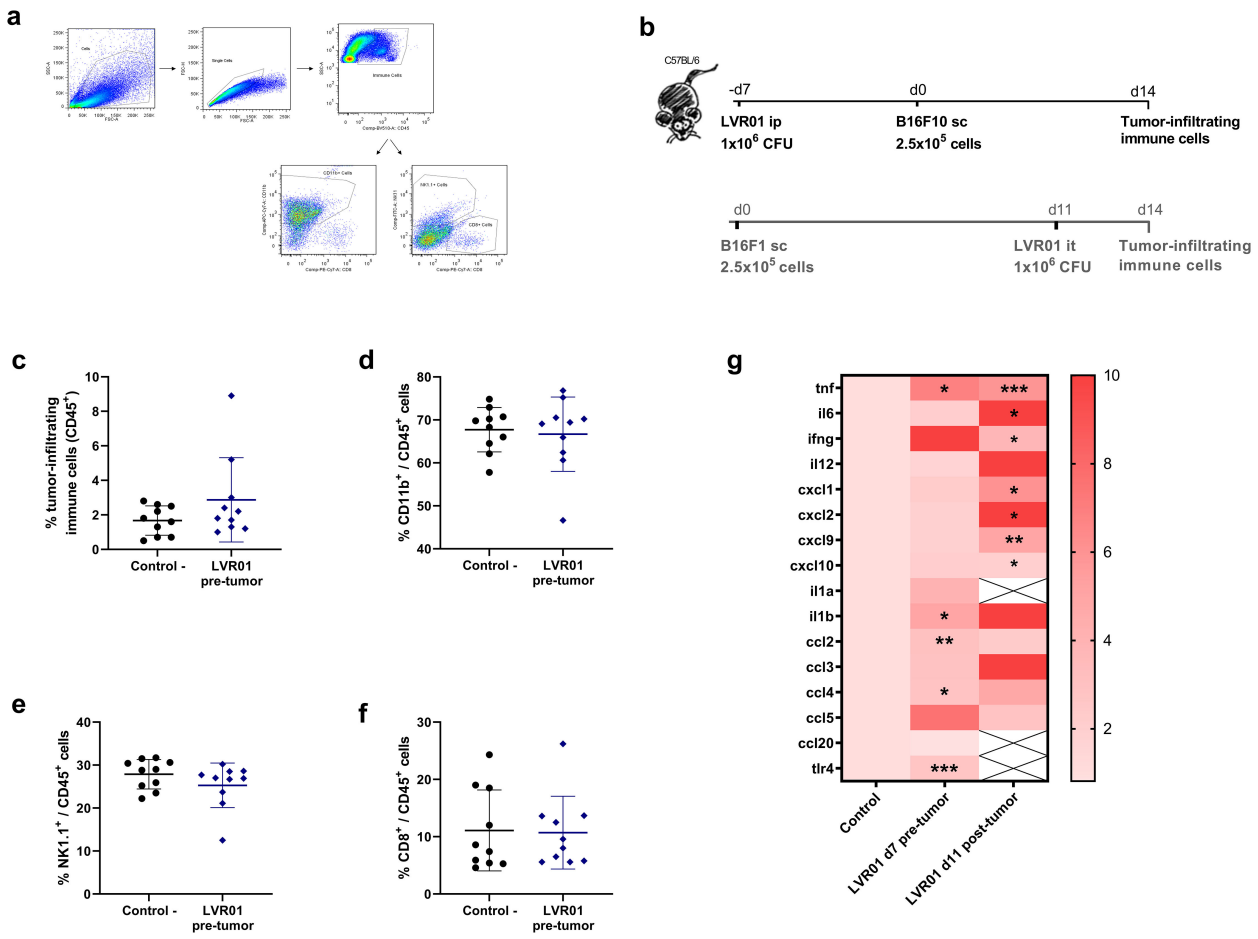


FIGURE 5
TME in mice pre-treated with *Salmonella*. **(a)** Representative flow cytometry plots and **(b)** experiment setups, "d" for days. Percentage of CD45+ **(c)**, CD45+CD11b+ **(d)**, CD45+NK1.1+ **(e)** and CD45+CD8+ **(f)** cells in the tumor microenvironment, 14 days after tumor implantation, assessed by flow cytometry in mice pre-treated with LVR01 one week before tumor implantation (n=10). **(g)** Heatmap representing cytokine/chemokine profile in *Salmonella* pre-treated (LVR01 pre-tumor, 7 days before tumor implantation) and treated (LVR01 it, 11 days after tumor implantation) mice, normalized against control untreated mice, expressed as mean Log2. Significance was calculated between the groups (*p < 0.05, ** p < 0.01, *** p < 0.01 by t test).

reported and reviewed by Geckin et al., that it is possible to induce trained immunity in multiple types of mononuclear myeloid cells like monocytes, macrophages, dendritic cells and neutrophils, and even in lymphoid cells such as NK cells and innate lymphoid cells (22, 26–31). We hypothesized that *Salmonella* is capable of inducing central changes that are beneficial for an anti-tumor immune response, but also induces peripheral tolerance, which may explain the transient effect of the treatment in preclinical models (13, 15).

To confirm if those changes are actually triggering an anti-tumor immune response, we examined the role of LVR01 on tumor development by giving the treatment one week before tumor implantation. This experimental design is an adaptation of Kalafati et al. work, where they demonstrate that trained immunity promotes anti-tumor activity in preclinical models pre-treated with β-glucan (32). When animals were pre-treated with *Salmonella* LVR01, there was a delay in tumor growth and a prolonged overall survival (Figure 4). This effect was observed even when mice were pre-treated with LVR01 one month before tumor implantation (Supplementary Figure 3). Strikingly, the anti-tumor effect was unrelated to increased tumor immune-infiltrating cells or a pro-inflammatory tumor microenvironment in the LVR01 group, which are hallmarks of the anti-tumor effect induced by therapeutic intratumoral injection of *Salmonella* (Figure 5). So far, the anti-tumor effect of *Salmonella*-based cancer therapies has always been related to the bacteria's ability to induce a strong inflammatory response in the tumor microenvironment, which is characterized by a significant increase in pro-inflammatory cytokines and chemokines, accompanied by the infiltration of immune cells, primarily neutrophils, macrophages, and NK cells (13, 15).

Kalafati et al. demonstrate that in the context of anti-tumor immunity, neutrophils and granulopoietic progenitors, not monocytes, are the major cellular effectors (32). Considering this, we continued exploring the kinetics of different immune effector cell populations in our pre-clinical model of trained immunity over time. As expected, after LVR01 treatment we observed an increase of myeloid cells in the blood and in bone marrow. This is reasonable

10.3389/fimmu.2025.1535131

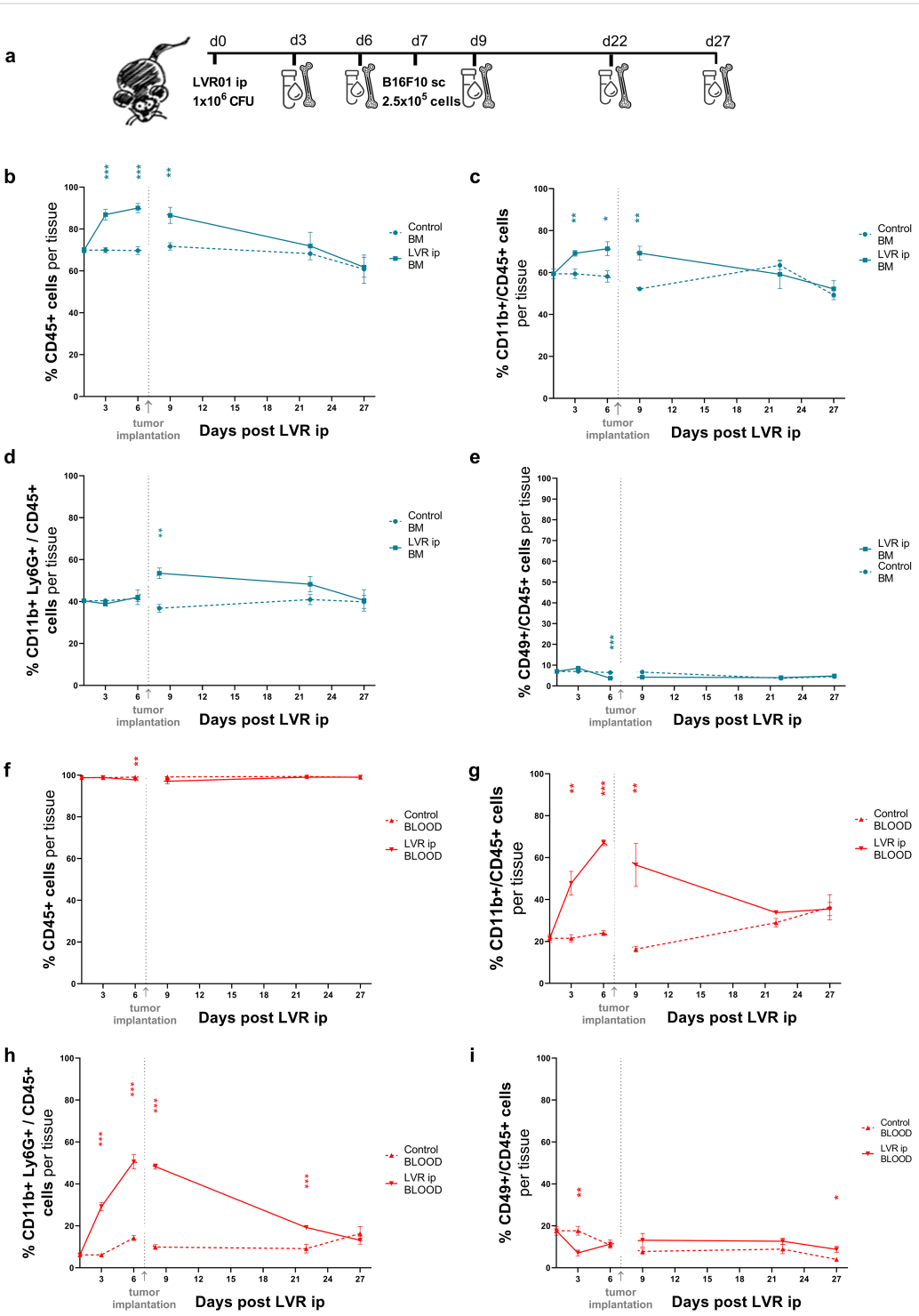


FIGURE 6
Kinetics of immune effector cells after *Salmonella* administration. **(a)** Experimental setup, "d" for days. Kinetics of CD45+ **(b)**, CD45+CD11b+ **(c)**, CD45+CD11b+Ly6G+ **(d)** and CD45+CD49b+ **(e)** cells in bone marrow samples from mice pre-treated with LVR01 one week before B16F10 tumor implantation. Kinetics of CD45+ **(f)**, CD45+CD11b+ **(g)**, CD45+CD11b+Ly6G+ **(h)** and CD45+CD49b+ **(i)** cells in blood samples from mice pre-treated with LVR01 one week before B16F10 tumor implantation. Data are presented as mean ± SEM (*p < 0.05, **p < 0.01, ***p < 0.001 by t test).

because we are administering attenuated bacteria that cause a controlled infection in the animals. The behavior of CD11b+ Ly6G+ cells in the bone marrow caught our attention; this population significantly increased in bone marrow after tumor implantation (Figure 6). These results are in line with the hypothesis of how BCG-trained cells could increase cytotoxic leukocyte responses; following cancer cell death, DAMPs can be released and act as a second stimulus for trained cells, leading to an enhanced anti-tumor effect (8). It is possible that the administration of tumor cells sends a second signal that modulates the

granulopoiesis in the bone marrow, reflected in an increase in the percentage of neutrophils and its progenitors (Figure 6). Yet, the role of neutrophils has not been demonstrated, because of major experimental limitations: (i) difficulty to deplete only neutrophils without affecting other immune cells, and (ii) impossibility to maintain neutrophil depletion over the time, due to the rapid turnover and the boost in cell numbers upon depletion. The fact that the anti-tumor effect of *Salmonella* persists even when tumors are implanted one month post-treatment suggests the induction of long-term alterations in immune cells (32).

All in all, our results show that administration of live attenuated *Salmonella* induces an immunological imprinting with a two counterposed behavior that nevertheless results in anti-tumor activity that lasts for at least one month after administration. Strikingly, this anti-tumor activity is developed in the absence of marked immune cell infiltration and inflammation in the tumor microenvironment suggesting a so far not described new mechanism for the anti-tumor effect of *Salmonella*. Digging into this new mechanism shall provide valuable information to leverage the design of new *Salmonella* mutants with improved anti-tumor effectiveness and clinical potential.

Data availability statement

The original contributions presented in the study are included in the article/Supplementary Material. Further inquiries can be directed to the corresponding authors.

Ethics statement

The studies involving humans were approved by Ethics Committee of Radboud University Nijmegen, the Netherlands. The studies were conducted in accordance with the local legislation and institutional requirements. The participants provided their written informed consent to participate in this study. The animal study was approved by University's Ethical Committee for Animal Experimentation, Uruguay (protocol number 1329). The study was conducted in accordance with the local legislation and institutional requirements.

Author contributions

SC: Conceptualization, Data curation, Formal analysis, Funding acquisition, Investigation, Methodology, Project administration, Resources, Software, Supervision, Validation, Visualization, Writing – original draft, Writing – review & editing. JS: Conceptualization, Investigation, Methodology, Supervision, Writing – review & editing. AM: Conceptualization, Funding acquisition, Visualization, Writing – review & editing. LJ: Conceptualization, Methodology, Resources, Supervision, Visualization, Writing – review & editing. MM: Conceptualization, Data curation, Formal analysis, Funding acquisition, Investigation, Methodology, Project administration, Resources, Software, Supervision, Validation, Visualization, Writing – original draft, Writing – review & editing. JC: Conceptualization, Formal analysis, Funding acquisition, Methodology, Project administration, Resources, Supervision, Validation, Visualization, Writing – original draft, Writing – review & editing.

Funding

The author(s) declare that financial support was received for the research and/or publication of this article. This research is financially supported by Agencia Nacional de Investigación e Innovación (Montevideo, Uruguay), Comisión Sectorial de Investigación Científica (Montevideo, Uruguay) and Programa de Posgrado en Biotecnología (Montevideo, Uruguay).

Conflict of interest

The authors declare that the research was conducted in the absence of any commercial or financial relationships that could be construed as a potential conflict of interest.

Generative AI statement

The author(s) declare that no Generative AI was used in the creation of this manuscript.

Publisher's note

All claims expressed in this article are solely those of the authors and do not necessarily represent those of their affiliated organizations, or those of the publisher, the editors and the reviewers. Any product that may be evaluated in this article, or claim that may be made by its manufacturer, is not guaranteed or endorsed by the publisher.

Supplementary material

The Supplementary Material for this article can be found online at: https://www.frontiersin.org/articles/10.3389/fimmu.2025.1535131/full#supplementary-material

References

1. Domínguez-Andrés J, Novakovic B, Li Y, Scicluna BP, Gresnigt MS, Arts RJW, et al. The itaconate pathway is a central regulatory node linking innate immune tolerance and trained immunity. *Cell Metab.* (2019) 29:211–220.e5. doi: 10.1016/j.cmet.2018.09.003

2. Foster SL, Hargreaves DC, Medzhitov R. Gene-specific control of inflammation by TLR-induced chromatin modifications. *Nature*. (2007) 447:972–8. doi: 10.1038/nature05836

3. Netea MG, Joosten LAB, Latz E, Mills KHG, Natoli G, Stunnenberg HG, et al. Trained immunity: A program of innate immune memory in health and disease. *Sci (80-.)*. (2016) 352:1–23. doi: 10.1126/science.aaf1098

4. Novakovic B, Habibi E, Wang SY, Arts RJW, Davar R, Megchelenbrink W, et al. β-glucan reverses the epigenetic state of LPS-induced immunological tolerance. *Cell*. (2016) 167:1354–1368.e14. doi: 10.1016/j.cell.2016.09.034

5. Dos Santos JC, Moreno M, Teufel LU, Chilibroste S, Keating ST, Groh L, et al. Leishmania Braziliensis enhances monocyte responses to promote anti-tumor activity. *Cell Rep*. (2024) 43(3):113932. doi: 10.1016/j.celrep.2024.113932

6. Vuscan P, Kischkel B, Joosten LAB, Netea MG. Trained immunity: General and emerging concepts. *Immunol Rev*. (2024) 323(1):164–85. doi: 10.1111/imr.13326

7. Bekkering S, Blok BA, Joosten LAB, Riksen NP, Van Crevel R, Netea MG. *In Vitro* experimental model of trained innate immunity in human primary monocytes. *Clin Vaccine Immunol*. (2016) 23:926–33. doi: 10.1128/CVI.00349-16

8. van Puffelen JH, Keating ST, Oosterwijk E, van der Heijden AG, Netea MG, Joosten LAB, et al. Trained immunity as a molecular mechanism for BCG immunotherapy in bladder cancer. *Nat Rev Urol*. (2020) 17:513–25. doi: 10.1038/s41585-020-0346-4

9. Alexandroff AB, Jackson AM, O'Donnell MA, James K. BCG immunotherapy of bladder cancer: 20 years on. *Lancet*. (1999) 353:1689–94. doi: 10.1016/S0140-6736(98)07422-4

10. Forbes NS, Coffin RS, Deng L, Evgin L, Fiering S, Giacalone M, et al. White paper on microbial anti-cancer therapy and prevention. *J Immunother Cancer*. (2018) 6:1–24. doi: 10.1186/s40425-018-0381-3

11. Pangilinan CR, Lee C-H. Salmonella-based targeted cancer therapy: updates on A promising and innovative tumor immunotherapeutic strategy. *Biomedicines*. (2019) 7:36. doi: 10.3390/biomedicines7020036

12. Pawelek JM, Low KB, Bermudes D. Tumor-targeted salmonella as a novel anti-melanoma vector. *Melanoma Res*. (1997) 7:S141. doi: 10.1097/00008390-199706001-00491

13. Grille S, Moreno M, Bascuas T, Marqués JM, Muñoz N, Lens D, et al. Salmonella enterica serovar Typhimurium immunotherapy for B-cell lymphoma induces broad anti-tumour immunity with therapeutic effect. *Immunology*. (2014) 143:428–37. doi: 10.1111/imm.12320

14. Mónaco A, Chilibroste S, Yim L, Chabalgoity JA, Moreno M. Inflammasome activation, NLRP3 engagement and macrophage recruitment to tumor microenvironment are all required for Salmonella antitumor effect. *Cancer Immunol Immunother*. (2022) 71(9):2141–50. doi: 10.1007/s00262-022-03148-x

15. Mónaco A, Plata MC, Chilibroste S, Vola M, Chabalgoity JA, Moreno M. Salmonella-induced immune response reduces recurrence and tumor dissemination in preclinical melanoma model. *Curr Res Immunol*. (2022) 3:159–66. doi: 10.1016/j.crimmu.2022.08.001

16. Li H, Breedijk A, Dietrich N, Nitschke K, Jarczyk J, Nuhn P, et al. Lipopolysaccharide tolerance in human primary monocytes and polarized macrophages. *Int J Mol Sci*. (2023) 24:12196. doi: 10.3390/ijms241512196

17. Howell LM, Manole S, Reitter AR, Forbes NS. Controlled production of lipopolysaccharides increases immune activation in Salmonella treatments of cancer. *Microb Biotechnol*. (2024) 17:1–16. doi: 10.1111/1751-7915.14461

18. Chabalgoity JA, Moreno M, Carol H, Dougan G, Hormaeche CE. Salmonella typhimurium as a basis for a live oral Echinococcus granulosus vaccine. *Vaccine*. (2000) 19:460–9. doi: 10.1016/S0264-410X(00)00197-3

19. Vola M, Mónaco A, Bascuas T, Rimsky G, Agorio CI, Chabalgoity JA, et al. TLR7 agonist in combination with Salmonella as an effective antimelanoma immunotherapy. *Immunotherapy*. (2018) 10:665–79. doi: 10.2217/imt-2017-0188

20. Livak KJ, Schmittgen TD. Analysis of relative gene expression data using real-time quantitative PCR and the 2-ΔΔCT method. *Methods*. (2001) 25:402–8. doi: 10.1006/meth.2001.1262

21. Zhu CT, Rand DM. A hydrazine coupled cycling assay validates the decrease in redox ratio under starvation in Drosophila. *PLoS One*. (2012) 7(10):e47584. doi: 10.1371/journal.pone.0047584

22. Geckin B, Konstantin Föhse F, Domínguez-Andrés J, Netea MG. Trained immunity: implications for vaccination. *Curr Opin Immunol*. (2022) 77:102190. doi: 10.1016/j.coi.2022.102190

23. Van Der Poll T, Van De Veerdonk FL, Scicluna BP, Netea MG. The immunopathology of sepsis and potential therapeutic targets. *Nat Rev Immunol*. (2017) 17:407–20. doi: 10.1038/nri.2017.36

24. Lajqi T, Braun M, Kranig SA, Frommhold D, Pöschl J, Hudalla H. LPS induces opposing memory-like inflammatory responses in mouse bone marrow neutrophils. *Int J Mol Sci*. (2021) 22:9803. doi: 10.3390/ijms22189803

25. Lajqi T, Köstlin-Gille N, Bauer R, Zarogiannis SG, Lajqi E, Ajeti V, et al. Training vs. Tolerance: the yin/yang of the innate immune system. *Biomedicines*. (2023) 11:766. doi: 10.3390/biomedicines11030766

26. Hole CR, Wager CML, Castro-Lopez N, Campuzano A, Cai H, Wozniak KL, et al. Induction of memory-like dendritic cell responses in *vivo*. *Nat Commun*. (2019) 10:2955. doi: 10.1038/s41467-019-10486-5

27. Kleinnijenhuis J, Quintin J, Preijers F, Joosten LAB, Ifrim DC, Saeed S, et al. Bacille Calmette-Guérin induces NOD2-dependent nonspecific protection from reinfection via epigenetic reprogramming of monocytes. *Proc Natl Acad Sci*. (2012) 109:17537–42. doi: 10.1073/pnas.1202870109

28. Moorlag S.J.C.F.M., Rodriguez-Rosales YA, Gillard J, Fanucchi S, Theunissen K, Novakovic B, et al. BCG vaccination induces long-term functional reprogramming of human neutrophils. *Cell Rep*. (2020) 33:108387. doi: 10.1016/j.celrep.2020.108387

29. Quintin J, Saeed S, Martens JHA, Giamarellos-Bourboulis EJ, Ifrim DC, Logie C, et al. Candida albicans Infection Affords Protection against Reinfection via Functional Reprogramming of Monocytes. *Cell Host Microbe*. (2012) 12:223–32. doi: 10.1016/j.chom.2012.06.006

30. Saeed S, Quintin J, Kerstens HHD, Rao NA, Aghajanirefah A, Matarese F, et al. Epigenetic programming of monocyte-to-macrophage differentiation and trained innate immunity. *Sci (80-.)*. (2014) 345:1–26. doi: 10.1126/science.1251086

31. Sun JC, Beilke JN, Lanier LL. Adaptive immune features of natural killer cells. *Nature*. (2009) 457:557–61. doi: 10.1038/nature07665

32. Kalafati L, Kourtzelis I, Schulte-Schrepping J, Li X, Hatzioannou A, Grinenko T, et al. Innate immune training of granulopoiesis promotes anti-tumor activity. *Cell*. (2020) 183:771–785.e12. doi: 10.1016/j.cell.2020.09.058

biomedicines

MDPI

Review

Salmonella-Induced Cell Death in Cancer Immunotherapy: What Lies Beneath?

Amy Mónaco, Sofía Chilibroste, María Clara Plata, Jose Alejandro Chabalgoity * and María Moreno *

Unidad Académica de Desarrollo Biotecnológico, Instituto de Higiene, Facultad de Medicina, Universidad de la República, Montevideo 11600, Uruguay; amonaco@higiene.edu.uy (A.M.); schilibroste@higiene.edu.uy (S.C.); mplata@higiene.edu.uy (M.C.P.)

* Correspondence: jachabal@higiene.edu.uy (J.A.C.); mmoreno@higiene.edu.uy (M.M.)

Abstract

Bacteria-based cancer immunotherapies are regaining attention due to recent advances in understanding the mechanisms underlying their efficacy, making them promising tools for cancer treatment. Among these, *Salmonella* stands out as one of the most extensively studied microorganisms in this field. Its ability to directly induce tumor cell death while stimulating the immune system offers unique therapeutic advantages, as cell death within an inflammatory environment may enhance the release of tumor antigens and promote effective antitumor immune responses. Although multiple studies have addressed *Salmonella*-induced cell death, the nomenclature and classification of death modalities are often inconsistent—either because earlier reports predate the formalization of certain death pathways, or due to overlapping criteria between different types of cell death. This review aims to comprehensively analyze the available evidence on *Salmonella*-induced apoptosis, pyroptosis and autophagy, as well as other less characterized death modalities. Given that most mechanistics evidence on *Salmonella*-induced cell death has been generated in myeloid cells, we primarily focus on the myeloid compartment while integrating available observations from tumor cells and other immune populations when relevant, organizing the existing data under current definitions and concepts, and highlighting the challenges of manipulating these pathways to optimize bacterial-based immunotherapies.

Keywords: *Salmonella*; cancer immunotherapy; cell death; apoptosis; pyroptosis; autophagy

Academic Editor: Adrian-Bogdan Țigu

Received: 6 November 2025
Revised: 13 December 2025
Accepted: 14 December 2025
Published: 20 December 2025

Copyright: © 2025 by the authors. Licensee MDPI, Basel, Switzerland. This article is an open access article distributed under the terms and conditions of the Creative Commons Attribution (CC BY) license.

1. Introduction

The use of microorganisms as therapeutic agents in cancer has gained increasing interest over the past two decades. This approach, often referred to as bacterial cancer therapy or microbial-based immunotherapy, exploits the unique ability of certain microbes to preferentially colonize tumor tissues, modulate the tumor microenvironment (TME), and stimulate robust antitumor immune responses. Historically, the concept dates back to the late 19th century with the work of Dr. William Coley, who used heat-killed *Streptococcus pyogenes* and *Serratia marcescens* to treat sarcomas—an early form of immunotherapy now known as "Coley's toxins" [1]. An early and clinically impactful milestone that followed Coley's work was the introduction of Bacillus Calmette–Guérin (BCG), a live-attenuated *Mycobacterium bovis* strain, for the treatment of non-muscle-invasive bladder cancer

(NMIBC). Since its approval in the 1970s, intravesical BCG remains the gold-standard adjuvant immunotherapy for NMIBC and represents one of the most successful examples of microbial use in cancer treatment, achieving durable responses through local inflammation, antigen presentation enhancement, and recruitment of cytotoxic immune cells [2]. Recently, the Argentine therapeutic melanoma vaccine VACCIMEL—composed of four lethally irradiated allogeneic melanoma cell lines—received regulatory approval, and is administered specifically in combination with BCG (and GM-CSF) as adjuvants [3], underscoring not only the resurgence of microbial-based immunotherapy but also the enduring relevance of BCG as a potent immune stimulant in treatment-adjunct settings. Other live-attenuated or genetically engineered bacteria such as *Salmonella*, *Listeria monocytogenes*, *Clostridium*, and *Bifidobacterium* have also been investigated as vectors for cancer-targeted therapy [4]. These microbes can deliver therapeutic molecules, induce immunogenic cell death, and enhance tumor-associated antigen presentation. Moreover, their capacity to reshape the suppressive TME into a proinflammatory one, by inducing proinflammatory cytokines and recruiting immune cells, places them as promising agents in both monotherapy and combination immunotherapy strategies. It is important to state that an effective bacterial candidate for anticancer therapy must strike an adequate balance between attenuation and antitumor activity. While wild-type strains are not suitable for clinical use due to their ability to induce severe systemic infections, overly attenuated derivatives may show reduced therapeutic efficacy because they fail to elicit a sufficient immune response for tumor regression [5].

Salmonella enterica serovar Typhimurium has been extensively studied as a vector for cancer immunotherapy due to its ability to preferentially colonize tumors, kill tumor cells and stimulate robust immune responses [6]. This is in part because of its capacity to use its flagella to move towards the TME, attracted by the available nutrients [7,8]. In addition, being a facultative anaerobe, *Salmonella* thrives in the typical hypoxic, poorly vascularized microenvironments of solid tumors, a property that has been exploited to design hypoxia-conditional strains such as YB1 that survive and replicate selectively within tumor cores [9]. Therefore, in this way, *Salmonella* acts at different levels: by starving tumor cells through competition for the same nutrients [10] or metabolically disrupting the TME [11]. In addition, *Salmonella* can invade tumor cells within the whole tumor mass (both viable margins and also the necrotic core, inaccessible for other therapies) and directly induce their death.

Beyond preclinical evidence, some attenuated *Salmonella* strains have already been evaluated in clinical settings, supporting the feasibility of exploiting the bacterium as an antitumoral agent. The first-in-human Phase I clinical trial administering intravenous attenuated *S. Typhimurium* VNP20009 to patients with metastatic melanoma demonstrated that treatment was safe at low doses, with occasional tumor colonization observed and evidence of immune activation, although without objective clinical responses [12]. A subsequent study using continuous intravenous infusion of the same strain further confirmed tolerability, setting safety parameters for future interventions [13]. More recently, an oral formulation engineered to express human IL-2 was tested in patients with metastatic gastrointestinal cancer, also showing an acceptable safety profile and preliminary immune engagement, thus reopening interest in clinical development [14]. Together, these trials highlight that *Salmonella*-based therapies are clinically implementable and provide a translational framework for next-generation tumor-targeting strains optimized for enhanced safety, delivery, and antitumor efficacy.

Although *Salmonella* exerts diverse antitumor activities beyond direct induction of tumor cell death, these aspects have been extensively covered elsewhere [15,16] and fall outside the specific scope of this review. The use of *Salmonella* in combination with other therapies has also been reviewed elsewhere [16]. Therefore, in this review we intend to

specifically address the different *Salmonella*-induced types of cell death (both in tumor and immune cells in the tumor bed) that, together with other phenomena, explain the preclinical success of cancer immunotherapies involving the use of attenuated *Salmonella*. The main objective of cancer therapies is the elimination of tumor cells, hence, the fact that *Salmonella* is able to induce diverse types of tumor cell death at the same time is highly relevant. The balance between these multiple cell death pathways dictates the final outcome of the therapy, which may favor the development of a tumor-specific effective immune response and therefore, disease eradication. Finally, we briefly discuss the rationale and challenges of manipulating tumor cell death mechanisms.

2. *Salmonella*-Induced Cell Death

Among the various contributing factors, *Salmonella*-mediated direct killing stands out as a major mechanism underlying the antitumor effects [17]. Different investigations have shown reduced tumor cell viability upon infection, using viability assays such as MTT [18] and resazurin reduction [19], or death assays as lactate dehydrogenase (LDH) release [20]. However, these approaches, while indicative of cytotoxicity, do not clarify the precise mode of cell death involved. A growing body of evidence indicates that *Salmonella* is capable of activating multiple cell death pathways, with outcomes depending on bacterial strain, host cell type, TME and other factors, as reviewed below. This distinction is biologically relevant, since different types of cell death can trigger distinct downstream immune consequences. Beyond the primary reduction in tumor burden through direct killing, the byproducts and danger signals released during each death process can differentially modulate antitumor immunity. Understanding these distinct mechanisms and their crosstalk is crucial for optimizing *Salmonella*-based cancer therapies. Therefore, in the following sections we provide an overview of each type of programmed cell death associated with *Salmonella* in cancer control, which are schematically represented in Figure 1.

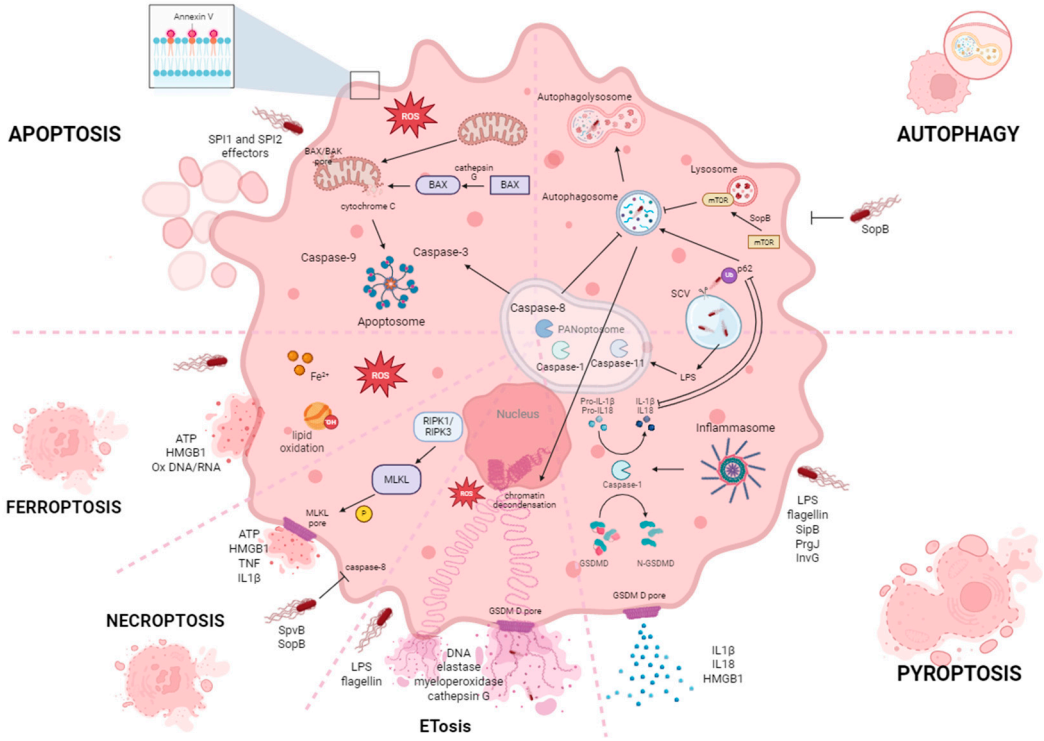


Figure 1. Schematic representation of *Salmonella*-induced cell death pathways, and their coordination and crosstalk. For the sake of clarity, only mouse protein names have been used (some may differ in humans) and several molecules have been omitted. BAX: Bcl-2-associated X protein; GSDM D: gasdermin D, HMGB1: high mobility group box 1, IL: interleukin, LPS: lipopolysaccharide,

mTOR: mammalian target of rapamycin, MLKL: mixed lineage kinase domain-like, RIPK: receptor-interacting protein kinase, ROS: Reactive oxygen species, SCV: *Salmonella*-containing vacuole, SPI: *Salmonella* Pathogenicity Island, TNF: tumor necrosis factor. Created in BioRender. Mónaco, A. (2025) https://BioRender.com/w25p0gr (accessed on 7th November 2025).

2.1. Apoptosis

This type of programmed cell death is one of the most studied in the context of *Salmonella*-mediated cancer therapy (Table 1). It consists of controlled self-destruction of cells, while the cell membrane remains intact and does not induce inflammation [21]. Notably, *S*. Typhimurium has been shown to both induce and modulate apoptosis in tumor cells through various mechanisms. Below, we summarize how *Salmonella* triggers apoptosis in different cells, the key molecular players involved, and how these phenomena contribute to tumor suppression and immunotherapy (Table 1).

The first report of *Salmonella* inducing apoptosis in infected macrophages dates back to 1996, in a work published by Monack et al. [22]. Subsequent work revealed the mechanism: the *Salmonella* pathogenicity island-1 (SPI-1) Type III secretion system (T3SS1) delivers an effector protein, SipB, into host macrophages that is both necessary and sufficient to induce apoptosis [23] (Figure 1). Notably, Caspase-1-mediated cell death is now termed pyroptosis (see Section 2.2 below) but earlier work described it as an apoptotic phenotype. In human macrophage-like THP-1 cells, *Salmonella* infection can also induce rapid DNA fragmentation in the host cells within hours. Valle and Guiney found that >70% of THP-1 cells became TUNEL-positive (indicating DNA breaks) after 4 h of infection, increasing to >90% by 5.5 h [24]. This effect depended on active bacterial infection and, surprisingly, did not require the SPI-1 or SPI-2 secretion systems or the spv virulence genes, but did require the *phoP* regulatory gene. Caspase-3 (an executioner caspase in classical apoptosis) was activated during *Salmonella* infection of THP-1 cells, though Caspase-8/9 (initiators of extrinsic/intrinsic apoptosis) were not, and blocking Caspase-3 did not fully prevent DNA fragmentation. These findings suggest *Salmonella* can initiate an atypical apoptotic program in macrophages, likely through Caspase-1 (pyroptotic) pathways and additional PhoP-regulated factors. The death of infected macrophages via apoptosis/pyroptosis may benefit the pathogen by releasing it from the macrophage, but in the context of cancer therapy, pyroptosis, but not apoptosis, can help expose tumor antigens and promote inflammation in the TME. In contrast with the pro-apoptotic effect seen in macrophages, *Salmonella* can actively suppress apoptosis in intestinal epithelial cells during the early stages of natural infection, ensuring a stable intracellular niche for replication. A key SPI-1 effector, SopB (also known as SigD), has been shown to protect infected epithelial cells from undergoing apoptosis [25]. In this work, Knodler et al. also demonstrated that wild-type *Salmonella* induces sustained Akt activation in epithelial cells in a SopB-dependent manner, and this prevents the normal apoptotic cascade.

Regarding the use of *Salmonella* in cancer therapy, studies in mouse tumor models have shown that systemically delivered *Salmonella* accumulate inside tumors and can trigger tumor cell death. Ganai et al. tracked *S. Typhimurium* in 4T1 mammary carcinoma and found that, within 48 h of intravenous injection, the bacteria had migrated away from well-vascularized tumor edges into the hypoxic tumor core, coinciding with elevated apoptosis in this central tumor region [26]. Hence, this study demonstrated that *Salmonella* not only penetrate deep into tumor tissue but also induce cancer cell apoptosis in vivo, contributing to a temporary stagnation of tumor growth.

Engineering *Salmonella* can further enhance this pro-apoptotic oncolytic effect. Kasinskas and Forbes showed that deleting the bacterial ribose/galactose chemoreceptor (which normally guides *Salmonella* toward certain nutrients) causes the bacteria to linger in tumor

quiescent zones, thereby intensifying their apoptotic impact on tumor cells [8]. The chemotaxis-deficient strain accumulated more in poorly perfused tumor regions and induced higher Caspase-3 activity (i.e., more apoptosis) in the tumor compared to wild-type *Salmonella*. Thus, *Salmonella*'s inherent tumor tropism can be tuned to maximize direct tumor cell killing via apoptosis. Recent research confirms that *Salmonella*-mediated tumor cell apoptosis is a key mechanism of tumor suppression. Zhang et al. employed an attenuated *S. Typhimurium* strain in a "L-form" (cell wall-deficient state) to treat murine ovarian cancer, and observed a robust induction of apoptosis in the ovarian tumor cells, alongside with inhibited tumor growth [27]. Tumors from treated mice showed significantly more TUNEL-positive (apoptotic) cancer cells than controls, and the therapy reduced expression of pro-tumor proteins, like galectin-9 and MMP9, which are associated with tumor proliferation and metastasis. This confirms that *Salmonella* can directly trigger intrinsic cell death pathways in cancer cells, contributing to oncolysis. In some studies, *Salmonella* infection has also been noted to damage the tumor vasculature and endothelium, partly through inducing apoptosis of endothelial cells, which ends up in an anti-angiogenesis effect that feeds a positive loop [28].

Several bacterial and host factors underlie *Salmonella*-mediated apoptosis. Among them, SipB is a key *Salmonella* effector during macrophage infection that binds and activates Caspase-1. At the time, this was described as an "inflammatory apoptotic death" of the phagocyte; however, it is now recognized as pyroptosis [23]. SipA, another SPI-1 effector, can activate Caspase-3 in host cells, linking *Salmonella* infection to classical apoptosis execution pathways [29]. In infected macrophages, Caspase-1 activation by SipB can also indirectly activate Caspase-3 downstream or induce other apoptotic signals, although the exact signaling crosstalk is complex. In the tumor context, host cytokines like TNF induced by *Salmonella* are also key pro-apoptotic mediators. *Salmonella*'s lipopolysaccharide (LPS) triggers TNF secretion by macrophages and monocytes, which can cause apoptotic death of tumor endothelial cells and tumor cells, contributing to tumor oncolysis as stated above [6,30].

All in all, harnessing *Salmonella*-mediated apoptosis—through careful genetic attenuation and targeting—may offer a unique biotherapeutic route for cancer treatment. Ongoing research and clinical trials will reveal how this strategy can be optimally and safely integrated into cancer immunotherapy, potentially providing a powerful adjunct or alternative to conventional treatments.

Table 1. Programmed cell death events associated with *Salmonella* antitumor effect in in vivo preclinical models.

Tumor Type	*Salmonella* Strain and Route of Administration	Type of Induced Cell Death	Refs.
Breast cancer (MARY-X human xenograft)	A1-R (i.v.)	Apoptosis *	[31]
Breast carcinoma (4T1)	Engineered VNP20009 (i.v.)	Apoptosis	[26]
Colon adenocarcinoma (CT26)	StΔppGpp-lux (i.v.)	Apoptosis/Pyroptosis *	[32]
Colon adenocarcinoma (CT26)	Engineered SGKS1004 (i.v./i.t.) (*S. enterica* serovar Gallinarum)	Autophagy	[33]
Colon adenocarcinoma (MC38)	ΔppGpp (i.v.)	Pyroptosis *	[34]
Fibrosarcoma (HT1080)	A1-R (i.g.)	Autophagy	[35]
Glioma	YB1 (i.v.)	Ferroptosis	[36]

(U87)			
Laryngeal cancer (Hep-2)	Engineered LH430 (i.v.)	Apoptosis	[37]
Non-small cell lung carcinoma (A549)	Engineered VNP20009 (i.v.)	Apoptosis	[38]
Ovarian cancer (ID8)	L-form VNP20009 (route not specified)	Apoptosis	[27]
Prostate adenocarcinoma (PC-3)	A1-R (i.v.)	Apoptosis *	[39]
Skin melanoma (B16F1)	LVR01 (i.t.)	Apoptosis */ICD/Pyroptosis	[40]
Skin melanoma (B16F10)	VNP20009 (i.v.)	Apoptosis	[9],[41]
Skin melanoma (B16F10)	VNP20009 (i.p.)	Apoptosis/Autophagy	[42]
Skin melanoma (B16F10)	Engineered VNP20009 (i.g.)	Apoptosis	[43]
Skin melanoma (B16F10)	Engineered VNP20009 (i.p.)	Apoptosis	[44]
Skin melanoma (B16F10)	Engineered 14028 (i.t.)	Apoptosis	[45]

All strains were *S. enterica* serovar Typhimurium, unless specifically stated otherwise. * indicates indirect evidence of particular cell death, through a mechanism not directly named in the article. "Engineered" depicts bacterial modifications to enhance/delete/add certain molecules. Abbreviations: ICD, immunogenic cell death; i.v., intravenous; i.t., intratumoral; i.g., intragastric (gavage); i.p., intraperitoneal.

2.2. Pyroptosis

Pyroptosis is a lytic and highly inflammatory form of programmed cell death driven by the gasdermin family of pore-forming proteins [46]. It is characterized by cell swelling, membrane permeabilization, and release of pro-inflammatory intracellular contents, in contrast to the silent dismantling of apoptosis. Firstly discovered as a defense mechanism against intracellular bacteria, pyroptosis occurs when cytosolic pattern recognition receptors engage their ligand and trigger the assembly of cytosolic multiprotein complexes called inflammasomes, which activate inflammatory caspases (such as Caspase-1, -4/5 in humans, or -11 in mice) in response to microbial or danger signals [47,48]. These caspases cleave the inhibitory C-terminal domain off gasdermin (GSDM) proteins, unleashing the cytotoxic N-terminal domain to oligomerize in the plasma membrane and form large pores, thereby disrupting ionic homeostasis and causing cell lysis. This gasdermin-mediated pore formation is the executioner step of pyroptosis and is essential for its downstream effects [49,50]. Indeed, cells lacking GSDMD, the substrate of Caspase-1/4/5/11, are resistant to pyroptosis and fail to secrete the potent cytokines interleukin-1β (IL-1β) and IL-18 upon infection [49]. Cleavage of GSDMD by inflammatory caspases releases its N-terminal fragment, which not only perforates the membrane to induce pyroptotic death but also can prompt assembly of the NLRP3 inflammasome, amplifying IL-1β maturation in a positive feedback loop [49] (Figure 1).

Salmonella infection is a quintessential trigger of pyroptosis. It delivers pathogen-associated molecular patterns (PAMPs) into the host cell cytosol, activating multiple inflammasome pathways. In macrophages, *Salmonella*'s flagellin and type III secretion system rod proteins are recognized by NAIP/NLRC4 inflammasomes, while additional stress signals from infection (for example, phagosomal damage or bacterial toxins) can engage the

NLRP3 inflammasome [48]. Both NLRC4 and NLRP3 converge on Caspase-1 activation and were found to play partially redundant roles in host defense against *Salmonella:* mice deficient in both of these inflammasome sensors are markedly more susceptible to infection [48]. *Salmonella* can also induce "non-canonical" inflammasome activation via Caspase-11 in mice (Caspase-4/5 in humans) when its LPS enters the cytosol. Consequently, *Salmonella*-infected macrophages rapidly activate Caspase-1 and Caspase-11, leading to GSDMD cleavage and pyroptotic cell death [49]. Along with directly killing the pathogen's replicative niche, pyroptotic death of *Salmonella*-infected cells results in the maturation and release of IL-1β and IL-18 (Figure 1), which act on surrounding cells to induce fever, vascular permeability and the recruitment of immune effector cells [48,49]. Pyroptotic cells also release alarmins such as ATP, HMGB1, and inflammasome complexes themselves; for example, oligomerized ASC "specks" are expelled from pyroptotic cells and can be phagocytosed by bystander macrophages to propagate Caspase-1 activation and cytokine release in the local environment [51]. Through these inflammatory feedback mechanisms, *Salmonella*-induced pyroptosis serves to alert and mobilize the immune system, effectively linking innate pathogen sensing to a potent inflammatory response that contains infection. Given its powerful immunostimulatory nature, pyroptosis has consequences in the context of cancer and is being explored as a tool in cancer therapy. Notably, *Salmonella*-induced pyroptosis has been identified as a key mechanism by which these bacteria can provoke an anticancer immune response. In a mouse colon adenocarcinoma model, intratumoral administration of an attenuated *S.* typhimurium elicited significantly elevated IL-1β levels in the TME and resulted in suppressed tumor growth, an effect that was dependent on inflammasome signaling. In addition, *Salmonella*-treated tumors showed upregulation of inflammasome pathway components (including NLRC4, NLRP3, and the P2X7 purinergic receptor), indicating that the bacterium activates innate immune sensors within the tumor. Different mechanistic studies revealed that *Salmonella* triggers pyroptosis predominantly in tumor-infiltrating macrophages: the bacteria directly infect these phagocytes and activate their inflammasomes, and additionally, *Salmonella*-mediated damage to nearby tumor cells releases Danger-Associated Molecular Pattern (DAMPs) (e.g., extracellular ATP) that further engage macrophage NLRP3 [40][34]. The result of this coordinated activation is pyroptotic death of some tumor-associated macrophages and robust IL-1β release in the tumor milieu. Actually, it has been shown that levels of IL-1β (and also TNF) are markedly increased in tumors colonized by *Salmonella*, but when they restart growth, cytokine levels return to normal. In addition, local administration of IL-1β along with *Salmonella* therapy further prolonged tumor suppression [32]. IL-1β is a potent proinflammatory cytokine that, along with IL-18 (also produced during inflammasome activation), can promote the recruitment and activation of lymphocytes and other immune cells in the tumor [48]. Thus, *Salmonella*-induced pyroptosis turns the immunosuppressive TME into an acutely inflamed site, which is conducive to antitumor immune activity. Consistent with this, *Salmonella* therapy failed to inhibit tumor growth in mice lacking Caspase-1/11, despite having normal baseline levels of IL-1β. This indicates that the process of pyroptosis (Caspase-1/11-mediated cell death)—and not merely the presence of IL-1β—is required to achieve tumor suppression, likely because pyroptosis amplifies local inflammation and releases other immunostimulatory factors (such as IL-18, HMGB1, and cleaved gasdermin-D fragments) that together drive a productive antitumor response [40]. In support of pyroptosis being an immunogenic cell death, a study showed that *Salmonella*-infected tumors showed hallmarks of immunogenicity: dying tumor cells exposed calreticulin on their surface (an "eat me" signal for dendritic cells) and released HMGB1, indicating that pyroptosis was occurring in tumor cells as well as in macrophages. The involvement of tumor cell pyroptosis in *Salmonella* therapy is further suggested by observations that *Salmonella*-infected melanoma cells upregulate

Caspase-11 and gasdermin-D and undergo membrane permeabilization. Notably, the efficacy of *Salmonella* against tumors was also abolished in NLRP3-deficient mice and upon macrophage depletion [40], underscoring that both the sensor (NLRP3 inflammasome) and the effector cells (macrophages) driving pyroptosis are essential for this form of bacteria-mediated cancer therapy. Together, these findings illustrate that *Salmonella*-induced pyroptosis within the TME activates innate immunity in situ and can spark downstream adaptive immune responses that curb tumor progression. Pyroptosis thereby serves as a critical link between *Salmonella* infection and cancer treatment by acting as an engine for inflammation-driven antitumor immunity. Pyroptotic cell death releases a wealth of inflammatory mediators and tumor antigens that help the immune system recognize and attack cancer. For example, the GSDMD pores not only allow IL-1β and IL-18 secretion, but also permit the release of tumor-associated antigens and DAMPs from dying tumor cells, which can be taken up by dendritic cells to prime tumor-specific T cells [52,53]. The concomitant release of IL-18 can drive IFN-γ production by NK and T cells, while IL-1β and HMGB1 recruit and activate myeloid cells, altogether creating a highly immunostimulatory TME [52,53]. Accordingly, inducing pyroptosis in even a fraction of tumor cells can trigger a systemic anticancer immune response. Recent studies have demonstrated that pyroptotic death in as few as ~10–15% of 4T1 tumor cells is sufficient to generate an inflammatory cascade that recruits cytotoxic lymphocytes to eradicate the remaining tumor [54], and that *Salmonella*-mediated antitumor effect disappears if T cells or NK cells are absent [55]. Pyroptosis within these tumors has been shown to increase infiltration of $CD8^+$ T cells, $CD4^+$ T cells, and NK cells, while reducing immunosuppressive cell types such as myeloid-derived suppressor cells, and to drive macrophages toward a pro-inflammatory M1 phenotype. This shift from an "immune-cold" tumor (poorly infiltrated by T cells) to an "immune-hot" tumor (rich in T cell infiltration) is precisely what is needed to improve responsiveness to immunotherapies. Indeed, pyroptosis is now recognized as a form of immunogenic cell death that can convert the TME from suppressive to highly inflammatory, thereby potentiating therapies like immune checkpoint blockade (revised in [53]). In preclinical models of colon carcinoma and melanoma, combination strategies that pair checkpoint inhibitors with pyroptosis-inducing agents lead to superior tumor control, suggesting a synergistic effect where pyroptosis fuels antitumor T cell responses [56]. Accumulating evidence indicates that robust activation of pyroptosis pathways tends to halt tumor growth by activating immune surveillance, whereas defects or suppression of pyroptosis can allow tumors to evade immune detection. For instance, it has been reported that NLRP3 inflammasome components deficiency significantly correlates with advanced hepatocellular carcinoma stage [57]. Many cancers downregulate key pyroptosis executors, particularly different gasdermins. In gastric cancers GSDMA, C and D have been shown to downregulate their expression and have even been postulated as tumor suppressors [58–60], although in those studies pyroptosis was not yet described. In addition GSDMD is also downregulated in colorectal carcinoma (CRC) [61]. For all the above-mentioned situations, restoring or introducing the capacity for pyroptosis in such tumors can tip the balance toward inflammatory cell death and tumor rejection. In that regard, *Salmonella* has shown to induce GSDMD upregulation in B16F1 melanoma cells [40]. In that report, a single intratumoral injection with *Salmonella* also induced augmentation of transcription of *NLRP3* and *NLRC4* inflammasome receptor genes in tumor cells three days post treatment, as well as executors Caspase-1 and IL1β, the latter both at mRNA and protein levels, leading to delay in tumor growth and prolonged survival of melanoma bearing mice.

Pyroptosis has been described as a double-edged sword: while its chronic activation can drive inflammation that may promote tumor development, its acute induction during

therapy can exert potent anticancer effects. [62]. Therefore, harnessing this form of inflammatory cell death is a promising strategy in cancer treatment. *Salmonella*-induced pyroptosis exemplifies this strategy: by causing targeted immune cell death in the tumor and flooding the area with inflammatory signals, it effectively turns the patient's own immune system into a weapon against the cancer. Hence, the goal is to build on these insights—for example, engineering *Salmonella* or other vectors to trigger tumor-localized pyroptosis more efficiently—to overcome suppressive TME and amplify antitumor immunity, offering a potent adjunct or alternative to conventional cancer treatments that would improve cancer immunotherapy outcomes.

2.3. Autophagy

Autophagy is a lysosome-dependent form of cell death that occurs at a low rate under homeostatic conditions but it is amplified in response to cellular stresses such as nutrient deprivation, hypoxia, energy depletion or infection [63]. It is a conserved and essential cellular process through which dysfunctional organelles and cytoplasmatic components are degraded and recycled. Autophagy also targets intracellular bacteria for lysosomal degradation (a process known as xenophagy), thus playing a crucial role in innate immunity [64,65]. Mechanistically, autophagy is a catabolic process in which protein aggregates, invading pathogens and damaged organelles are sequestered into LC3-positive double-membrane vesicles called autophagosomes. These vesicles then fuse with lysosomes, where their cargo is degraded by lysosomal hydrolases [66] (Figure 1).

Host cells can trigger autophagy upon *Salmonella*-infection by directly recognizing cytosolic bacteria and by detecting damaged *Salmonella*-containing vacuoles (SCVs). Following the active invasion, *S. Typhimurium* typically resides within SCVs, whose integrity can be compromised by the activity of the T3SS1 [67]. When bacterial components are exposed to the cytosol, they induce host ubiquitination pathways and the recruitment of autophagy adaptor proteins that bind ubiquitinated bacteria/damaged SCV and LC3, facilitating their sequestration into autophagosomes [68]. In autophagy-deficient cells (e.g., *Atg5*$^{-/-}$), intracellular replication of *Salmonella* is enhanced, highlighting the role of autophagy in restricting bacterial proliferation and maintaining cytosolic integrity. *Salmonella* can also trigger autophagy through nutrient-sensing pathways. The serine/threonine kinase mTOR (mammalian Target of Rapamycin) acts as a central metabolic checkpoint that integrates signals related to nutrient availability, growth factors, and cellular energy status to regulate processes such as protein synthesis, cell growth, and autophagy. Under nutrient-rich conditions, mTOR activity suppresses autophagy. However, during active invasion, the insertion of the T3SS1 translocation apparatus into the host plasma membrane forms pores that cause acute leakage of amino acids from the cytosol. This sudden nutrient depletion triggers a starvation-like response, altering the subcellular localization of mTOR and reducing its activity. As a result, autophagy is rapidly initiated as part of the host defense. Notably, this autophagic response is transient, peaking at approximately 1 h post-infection and declining by 3 h, which coincides with the downregulation of T3SS1 and the upregulation of T3SS2. This transition may restore membrane integrity and normalize amino acid levels, contributing to the resolution of the autophagic cascade [69,70].

In addition to restricting bacterial replication, autophagy plays a crucial role in modulating inflammatory responses. Inflammatory stimuli can activate autophagy to limit IL-1β production by targeting ubiquitinated inflammasome components for lysosomal degradation [71]. Recently, the adaptor protein p62 was shown to inhibit IL-1β release in macrophages infected with *Salmonella Typhimurium* by promoting the autophagic degradation of inflammasome complexes [72]. These findings highlight the role of selective autophagy in disrupting inflammatory signaling by modulating other mechanisms such as pyroptosis.

Autophagy has a dual role in tumor development; it can promote tumor progression or regression depending on different features such as the type of cancer and the stage of the disease, the genetic background, and the TME characteristics, among others [73–75]. This opposing role is well illustrated by a study from Rao et al., who used a murine model of lung cancer to compare autophagy-competent and autophagy-deficient (*Atg5*-deleted) tumors. They found that loss of autophagy accelerated early tumor initiation but reduces progression from adenomas to adenocarcinomas. This context-dependent behavior highlights the need for caution when considering autophagy modulation as a therapeutic strategy in cancer [76]. The stage of cancer appears to be particularly critical: while autophagy is required for cancer immunosurveillance in early stages, once tumors are established, increased autophagy may favor tumor cell survival and growth [77,78] (reviewed in [79]).

In addition to its role in tumor cells, autophagy is also crucial in influencing the behavior of immune cells within the TME. For instance, pharmacological inhibition of autophagy with chloroquine in tumor-associated macrophages has been shown to promote a shift from an immunosuppressive M2 phenotype to a proinflammatory M1-like phenotype. This change leads to a reduction in immunosuppressive T cell populations and an enhancement of antitumor T cell immunity in mouse models [80]. Similarly, inhibition of autophagy in $CD8^+$ T cells enhanced tumor rejection by promoting a more effector memory-like phenotype associated with increased production of IFN-γ and TNF. These effects were linked to enhanced glucose metabolism and epigenetic remodeling in T cells [81].

These findings highlight the potential of targeting autophagy to modulate immune responses within tumors. In this regard, it has been demonstrated that *Salmonella* can induce autophagy in tumor cells by downregulating the AKT/mTOR pathway [82,83]. *Salmonella*-induced autophagy contributes to the suppression of indoleamine 2,3-dioxygenase 1 (IDO), a key immunosuppressive molecule in the tumor microenvironment, thereby hindering tumor immune tolerance and promoting antitumor immunity [84]. Furthermore, combining *Salmonella*-based therapy with pharmacological inhibitors of autophagy, such as chloroquine, has been shown to enhance antitumor effects. This combinatorial approach improves bacterial tumor targeting, increases tumor cell death, and boosts antitumor immune responses [42,85]. For instance, the use of *Salmonella* strains VNP20009 or A1-R in combination with chloroquine resulted in synergistic tumor eradication, both in vitro and in vivo, particularly in fibrosarcoma and other solid tumor models [35,85]. Similarly, the co-administration of chloroquine with *S*. Gallinarum expressing arginine deaminase (*PelB*-ADI) enhanced tumor growth inhibition by simultaneously targeting tumor metabolism and disrupting autophagic flux [33].

Altogether, the complex interplay between autophagy, immune modulation, and tumor progression highlights the therapeutic potential of strategically modulating autophagy within *Salmonella*-based approaches to boost antitumor immunity.

2.4. Emerging Cell Death Pathways Potentially Involved in Salmonella-Based Cancer Immunotherapy

While apoptosis, pyroptosis, and autophagy are the best-characterized forms of cell death associated with *Salmonella*-based cancer immunotherapy, other regulated cell death pathways may also influence therapeutic outcomes. Although experimental evidence directly linking them to cancer treatment efficacy remains limited, the following mechanisms could play relevant roles in shaping the immune and metabolic landscape of the TME:

2.4.1. Necroptosis

Necroptosis is a form of regulated necrosis mediated by death receptors and typically triggered by Caspase-8 inhibition. Although it represents another type of inflammatory

programmed cell death, it differs from pyroptosis in several aspects. One major distinction lies in the key signaling molecules involved, namely receptor-interacting protein kinase 1 (RIPK1), receptor-interacting protein kinase 3 (RIPK3) and their downstream substrate, mixed lineage kinase domain-like (MLKL). Upon activation, RIPK1 and RIPK3 interact to form the necrosome, initiating a phosphorilation cascade that recruits MLKL, ultimately leading to necroptotic cell death [86]. Activated MLKL oligomerizes and translocates to the plasma membrane, forming selective pores that cause calcium influx and culminate in explosive, lytic cell death [87]. To date, no direct association between *Salmonella* cancer immunotherapy and necroptosis has been established. However, Hancz et al. have demonstrated in Jurkat T cells that *Salmonella* can trigger RIPK1 (formerly depicted as RIP1)-dependent cell death through flagellin, while the apoptotic pathway remains unaffected and in the absence of caspases, also known as necroptosis [88]. Also, *Salmonella* infection leads to downregulation of Caspase-8 in infected macrophages and induces necroptosis through type I interferon in the presence of pancaspase inhibition [89,90]. In addition, it is known that intratumoral necroptosis potentiates antitumor immunity [91]. Thus, in a Caspase-8 inhibition scenario induced by *Salmonella*, the resulting necroptosis may lead to a better treatment outcome, pinpointing Caspase-8 as a good target for *Salmonella*-based cancer treatment. Nevertheless, since tumor expression of Caspase-8 varies within cancer types [92], this aspect needs to be further studied in each particular situation.

2.4.2. PANoptosis

As knowledge of programmed cell death has expanded, a recent unifying concept has emerged: PANoptosis, the coordinated execution of pyroptosis, apoptosis and necroptosis through a single regulatory node. This regulation allows for circumventing inhibition of individual death pathways [93], which may represent a tumor cell strategy to avoid elimination. Caspase-8 sits at the hub of this "death triad," acting as a molecular switch that can license or suppress each pathway depending on context [94,95], and all these processes are actually controlled by the same master regulators (ZBP1 and TAK1) [96]. A work in murine bone marrow macrophages showed that *Salmonella* activates the NAIP/NLRC4 inflammasome, recruiting Caspase-1/11 and Caspase-8 into a multimeric "PANoptosome". Only cells lacking all four enzymes (Caspase-1, -11, -8 and RIPK3) escape death, confirming simultaneous engagement of all three arms of PANoptosis, whereas single knockouts do not [93]. This fail-safe design thwarts *Salmonella*'s attempts to block individual pathways and ensures robust cytokine release (IL-1β, IL-18, HMGB1) together with lytic membrane rupture of infected host cells. Since the resulting microenvironment is flooded with danger cues, it constitutes an ideal setting for mounting antitumor immunity. Hence, the use of attenuated *Salmonella* as immunotherapy exploits the same circuitry inside tumors. An example of the combined forces is the evidence that *Salmonella* treatment in colon carcinoma model promoted tumor regression associated with increased IL-1β and TNF, Caspase-1 activation, and NLRC4 inflammasome signaling [32], even when by that time the term PANoptosis term was not coined yet. All in all, PANoptotic cell death converts "cold" tumors into inflamed foci rich in antigen, DAMPs and type-1 cytokines—conditions that foster dendritic-cell priming and cytotoxic-T/NK-cell recruitment. Harnessing or mimicking this integrated death program—rather than stimulating a single pathway—may offer a powerful route to next-generation cancer immunotherapies, although the implications of PANoptosis on cancer immunotherapies are not fully explored nor understood.

2.4.3. ETosis

Other less common ways of cell death have been reported by the use of *Salmonella*, as is the case of ETosis, in which the cell releases its contents into the extracellular space

forming DNA nets which are termed "extracellular traps" [97]. Particularly regarding METosis, the ETosis of macrophages, it has been reported that *Salmonella* infection steadily induces the release of Macrophage Extracellular Traps (METs) with the concomitant cell death by METosis in less than an hour [98]. Nevertheless, its role in cancer was not assessed. In this regard, the group of Cools-Lartigue et al. has found that a close relative of METs, which are the Neutrophil Extracellular Traps (NETs), may favor metastasis development by sequestering tumor cells and releasing them in distant places [99,100]. On the other hand, NETs have been reported to boost chemotherapy against CRC through cathepsin G-mediated translocation of cytosolic BAX to the mitochondrial membrane. There, BAX and BAK oligomerize to form pores that mediate cytochrome c release, promoting apoptosis. [101]. To the best of our knowledge, up to date no mechanistic link between METs and cancer has been described. However, since extracellular DNA acts as a DAMP that activates inflammasome [102,103], it is plausible that its detection may induce an inflammatory response, that together with antigen exposure caused by tumor cell death by other pathways (e.g., *Salmonella*-induced pyroptosis), may generate a specific antitumor response. Further studies are needed to elucidate the outcome of the occurrence of extracellular traps release in a tumoral context. However, there are reports indicating that protein components of these traps, such as myeloperoxidase and elastase, exhibit antitumor effects in vivo, both locally and even at distant metastatic sites [104][105]. Moreover, elastase has been shown to selectively kill tumor cells without affecting non-tumor cells [105]. In addition, NETs have been found to correlate positively with survival in patients with high-grade ovarian cancer, through the induction of NADPH oxidase 2-independent NETosis [106] and in the case of CRC, increased NET levels in tumors were also associated with longer progression-free survival [101].

Interestingly, the GSDMD pores required for pyroptosis may also be used to release the extracellular traps, so both processes have proven to be connected by this molecule [107,108], even when there are also reports regarding NETosis independent of GSDMD [109]. Therefore, a systematic simultaneous assessment of pyroptosis and ETosis, their interaction and contribution to *Salmonella*-based cancer immunotherapy is still required.

It is also worth mentioning that M1 macrophages, unlike their M2 counterparts, are capable of releasing METs as part of their antimicrobial and proinflammatory response [110]. As stated in Section 2.3, inhibition of autophagy favors M1 polarization [80], and this effect may partly result from impaired clearance of inflammasome components, which enhances Caspase-1 activation and IL-1β release, thereby amplifying inflammatory cell death [111,112]. We have previously reported that soon after intratumoral injection, *Salmonella* induces pyroptosis and promotes a transient shift from M2 to M1 macrophages that corresponds to antitumor effect, but this profile is then lost [40]. In this context, modulation of autophagy may represent a strategy to sustain or potentiate the M1 phenotype and the proinflammatory responses elicited by *Salmonella* within the TME, perpetuating its therapeutic effects. Interestingly, inhibition of autophagy has been shown to prevent intracellular chromatin decondensation, a key step for NETosis, leading instead to cell death resembling apoptosis [113]. This finding suggests that apoptosis might act as a backup program when ETosis pathways are impaired, highlighting the complex interplay between different cell death mechanisms.

2.4.4. Ferroptosis

Ferroptosis is a newly characterized iron-dependent form of regulated cell death triggered by disruption of cellular redox homeostasis, leading to the accumulation of lipid peroxides and oxidative damage [114]. The only report regarding *Salmonella*-induced ferroptosis as part of an immunotherapy is on glioma cells, showing that *Salmonella* YB1 infection disrupts the GPX4–glutathione redox axis, leading to mitochondrial damage and

tumor growth suppression in vivo, which can be reversed by the use of the ferroptosis inhibitor Fer-1 [36]. It has been reported that therapy-resistant cancer cells, particularly those of the mesenchymal state and prone to metastasis, are profoundly vulnerable to ferroptosis. Hence, modulation of ferroptosis, holds great potential for the treatment of cancers (revised in [115]). To date, the contribution of ferroptosis to *Salmonella*-mediated antitumor activity can be directly attributed to tumor mass cytoreduction resulting from cancer cell death. However, the consequences of ferroptosis activation in the TME should be addressed to help understanding its role in tumor suppression and immune surveillance within *Salmonella*-based cancer therapies.

3. Challenges Facing *Salmonella*-Induced Cell Death as Antitumor Strategy

The most straightforward approach to inducing cancer cell death was traditionally the use of conventional chemotherapy or radiotherapy. However, in the current era of immunotherapy, the most evident strategies are now immune checkpoint inhibitors and chimeric antigen receptor (CAR) T cell therapies. Although immune checkpoint inhibitors have shown remarkable success in a subset of patients, a significant proportion of treated individuals exhibit partial or no response, and their use remains limited by immune-related adverse events and high costs. On the other hand, CAR T cell therapy, while highly effective in hematological malignancies, faces considerable challenges in solid tumors, including limited efficacy, severe toxicity, and complex logistics associated with the use of autologous cells. In this context, the use of *Salmonella* as a tumor-targeting agent emerges as an innovative and potentially more cost-effective strategy to induce tumor cell death. Nevertheless, this approach is not exempt from challenges. One of the main difficulties lies in the synergy, crosstalk, and compensatory interactions between molecules that were previously thought to act exclusively within their representative cell death pathways. For instance, intracellular molecules released during one form of cell death (e.g., necroptosis) can be sensed by pattern recognition receptors such as NLRP3—which is notably promiscuous in detecting damage—thereby triggering pyroptosis. Regarding PANoptosis, it has been described that the PANoptosome complex consists of Caspase-8, ASC, RIPK1, RIPK3, NLRP3, and ZBP1, which directly interact with each other [116]. Because these molecules can participate in multiple cell death pathways, it becomes difficult to delineate the specific mechanisms induced by *Salmonella*. In addition, evidence suggests an interconnection between pyroptosis, apoptosis, and necroptosis during *S. Typhimurium* infection [93], and while deletion of molecules such as Caspases 1, 8 and 11 along with RIPK3 protects macrophages from cell death, individual deletions do not fully prevent it, highlighting the challenge of fine-tuning the system [117]. Furthermore, gasdermins, originally characterized for their role in pyroptosis, are now increasingly recognized as effectors in apoptosis as well. Certain members of this family, such as GSDME, directly contribute to mitochondrial permeabilization and the release of apoptotic factors, thus bridging pyroptosis and apoptosis [118]. This functional interplay may also explain why cells often display overlapping features of different death pathways.

Furthermore, it is essential to consider both species-specific and cell-type variations. For instance, murine keratinocytes lack NLRP1 expression and are hence unable to respond to NLRP1 activators, while humans constitutively express this receptor in barrier cells [119], highlighting significant interspecies differences in innate immune signaling pathways. Additionally, cell-type-specific responses further complicate the interpretation scenario as, for instance, myeloid and epithelial cells may engage distinct immune pathways upon sensing of infection [120], and many different kinds of cells coexist in the TME at the same time. In the case of ETosis, the existence of distinct subtypes or compositions

depending on the cell and the initial trigger also remains a source of heterogeneity that has to be considered.

Although the focus of this review is on myeloid populations due to their abundance and functional relevance within the TME, it is important to acknowledge that lymphocytes may also undergo *Salmonella*-induced cell death through different mechanisms. However, the current evidence specifically addressing these pathways in lymphoid cells during *Salmonella*-based cancer therapies remains limited. For instance, a report suggests that *Salmonella* Typhi can induce apoptosis in lymphoma-derived T cells in vitro and contributes to tumor regression in murine T cell lymphoma models [121]. However, in this case, lymphocytes are not other than tumor cells. Other studies show that *Salmonella* inhibits both pyroptosis [122,123] and autophagy [124] in B cells to persist, but those reports do not address bacteria as cancer therapy. This knowledge gap represents an opportunity for future investigation to clarify whether and how distinct lymphocyte subsets undergo programmed cell death following bacterial targeting in the TME.

Finally, as described in Section 2.3, considering cell death modulation as a therapeutic strategy in cancer also has to take into account the stage of cancer [125,126].

4. Conclusions

In this review, we have discussed the different types of cell death triggered by *Salmonella* that may contribute to tumor shrinkage and, ultimately, tumor eradication. We also summarized the mechanisms by which these processes can be modulated, as well as the challenges associated with their regulation—largely arising from the fact that cellular context critically determines whether induction or inhibition of specific death pathways is the most beneficial strategy. All things considered, the ability of *Salmonella* to induce tumor cell death stands as a cornerstone of its oncolytic and immunotherapeutic potential. Through both direct and indirect mechanisms, this approach not only eliminates tumor cells and release tumor antigens, thereby priming antitumor immunity, but also reshapes the TME by promoting inflammation and immune cell infiltration, effectively converting immunosuppressive "cold" tumors into immunologically active "hot" tumors. Importantly, many antitumor agents previously thought to act primarily through one mechanism are now recognized to act through another or a combination of them or to mutually regulate. This paradigm shift underscores the need to reassess the mechanisms underlying *Salmonella*-based immunotherapies and to exploit the full spectrum of programmed cell death modalities they can trigger. Understanding and harnessing these processes is essential to optimize therapeutic outcomes and to advance the rational design and clinical translation of *Salmonella*-based cancer immunotherapies.

Author Contributions: Conceptualization, A.M.; literature research, A.M. and S.C.; writing—original draft preparation, A.M.; writing—review and editing, A.M., S.C., M.C.P., J.A.C. and M.M.; image design, A.M., S.C. and M.C.P.; funding acquisition, A.M., J.A.C. and M.M. All authors have read and agreed to the published version of the manuscript.

Funding: The APC was funded by Agencia Nacional de Investigación e Innovación, project ID FCE_3_2022_1_172209.

Conflicts of Interest: The authors declare no conflicts of interest.

References

1. McCarthy, E.F. The toxins of William B. Coley and the treatment of bone and soft-tissue sarcomas. *Iowa Orthop. J.* **2006**, *26*, 154–158. Available online: http://www.ncbi.nlm.nih.gov/pubmed/16789469 (accessed on 13 December 2025)
2. Redelman-sidi, G.; Glickman, M.S.; Bochner, B.H. The mechanism of action of BCG therapy for bladder cancer—A current perspective. *Nat. Rev. Urol.* **2014**, *11*, 153–162. https://doi.org/10.1038/nrurol.2014.15.

3. Carri, I.; Schwab, E.; Trivino, J.C.; Von Euw, E.M.; Nielsen, M.; Mordoh, J.; Barrio, M.M. VACCIMEL, an allogeneic melanoma vaccine, efficiently triggers T cell immune responses against neoantigens and alloantigens, as well as against tumor-associated antigens. *Front. Immunol.* **2025**, *15*, 1496204. https://doi.org/10.3389/fimmu.2024.1496204.
4. Zhou, S.; Gravekamp, C.; Bermudes, D.; Liu, K. Tumour-targeting bacteria engineered to fight cancer. *Nat. Rev. Cancer* **2018**, *18*, 727–743. https://doi.org/10.1038/s41568-018-0070-z.
5. Frahm, M.; Felgner, S.; Kocijancic, D.; Rohde, M.; Hensel, M.; Curtis III, R.; Erhardt, M.; Weiss, S. Efficiency of Conditionally Attenuated Salmonella enterica Serovar Typhimurium in Bacterium-Mediated Tumor Therapy. *mBio* **2015**, *6*, e00254-15. https://doi.org/10.1128/mBio.00254-15.
6. Wang, D.; Wei, X.; Kalvakolanu, D.V.; Guo, B.; Zhang, L. Perspectives on Oncolytic Salmonella in Cancer Immunotherapy—A Promising Strategy. *Front. Immunol.* **2021**, *12*, 615930. https://doi.org/10.3389/fimmu.2021.615930.
7. Kasinskas, R.W.; Forbes, N.S. Salmonella typhimurium specifically chemotax and proliferate in heterogeneous tumor tissue in vitro. *Biotechnol. Bioeng.* **2006**, *94*, 710–721. https://doi.org/10.1002/bit.20883.
8. Kasinskas, R.W.; Forbes, N.S. Salmonella typhimurium lacking ribose chemoreceptors localize in tumor quiescence and induce apoptosis. *Cancer Res.* **2007**, *67*, 3201–3209. https://doi.org/10.1158/0008-5472.CAN-06-2618.
9. Chen, W.; Wang, Y.; Qin, M.; Zhang, X.; Zhang, Z.; Sun, X.; Gu, Z. Bacteria-Driven Hypoxia Targeting for Combined Biotherapy and Photothermal Therapy. *ACS Nano* **2018**, *12*, 5995–6005. https://doi.org/10.1021/acsnano.8b02235.
10. Mi, Z.; Feng, Z.-C.; Li, C.; Yang, X.; Ma, M.-T.; Rong, P.-F. Salmonella-Mediated Cancer Therapy: An Innovative Therapeutic Strategy. *J. Cancer* **2019**, *10*, 4765–4776. https://doi.org/10.7150/jca.32650.
11. [11] Copland, A.; Mackie, G.M.; Scarfe, L.; Jinks, E.; Lecky, D.A.J.; Gudgeon, N.; McQuade, R.; Ono, M.; Barthel, M.; Hardt, W.-D.; et al. Salmonella cancer therapy metabolically disrupts tumours at the collateral cost of T cell immunity. *EMBO Mol. Med.* **2024**, *16*, 3057–3088. https://doi.org/10.1038/s44321-024-00159-2.
12. Toso, J.F.; Gill, V.J.; Hwu, P.; Marincola, F.M.; Restifo, N.P.; Schwartzentruber, D.J.; Sherry, R.M.; Topalian, S.L.; Yang, J.C.; Stock, F.; et al. Phase I study of the intravenous administration of attenuated Salmonella typhimurium to patients with metastatic melanoma. *J. Clin. Oncol.* **2002**, *20*, 142–152. https://doi.org/10.1200/JCO.20.1.142.
13. Heimann, D.; Rosenberg, S.A. Continuous Intravenous Administration of Live Genetically Modified Salmonella Typhimurium in Patients with Metastatic Melanoma. *J. Immunother.* **2003**, *26*, 179–180.
14. Gniadek, T.J.; Augustin, L.; Schottel, J.; Leonard, A.; Saltzman, D.; Greeno, E.; Batist, G. A Phase I, Dose Escalation, Single Dose Trial of Oral Attenuated Salmonella typhimurium Containing Human IL-2 in Patients with Metastatic Gastrointestinal Cancers. *J. Immunother.* **2020**, *43*, 217–221. https://doi.org/10.1097/CJI.0000000000000325.
15. Pangilinan, C.R.; Lee, C.-H. Salmonella-Based Targeted Cancer Therapy: Updates on A Promising and Innovative Tumor Immunotherapeutic Strategy. *Biomedicines* **2019**, *7*, 36.
16. Al-Saafeen, B.H.; Fernandez-Cabezudo, M.J.; Al-Ramadi, B.K. Integration of Salmonella into Combination Cancer Therapy. *Cancers* **2021**, *13*, 3228. https://doi.org/10.3390/cancers13133228.
17. Vola, M.; Mónaco, A.; Bascuas, T.; Rimsky, G.; Agorio, C.I.; Chabalgoity, J.A.; Moreno, M. TLR7 agonist in combination with Salmonella as an effective antimelanoma immunotherapy. *Immunotherapy* **2018**, *10*, 665–679. https://doi.org/10.2217/imt-2017-0188.
18. Kumar, P.; Nagarajan, A.; Uchil, P.D. Analysis of Cell Viability by the MTT Assay. *Cold Spring Harb. Protoc.* **2018**, *2018*, pdb.prot095505. https://doi.org/10.1101/pdb.prot095505.
19. Kumar, P.; Nagarajan, A.; Uchil, P.D. Analysis of Cell Viability by the alamarBlue Assay. *Cold Spring Harb. Protoc.* **2018**, *2018*, pdb.prot095489. https://doi.org/10.1101/pdb.prot095489.
20. Kumar, P.; Nagarajan, A.; Uchil, P.D. Analysis of Cell Viability by the Lactate Dehydrogenase Assay. *Cold Spring Harb. Protoc.* **2018**, *2018*, pdb.prot095497. https://doi.org/10.1101/pdb.prot095497.
21. Haanen, C.; Vermes, I. Apoptosis and inflammation. *Mediat. Inflamm.* **1995**, *4*, 5–15.
22. Monack, D.M.; Raupach, B.; Hromockyj, A.E.; Falkow, S. Salmonella typhimurium invasion induces apoptosis in infected macrophages. *Proc. Natl. Acad. Sci. USA* **1996**, *93*, 9833–9838. https://doi.org/10.1073/pnas.93.18.9833.
23. Hersh, D.; Monack, D.M.; Smith, M.R.; Ghori, N.; Falkow, S.; Zychlinsky, A. The Salmonella invasin SipB induces macrophage apoptosis by binding to caspase-1. *Proc. Natl. Acad. Sci. USA* **1999**, *96*, 2396–2401. https://doi.org/10.1073/pnas.96.5.2396.
24. Valle, E.; Guiney, D.G. Characterization of Salmonella-Induced Cell Death in Human Macrophage-Like THP-1 Cells. *Infect. Immun.* **2005**, *73*, 2835–2840. https://doi.org/10.1128/IAI.73.5.2835-2840.2005.
25. Knodler, L.A.; Finlay, B.B.; Steele-Mortimer, O. The Salmonella Effector Protein SopB Protects Epithelial Cells from Apoptosis by Sustained Activation of Akt. *J. Biol. Chem.* **2005**, *280*, 9058–9064. https://doi.org/10.1074/jbc.M412588200.

26. Ganai, S.; Arenas, R.B.; Sauer, J.P.; Bentley, B.; Forbes, N.S. In tumors Salmonella migrate away from vasculature toward the transition zone and induce apoptosis. *Cancer Gene Ther.* **2011**, *18*, 457–466. https://doi.org/10.1038/cgt.2011.10.
27. Zhang, Y.; Tang, Z.; Shao, Y.; Yue, X.; Chu, Y.; Chen, D. Attenuated Salmonella typhimurium L forms suppress tumor growth and promote apoptosis in murine ovarian tumors. *Sci. Rep.* **2024**, *14*, 16045. https://doi.org/10.1038/s41598-024-66898-x.
28. Badie, F.; Ghandali, M.; Tabatabaei, S.A.; Safari, M.; Khorshidi, A.; Shayestehpour, M.; Mahjoubin-Tehran, M.; Morshedi, K.; Jalili, A.; Tajiknia, V.; et al. Use of Salmonella Bacteria in Cancer Therapy: Direct, Drug Delivery and Combination Approaches. *Front. Oncol.* **2021**, *11*, 624759. https://doi.org/10.3389/fonc.2021.624759.
29. Srikanth, C.V.; Wall, D.M.; Maldonado-Contreras, A.; Shi, H.N.; Zhou, D.; Demma, Z.; Mumy, K.L.; McCormick, B.A. Salmonella Pathogenesis and Processing of Secreted Effectors by Caspase-3. *Science* **2010**, *330*, 390–393. https://doi.org/10.1126/science.1194598.
30. Chilibroste, S.; dos Santos, J.C.; Mónaco, A.; Joosten, L.A.B.; Moreno, M.; Chabalgoity, J.A. Salmonella LVR01 triggers antagonistic two-armed innate immune memory that impacts on antitumor efficacy. *Front. Immunol.* **2025**, *16*, 1535131. https://doi.org/10.3389/fimmu.2025.1535131.
31. Zhao, M.; Yang, M.; Ma, H.; Li, X.; Tan, X.; Li, S.; Yang, Z.; Hoffman, R.M. Targeted Therapy with a Salmonella Typhimurium Leucine-Arginine Auxotroph Cures Orthotopic Human Breast Tumors in Nude Mice. *Cancer Res.* **2006**, *66*, 7647–7652. https://doi.org/10.1158/0008-5472.CAN-06-0716.
32. Kim, J.-E.; Phan, T.X.; Nguyen, V.H.; Dinh-Vu, H.-V.; Zheng, J.H.; Yun, M.; Park, S.-G.; Hong, Y.; Choy, H.E.; Szardenings, M.; et al. Salmonella typhimurium suppresses tumor growth via the pro-inflammatory cytokine interleukin-1β. *Theranostics* **2015**, *5*, 1328–1342. https://doi.org/10.7150/thno.11432.
33. Duysak, T.; Kim, K.; Yun, M.; Jeong, J.-H.; Choy, H.E. Enhanced anti-cancer efficacy of arginine deaminase expressed by tumor-seeking Salmonella Gallinarum. *Oncogene* **2024**, *43*, 3378–3387. https://doi.org/10.1038/s41388-024-03176-0.
34. Phan, T.X.; Nguyen, V.H.; Duong, M.T.-Q.; Hong, Y.; Choy, H.E.; Min, J.-J. Activation of inflammasome by attenuated Salmonella typhimurium in bacteria-mediated cancer therapy. *Microbiol. Immunol.* **2015**, *59*, 664–675. https://doi.org/10.1111/1348-0421.12333.
35. Morinaga, S.; Zhao, M.; Mizuta, K.; Kang, B.M.; Bouvet, M.; Yamamoto, N.; Hayashi, K.; Kimura, H.; Miwa, S.; Igarashi, K.; et al. The Combination of Tumor-targeting Salmonella typhimurium A1-R Plus the Autophagy-inhibitor Chloroquine Synergistically Eradicates HT1080 Fibrosarcoma Cells In Vitro and In Vivo. *In Vivo* **2025**, *39*, 102–109. https://doi.org/10.21873/invivo.13807.
36. Chen, J.; Li, T.; Zhou, N.; He, Y.; Zhong, J.; Ma, C.; Zeng, M.; Ji, J.; Huang, J.-D.; Ke, Y.; et al. Engineered Salmonella inhibits GPX4 expression and induces ferroptosis to suppress glioma growth in vitro and in vivo. *J. Neurooncol.* **2023**, *163*, 607–622. https://doi.org/10.1007/s11060-023-04369-5.
37. Guan, G.; Zhao, M.; Liu, L.; Jin, C.; Sun, K.; Zhang, D.; Yu, D.; Cao, H.; Lu, Y.Q.; Wen, L. Salmonella typhimurium Mediated Delivery of Apoptin in Human Laryngeal Cancer. *Int. J. Med. Sci.* **2013**, *10*, 1639–1648. https://doi.org/10.7150/ijms.6960.
38. Zhao, C.; He, J.; Cheng, H.; Zhu, Z.; Xu, H. Enhanced therapeutic effect of an antiangiogenesis peptide on lung cancer in vivo combined with salmonella VNP20009 carrying a Sox2 shRNA construct. *J. Exp. Clin. Cancer Res.* **2016**, *35*, 107. https://doi.org/10.1186/s13046-016-0381-4.
39. Zhao, M.; Geller, J.; Ma, H.; Yang, M.; Penman, S.; Hoffman, R.M. Monotherapy with a tumor-targeting mutant of Salmonella typhimurium cures orthotopic metastatic mouse models of human prostate cancer. *Proc. Natl. Acad. Sci. USA* **2007**, *104*, 10170–10174. https://doi.org/10.1073/pnas.0703867104.
40. Mónaco, A.; Chilibroste, S.; Yim, L.; Chabalgoity, J.A.; Moreno, M. Inflammasome activation, NLRP3 engagement and macrophage recruitment to tumor microenvironment are all required for Salmonella antitumor effect. *Cancer Immunol. Immunother.* **2022**, *71*, 2141–2150. https://doi.org/10.1007/s00262-022-03148-x.
41. Wang, Y.; Zhou, Z.; Chen, W.; Qin, M.; Zhang, Z.; Gong, T.; Sun, X. Potentiating bacterial cancer therapy using hydroxychloroquine liposomes. *J. Control. Release* **2018**, *280*, 39–50. https://doi.org/10.1016/j.jconrel.2018.04.046.
42. Zhang, X.; Xu, Q.; Zhang, Z.; Cheng, W.; Cao, W.; Jiang, C.; Han, C.; Li, J.; Hua, Z. Chloroquine enhanced the anticancer capacity of VNP20009 by inhibiting autophagy. *Sci. Rep.* **2016**, *6*, 29774. https://doi.org/10.1038/srep29774.
43. Wang, H.; Chen, T.; Wan, L.; Lu, J.; Wei, H.; Deng, K.-Y.; Wei, J.; Xin, H.-B. Attenuated Salmonella engineered with an apoptosis-inducing factor (AIF) eukaryotic expressing system enhances its anti-tumor effect in melanoma in vitro and in vivo. *Appl. Microbiol. Biotechnol.* **2020**, *104*, 3517–3528. https://doi.org/10.1007/s00253-020-10485-3.

44. Chen, J.; Yang, B.; Cheng, X.; Qiao, Y.; Tang, B.; Chen, G.; Wei, J.; Liu, X.; Cheng, W.; Du, P.; et al. Salmonella-mediated tumor-targeting TRAIL gene therapy significantly suppresses melanoma growth in mouse model. *Cancer Sci.* **2012**, *103*, 325–333. https://doi.org/10.1111/j.1349-7006.2011.02147.x.
45. Pérez Jorge, G.; Gontijo, M.; Flóro e Silva, M.; Rodriguez Dos Santos Goes, I.C.; Jaimes-Florez, Y.P.; De Oliveira Coser, L.; Soares Rocha, F.J.; Giorgio, S.; Brocchi, M. Attenuated mutants of Salmonella enterica Typhimurium mediate melanoma regression via an immune response. *Exp. Biol. Med.* **2024**, 249, 10081. https://doi.org/10.3389/ebm.2024.10081.
46. Xia, X.; Wang, X.; Cheng, Z.; Qin, W.; Lei, L.; Jiang, J.; Hu, J. The role of pyroptosis in cancer: Pro-cancer or pro-"host"? *Cell Death Dis.* **2019**, *10*, 650. https://doi.org/10.1038/s41419-019-1883-8.
47. Lu, X.; Guo, T.; Zhang, X. Pyroptosis in Cancer: Friend or Foe? *Cancers* **2021**, *13*, 3620. https://doi.org/10.3390/cancers13143620.
48. Broz, P.; Newton, K.; Lamkanfi, M.; Mariathasan, S.; Dixit, V.M.; Monack, D.M. Redundant roles for inflammasome receptors NLRP3 and NLRC4 in host defense against Salmonella. *J. Exp. Med.* **2010**, *207*, 1745–1755. https://doi.org/10.1084/jem.20100257.
49. Kayagaki, N.; Stowe, I.B.; Lee, B.L.; O'Rourke, K.; Anderson, K.; Warming, S.; Cuellar, T.; Haley, B.; Roose-Girma, M.; Phung, Q.T.; et al. Caspase-11 cleaves gasdermin D for non-canonical inflammasome signalling. *Nature* **2015**, *526*, 666–671. https://doi.org/10.1038/nature15541.
50. Shi, J.; Zhao, Y.; Wang, K.; Shi, X.; Wang, Y.; Huang, H.; Zhuang, Y.; Cai, T.; Wang, F.; Shao, F. Cleavage of GSDMD by inflammatory caspases determines pyroptotic cell death. *Nature* **2015**, *526*, 660–665. https://doi.org/10.1038/nature15514.
51. Baroja-Mazo, A.; Martín-Sánchez, F.; Gomez, A.I.; Martínez, C.M.; Amores-Iniesta, J.; Compan, V.; Barberà-Cremades, M.; Yagüe, J.; Ruiz-Ortiz, E.; Antón, J.; et al. The NLRP3 inflammasome is released as a particulate danger signal that amplifies the inflammatory response. *Nat. Immunol.* **2014**, *15*, 738–748. https://doi.org/10.1038/ni.2919.
52. Tan, Y.; Chen, Q.; Li, X.; Zeng, Z.; Xiong, W.; Li, G.; Li, X.; Yang, J.; Xiang, B.; Yi, M. Pyroptosis: A new paradigm of cell death for fighting against cancer. *J. Exp. Clin. Cancer Res.* **2021**, *40*, 153. https://doi.org/10.1186/s13046-021-01959-x.
53. Wang, W.; Zhang, L.; Sun, Z. Eliciting pyroptosis to fuel cancer immunotherapy: Mechanisms and strategies. *Cancer Biol. Med.* **2022**, *19*, 948–964. https://doi.org/10.20892/j.issn.2095-3941.2022.0049.
54. Wang, Q.; Wang, Y.; Ding, J.; Wang, C.; Zhou, X.; Gao, W.; Huang, H.; Shao, F.; Liu, Z. A bioorthogonal system reveals antitumour immune function of pyroptosis. *Nature* **2020**, *579*, 421–426. https://doi.org/10.1038/s41586-020-2079-1.
55. Mónaco, A.; Plata, M.C.; Chilibroste, S.; Vola, M.; Chabalgoity, J.A.; Moreno, M. Salmonella-induced immune response reduces recurrence and tumor dissemination in preclinical melanoma model. *Curr. Res. Immunol.* **2022**, *3*, 159–166. https://doi.org/10.1016/j.crimmu.2022.08.001.
56. Zhou, Z.; He, H.; Wang, K.; Shi, X.; Wang, Y.; Su, Y.; Wang, Y.; Li, D.; Liu, W.; Zhang, Y.; et al. Granzyme A from cytotoxic lymphocytes cleaves GSDMB to trigger pyroptosis in target cells. *Science* **2020**, *368*, aaz7548. https://doi.org/10.1126/science.aaz7548.
57. Wei, Q.; Mu, K.; Li, T.; Zhang, Y.; Yang, Z.; Jia, X.; Zhao, W.; Huai, W.; Guo, P.; Han, L. Deregulation of the NLRP3 inflammasome in hepatic parenchymal cells during liver cancer progression. *Lab. Investig.* **2014**, *94*, 52–62. https://doi.org/10.1038/labinvest.2013.126.
58. Saeki, N.; Kim, D.H.; Usui, T.; Aoyagi, K.; Tatsuta, T.; Aoki, K.; Yanagihara, K.; Tamura, M.; Mizushima, H.; Sakamoto, H.; et al. GASDERMIN, suppressed frequently in gastric cancer, is a target of LMO1 in TGF-β-dependent apoptotic signalling. *Oncogene* **2007**, *26*, 6488–6498. https://doi.org/10.1038/sj.onc.1210475.
59. Saeki, N.; Usui, T.; Aoyagi, K.; Kim, D.H.; Sato, M.; Mabuchi, T.; Yanagihara, K.; Ogawa, K.; Sakamoto, H.; Yoshida, T.; et al. Distinctive expression and function of four GSDM family genes (GSDMA-D) in normal and malignant upper gastrointestinal epithelium. *Genes Chromosom. Cancer* **2009**, *48*, 261–271. https://doi.org/10.1002/gcc.20636.
60. Miguchi, M.; Hinoi, T.; Shimomura, M.; Adachi, T.; Saito, Y.; Niitsu, H.; Kochi, M.; Sada, H.; Sotomaru, Y.; Ikenoue, T.; et al. Gasdermin C Is Upregulated by Inactivation of Transforming Growth Factor β Receptor Type II in the Presence of Mutated Apc, Promoting Colorectal Cancer Proliferation. *PLoS ONE* **2016**, *11*, e0166422. https://doi.org/10.1371/journal.pone.0166422.
61. Orita, H.; Tanaka, S.; Watanabe, S.; Matsuzawa, H.; Mizuguchi, K.; Ito, T.; Senuma, K.; Kushida, T.; Sakurada, M.; Maekawa, H.; et al. Abstract 3424: The efficacy of Gasdermin gene family for tumor marker in colorectal cancer. *Cancer Res.* **2015**, *75*, 3424. https://doi.org/10.1158/1538-7445.AM2015-3424.
62. Liu, Z.; Wang, C.; Lin, C. Pyroptosis as a double-edged sword: The pathogenic and therapeutic roles in inflammatory diseases and cancers. *Life Sci.* **2023**, *318*, 121498. https://doi.org/10.1016/j.lfs.2023.121498.
63. Casanova, J.E. Bacterial Autophagy: Offense and Defense at the Host–Pathogen Interface. *Cell. Mol. Gastroenterol. Hepatol.* **2017**, *4*, 237–243. https://doi.org/10.1016/j.jcmgh.2017.05.002.

64. Tattoli, I.; Sorbara, M.T.; Philpott, D.J.; Girardin, S.E. Bacterial autophagy. *Autophagy* **2012**, *8*, 1848–1850. https://doi.org/10.4161/auto.21863.
65. Wu, S.; Shen, Y.; Zhang, S.; Xiao, Y.; Shi, S. Salmonella Interacts with Autophagy to Offense or Defense. *Front. Microbiol.* **2020**, *11*, 721. https://doi.org/10.3389/fmicb.2020.00721.
66. Lamark, T.; Johansen, T. Mechanisms of Selective Autophagy. *Annu. Rev. Cell Dev. Biol.* **2021**, *37*, 143–169. https://doi.org/10.1146/annurev-cellbio-120219-035530.
67. Birmingham, C.L.; Smith, A.C.; Bakowski, M.A.; Yoshimori, T.; Brumell, J.H. Autophagy Controls Salmonella Infection in Response to Damage to the Salmonella-containing Vacuole. *J. Biol. Chem.* **2006**, *281*, 11374–11383. https://doi.org/10.1074/jbc.M509157200.
68. Zheng, Y.T.; Shahnazari, S.; Brech, A.; Lamark, T.; Johansen, T.; Brumell, J.H. The Adaptor Protein p62/SQSTM1 Targets Invading Bacteria to the Autophagy Pathway. *J. Immunol.* **2009**, *183*, 5909–5916. https://doi.org/10.4049/jimmunol.0900441.
69. Tattoli, I.; Sorbara, M.T.; Vuckovic, D.; Ling, A.; Soares, F.; Carneiro, L.A.M.; Yang, C.; Emili, A.; Philpott, D.J.; Girardin, S.E. Amino Acid Starvation Induced by Invasive Bacterial Pathogens Triggers an Innate Host Defense Program. *Cell Host Microbe* **2012**, *11*, 563–575. https://doi.org/10.1016/j.chom.2012.04.012.
70. Tattoli, I.; Philpott, D.J.; Girardin, S.E. The bacterial and cellular determinants controlling the recruitment of mTOR to the Salmonella-containing vacuole. *Biol. Open* **2012**, *1*, 1215–1225. https://doi.org/10.1242/bio.20122840.
71. Shi, C.; Shenderov, K.; Huang, N.; Kabat, J.; Abu-Asab, M.; Fitzgerald, K.A.; Sher, A.; Kehrl, J.H. Activation of autophagy by inflammatory signals limits IL-1β production by targeting ubiquitinated inflammasomes for destruction. *Nat. Immunol.* **2012**, *13*, 255–263. https://doi.org/10.1038/ni.2215.
72. Hos, N.J.; Fischer, J.; Murthy, A.M.V.; Hejazi, Z.; Krönke, M.; Hos, D.; Robinson, N. P62 inhibits IL-1β release during Salmonella Typhimurium infection of macrophages. *Front. Cell. Infect. Microbiol.* **2025**, *15*, 1495567. https://doi.org/10.3389/fcimb.2025.1495567.
73. Towers, C.G.; Wodetzki, D.; Thorburn, A. Autophagy and cancer: Modulation of cell death pathways and cancer cell adaptations. *J. Cell Biol.* **2019**, *219*, e201909033. https://doi.org/10.1083/jcb.201909033.
74. Gao, W.; Wang, X.; Zhou, Y.; Wang, X.; Yu, Y. Autophagy, ferroptosis, pyroptosis, and necroptosis in tumor immunotherapy. *Signal Transduct. Target. Ther.* **2022**, *7*, 196. https://doi.org/10.1038/s41392-022-01046-3.
75. Dikic, I.; Elazar, Z. Mechanism and medical implications of mammalian autophagy. *Nat. Rev. Mol. Cell Biol.* **2018**, *19*, 349–364. https://doi.org/10.1038/s41580-018-0003-4.
76. Rao, S.; Tortola, L.; Perlot, T.; Wirnsberger, G.; Novatchkova, M.; Nitsch, R.; Sykacek, P.; Frank, L.; Schramek, D.; Komnenovic, V.; et al. A dual role for autophagy in a murine model of lung cancer. *Nat. Commun.* **2014**, *5*, 3056. https://doi.org/10.1038/ncomms4056.
77. Amaravadi, R.; Kimmelman, A.C.; White, E. Recent insights into the function of autophagy in cancer. *Genes Dev.* **2016**, *30*, 1913–1930. https://doi.org/10.1101/gad.287524.116.
78. White, E. Deconvoluting the context-dependent role for autophagy in cancer. *Nat. Rev. Cancer* **2012**, *12*, 401–410. https://doi.org/10.1038/nrc3262.
79. Galluzzi, L.; Pietrocola, F.; Pedro, J.M.B.; Ravi, K.; Maiuri, M.C.; Martin, S.J.; Penninger, J.; Piacentini, M. Autophagy in malignant transformation and cancer progression. *EMBO J.* **2015**, *34*, 856–880.
80. Chen, D.; Xie, J.; Fiskesund, R.; Dong, W.; Liang, X.; Lv, J.; Jin, X.; Liu, J.; Mo, S.; Zhang, T.; et al. Chloroquine modulates antitumor immune response by resetting tumor-associated macrophages toward M1 phenotype. *Nat. Commun.* **2018**, *9*, 873. https://doi.org/10.1038/s41467-018-03225-9.
81. DeVorkin, L.; Pavey, N.; Carleton, G.; Comber, A.; Ho, C.; Lim, J.; McNamara, E.; Huang, H.; Kim, P.; Zacharias, L.G.; et al. Autophagy Regulation of Metabolism Is Required for CD8+ T Cell Anti-tumor Immunity. *Cell Rep.* **2019**, *27*, 502–513.e5. https://doi.org/10.1016/j.celrep.2019.03.037.
82. Wu, L.; Pangilinan, C.R.; Lee, C. Downregulation of AKT/mTOR signaling pathway for Salmonella-mediated autophagy in human anaplastic thyroid cancer. *J. Cancer* **2022**, *13*, 3268–3279. https://doi.org/10.7150/jca.75163.
83. Lee, C.; Lin, S.; Liu, J.; Chang, W.; Hsieh, J.; Wang, W. Salmonella induce autophagy in melanoma by the downregulation of AKT/mTOR pathway. *Gene Ther.* **2014**, *21*, 309–316. https://doi.org/10.1038/gt.2013.86.
84. Kuan, Y.-D.; Lee, C.-H. Salmonella overcomes tumor immune tolerance by inhibition of tumor indoleamine 2, 3-dioxygenase 1 expression. *Oncotarget* **2016**, *7*, 374–385. https://doi.org/10.18632/oncotarget.6258.
85. Liu, B.; Jiang, Y.; Dong, T.; Zhao, M.; Wu, J.; Li, L.; Chu, Y.; She, S.; Zhao, H.; Hoffman, R.M.; et al. Blockage of autophagy pathway enhances Salmonella tumor-targeting. *Oncotarget* **2016**, *7*, 22873–22882. https://doi.org/10.18632/oncotarget.8251.

86. Berghe, T.V.; Linkermann, A.; Jouan-Lanhouet, S.; Walczak, H.; Vandenabeele, P. Regulated necrosis: The expanding network of non-apoptotic cell death pathways. *Nat. Rev. Mol. Cell Biol.* **2014**, *15*, 135–147. https://doi.org/10.1038/nrm3737.
87. Chen, X.; He, W.; Hu, L.; Li, J.; Fang, Y.; Wang, X.; Xu, X.; Wang, Z.; Huang, K.; Han, J. Pyroptosis is driven by non-selective gasdermin-D pore and its morphology is different from MLKL channel-mediated necroptosis. *Cell Res.* **2016**, *26*, 1007–1020. https://doi.org/10.1038/cr.2016.100.
88. Hancz, D.; Szabo, A.; Molnar, T.; Varga, Z.; Hancz, A.; Gregus, A.; Hueber, A.-O.; Rajnavolgyi, E.; Koncz, G. Flagellin increases death receptor-mediated cell death in a RIP1-dependent manner. *Immunol. Lett.* **2018**, *193*, 42–50. https://doi.org/10.1016/j.imlet.2017.11.007.
89. Robinson, N.; McComb, S.; Mulligan, R.; Dudani, R.; Krishnan, L.; Sad, S. Type I interferon induces necroptosis in macrophages during infection with Salmonella enterica serovar Typhimurium. *Nat. Immunol.* **2012**, *13*, 954–962. https://doi.org/10.1038/ni.2397.
90. Satkovich, J.; Anderson, C.J.; Medina, C.B.; Ottolini, M.; Lukens, J.R.; Kendall, M.M. RIPK3-Dependent Recruitment of Low-Inflammatory Myeloid Cells Does Not Protect from Systemic Salmonella Infection. *mBio* **2020**, *11*, e02588-20. https://doi.org/10.1128/mBio.02588-20.
91. Snyder, A.G.; Hubbard, N.W.; Messmer, M.N.; Kofman, S.B.; Hagan, C.E.; Orozco, S.L.; Chiang, K.; Daniels, B.P.; Baker, D.; Oberst, A. Intratumoral activation of the necroptotic pathway components RIPK1 and RIPK3 potentiates antitumor immunity. *Sci. Immunol.* **2019**, *4*, eaaw2004. https://doi.org/10.1126/sciimmunol.aaw2004.
92. Müller, I.; Strozyk, E.; Schindler, S.; Beissert, S.; Oo, H.Z.; Sauter, T.; Lucarelli, P.; Raeth, S.; Hausser, A.; Al Nakouzi, N.; et al. Cancer Cells Employ Nuclear Caspase-8 to Overcome the p53-Dependent G2/M Checkpoint through Cleavage of USP28. *Mol. Cell* **2020**, *77*, 970–984.e7. https://doi.org/10.1016/j.molcel.2019.12.023.
93. Christgen, S.; Zheng, M.; Kesavardhana, S.; Karki, R.; Malireddi, R.K.S.; Banoth, B.; Place, D.E.; Briard, B.; Sharma, B.R.; Tuladhar, S.; et al. Identification of the PANoptosome: A Molecular Platform Triggering Pyroptosis, Apoptosis, and Necroptosis (PANoptosis). *Front. Cell. Infect. Microbiol.* **2020**, *10*, 237. https://doi.org/10.3389/fcimb.2020.00237.
94. Jiang, M.; Qi, L.; Li, L.; Wu, Y.; Song, D.; Li, Y. Caspase-8: A key protein of cross-talk signal way in "PANoptosis" in cancer. *Int. J. Cancer* **2021**, *149*, 1408–1420. https://doi.org/10.1002/ijc.33698.
95. Fritsch, M.; Günther, S.D.; Schwarzer, R.; Albert, M.-C.; Schorn, F.; Werthenbach, J.P.; Schiffmann, L.M.; Stair, N.; Stocks, H.; Seeger, J.M.; et al. Caspase-8 is the molecular switch for apoptosis, necroptosis and pyroptosis. *Nature* **2019**, *575*, 683–687. https://doi.org/10.1038/s41586-019-1770-6.
96. Malireddi, R.K.S.; Kesavardhana, S.; Kanneganti, T. ZBP1 and TAK1: Master Regulators of NLRP3 Inflammasome/Pyroptosis, Apoptosis, and Necroptosis (PAN-optosis). *Front. Cell. Infect. Microbiol.* **2019**, *9*, 406. https://doi.org/10.3389/fcimb.2019.00406.
97. Brinkmann, V.; Reichard, U.; Goosmann, C.; Fauler, B.; Uhlemann, Y.; Weiss, D.S.; Weinrauch, Y.; Zychlinsky, A. Neutrophil Extracellular Traps Kill Bacteria. *Science* **2004**, *303*, 1532–1535. https://doi.org/10.1126/science.1092385.
98. Mónaco, A.; Canales-Huerta, N.; Jara-Wilde, J.; Härtel, S.; Chabalgoity, J.A.; Moreno, M.; Scavone, P. Salmonella Typhimurium Triggers Extracellular Traps Release in Murine Macrophages. *Front. Cell. Infect. Microbiol.* **2021**, *11*, 639768. https://doi.org/10.3389/fcimb.2021.639768.
99. Cools-Lartigue, J.; Spicer, J.; McDonald, B.; Gowing, S.; Chow, S.; Giannias, B.; Bourdeau, F.; Kubes, P.; Ferri, L. Neutrophil extracellular traps sequester circulating tumor cells and promote metastasis. *J. Clin. Investig.* **2013**, *123*, 3446–3458. https://doi.org/10.1172/JCI67484.
100. Cools-Lartigue, J.; Spicer, J.; Najmeh, S.; Ferri, L. Neutrophil extracellular traps in cancer progression. *Cell. Mol. Life Sci.* **2014**, *71*, 4179–4194. https://doi.org/10.1007/s00018-014-1683-3.
101. Li, Y.; Wu, S.; Zhao, Y.; Dinh, T.; Jiang, D.; Selfridge, J.E.; Myers, G.; Wang, Y.; Zhao, X.; Tomchuck, S.; et al. Neutrophil extracellular traps induced by chemotherapy inhibit tumor growth in murine models of colorectal cancer. *J. Clin. Investig.* **2024**, *134*, e175031. https://doi.org/10.1172/JCI175031.
102. Kahlenberg, J.M.; Carmona-Rivera, C.; Smith, C.K.; Kaplan, M.J. Neutrophil Extracellular Trap–Associated Protein Activation of the NLRP3 Inflammasome Is Enhanced in Lupus Macrophages. *J. Immunol.* **2013**, *190*, 1217–1226. https://doi.org/10.4049/jimmunol.1202388.
103. Hu, Q.; Shi, H.; Zeng, T.; Liu, H.; Su, Y.; Cheng, X.; Ye, J.; Yin, Y.; Liu, M.; Zheng, H.; et al. Increased neutrophil extracellular traps activate NLRP3 and inflammatory macrophages in adult-onset Still's disease. *Arthritis Res. Ther.* **2019**, *21*, 9. https://doi.org/10.1186/s13075-018-1800-z.

104. Ali, M.; Fulci, G.; Grigalavicius, M.; Pulli, B.; Li, A.; Wojtkiewicz, G.R.; Wang, C.; Hsieh, K.L.C.; Linnoila, J.J.; Theodossiou, T.A.; et al. Myeloperoxidase exerts anti-tumor activity in glioma after radiotherapy. *Neoplasia* **2022**, *26*, 100779. https://doi.org/10.1016/j.neo.2022.100779.
105. Cui, C.; Chakraborty, K.; Tang, X.A.; Zhou, G.; Schoenfelt, K.Q.; Becker, K.M.; Hoffman, A.; Chang, Y.-F.; Blank, A.; Reardon, C.A.; et al. Neutrophil elastase selectively kills cancer cells and attenuates tumorigenesis. *Cell* **2021**, *184*, 3163–3177.e21. https://doi.org/10.1016/j.cell.2021.04.016.
106. Muqaku, B.; Pils, D.; Mader, J.C.; Aust, S.; Mangold, A.; Muqaku, L.; Slany, A.; Del Favero, G.; Gerner, C. Neutrophil Extracellular Trap Formation Correlates with Favorable Overall Survival in High Grade Ovarian Cancer. *Cancers* **2020**, *12*, 505. https://doi.org/10.3390/cancers12020505.
107. Sollberger, G.; Choidas, A.; Burn, G.L.; Habenberger, P.; Di Lucrezia, R.; Kordes, S.; Menninger, S.; Eickhoff, J.; Nussbaumer, P.; Klebl, B.; et al. Gasdermin D plays a vital role in the generation of neutrophil extracellular traps. *Sci. Immunol.* **2018**, *3*, eaar6689. https://doi.org/10.1126/sciimmunol.aar6689.
108. Chen, K.W.; Monteleone, M.; Boucher, D.; Sollberger, G.; Ramnath, D.; Condon, N.D.; von Pein, J.B.; Broz, P.; Sweet, M.J.; Schroder, K. Noncanonical inflammasome signaling elicits gasdermin D–dependent neutrophil extracellular traps. *Sci. Immunol.* **2018**, *3*, eaar6676. https://doi.org/10.1126/sciimmunol.aar6676.
109. Chauhan, D.; Demon, D.; Vande Walle, L.; Paerewijck, O.; Ribo, S.; Fossoul, A.; Zecchin, A.; Bosseler, L.; Santoni, K.; Gonçalves, A.; et al. GSDMD drives canonical inflammasome-induced neutrophil pyroptosis and is dispensable for NETosis. *EMBO Rep.* **2022**, *23*, EMBR202154277. https://doi.org/10.15252/embr.202154277.
110. Rayner, B.S.; Zhang, Y.; Brown, B.E.; Reyes, L.; Cogger, V.C.; Hawkins, C.L. Role of hypochlorous acid (HOCl) and other inflammatory mediators in the induction of macrophage extracellular trap formation. *Free Radic. Biol. Med.* **2018**, *129*, 25–34. https://doi.org/10.1016/j.freeradbiomed.2018.09.001.
111. Harris, J.; Hartman, M.; Roche, C.; Zeng, S.G.; O'Shea, A.; Sharp, F.A.; Lambe, E.M.; Creagh, E.M.; Golenbock, D.T.; Tschopp, J.; et al. Autophagy Controls IL-1β Secretion by Targeting Pro-IL-1β for Degradation. *J. Biol. Chem.* **2011**, *286*, 9587–9597. https://doi.org/10.1074/jbc.M110.202911.
112. Gao, Z.; Feng, S.-R.; Chen, J.; Li, X.; Shi, Y.; Tang, Z.; Liu, W.; Zhang, X.; Huang, A.; Luo, X.; et al. Inhibition of autophagy in macrophage promotes IL-1β-mediated hepatocellular carcinoma progression via inflammasome accumulation and self-recruitment. *Biomed. Pharmacother.* **2023**, *161*, 114560. https://doi.org/10.1016/j.biopha.2023.114560.
113. Remijsen, Q.; Berghe, T.V.; Wirawan, E.; Asselbergh, B.; Parthoens, E.; De Rycke, R.; Noppen, S.; Delforge, M.; Willems, J.; Vandenabeele, P. Neutrophil extracellular trap cell death requires both autophagy and superoxide generation. *Cell Res.* **2011**, *21*, 290–304. https://doi.org/10.1038/cr.2010.150.
114. Dixon, S.J.; Lemberg, K.M.; Lamprecht, M.R.; Skouta, R.; Zaitsev, E.M.; Gleason, C.E.; Patel, D.N.; Bauer, A.J.; Cantley, A.M.; Yang, W.S.; et al. Ferroptosis: An Iron-Dependent Form of Nonapoptotic Cell Death. *Cell* **2012**, *149*, 1060–1072. https://doi.org/10.1016/j.cell.2012.03.042.
115. Jiang, X.; Stockwell, B.R.; Conrad, M. Ferroptosis: Mechanisms, biology and role in disease. *Nat. Rev. Mol. Cell Biol.* **2021**, *22*, 266–282. https://doi.org/10.1038/s41580-020-00324-8.
116. Sundaram, B.; Kanneganti, T.-D. Advances in Understanding Activation and Function of the NLRC4 Inflammasome. *Int. J. Mol. Sci.* **2021**, *22*, 1048. https://doi.org/10.3390/ijms22031048.
117. Doerflinger, M.; Deng, Y.; Whitney, P.; Salvamoser, R.; Engel, S.; Kueh, A.J.; Tai, L.; Bachem, A.; Gressier, E.; Geoghegan, N.D.; et al. Flexible Usage and Interconnectivity of Diverse Cell Death Pathways Protect against Intracellular Infection. *Immunity* **2020**, *53*, 533–547.e7. https://doi.org/10.1016/j.immuni.2020.07.004.
118. Rogers, C.; Alnemri, E.S. Gasdermins in Apoptosis: New players in an Old Game. *Yale J. Biol. Med.* **2019**, *92*, 603–617. Available online: http://www.ncbi.nlm.nih.gov/pubmed/31866776.
119. Barry, K.; Murphy, C.; Mansell, A. NLRP1-A CINDERELLA STORY: A perspective of recent advances in NLRP1 and the questions they raise. *Commun. Biol.* **2023**, *6*, 1274. https://doi.org/10.1038/s42003-023-05684-3.
120. Guy, C.; Baran, M.; Ribó-Molina, P.; van den Hoogen, B.G.; Bowie, A.G. Viral sensing by epithelial cells involves PKR- and caspase-3-dependent generation of gasdermin E pores. *iScience* **2023**, *26*, 107698. https://doi.org/10.1016/j.isci.2023.107698.
121. Vendrell, A.; Gravisaco, M.J.; Goin, J.C.; Pasetti, M.F.; Herschllik, L.; De Toro, J.; Rodríguez, C.; Larotonda, G.; Mongini, C.; Waldner, C.I. Therapeutic Effects of Salmonella Typhi in a Mouse Model of T-Cell Lymphoma. *J. Immunother.* **2013**, *36*, 171–180. https://doi.org/10.1097/CJI.0b013e3182886d95.

122. Rosales-Reyes, R.; Pérez-López, A.; Sánchez-Gómez, C.; Hernández-Mote, R.R.; Castro-Eguiluz, D.; Ortiz-Navarrete, V.; Alpuche-Aranda, C.M. Salmonella infects B cells by macropinocytosis and formation of spacious phagosomes but does not induce pyroptosis in favor of its survival. *Microb. Pathog.* **2012**, *52*, 367–374. https://doi.org/10.1016/j.micpath.2012.03.007.
123. Perez-Lopez, A.; Rosales-Reyes, R.; Alpuche-Aranda, C.M.; Ortiz-Navarrete, V. Salmonella Downregulates Nod-like Receptor Family CARD Domain Containing Protein 4 Expression To Promote Its Survival in B Cells by Preventing Inflammasome Activation and Cell Death. *J. Immunol.* **2013**, *190*, 1201–1209. https://doi.org/10.4049/jimmunol.1200415.
124. Luis, L.; Ana, G.; Abraham, G.; Iris, E.; Martha, M.; Vianney, O. Salmonella Promotes Its Own Survival in B Cells by Inhibiting Autophagy. *Cells* **2022**, *11*, 2061. https://doi.org/10.3390/cells11132061.
125. Hsu, P.-C.; Tsai, C.-C.; Lin, Y.-H.; Kuo, C.-Y. Therapeutic Targeting of Apoptosis, Autophagic Cell Death, Necroptosis, Pyroptosis, and Ferroptosis Pathways in Oral Squamous Cell Carcinoma: Molecular Mechanisms and Potential Strategies. *Biomedicines* **2025**, *13*, 1745. https://doi.org/10.3390/biomedicines13071745.
126. Gong, Y.; Fan, Z.; Luo, G.; Yang, C.; Huang, Q.; Fan, K.; Cheng, H.; Jin, K.; Ni, Q.; Yu, X.; et al. The role of necroptosis in cancer biology and therapy. *Mol. Cancer* **2019**, *18*, 100. https://doi.org/10.1186/s12943-019-1029-8.

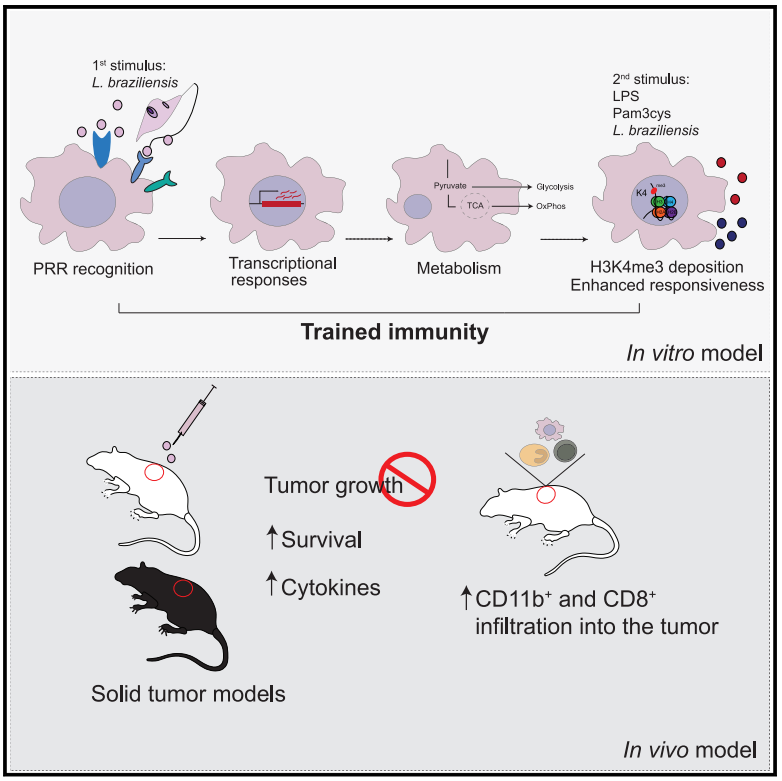
Disclaimer/Publisher's Note: The statements, opinions and data contained in all publications are solely those of the individual author(s) and contributor(s) and not of MDPI and/or the editor(s). MDPI and/or the editor(s) disclaim responsibility for any injury to people or property resulting from any ideas, methods, instructions or products referred to in the content.

Cell Reports

Article

Leishmania braziliensis enhances monocyte responses to promote anti-tumor activity

Graphical abstract



Authors

Jéssica Cristina dos Santos, María Moreno, Lisa U. Teufel, ..., Mihai G. Netea, José A. Chabalgoity, Leo A.B. Joosten

Correspondence

leo.joosten@radboudumc.nl

In brief

dos Santos et al. report the ability of *Leishmania* parasites to improve the responses of monocytes through trained immunity. Trained macrophages impact tumor growth and survival of mice bearing lymphoma and melanoma, offering opportunities for the use of trained immunity in cancer therapy.

Highlights

- *Leishmania braziliensis* induces trained immunity (TI) in human monocytes
- The secondary stimulus dictates the effector responses produced by trained monocytes
- *L. braziliensis* reduces tumor growth and improves survival in solid tumor models
- *L. braziliensis* impacts the myeloid and T cell accumulation in the tumor environment

dos Santos et al., 2024, Cell Reports *43*, 113932
March 26, 2024 © 2024 The Author(s).
https://doi.org/10.1016/j.celrep.2024.113932

CellPress

Cell Reports

CellPress
OPEN ACCESS

Article

Leishmania braziliensis enhances monocyte responses to promote anti-tumor activity

Jéssica Cristina dos Santos,[1] María Moreno,[2] Lisa U. Teufel,[1] Sofía Chilibroste,[2] Samuel T. Keating,[1] Laszlo Groh,[1] Jorge Domínguez-Andrés,[1] David L. Williams,[3] Zuchao Ma,[3] Douglas W. Lowman,[3] Harry E. Ensley,[3] Boris Novakovic,[1,4] Fátima Ribeiro-Dias,[5] Mihai G. Netea,[1,6] José A. Chabalgoity,[2] and Leo A.B. Joosten[1,7,8,*]

[1]Department of Internal Medicine and Radboud Center of Infectious Diseases (RCI), Radboud University Medical Center, Nijmegen, the Netherlands

[2]Laboratory for Vaccine Research, Departamento de Desarrollo Biotecnológico, Instituto de Higiene, Facultad de Medicina, Universidad de la República, Montevideo, Uruguay

[3]Department of Surgery, Quillen College of Medicine, Center of Excellence in Inflammation, Infectious Disease and Immunity, East Tennessee State University, Johnson City, TN, USA

[4]Murdoch Children's Research Institute and Department of Pediatrics, University of Melbourne, Melbourne, VIC, Australia

[5]Instituto de Patologia Tropical e Saúde Pública, Universidade Federal de Goiás, Goiânia, Goiás, Brazil

[6]Department for Immunology and Metabolism, Life and Medical Sciences Institute (LIMES), University of Bonn, Bonn, Germany

[7]Department of Medical Genetics, Iuliu Hatieganu University of Medicine and Pharmacy, Cluj-Napoca, Romania

[8]Lead contact

*Correspondence: leo.joosten@radboudumc.nl

https://doi.org/10.1016/j.celrep.2024.113932

SUMMARY

Innate immune cells can undergo long-term functional reprogramming after certain infections, a process called trained immunity (TI). Here, we focus on antigens of *Leishmania braziliensis*, which induced anti-tumor effects via trained immunity in human monocytes. We reveal that monocytes exposed to promastigote antigens of *L. braziliensis* develop an enhanced response to subsequent exposure to Toll-like receptor (TLR)2 or TLR4 ligands. Mechanistically, the induction of TI in monocytes by *L. braziliensis* is mediated by multiple pattern recognition receptors, changes in metabolism, and increased deposition of H3K4me3 at the promoter regions of immune genes. The administration of *L. braziliensis* exerts potent anti-tumor capabilities by delaying tumor growth and prolonging survival of mice with non-Hodgkin lymphoma. Our work reveals mechanisms of TI induced by *L. braziliensis in vitro* and identifies its potential for cancer immunotherapy.

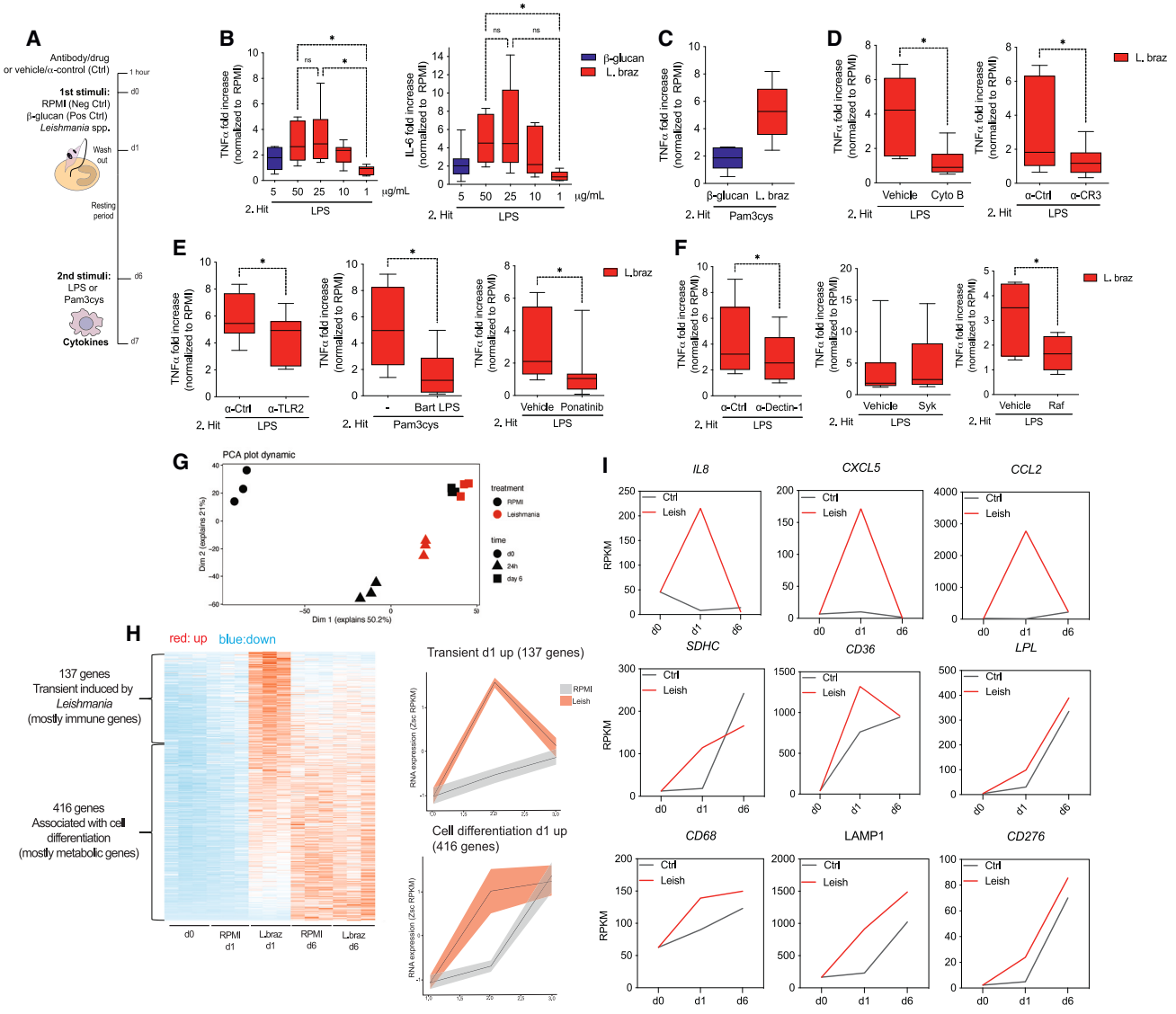
INTRODUCTION

Leishmania (*Viannia*) *braziliensis* is the most prevalent species causing American tegumentary leishmaniasis (ATL) in Latin America. The spectrum of clinical manifestations of *L. braziliensis* infections ranges from self-healing cutaneous lesions to chronic ulcers and mucosal involvement.[1,2] Macrophages are the main host cells used by the parasites for intracellular replication and long-term survival.[3] Activation of macrophages by interferon-γ and tumor necrosis factor (TNF) contributes to the control of growth of the parasite. Nevertheless, increased numbers of macrophages in the lesion site have been associated with lesion size in early lesions and with necrosis throughout the course of the disease, suggesting a direct role for macrophages in the pathology of *L. braziliensis*-induced lesions.[4–7]

It was recently shown that monocytes and macrophages can build memory traits through previous immune exposure and develop long-term functional reprogramming via a process called trained immunity (TI). TI occurs upon the contact of monocytes to vaccines such as bacillus Calmette-Guérin vaccine (BCG) or to pathogen-associated molecular patterns and damage-associated molecular patterns, including the cell-wall component from *Candida albicans*, β-glucan, oxidized low-density lipoprotein (oxLDL), and urate, respectively.[8–11] The increased responsiveness of trained monocytes after encountering a secondary stimulus has been associated with metabolic and epigenetic rewiring.[12,13] Numerous metabolites that are generated as a product of changes in cellular metabolism can act as cofactors for epigenetic writers and erasers, linking immunometabolism with long-term changes in gene regulation.[14] At the chromatin level, enrichment of trimethylation of lysine 4 of H3 histones (H3K4me3), H3K4 monomethylation (H3K4me1), and H3K27 acetylation at regulatory elements of proinflammatory cytokine genes are associated with increased transcriptional competency.[15–17] The clinical relevance of the induction of TI has been explored in areas of atherosclerosis, immunodeficiency, autoinflammatory diseases, non-related infections, and anti-cancer therapy.[11,18–20]

The induction of inflammatory responses by macrophages in response to *L. braziliensis* might offer pragmatic benefits for

This is an open access article under the CC BY license (http://creativecommons.org/licenses/by/4.0/).



J

Leishmania upregulated genes (n= 381)	P.value
Metabolism	5.8×10^{-11}
Neutrophil degranulation	2.4×10^{-8}
ATP synthesis	5.0×10^{-8}
Citrate cycle (TCA cycle)	6.7×10^{-8}
Oxidative phosphorylation	3.8×10^{-6}
PPAR signaling	6.5×10^{-6}
Glutathione metabolism	1.7×10^{-4}
Lipid metabolism	7.0×10^{-4}
Fatty acid metabolism	9.3×10^{-4}

K

Leishmania down genes (n= 350)	P.value
Cytokine signaling	6.5×10^{-10}
Neutrophil degranulation	3.0×10^{-8}
Interferon gamma signaling	8.3×10^{-7}
Interferon alpha/beta signaling	2.5×10^{-5}
Antigen processing and presentation	4.2×10^{-5}
PD-1 signaling	1.3×10^{-4}
Circadian clock	1.7×10^{-4}

Figure 1. *L. braziliensis* induces trained immunity *in vitro*

(A) Experimental setup.

(B) TNF and IL-6 release from monocytes trained with RPMI, β-glucan (5 μg/mL), or *L. braziliensis* lysates (50, 25, 10, and 1 μg/mL) for 24 h after LPS (10 ng/mL) restimulation at day 7, measured by ELISA.

(C–F) (C) TNF release from *L. braziliensis* lysates-trained macrophages (25 μg/mL) after restimulation with Pam_3Cys (10 μg/mL) at day 7. TNF production after LPS restimulation at day 7 of *L. braziliensis*-trained (25 μg/mL) macrophages ± (D) cytochalasin B and anti-CR3, (E) anti-TLR2 and *B. quintana* LPS (Bart. LPS, TLR4 antagonist), the RIP2 kinase inhibitor ponatinib, and (F) anti-dectin-1 and the Syk and Raf inhibitors R406 and GW5074, respectively. As controls, isotype control antibody, RPMI (−), or RPMI + DMSO (vehicle) were used as indicated. n = 6 independent donors. Cytokine measurements are represented as fold increase

(legend continued on next page)

the treatment of pathologies in which immunosuppression is harmful, most notably, e.g., while treating certain cancers. Overcoming the immunosuppressive tumor microenvironment attributed mainly to the presence of tumor-associated macrophages, regulatory T cells, and myeloid-derived suppressor cells remains the major challenge to the successful application of immunotherapy.[21,22] In the present study, we postulated that the exposure of human monocytes to *Leishmania* spp. induces functional reprogramming of monocytes and macrophages via induction of TI. In addition, we hypothesized that activation of TI by *Leishmania* may induce anti-tumor effects. Deciphering how myeloid cells are epigenetically reprogrammed for a hyperinflammatory state during *Leishmania* infections could provide a potential breakthrough not only in targeting the induction of deleterious inflammation but also in inducing anti-tumor macrophages with effector responses in the tumor microenvironment.

RESULTS

Leishmania parasites induce TI in human primary monocytes

Given the importance of monocytes and macrophages for *Leishmania* infections,[7,23] we hypothesize that the exposure of human monocytes to *Leishmania* parasites induces TI. We exposed human primary monocytes to different lysate concentrations obtained from stationary-phase *L. braziliensis* promastigotes. As positive and negative control we used β-glucan from *Candida albicans*[17] and a non-stimulated RPMI medium condition, respectively. After 24 h of exposure with the first stimuli, the cells were challenged at day 6 with Toll-like receptor 4 (TLR4) (lipopolysaccharide [LPS]) or TLR2 (Pam_3Cys) ligands as a secondary stimulus (Figure 1A). The exposure of monocytes to different concentrations (1, 10, 25, and 50 μg/mL) of *L. braziliensis* lysates led to increased production of TNF and interleukin-6 (IL-6) upon LPS restimulation 6 days later, measured as fold increase normalized to RPMI (Figure 1B). The concentrations of 50 and 25 μg/mL *L. braziliensis* lysates induced a 2-fold higher increase in TNF production than 1 μg/mL, and no significant differences were observed between lysates at 50 and 25 μg/mL. For IL-6, the exposure of monocytes to 50 μg/mL lysates led to a higher fold increase than with 1 μg/mL, and no differences were observed among the other doses of lysates (Figure 1B). Including β-glucan as a well-established inducer of TI allowed us to conclude that lysates of *L. braziliensis* induce TI based on the production of TNF and IL-6; therefore, we chose the dose of 25 μg/mL lysates to continue with in the *in vitro* experiments. Of note, the addition of Pam_3Cys as a secondary stimulus resulted in similar effects on TNF release as observed with LPS (Figure 1C).

Next, we exposed primary monocytes to different ratios of live promastigotes of *L. braziliensis* per cell (MOI 50:1, 10:1, 5:1, or 2:1) to assess whether the live form of the parasite could exert lysate-like effects on monocytes. Upon LPS restimulation, we observed an increase in the fold induction of TNF and IL-6, indicating that the live forms of the parasites were also able to induce TI responses in monocytes *in vitro* (Figure S1A). We further characterized the ability of other *Leishmania* species to induce TI by exposing monocytes to lysates of *L. guyanensis* and *L. amazonensis*. Similar to *L. braziliensis*, both *L. guyanensis* and *L. amazonensis* enhanced the fold induction of TNF and IL-6 when the cells were restimulated with LPS. Interestingly, when the production of the anti-inflammatory cytokine IL-10 was assessed, a tendency to increased IL-10 production was observed in monocytes exposed to *L. amazonensis* in comparison to *L. braziliensis*-exposed monocytes (Figure S1B). The presence of lipophosphoglycan (LPG) in the *L. braziliensis* extracts was established by 1D ^{1}H NMR analysis at 60°C (Figure S1C). We observed two anomeric proton resonances at 5.47 and 4.49 ppm and lipid resonances between 0.5 and 1.5 ppm. Based on 2D correlation spectroscopy analysis and comparison with the structural analysis of an LPG from *L. donovani*[24] and *L. major*,[25] these anomeric ^{1}H resonances were assigned to αDManp and βDGalp repeat units, respectively, in the -6Galβ1-4Manα1-PO_4- structural fragment of the LPG fraction. Based on these data, we conclude that *L. braziliensis* contains an LPG-like molecule. Other carbohydrate repeat units were not observed in the NMR spectrum. The addition of different concentrations of LPG to monocytes triggered increased TNF production upon LPS restimulation, suggesting the importance of this glycoconjugate in the induction of TI by *Leishmania* (Figure S1D).

To assess which receptors were involved in *L. braziliensis*-induced TI in human monocytes, we used antibodies and small molecules as inhibitors of pattern recognition receptors (PRRs) or their downstream signaling mediators. Monocytes were incubated in the presence of different inhibitors and controls 1 h prior the addition of *L. braziliensis* or β-glucan. Thereafter, the procedures of the *in vitro* protocol of training were followed as described previously (Figure 1A). To study whether endocytosis and complement receptor 3 (CR3)-mediated phagocytosis are involved in the induction of TI by *L. braziliensis*, we pre-incubated monocytes with cytochalasin B and a neutralizing antibody for CR3. The TI phenotype was assessed by the ability of trained monocytes to release TNF upon LPS restimulation. The blockade of the uptake of *L. braziliensis* lysates by cytochalasin B and the

normalized to RPMI (non-trained cells). Data in (B–F) are shown in box-and-whiskers (minimum-to-maximum) plots from two independent experiments (*$p < 0.05$ by Wilcoxon test; ns, $p > 0.05$).

(G) Principal component analysis (PCA) plot of gene expression dynamic across treatment and time points (RPMI, black; *L. braziliensis* lysates, red; day 0, circles; 24 h, triangles; day 6, squares).

(H) Heatmap of differentiated expressed genes (upregulated, red; downregulated, blue) at baseline (day 0) and at the indicated time points (day 1 and day 6) after RPMI or *L. braziliensis* lysates exposure (25 μg/mL).

(I) Time-resolved median expression of genes transiently or gradually induced in *L. braziliensis*-exposed cells.

(J and K) Most abundant pathways (J) upregulated and (K) downregulated based on gene expression analysis 24 h after treatment. n = 3 independent donors from one experiment.

See also Figures S1 and S2.

anti-CR3 antibody led to a significant decrease in the fold induction of TNF after LPS restimulation in comparison to the vehicle and isotype control, respectively (Figure 1D). We further investigated the role of TLRs, nucleotide oligomerization domain 1 (NOD1) and NOD2, and C-type lectin receptors in the induction of TI by *L. braziliensis*. The blockade of TLR2 and TLR4 using a neutralizing antibody (anti-TLR2) and the natural TLR4 antagonist *Bartonella quintana* LPS[26] caused a significant reduction in the fold induction of TNF upon training with *L. braziliensis* (Figure 1E). The cytosolic NOD1/2 receptors are also important for *L. braziliensis*-induced TI, as the inhibition of their downstream signaling molecule RIP2 kinase by ponatinib resulted in a significant reduction of TNF production in comparison to the vehicle (Figure 1E). The blockade of several C-type lectin receptors with specific antibodies including dectin-2, mincle mannose receptor, and DC-SIGN did not result in changes in TNF production upon training with *L. braziliensis* (Figure S1E). The involvement of TLR4, NOD1/2, and dectin-1 receptors were also shown to be important for the induction of IL-6 by *L. braziliensis*-trained macrophages, as the blockade of these receptors in the same manner as mentioned above diminished the IL-6 production (Figure S1F). Similar to β-glucan (Figure S1G), the exposure of monocytes to neutralizing antibodies against dectin-1 or to Raf inhibitor led to a significant decrease in the fold induction of TNF in *L. braziliensis*-trained macrophages compared to the isotype control and vehicle conditions. The inhibition of spleen tyrosine kinase (Syk) signaling did not result in differences in the fold induction of TNF in trained macrophages (Figure 1F). Collectively, the engagement of multiple immune receptors is required for the increased TNF and IL-6 production induced upon training of monocytes with *L. braziliensis*.

L. braziliensis modulates the transcriptional response of human monocytes

Next, we performed transcriptional characterization of *L. braziliensis* lysate-exposed monocytes across different time points of the *in vitro* protocol using RNA sequencing (RNA-seq). The time points constitute the basal expression levels at day 0 prior to the addition of the first stimulus and the initial exposure to the first stimulus at day 1, followed by culture media removal and differentiation to macrophages at day 6 in the presence or absence of LPS for 4 h (Figure 1A;[13]). More than 2.505 genes were differentially expressed (fold change >2.5, adjusted p value <0.05) in our model between either treatments or time points. Over the time course, the major changes in gene expression patterns were already seen by day 1 (principal component [PC] 1, 50.2% of the variance), which was most pronounced between RPMI and *L. braziliensis* lysate-treated monocytes, and by day 0 prior to stimulation (PC2, 21% of the variance) (Figure 1G). Of note, when merging the RNA-seq dataset from a previous study in which β-glucan and RPMI conditions were used with the samples of our current study, a similar transcriptional pattern was observed for β-glucan- and *L. braziliensis*-exposed monocytes where most differences were seen after 24 h of stimulation (Figure S2A). Among the genes that changed in expression after 24 h, 137 genes, mostly immune genes, were transiently induced by *L. braziliensis*. Moreover, another set of 416 genes, mostly metabolic genes and genes associated with cell differentiation, changed in expression gradually over time during the transition from monocytes to macrophages in both RPMI-exposed and *L. braziliensis*-treated cells. Of note, the differentiation process was faster in *L. braziliensis* than in RPMI-exposed cells (Figure 1H). Chemokine genes such as *IL8*, *CXCL5*, and *CCL2* were examples of genes that were transiently upregulated in *Leishmania*-exposed monocytes after 24 h and rapidly decreased in expression at day 6. Genes associated with cell metabolism including *succinate dehydrogenase complex subunit C* (*SDHC*), *CD36*, and *lipoprotein lipase* (*LPL*) had an increased expression in *Leishmania*-treated cells after 24 h and remained elevated on day 6. However, the expression levels of these genes were similar to the RPMI control condition at day 6. The genes associated with cell differentiation, *CD68*, *LAMP1*, and *CD276*, gradually increased in expression over time and remained higher in *Leishmania*-exposed macrophages at day 6 in comparison to the untreated RPMI condition (Figure 1I). We studied the overlap between the transcriptional response induced after 24 h of exposure with *L. braziliensis* and β-glucan using the dataset from Novakovic et al.[13] and observed that 15.5% (162) of the genes were commonly induced by both stimuli, whereas 37.1% (391) and 47.5% (501) of the genes were specific for *L. braziliensis* and β-glucan, respectively (Figure S2B). The major ontologies of *L. braziliensis*-induced genes (381 genes at day 1) were metabolic pathways and peroxisome proliferator-activated receptor signaling (Figure 1J). The ontologies of genes downregulated by *L. braziliensis* (350 genes at day 1) were cytokine signaling, antigen processing and presentation, and circadian clock (Figure 1K).

Given that only few differences were observed in the overall transcriptional landscape of *L. braziliensis*-stimulated macrophages at day 6 in comparison to the control (Figure 1H), we sought to interrogate the gene responsiveness of RPMI and *L. braziliensis*-treated cells upon LPS restimulation for 4 h. Based on the mean and individual expression profile, most genes remained equal in expression when comparing *L. braziliensis*- and RPMI-treated macrophages upon LPS restimulation. However, some genes had higher (trained) and lower (tolerized) expression in response to LPS stimulation (Figure S2C). *IL12B*, *NFKB1*, and *IL1A* were examples of genes classified as trained, equal, and tolerized, respectively in *L. braziliensis*-trained macrophages after LPS stimulation (Figure S2D).

We used motif analysis to gain insights into which pathways and transcription factors were involved in the upregulation of transient, metabolic, and cell differentiation associated genes upon *L. braziliensis* exposure after 24 h. Interestingly, the strongest predicted motifs include basic-helix-loop-helix family members (BHLHE) 40/41 and clock circadian regulator CLOCK, which were associated with the transient upregulated subset of genes (Figure S2E). *L. braziliensis*-exposed cells induced the expression of *BHLHE41* (Figure S2F), and the accumulation of this transcription factor has been associated with increased expression of cytokines and proliferation genes in macrophages.[27]

TI induced by *L. braziliensis* is mediated by JNK pathway, changes in metabolism, and chromatin accessibility

To understand the mechanisms involved in the transcriptional response and increased cytokine release upon *L. braziliensis* exposure, we investigated the role of phosphatidylinositol

3-kinase (PI3K/AKT), mammalian target of rapamycin (mTOR), and c-Jun N-terminal kinase (JNK) pathways. We assessed LPS-induced TNF levels upon training of monocytes with *L. braziliensis* or RPMI in the presence or absence of specific inhibitors for the aforementioned pathways (Figure 2A). The PI3K/AKT and mTOR inhibition with wortmannin, rapamycin, and torin had no effect on the induction of TNF. However, the treatment of monocytes with a JNK inhibitor significantly decreased the fold induction of TNF, confirming the involvement of this pathway in the induction of TI by *L. braziliensis* (Figure 2B).

We next investigated the glucose metabolism and oxidative phosphorylation (OXPHOS) in monocytes trained with lysates of *L. braziliensis* by assessing basal and maximum extracellular acidification rate (ECAR), oxygen consumption rate (OCR), and the accumulation of lactate. The basal and maximum ECAR was higher in *L. braziliensis*-treated macrophages than in RPMI-treated cells, whereas for the OCR, significant differences were observed for basal rates only (Figures 2C and 2E). Moreover, an increase in lactate levels was observed in the supernatants of *L. braziliensis*-trained macrophages (Figure 2D). In line with previous reports,[28] the addition of β-glucan, used as positive control in our study, also led to increased ECAR, lactate, and OXPHOS (Figures S3A–S3C). Of note, the inhibition of glycolysis and OXPHOS by deoxyglucose and oligomycin, respectively, abolished the increase in TNF production by *L. braziliensis*-trained macrophages (Figure S3D). Collectively, our results demonstrate the importance of glycolysis and OXPHOS in the induction of the trained phenotype induced by *L. braziliensis*.

To assess whether training of monocytes induced by *L. braziliensis* was dependent on changes in chromatin accessibility, we pre-incubated monocytes with methylthioadenosine (MTA, a pan-methyltransferase inhibitor) for 24 h prior the addition of *Leishmania* during the *in vitro* training protocol (Figure 2A). The presence of MTA abrogated the production of TNF by macrophages exposed to *L. braziliensis* and restimulated with LPS. Moreover, and based on a previous study identifying Set7 lysine methyltransferase (SET7) as an important regulator of TI induced by β-glucan,[28] we tested the role of Set7 in *L. braziliensis*-induced TI by incubating monocytes with cyproheptadine (CPH) for 24 h. After training and restimulation with LPS, the levels of TNF were significantly decreased in the CPH-treated macrophages in comparison to the vehicle control (Figure 2F). Next, we assessed the enrichment of transcriptionally permissive histone modification (H3K4me3) at the proximal promoter regions of genes that have been linked to the increased responsiveness of *Leishmania*-trained monocytes including *TNF*, *IL6*, and *CCL2*. An increased deposition of H3K4me3 was observed on the promoters of *TNF*, *IL6*, and *CCL2* of *L. braziliensis*-trained macrophages at day 6 in comparison to RPMI controls (Figure 2G). We extended our analysis to metalloproteinase genes that were previously associated with the TI phenotype induced by oxLDL.[11] A significantly increased deposition of H3K4me3 was observed for *MMP2* in cells exposed to *L. braziliensis* in comparison to RPMI. Although the differences in H3K4me3 levels were not significant for *MMP9*, a tendency to being increased was observed in the *L. braziliensis* condition (Figure S3E). These data highlight the importance of chromatin modifications in modulating the production of mediators associated with the increased responsiveness of macrophages during TI induced by *L. braziliensis*.

L. braziliensis-trained macrophages are permissive for the infection with live promastigotes

So far, we have provided experimental evidence that *L. braziliensis* can trigger an increased responsiveness of macrophages upon exposure to an unrelated secondary stimulus. We investigated whether the macrophages that underwent training with *L. braziliensis* lysates were able to control the intracellular growth of live promastigote forms of the same species. We addressed this question by infecting RPMI- and *L. braziliensis*-exposed macrophages with live promastigote forms of *L. braziliensis* at day 6, and thereafter the percentage of infected cells and number of parasites per cell were monitored after 2, 24, and 48 h of incubation (Figure 3A). In *Leishmania*-trained macrophages, a significant increase in the percentages of infected cells was observed after 24 h and 48 h of infection in comparison to the RPMI-exposed cells (Figure 3B). No significant differences were observed in the number of parasites per infected cell between the conditions at the aforementioned time points (Figure 3C). Of note, there was a tendency to a higher infection index in *L. braziliensis*-trained macrophages after 24 h and 48 h ($p = 0.0781$ and 0.0625, respectively) infected with promastigote forms in comparison to the RPMI controls (Figure 3D). A representation of how the macrophages were displayed 2 h, 24 h, and 48 h post infection with live promastigote forms of *L. braziliensis* is shown in Figures 3E–3G. In ATL, the balance between production of pro- and anti-inflammatory cytokines is associated with parasite control and disease immunopathogenesis.[29] Interestingly, after assessing the TNF and IL-6 production of RPMI- and *L. braziliensis*-exposed macrophages followed by live *Leishmania* re-exposure, no significant differences were observed between conditions (Figure 3H). In addition, *L. braziliensis*-trained macrophages led to an increased production of reactive oxygen species (ROS) upon restimulation with zymosan, used as positive control, and *Leishmania* in comparison to RPMI (Figure 3I). Next, we assessed the deposition of H3K4me3 at *IL1B* and *IL1RN* promoters in RPMI- and *L. braziliensis*-trained macrophages. We observed a significant increase on the promoters of both *IL1B* and *IL1RN* of *L. braziliensis*-trained macrophages (Figure 3J). The enrichment of H3K4me3 on the promoter of *IL1B* contributed to an enhanced *IL1B* mRNA expression in trained macrophages after live *Leishmania* restimulation as well increased production of total intracellular IL-1β. No significant difference in total intracellular IL-1β production was found in trained macrophages restimulated with LPS (Figures 3K and 3L). Importantly, IL-1β secretion only occurred when ATP was added in combination with both LPS and *Leishmania* as secondary stimuli for additional triggering of inflammasome activation. The addition of ATP contributed to an increased release of IL-1β in the supernatants of trained macrophages in comparison to RPMI-exposed macrophages (Figure 3M). Additionally, we observed increased production of IL-1Ra in macrophages trained with *L. braziliensis* in comparison to RPMI upon restimulation with both LPS and live *Leishmania* (Figure 3N). Collectively, we have shown that live *L. braziliensis*, when used as a secondary stimulus, elicits a different cellular response in terms of TNF

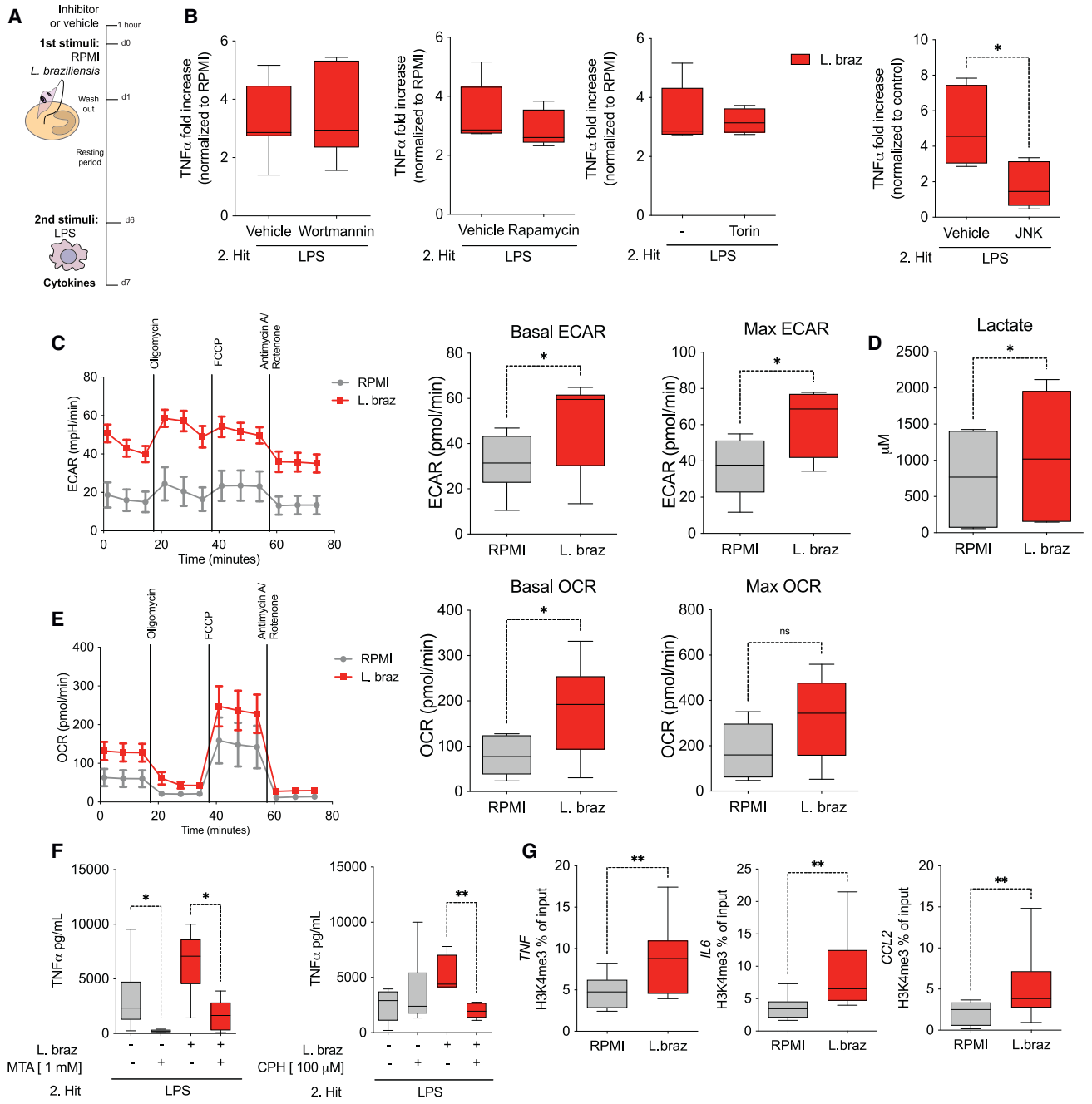


Figure 2. *L. braziliensis* training relies on JNK activation, metabolism, and H3K4me3 deposition

(A and B) (A) Experimental setup. TNF production after LPS (10 ng/mL) restimulation at day 7 of *L. braziliensis*-trained (25 μg/mL) macrophages ± (B) the PI3K/AKT, mTOR inhibitors wortmannin and rapamycin/torin, respectively, and the JNK inhibitor SP600125. As controls, RPMI (–) or RPMI + DMSO (vehicle) were used as indicated.

(C) Basal and maximum extracellular acidification rates (ECAR) of RPMI- and *L. braziliensis*-trained macrophages at day 6, measured by Seahorse.

(D) Lactate production assessed in the supernatant of trained macrophages at day 6 by fluorometric assay.

(E) Basal and maximum oxygen consumption rate (OCR) of RPMI- and *L. braziliensis*-trained macrophages at day 6, measured by Seahorse.

(F) TNF production after LPS restimulation at day 7 of RPMI-exposed and *L. braziliensis*-trained (25 μg/mL) macrophages ± the methyltransferase inhibitors MTA and CPH.

(G) Levels of H3K4me3 at *TNF*, *IL6*, and *CCL2* promoters of RPMI- and *L. braziliensis*-exposed macrophages assessed by chromatin immunoprecipitation-qPCR. n = 6 independent donors. Cytokine measurements are presented as fold increase normalized to RPMI (non-trained cells). Data are shown in box-and-whiskers (minimum-to-maximum) plots from two independent experiments (*p < 0.05; **p < 0.01 by Wilcoxon test; ns, p > 0.05). See also Figure S3.

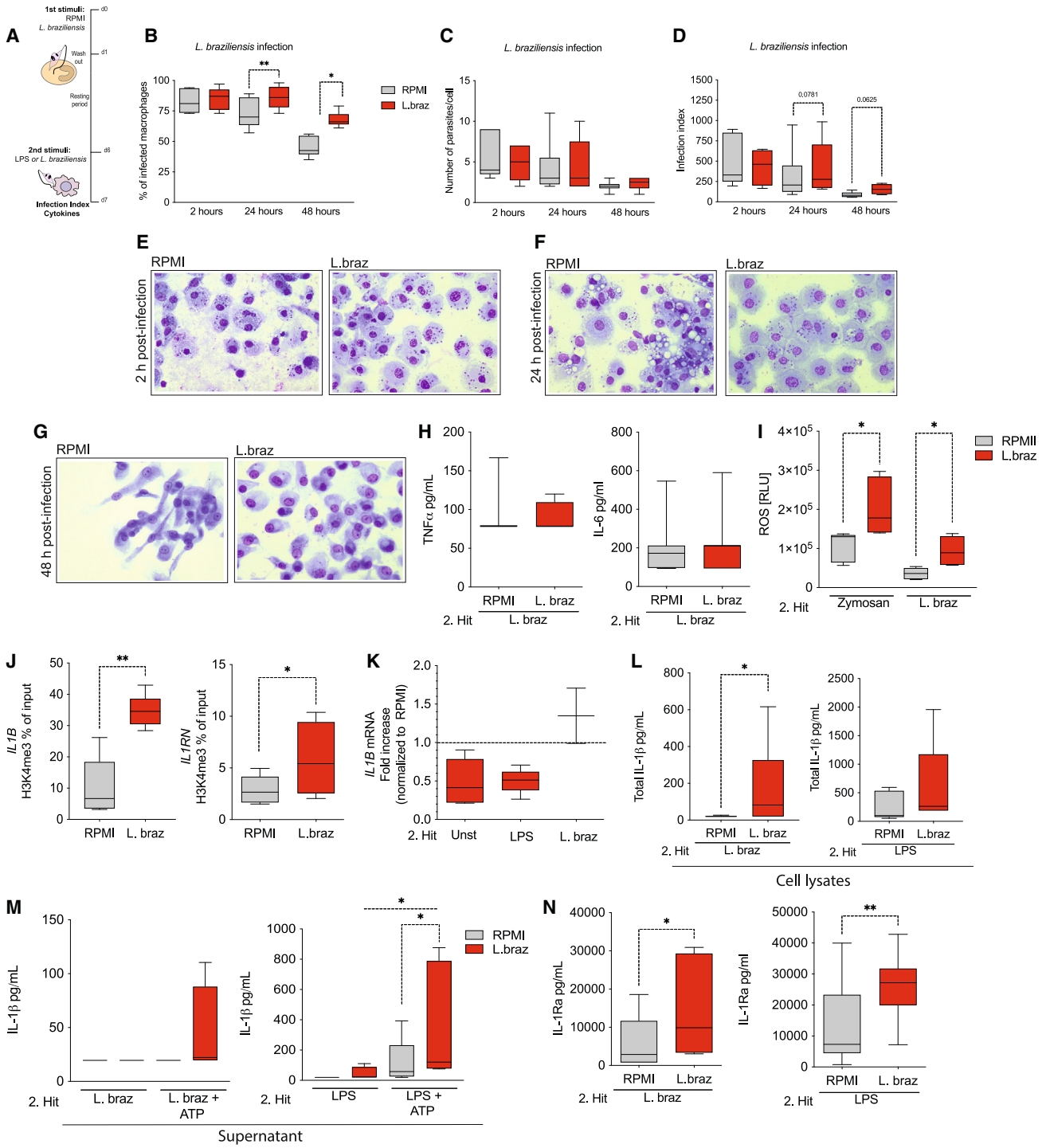


Figure 3. *L. braziliensis*-trained macrophages are permissive for intracellular growth of *Leishmania* amastigotes *in vitro*

(A) Experimental setup.

(B–D) (B) Percentages of infected macrophages, (C) number of parasites per infected cell, and (D) infection index were assessed in RPMI- and *L. braziliensis*-trained (25 μg/mL) macrophages on day 6, 2 h, 24 h, and 48 h post infection with *L. braziliensis* promastigotes (MOI 5) by Giemsa.

(E–G) Representative figures of RPMI- and *L. braziliensis*-treated macrophages (E) 2 h, (F) 24 h, and (G) 48 h post infection captured by light microscope (20×).

(H) TNF and IL-6 release from *L. braziliensis* lysates-trained macrophages (25 μg/mL) after exposure to *L. braziliensis* promastigotes (MOI 5) measured by ELISA at day 7, 24 h post infection.

(legend continued on next page)

and IL-6 induction. Moreover, *L. braziliensis*-trained macrophages have an increased production of intracellular IL-1β in which an additional signal is required to trigger its release. These mechanisms together may favor parasite survival in *L. braziliensis*-trained macrophages.

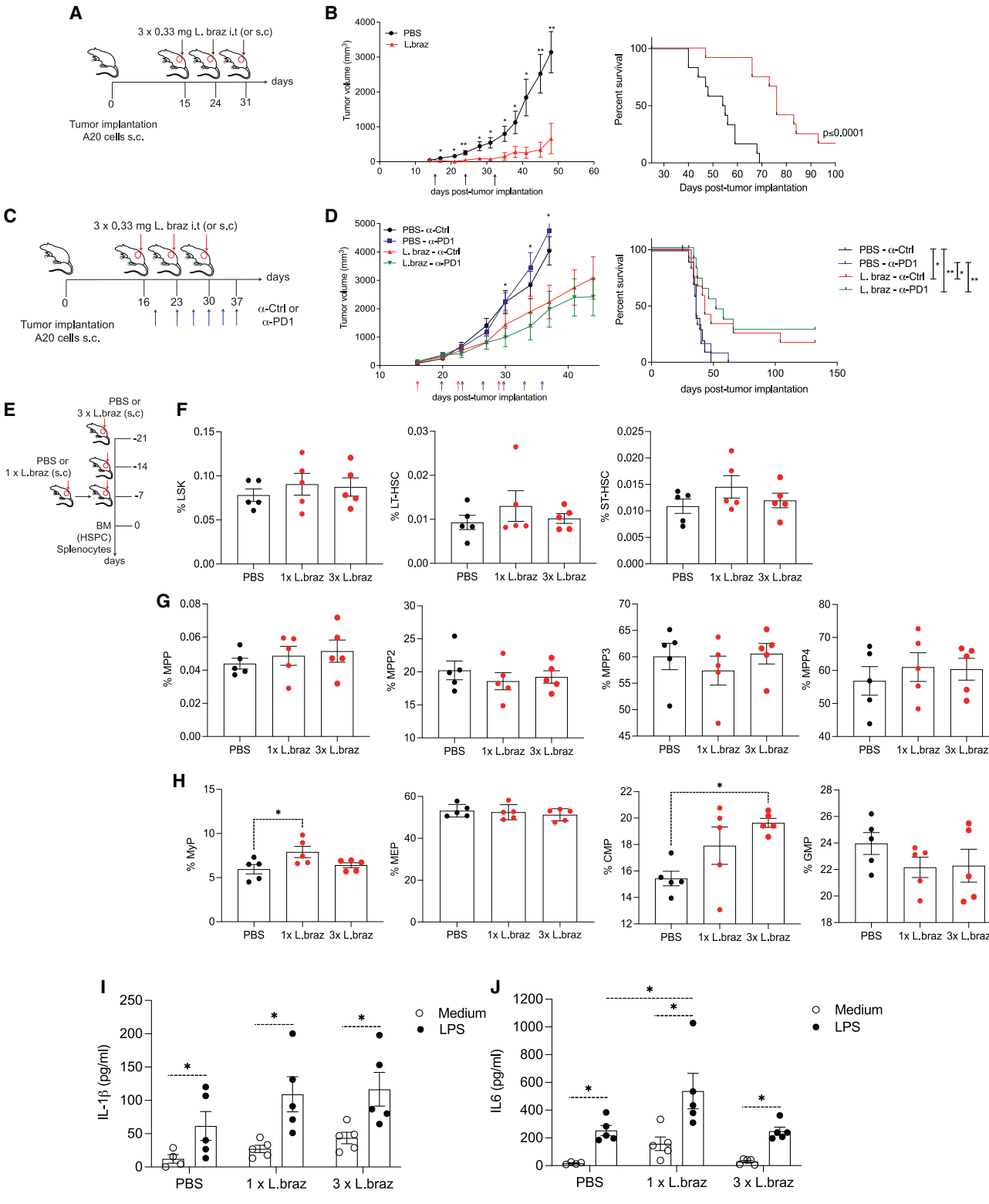
TI induced by *L. braziliensis in vivo* promotes anti-tumor activities

Having established *L. braziliensis* as an initial stimulus resulted in trained macrophages, we wanted to extend our findings to the potential anti-tumor responses of TI induced by *Leishmania* lysates *in vivo*. We used a therapeutic setting in which A20 (B cell lymphoma) tumor cells were injected subcutaneously in BALB/c mice (Figure 4A). We observed a significant tumor-growth inhibition exerted by the treatment of mice with *L. braziliensis* lysates in comparison to the PBS-treated group. Interestingly, the tumor volume of *L. braziliensis*-treated mice remained significantly smaller than that of the PBS group up to 40 days after treatment (Figure 4B). Of importance, after monitoring the tumor volume of each animal post tumor implantation, we noticed that most of the mice in the *L. braziliensis*-treated group had a substantial delay in tumor growth in comparison to animals receiving PBS (Figures S4A and S4B). In addition, animals treated with three doses of *L. braziliensis* lysates showed significantly prolonged survival compared to the PBS group (Figure 4B). To further explore whether the effects of *L. braziliensis* were applicable to other tumor models, we tested the effects of the lysates in the experimental model of melanoma. *L. braziliensis* lysates also exerted anti-tumor activities in the melanoma model, demonstrated by significant tumor-growth inhibition and prolonged survival in the animals treated with the lysates in comparison to the PBS group (Figures S4F and S4G).

We next performed experiments to compare anti-tumoral effects of immunotherapy with checkpoint inhibitors alone versus a combination with our TI-inducing *L. braziliensis* therapy. To explore this, we first performed an experiment to confirm the expression of programmed cell death-ligand 1 (PD-L1) in the A20 cell line (Figure S4C). Next, after 2 weeks of tumor implantation using A20 cells, mice were randomized and allocated to four treatment groups in which PBS and *L. braziliensis* was combined with anti-programmed cell death-1 (PD-1) and isotype control antibody regimens (Figure 4C). In the PBS-treated group, the anti-PD-1 therapy alone did not affect tumor growth in comparison to the PBS-treated isotype control group. Combining *L. braziliensis* with anti-PD-1 or isotype control significantly lowered tumor-growth rate compared to the PBS-treated groups with anti-PD-1 or isotype control regimens. We did not observe significant differences in tumor growth between *L. braziliensis*-treated groups combined with anti-PD-1 or isotype control (Figure 4D). As seen in the first experiments, we demonstrated that the treatment of tumor-bearing mice with *L. braziliensis* improved the survival of the animals to up to 100 days in comparison to the PBS groups, a process that was observed for both anti-PD-1 and isotype control *L. braziliensis*-treated groups (Figure 4D). Interestingly, after assessing the cytotoxic activity of immune cells against A20 cells in splenocytes taken either from PBS- or *L. braziliensis*-treated mice that survived the tumor and non-tumor exposed control mice (naive), we observed a significant increase in cytotoxic activity of splenocytes derived from *L. braziliensis*-treated mice when a 100:1 effector/target ratio was used (Figure S4D). Moreover, these increased cytotoxic effects were seen in splenocytes derived from *L. braziliensis*-treated mice in which the treatment was combined with anti-PD-1 and isotype control antibodies (Figure S4E).

So far, our results showed a potent ability of *L. braziliensis* lysates to inhibit tumor growth *in vivo*. We hypothesized that these anti-tumor effects were exerted through the amplification of myelopoiesis at bone marrow level, which is an intrinsic mechanism associated with the TI phenotype induced by β-glucan.[30] Using a different animal group, we performed three additional experiments: (1) mice were injected with a single dose of *L. braziliensis*; (2) mice were injected with three doses of *L. braziliensis* or PBS every 7 days; and (3) functional responses of bone marrow cells were studied through the assessment of cytokine production upon LPS restimulation *ex vivo*. In both experiments, bone marrow cells were collected for *ex vivo* immunophenotyping analysis (Figures 4E and S5A). The subcutaneous injection of *L. braziliensis* lysates did not induce major changes in either the absolute numbers and percentages of total hematopoietic bone marrow progenitor cells (LSKs, $Lin^{-}cKit^{+}Sca1^{+}$) or in the long- and short-term hematopoietic stem cells (LT-HSCs, $CD48^{-}CD150^{+}$LSK and ST-HSCs, $CD48^{-}CD150^{+}$LSK, respectively), as compared to PBS-treated mice (Figures 4F and S5B). Moreover, no differences were observed after the analysis was extended to the percentages and numbers of multipotent progenitors (MMPs, $CD48^{+}CD150^{-}$LSK) as well as of MMP2 ($Flt3^{-}CD48^{+}CD150^{+}$LSK), MMP3 ($Flt3^{-}CD48^{+}CD150^{-}$LSK), and MMP4 ($Flt3^{+}CD48^{+}CD150^{-}$LSK) subsets among the PBS- and *L. braziliensis*-injected groups (Figures 4G and S5C). Seven days after one injection of *L. braziliensis*, an increase in the percentages of myeloid progenitors (MyPs, $Lin^{-}cKit^{+}Sca1^{-}$) was observed in comparison to PBS-injected control mice. No

(I) Reactive oxygen species (ROS) represented as area under the curve of a total 1-h period of RPMI- and *L. braziliensis*-trained macrophages restimulated with zymosan (1 mg/mL, positive control) and *L. braziliensis* lysates (25 μg/mL). ROS production was assessed by luminol-enhanced chemiluminescence assay.
(J) Levels of H3K4me3 at *IL1B* and *IL1RN* promoters of RPMI- and *L. braziliensis*-exposed macrophages assessed by ChiP-qPCR.
(K and L) (K) *IL1B* mRNA expression and (L) total intracellular IL-1β production measured in cell lysates of *L. braziliensis*-trained (25 μg/mL) macrophages on day 6 after *L. braziliensis* lysates (25 μg/mL) and LPS (10 ng/mL) restimulation by qPCR and ELISA, respectively.
(M) IL-1β secretion in the supernatant of RPMI- and *L. braziliensis*-trained macrophages after restimulation of LPS (10 ng/mL) and *L. braziliensis* lysates (25 μg/mL) for 23 h followed by an additional 1-h incubation with ATP (1.25 mM).
(N) IL-1Ra secretion in the supernatant of RPMI- and *L. braziliensis*-trained macrophages after LPS (10 ng/mL) and *L. braziliensis* restimulation. Both IL-1β and IL-1Ra were assessed in the supernatants using ELISA.
n = 6 independent donors. *IL1B* mRNA are presented as fold increase normalized to RPMI (non-trained cells). Data are shown in box-and-whiskers (minimum-to-maximum) plots from two independent experiments (*$p < 0.05$; **$p < 0.01$ by Wilcoxon test; ns, $p > 0.05$).



(legend on next page)

differences were observed for the MyP absolute numbers (Figure S5C). Furthermore, the administration of three doses of *Leishmania* lysates led to increased proportions of common myeloid progenitors (CMPs, $Lin^{-}cKit^{+}Sca1^{-}CD16/CD32^{-}CD34^{+}$) compared to control mice. The proportions of granulocyte-macrophage progenitors (GMPs, $Lin^{-}cKit^{+}Sca1^{-}CD16/CD32^{+}CD34^{+}$) were not affected by the injection of one or three doses of *Leishmania* lysates (Figure 4H). No differences were observed in the production of TNF, IL-6, and IL-1β by bone marrow cells isolated from A20 lymphoma-bearing mice treated with PBS and *L. braziliensis* after LPS restimulation *ex vivo* (Figure S6H).

After investigating the effects of *L. braziliensis* lysates on bone marrow hematopoietic stem and progenitor cell (HSPC) expansion and composition, we assessed "peripheral" TI by evaluating the *ex vivo* response of splenocytes to LPS restimulation. IL-1β production by LPS-exposed splenocytes was greater than in splenocytes exposed to control medium in all three groups of mice. However, the production of IL-1β in PBS-treated versus *L. braziliensis*-treated groups did not differ (Figure 4I). Interestingly, the addition of LPS triggered higher IL-6 production in splenocytes from mice exposed to a single dose of *L. braziliensis* compared to the PBS-treated group. Similarly to IL-1β, the IL-6 concentrations were higher in LPS-exposed splenocytes than in control medium for all groups (Figure 4J). Subcutaneous injection of various doses of *L. braziliensis* mildly affects HSPC composition. Functionally, these cells do not exhibit enhanced cytokine production upon restimulation. Instead, *L. braziliensis* lysates induced peripheral TI by modulating splenocyte cytokine and cytotoxic responses.

L. braziliensis induces the infiltration of myeloid and $CD8^{+}$ T cells into the tumor

After evaluating the effect of multiple doses of *L. braziliensis* lysates in the absence of the tumor, we continued our analysis to evaluate the central versus peripheral induction of TI 21 and 35 days after tumor implantation. We assessed the HSPC composition, the infiltration of $CD11b^{+}$ and $CD8^{+}$ cells into the tumor, the *ex vivo* production of cytokines by splenocytes, and the systemic release of inflammatory mediators in the serum of both PBS- and *L. braziliensis*-treated mice (Figure 5A).

Assessment of the bone marrow composition in mice exposed to one or three doses of *L. braziliensis* at days 21 and 35 did not show differences in the absolute numbers and percentages of LSKs, LT- and ST-HSCs, and MMPs in comparison to the PBS group (Figures 5B and S6B–S6E). In addition, there was a decrease in the percentages of the myeloid-biased MMP3 cells in *L. braziliensis*-treated mice 21 days post tumor implantation, in comparison to the PBS-injected group. The percentages of lymphoid-based MMP4 and MMP2 cells were the same in both groups and at both time points post tumor implantation (Figures 5C and S6E). Analysis of MyP percentages did not show significant differences between the groups and time points (Figure S6F). Moreover, the CMP proportions were decreased at day 21 in *L. braziliensis*-treated mice, yet no significant differences between groups were observed at day 35. As for the GMPs, a significant decrease in the percentages of cells was observed in *L. braziliensis*-treated mice at day 35 post tumor implantation (Figure 5D). Collectively, our data indicate the presence of a negative regulation of the induction of myelopoiesis centrally at the bone marrow of *L. braziliensis*-treated mice after tumor implantation.

Next, we studied the influx of mature myeloid and lymphoid cells to the periphery, more specifically at the tumor environment, by assessing the presence of total $CD45^{+}$, $CD11b^{+}$, and $CD8^{+}$ cells after 21 and 35 days of tumor establishment (Figure 5E). We observed an increase in the influx of $CD11b^{+}$ into the tumor in *L. braziliensis*-treated mice at days 21 and 35 in comparison to the PBS group. At day 21, the proportion of $CD11b^{+}$ cells in the tumor of PBS-treated mice were higher than at day 35 (Figure 5F). The injection of *L. braziliensis* significantly increased the influx of $CD8^{+}$ cells at day 21 in comparison to the PBS group. Moreover, the proportions of $CD8^{+}$ in the tumor decreased by day 35 in both PBS- and *L. braziliensis*-treated groups, demonstrating that this influx is transient (Figure 5G). Thereafter, we performed an independent experiment aiming to further characterize the phenotype of $CD11b^{+}$ cells found to be increased in the tumor environment. Our results indicated a trend toward increased $CD11b^{+}F4/80^{+}$ macrophages in *L. braziliensis*-treated mice in comparison to the control group, whereas no differences were seen for $CD11b^{+}Ly6G^{+}$ cells between the groups (Figures S6G and S6I).

Figure 4. *L. braziliensis* injection delays tumor growth and prolonged survival of A20 non-Hodgkin-lymphoma-bearing mice

(A) Experimental setup.

(B) *In vivo* tumor growth and survival curves of BALB/c mice, which were inoculated with 1×10^{6} A20 tumor cells and submitted to a regimen consisted of three subcutaneous injections of PBS or *L. braziliensis* lysates (0.33 mg/mL each injection). Overall survival was followed up for 100 days (n = 12). Significance was calculated between the groups (*$p < 0.05$, **$p < 0.01$ by t test and log rank, respectively).

(C) Experimental setup of checkpoint inhibitor experiment.

(D) *In vivo* tumor growth and survival curves of tumor-bearing BALB/c mice, which were randomized into one of the four treatment groups consisting of PBS and *L. braziliensis* in combination with anti-PD-1 (200 μg/mouse) and isotype control (200 μg/mouse) antibody regimens. The antibodies were administered intraperitoneally twice a week, starting after the administration of the first dose of PBS or *L. braziliensis* and lasted until day 37 post tumor implantation. Overall survival was followed up for 130 days (n = 12). Significance was calculated between all groups (*$p < 0.05$ by t test and log rank, respectively).

(E) Experimental setup of *ex vivo* bone marrow phenotyping and splenocyte-derived cytokine production. Mice were injected with a single dose of *L. braziliensis* for 7 days or three doses of *L. braziliensis* or PBS every 7 days. Bone marrow cells were collected for *ex vivo* immunophenotyping analysis by flow cytometry.

(F–H) Percentages of (F) LSKs, LT-HSCs, and ST-HSCs, (G) MMPs, MMP2, MMP3, and MMP4, and (H) MyPs, MEPs, CMPs, and GMPs in PBS- and *L. braziliensis*-treated mice (n = 5).

(I and J) Splenocytes (5×10^{5}) of PBS- and *L. braziliensis*-treated mice submitted to both single- and triple-dose regimens were restimulated for 24 h with LPS (100 ng/mL). Production of (I) IL-1β and (J) IL-6 was assessed in the supernatant by ELISA (n = 5).

Data in bar plots are shown as mean ± SD (*$p < 0.05$ by t test). See also Figures S4 and S5.

CellPress
OPEN ACCESS

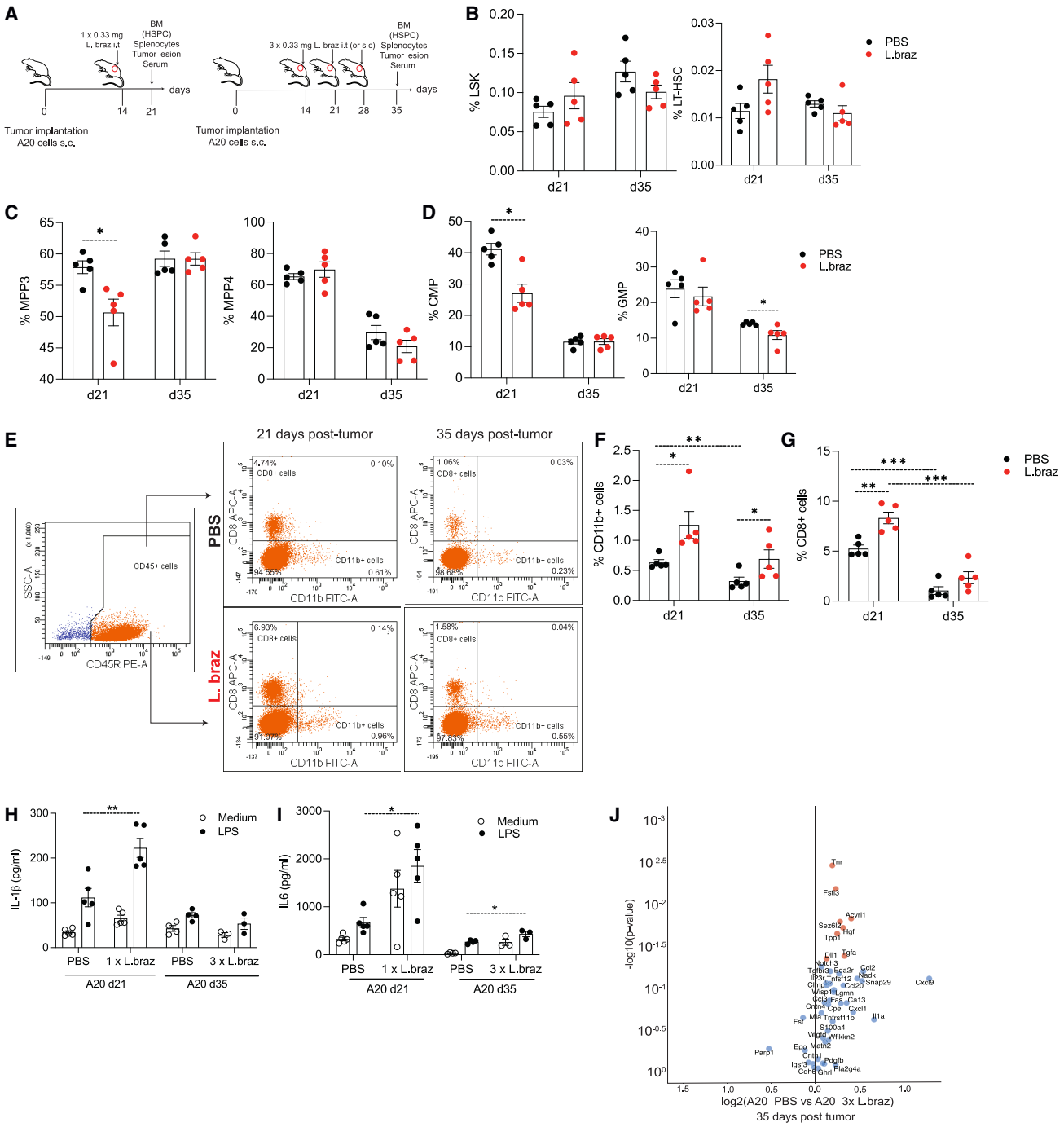


Figure 5. *L. braziliensis* injection promotes the infiltration of immune cells into the tumor

(A) Experimental setup. *Ex vivo* bone marrow phenotyping of tumor-bearing PBS- and *L. braziliensis*-treated (0.33 mg/mL) mice submitted to both single-dose (day 21) and triple-dose (day 35) regimens injected subcutaneously.

(B–D) Percentages of (B) LSKs and LT-HSCs, (C) MMP3 and MMP4, and (D) CMP and GMP were assessed by flow cytometry (n = 5).

(E) Representative flow-cytometry plots.

(F and G) Percentages of (F) $CD45^+CD11b^+$ and (G) $CD45^+CD8^+$ cells in the tumor lesion were assessed by flow cytometry (n = 5). 5×10^5 splenocytes of were restimulated for 24 h with LPS (100 ng/mL).

(H and I) Production of (H) IL-1β and (I) IL-6 was assessed in the supernatant by ELISA (n = 5).

(J) Proteins measured in the serum by Olink in both tumor-bearing PBS- and *L. braziliensis*-treated mice 35 days after tumor implantation. Volcano plot showing the differentially expressed proteins between the two groups (log_2 values; significant proteins are marked in red; false discovery rate adjusted *p < 0.05).

Data in bar plots are shown as mean ± SD (*p < 0.05, ** p < 0.01 by t test). See also Figure S6.

To investigate whether the peripheral cells displayed an increased responsiveness upon restimulation, we measured the *ex vivo* cytokine production of splenocytes upon LPS restimulation. The splenocytes of *L. braziliensis*-treated mice released higher amounts of IL-1β and IL-6 than the PBS control group at day 21 post tumor implantation. At day 35, no significant differences in the secretion of IL-1β was observed between the groups, whereas for IL-6, higher production was observed in the *L. braziliensis*-treated mice than in the PBS control group (Figures 5H and 5I). To assess the systemic effects of the injection of *L. braziliensis* lysates, we measured the presence of immune mediators in the serum of the animals at day 35 post tumor implantation. The results showed increased production of proteins associated with signal transduction (tenascin R), transforming growth factor β signaling (follistatin-like 3 and activin A receptor type II-like 1), regulation of cell chemotaxis, apoptosis, and inflammatory responses (hepatocyte growth factor) in *L. braziliensis*-treated mice 35 days after tumor establishment (Figure 5J). Taken together, our data suggest that not only do *L. braziliensis* lysates incite a trained phenotype in peripheral immune cells, but also the induced anti-tumor effects are exerted locally into the tumor in a transient manner, a mechanism which is likely relevant for future clinical applications in treating solid tumors.

DISCUSSION

In this study, we describe for the first time the molecular mechanisms through which the parasite *L. braziliensis* induces TI, resulting in a robust innate host response after a secondary challenge. Training of monocytes with *L. braziliensis* lysates induced a significant increase in the production of cytokines, which was attributed to metabolic and epigenetic mechanisms. Although trained macrophages did not confer protection against reinfection with *Leishmania*, we demonstrated an anti-tumor response exerted by the parasites *in vivo*, which contributed to prolonged survival of mice bearing non-Hodgkin lymphoma.

We have shown in this study that stimulation with *L. braziliensis*-induced TI results in increased responsiveness of monocytes and macrophages upon binding of a secondary TLR ligand. Importantly, we observed that the nature of the secondary stimulus contributes to the effector responses exerted by trained macrophages, as we showed that cells were not able to respond with higher production of cytokines upon reinfection with *L. braziliensis* promastigotes. Therefore, even though *L. braziliensis* induces TI, different pathways are required for effective control of parasite growth. Similar to BCG, monocytes exposed to *L. braziliensis* increase their ROS production upon restimulation.[31,32] The induction of TI by β-glucan was shown to be beneficial in controlling infections caused by *L. braziliensis* via the activation of the IL-32-IL-1β axis. Both IL-32 and IL-1β are important for the induction of microbicidal molecules against *Leishmania*.[32,33] *L. braziliensis* used as a secondary stimulus on trained macrophages led to an increased production of intracellular IL-1β but did not increase the amounts of IL-1β released in the supernatant. IL-1β secretion by trained macrophages occurred only in the presence of ATP, which is required for inflammasome assembly leading to caspase-1 activation and cleavage of the intracellular pro-IL-1β.[34] The presence of IL-1Ra in combination with the absence of IL-1β secretion, together with the low production of TNF, could lead to the impairment of macrophage-mediated responses, which are important for parasite killing. In ATL, proinflammatory cytokines act like a double-edged sword that may induce protection against secondary infections but at the same time may be implicated in severe tissue destruction typical of this infection.[35]

The transcriptional response of monocytes upon training with *L. braziliensis* showed dynamic expression of genes and pathways modulated over time. *L. braziliensis* amplified the expression of genes involved in chemokine signaling, cell metabolism, and cell differentiation. We showed that increased *CCL2* mRNA expression in *L. braziliensis*-trained cells was accompanied by an enhanced H3K4me3 deposition at the promoter region of *CCL2*. The presence of myeloid cells that are prompted to produce CCL2 has important implications for the induction of peripheral TI, as it can favor the influx of immune cells that exert effector responses.[36] Moreover, changes in the induction of cellular metabolism are a hallmark of trained monocytes.[28] In the present study, we showed that glucose metabolism is crucial for *L. braziliensis*-induced TI. To accommodate the increased energy requirements needed for enhanced immune responsiveness, *L. braziliensis*' induction of TI is dependent on the use of glycolysis and oxidative phosphorylation. Moreover, the increased inflammatory responses observed in human monocytes upon training with *L. braziliensis* were shown to be associated with the enrichment of transcriptionally permissive H3K4me3 chromatin modification at the promoter sites of the immune genes *TNF*, *IL6*, *IL1B*, *IL1RA*, and *MMP2*. Thus, our data indicate that the enhanced responsiveness of trained monocytes by *L. braziliensis* is dependent on complementary transcriptional, metabolic, and epigenetic programs. Importantly, even though the phenotype of trained macrophages induced by *L. braziliensis* shares similarities or additive effects when compared to well-established inducers of TI such as β-glucan and BCG, we also identified unique features that are specific for an *L. braziliensis*-induced TI program (including specific genes and PRRs). Moreover, synergistic effects of these inducers in exerting beneficial effects are shown by studies of patients with diffuse cutaneous leishmaniasis who were treated with BCG in combination with promastigote antigens of *Leishmania* spp., allowing control of parasites and long periods without relapses.[37,38]

The beneficial effects of TI were demonstrated in two independent studies using a B16-F10 melanoma model *in vivo*, in which the treatment of melanoma-bearing mice with either β-glucan or MTP-HDL (muramyl tripeptide-high-density lipoprotein) inhibited tumor growth.[39,40] Moreover, TI induced by MTP-HDL was shown to potentiate the checkpoint blockage therapy using anti-PD-1.[40] Likewise, we demonstrate in the present study that *L. braziliensis* immunotherapy can delay tumor growth and improve the survival rate of non-Hodgkin-lymphoma-bearing mice. Moreover, *L. braziliensis*-treated mice exerted the same effects in inhibiting tumor growth when compared with *L. braziliensis* + anti-PD-1-treated mice. In accordance with the literature, anti-PD-1 therapy alone had no survival benefit in the PBS group while the combination of *L. braziliensis* and anti-PD-1 induced a

better survival outcome. Unresponsiveness to PD-1/PD-L1 blockade therapies has been reported previously in advanced stages of lymphoma, a process that was overcome by local delivery of an armed anti-PD-L1 antibody with type I interferon-α to create feedforward responses.[41]

TI-mediated long-term effects on myeloid cells occur via the modulation of progenitor cells centrally in the bone marrow, and these cells can transfer their trained phenotype to circulating immune cells.[42] In addition, circulating monocytes and tissue-resident macrophages can develop innate immune memory at the tissue level, a process known as peripheral induction of TI. In the melanoma model, anti-tumor activities were achieved upon administration of β-glucan and MTP-HDL intraperitoneally and intravenously, respectively.[39,40] In both cases, the involvement of myeloid progenitors was shown to be associated with the induction of TI. We have assessed the anti-tumor responses of *L. braziliensis* using a subcutaneous model in which the parasite fragments were injected intratumorally. We showed that the injection of the parasite lysates subcutaneously had mild effects centrally at the level of bone marrow progenitors. Importantly, we suggest the presence of induction of peripheral TI, as splenocytes of *L. braziliensis*-treated mice were able to build a stronger inflammatory response upon restimulation with LPS, a process that was exerted in the absence of tumor and in non-Hodgkin-lymphoma-bearing mice. In addition to cytokine release, we showed that these cells have a greater ability to exert cytotoxicity to tumor cells. In fact, in a recent study, the authors reported that β-glucan-trained macrophages can be activated upon exposure to tumor cells, contributing to the enhancement of anti-tumor responses such as increased cytotoxicity against pancreatic tumor cells.[36] Locally at the tumor site, the anti-tumor activities in our model are likely to be attributed to the influx of myeloid cells characterized by the accumulation of $CD11b^+$ cells and $CD8^+$ T cells.

In conclusion, we provide comprehensive evidence that *L. braziliensis* exposure of human monocytes induces TI. The identification of the metabolic pathways and epigenetic markers contributing to induction of TI by *L. braziliensis* improves our understanding of pathogenesis of leishmaniasis and identifies potential therapeutic strategies for other non-related infectious diseases and cancer. Importantly, we demonstrate a capability of *L. braziliensis* lysates to exert anti-tumor responses locally by engaging myeloid cells *in vivo*. These findings emphasize the potential of using *L. braziliensis* lysates to therapeutically target myeloid cells within the tumor environment through the induction of peripheral TI. Thus, our results open the possibility to extend the life of patients with therapy for non-responsive malignancies by using agents that induce TI.

Limitations of the study

Further studies aiming to investigate the effects of different doses of *L. braziliensis* lysates, as well as exploring the impact of the route of administration in the induction of anti-tumor activities *in vivo*, are of interest. Additionally, these studies may further elucidate the mechanisms associated with the induction of TI by *Leishmania* lysates *in vivo*, whether it occurs centrally at the level of progenitor cells or locally in peripheral tissues.

STAR★METHODS

Detailed methods are provided in the online version of this paper and include the following:

- KEY RESOURCES TABLE
- RESOURCE AVAILABILITY
  - Lead contact
  - Materials availability
  - Data and code availability
- EXPERIMENTAL MODEL AND STUDY PARTICIPANT DETAILS
  - Human subjects
  - Animals
- METHOD DETAILS
  - NMR structural analysis of LPG derived from *L. braziliensis*
  - *In vivo* L. *braziliensis*-induced trained immunity
- QUANTIFICATION AND STATISTICAL ANALYSIS

SUPPLEMENTAL INFORMATION

Supplemental information can be found online at https://doi.org/10.1016/j.celrep.2024.113932.

ACKNOWLEDGMENTS

L.A.B.J. received funding from the European Union Horizon 2020 research and innovation program under grant agreement no. 667837, as well as the IN-CONTROL grant from the Heart Foundation, the Netherlands. M.G.N. was supported by an ERC advanced grant (833247) and a Spinoza grant of the Netherlands Organization for Scientific Research. B.N. was supported by an NHMRC (Australia) investigator grant (APP1173314). D.L.W. was supported, in part, by the National Institutes of Health grants R01GM119197 and RO1GM083016 and the Carroll H. Long endowment, United States. F.R.-D. is fellow researcher of National Council for Scientific and Technological Development/CNPq/Brazil; F.R.-D. and L.A.B.J. are members of INCT-IPH (National Institute of Science and Technology for strategies in Parasite-Host Interactions/FAPEG/Brazil).

AUTHOR CONTRIBUTIONS

Conceptualization, J.C.d.S., L.A.B.J., and M.G.N.; methodology, J.C.d.S., M.M., L.U.T., S.C., S.T.K., L.G., J.D.-A., D.L.W., Z.M., D.W.L., H.E.E., and B.N.; investigation, J.C.d.S., M.M., and L.U.T.; visualization, J.C.d.S., M.M., S.C., L.U.T., and B.N.; funding acquisition, L.A.B.J. and M.G.N.; project administration, L.A.B.J.; supervision, L.A.B.J. and J.A.C.; writing – original draft, J.C.d.S. and M.M.; writing – review & editing, J.C.d.S., M.M., F.R.-D., J.A.C., L.A.B.J., and M.G.N.

DECLARATION OF INTERESTS

The authors declare no competing interests.

Received: April 16, 2023
Revised: November 7, 2023
Accepted: February 21, 2024

REFERENCES

1. Murray, H.W., Berman, J.D., Davies, C.R., and Saravia, N.G. (2005). Advances in leishmaniasis. Lancet *366*, 1561–1577. https://doi.org/10.1016/S0140-6736(05)67629-5.

2. Araujo-Pereira, T.d., Pita-Pereira, D.d., Moreira, R.B., Silva-Galdino, T., Duarte, M.P.d.O., Brazil, R.P., and Britto, C. (2018). Molecular diagnosis of cutaneous leishmaniasis in an endemic area of Acre State in the Amazonian Region of Brazil. Rev. Soc. Bras. Med. Trop. *51*, 376–381. https://doi.org/10.1590/0037-8682-0232-2017.

3. Beattie, L., and Kaye, P.M. (2011). Leishmania-host interactions: what has imaging taught us? Cell Microbiol. *13*, 1659–1667. https://doi.org/10.1111/j.1462-5822.2011.01658.x.

4. Liese, J., Schleicher, U., and Bogdan, C. (2008). The innate immune response against Leishmania parasites. Immunobiology *213*, 377–387. https://doi.org/10.1016/j.imbio.2007.12.005.

5. Ibraim, I.C., de Assis, R.R., Pessoa, N.L., Campos, M.A., Melo, M.N., Turco, S.J., and Soares, R.P. (2013). Two biochemically distinct lipophosphoglycans from Leishmania braziliensis and Leishmania infantum trigger different innate immune responses in murine macrophages. Parasit. Vectors *6*, 54. https://doi.org/10.1186/1756-3305-6-54.

6. Bottrel, R.L., Dutra, W.O., Martins, F.A., Gontijo, B., Carvalho, E., Barral-Netto, M., Barral, A., Almeida, R.P., Mayrink, W., Locksley, R., and Gollob, K.J. (2001). Flow cytometric determination of cellular sources and frequencies of key cytokine-producing lymphocytes directed against recombinant LACK and soluble Leishmania antigen in human cutaneous leishmaniasis. Infect. Immun. *69*, 3232–3239. https://doi.org/10.1128/IAI.69.5.3232-3239.2001.

7. Saldanha, M.G., Queiroz, A., Machado, P.R.L., de Carvalho, L.P., Scott, P., de Carvalho Filho, E.M., and Arruda, S. (2017). Characterization of the Histopathologic Features in Patients in the Early and Late Phases of Cutaneous Leishmaniasis. Am. J. Trop. Med. Hyg. *96*, 645–652. https://doi.org/10.4269/ajtmh.16-0539.

8. Crișan, T.O., Cleophas, M.C.P., Oosting, M., Lemmers, H., Toenhake-Dijkstra, H., Netea, M.G., Jansen, T.L., and Joosten, L.A.B. (2016). Soluble uric acid primes TLR-induced proinflammatory cytokine production by human primary cells via inhibition of IL-1Ra. Ann. Rheum. Dis. *75*, 755–762. https://doi.org/10.1136/annrheumdis-2014-206564.

9. Netea, M.G., Joosten, L.A.B., Latz, E., Mills, K.H.G., Natoli, G., Stunnenberg, H.G., O'Neill, L.A.J., and Xavier, R.J. (2016). Trained immunity: A program of innate immune memory in health and disease. Science *352*, aaf1098. https://doi.org/10.1126/science.aaf1098.

10. Arts, R.J.W., Joosten, L.A.B., and Netea, M.G. (2016). Immunometabolic circuits in trained immunity. Semin. Immunol. *28*, 425–430. https://doi.org/10.1016/j.smim.2016.09.002.

11. Bekkering, S., Quintin, J., Joosten, L.A.B., van der Meer, J.W.M., Netea, M.G., and Riksen, N.P. (2014). Oxidized low-density lipoprotein induces long-term proinflammatory cytokine production and foam cell formation via epigenetic reprogramming of monocytes. Arterioscler. Thromb. Vasc. Biol. *34*, 1731–1738. https://doi.org/10.1161/ATVBAHA.114.303887.

12. Cheng, S.C., Quintin, J., Cramer, R.A., Shepardson, K.M., Saeed, S., Kumar, V., Giamarellos-Bourboulis, E.J., Martens, J.H.A., Rao, N.A., Aghajanirefah, A., et al. (2014). mTOR- and HIF-1alpha-mediated aerobic glycolysis as metabolic basis for trained immunity. Science *345*, 1250684. https://doi.org/10.1126/science.1250684.

13. Novakovic, B., Habibi, E., Wang, S.Y., Arts, R.J.W., Davar, R., Megchelenbrink, W., Kim, B., Kuznetsova, T., Kox, M., Zwaag, J., et al. (2016). beta-Glucan Reverses the Epigenetic State of LPS-Induced Immunological Tolerance. Cell *167*, 1354–1368 e1314. https://doi.org/10.1016/j.cell.2016.09.034.

14. Groh, L., Netea, M.G., Riksen, N.P., and Keating, S.T. (2018). Getting to the marrow of trained immunity. Epigenomics *10*, 1151–1154. https://doi.org/10.2217/epi-2018-0098.

15. Saeed, S., Quintin, J., Kerstens, H.H.D., Rao, N.A., Aghajanirefah, A., Matarese, F., Cheng, S.C., Ratter, J., Berentsen, K., van der Ent, M.A., et al. (2014). Epigenetic programming of monocyte-to-macrophage differentiation and trained innate immunity. Science *345*, 1251086. https://doi.org/10.1126/science.1251086.

16. Kleinnijenhuis, J., Quintin, J., Preijers, F., Joosten, L.A.B., Ifrim, D.C., Saeed, S., Jacobs, C., van Loenhout, J., de Jong, D., Stunnenberg, H.G., et al. (2012). Bacille Calmette-Guerin induces NOD2-dependent nonspecific protection from reinfection via epigenetic reprogramming of monocytes. Proc. Natl. Acad. Sci. USA *109*, 17537–17542. https://doi.org/10.1073/pnas.1202870109.

17. Quintin, J., Saeed, S., Martens, J.H.A., Giamarellos-Bourboulis, E.J., Ifrim, D.C., Logie, C., Jacobs, L., Jansen, T., Kullberg, B.J., Wijmenga, C., et al. (2012). Candida albicans infection affords protection against reinfection via functional reprogramming of monocytes. Cell Host Microbe *12*, 223–232. https://doi.org/10.1016/j.chom.2012.06.006.

18. Buffen, K., Oosting, M., Quintin, J., Ng, A., Kleinnijenhuis, J., Kumar, V., van de Vosse, E., Wijmenga, C., van Crevel, R., Oosterwijk, E., et al. (2014). Autophagy controls BCG-induced trained immunity and the response to intravesical BCG therapy for bladder cancer. PLoS Pathog. *10*, e1004485. https://doi.org/10.1371/journal.ppat.1004485.

19. van der Meer, J.W.M., Joosten, L.A.B., Riksen, N., and Netea, M.G. (2015). Trained immunity: A smart way to enhance innate immune defence. Mol. Immunol. *68*, 40–44. https://doi.org/10.1016/j.molimm.2015.06.019.

20. Arts, R.J.W., Moorlag, S.J.C.F.M., Novakovic, B., Li, Y., Wang, S.Y., Oosting, M., Kumar, V., Xavier, R.J., Wijmenga, C., Joosten, L.A.B., et al. (2018). BCG Vaccination Protects against Experimental Viral Infection in Humans through the Induction of Cytokines Associated with Trained Immunity. Cell Host Microbe *23*, 89–100.e5. https://doi.org/10.1016/j.chom.2017.12.010.

21. Wang, W., Marinis, J.M., Beal, A.M., Savadkar, S., Wu, Y., Khan, M., Taunk, P.S., Wu, N., Su, W., Wu, J., et al. (2020). RIP1 Kinase Drives Macrophage-Mediated Adaptive Immune Tolerance in Pancreatic Cancer. Cancer Cell *38*, 585–590. https://doi.org/10.1016/j.ccell.2020.09.020.

22. Karamitopoulou, E. (2019). Tumour microenvironment of pancreatic cancer: immune landscape is dictated by molecular and histopathological features. Br. J. Cancer *121*, 5–14. https://doi.org/10.1038/s41416-019-0479-5.

23. Passos, S., Carvalho, L.P., Costa, R.S., Campos, T.M., Novais, F.O., Magalhães, A., Machado, P.R.L., Beiting, D., Mosser, D., Carvalho, E.M., and Scott, P. (2015). Intermediate monocytes contribute to pathologic immune response in Leishmania braziliensis infections. J. Infect. Dis. *211*, 274–282. https://doi.org/10.1093/infdis/jiu439.

24. Homans, S.W., Mehlert, A., and Turco, S.J. (1992). Solution structure of the lipophosphoglycan of Leishmania donovani. Biochemistry *31*, 654–661. https://doi.org/10.1021/bi00118a004.

25. McConville, M.J., Thomas-Oates, J.E., Ferguson, M.A., and Homans, S.W. (1990). Structure of the lipophosphoglycan from Leishmania major. J. Biol. Chem. *265*, 19611–19623.

26. Malgorzata-Miller, G., Heinbockel, L., Brandenburg, K., van der Meer, J.W.M., Netea, M.G., and Joosten, L.A.B. (2016). Bartonella quintana lipopolysaccharide (LPS): structure and characteristics of a potent TLR4 antagonist for in-vitro and in-vivo applications. Sci. Rep. *6*, 34221. https://doi.org/10.1038/srep34221.

27. Cook, M.E., Jarjour, N.N., Lin, C.C., and Edelson, B.T. (2020). Transcription Factor Bhlhe40 in Immunity and Autoimmunity. Trends Immunol. *41*, 1023–1036. https://doi.org/10.1016/j.it.2020.09.002.

28. Keating, S.T., Groh, L., van der Heijden, C.D.C.C., Rodriguez, H., Dos Santos, J.C., Fanucchi, S., Okabe, J., Kaipananickal, H., van Puffelen, J.H., Helder, L., et al. (2020). The Set7 Lysine Methyltransferase Regulates Plasticity in Oxidative Phosphorylation Necessary for Trained Immunity Induced by beta-Glucan. Cell Rep. *31*, 107548. https://doi.org/10.1016/j.celrep.2020.107548.

29. Volpedo, G., Pacheco-Fernandez, T., Holcomb, E.A., Cipriano, N., Cox, B., and Satoskar, A.R. (2021). Mechanisms of Immunopathogenesis in Cutaneous Leishmaniasis And Post Kala-azar Dermal Leishmaniasis (PKDL). Front. Cell. Infect. Microbiol. *11*, 685296. https://doi.org/10.3389/fcimb.2021.685296.

30. Mitroulis, I., Ruppova, K., Wang, B., Chen, L.S., Grzybek, M., Grinenko, T., Eugster, A., Troullinaki, M., Palladini, A., Kourtzelis, I., et al. (2018). Modulation of Myelopoiesis Progenitors Is an Integral Component of Trained Immunity. Cell *172*, 147–161.e12. https://doi.org/10.1016/j.cell.2017.11.034.

31. Silva, M.V.T., Dos Santos, J.C., Figueiredo, A.M.B.d., Teufel, L.U., Pereira, J.X., Matos, G.G.d., Pinto, S.A., Netea, M.G., Gomes, R.S., Joosten, L.A.B., and Ribeiro-Dias, F. (2021). The role of IL-32 in Bacillus Calmette-Guerin (BCG)-induced trained immunity in infections caused by different Leishmania spp. Microb. Pathog. *158*, 105088. https://doi.org/10.1016/j.micpath.2021.105088.

32. Dos Santos, J.C., Barroso de Figueiredo, A.M., Teodoro Silva, M.V., Cirovic, B., de Bree, L.C.J., Damen, M., Moorlag, S., Gomes, R.S., Helsen, M.M., Oosting, M., et al. (2019). beta-Glucan-Induced Trained Immunity Protects against Leishmania braziliensis Infection: a Crucial Role for IL-32. Cell Rep. *28*, 2659–2672 e2656. https://doi.org/10.1016/j.celrep.2019.08.004.

33. de Carvalho, R.V.H., Lima-Junior, D.S., da Silva, M.V.G., Dilucca, M., Rodrigues, T.S., Horta, C.V., Silva, A.L.N., da Silva, P.F., Frantz, F.G., Lorenzon, L.B., et al. (2019). Leishmania RNA virus exacerbates Leishmaniasis by subverting innate immunity via TLR3-mediated NLRP3 inflammasome inhibition. Nat. Commun. *10*, 5273. https://doi.org/10.1038/s41467-019-13356-2.

34. Marchetti, C., Swartzwelter, B., Gamboni, F., Neff, C.P., Richter, K., Azam, T., Carta, S., Tengesdal, I., Nemkov, T., D'Alessandro, A., et al. (2018). OLT1177, a beta-sulfonyl nitrile compound, safe in humans, inhibits the NLRP3 inflammasome and reverses the metabolic cost of inflammation. Proc. Natl. Acad. Sci. USA *115*, E1530–E1539. https://doi.org/10.1073/pnas.1716095115.

35. Oliveira, F., Bafica, A., Rosato, A.B., Favali, C.B.F., Costa, J.M., Cafe, V., Barral-Netto, M., and Barral, A. (2011). Lesion size correlates with Leishmania antigen-stimulated TNF-levels in human cutaneous leishmaniasis. Am. J. Trop. Med. Hyg. *85*, 70–73. https://doi.org/10.4269/ajtmh.2011.10-0680.

36. Geller, A.E., Shrestha, R., Woeste, M.R., Guo, H., Hu, X., Ding, C., Andreeva, K., Chariker, J.H., Zhou, M., Tieri, D., et al. (2022). The induction of peripheral trained immunity in the pancreas incites anti-tumor activity to control pancreatic cancer progression. Nat. Commun. *13*, 759. https://doi.org/10.1038/s41467-022-28407-4.

37. Pereira, L.I.A., Dorta, M.L., Pereira, A.J.C.S., Bastos, R.P., Oliveira, M.A.P., Pinto, S.A., Galdino, H., Jr., Mayrink, W., Barcelos, W., Toledo, V.P.C.P., et al. (2009). Increase of NK cells and proinflammatory monocytes are associated with the clinical improvement of diffuse cutaneous leishmaniasis after immunochemotherapy with BCG/Leishmania antigens. Am. J. Trop. Med. Hyg. *81*, 378–383.

38. Convit, J., Ulrich, M., Polegre, M.A., Avila, A., Rodríguez, N., Mazzedo, M.I., and Blanco, B. (2004). Therapy of Venezuelan patients with severe mucocutaneous or early lesions of diffuse cutaneous leishmaniasis with a vaccine containing pasteurized Leishmania promastigotes and bacillus Calmette-Guerin: preliminary report. Mem. Inst. Oswaldo Cruz *99*, 57–62. https://doi.org/10.1590/s0074-02762004000100010.

39. Kalafati, L., Kourtzelis, I., Schulte-Schrepping, J., Li, X., Hatzioannou, A., Grinenko, T., Hagag, E., Sinha, A., Has, C., Dietz, S., et al. (2020). Innate Immune Training of Granulopoiesis Promotes Anti-tumor Activity. Cell *183*, 771–785.e12. https://doi.org/10.1016/j.cell.2020.09.058.

40. Priem, B., van Leent, M.M.T., Teunissen, A.J.P., Sofias, A.M., Mourits, V.P., Willemsen, L., Klein, E.D., Oosterwijk, R.S., Meerwaldt, A.E., Munitz, J., et al. (2020). Trained Immunity-Promoting Nanobiologic Therapy Suppresses Tumor Growth and Potentiates Checkpoint Inhibition. Cell *183*, 786–801.e19. https://doi.org/10.1016/j.cell.2020.09.059.

41. Liang, Y., Tang, H., Guo, J., Qiu, X., Yang, Z., Ren, Z., Sun, Z., Bian, Y., Xu, L., Xu, H., et al. (2018). Targeting IFNalpha to tumor by anti-PD-L1 creates feedforward antitumor responses to overcome checkpoint blockade resistance. Nat. Commun. *9*, 4586. https://doi.org/10.1038/s41467-018-06890-y.

42. Cirovic, B., de Bree, L.C.J., Groh, L., Blok, B.A., Chan, J., van der Velden, W.J.F.M., Bremmers, M.E.J., van Crevel, R., Händler, K., Picelli, S., et al. (2020). BCG Vaccination in Humans Elicits Trained Immunity via the Hematopoietic Progenitor Compartment. Cell Host Microbe *28*, 322–334.e5. https://doi.org/10.1016/j.chom.2020.05.014.

43. Grille, S., Brugnini, A., Nese, M., Corley, E., Falkenberg, F.W., Lens, D., and Chabalgoity, J.A. (2010). A B-cell lymphoma vaccine using a depot formulation of interleukin-2 induces potent antitumor immunity despite increased numbers of intratumoral regulatory T cells. Cancer Immunol. Immunother. *59*, 519–527. https://doi.org/10.1007/s00262-009-0768-6.

44. Turco, S.J., Wilkerson, M.A., and Clawson, D.R. (1984). Expression of an unusual acidic glycoconjugate in Leishmania donovani. J. Biol. Chem. *259*, 3883–3889.

45. Nogueira, P.M., Assis, R.R., Torrecilhas, A.C., Saraiva, E.M., Pessoa, N.L., Campos, M.A., Marialva, E.F., Ríos-Velasquez, C.M., Pessoa, F.A., Secundino, N.F., et al. (2016). Lipophosphoglycans from Leishmania amazonensis Strains Display Immunomodulatory Properties via TLR4 and Do Not Affect Sand Fly Infection. PLoS Negl. Trop. Dis. *10*, e0004848. https://doi.org/10.1371/journal.pntd.0004848.

46. Lowman, D.W., Ensley, H.E., Greene, R.R., Knagge, K.J., Williams, D.L., and Kruppa, M.D. (2011). Mannan structural complexity is decreased when Candida albicans is cultivated in blood or serum at physiological temperature. Carbohydr. Res. *346*, 2752–2759. https://doi.org/10.1016/j.carres.2011.09.029.

47. Dos Santos, J.C., Damen, M.S.M.A., Oosting, M., de Jong, D.J., Heinhuis, B., Gomes, R.S., Araújo, C.S., Netea, M.G., Ribeiro-Dias, F., and Joosten, L.A.B. (2017). The NOD2 receptor is crucial for immune responses towards New World Leishmania species. Sci. Rep. *7*, 15219. https://doi.org/10.1038/s41598-017-15412-7.

48. Repnik, U., Knezevic, M., and Jeras, M. (2003). Simple and cost-effective isolation of monocytes from buffy coats. J. Immunol. Methods *278*, 283–292. https://doi.org/10.1016/s0022-1759(03)00231-x.

49. Domínguez-Andrés, J., Arts, R.J.W., Bekkering, S., Bahrar, H., Blok, B.A., de Bree, L.C.J., Bruno, M., Bulut, Ö., Debisarun, P.A., Dijkstra, H., et al. (2021). In vitro induction of trained immunity in adherent human monocytes. STAR Protoc. *2*, 100365. https://doi.org/10.1016/j.xpro.2021.100365.

50. Popa, C., Abdollahi-Roodsaz, S., Joosten, L.A.B., Takahashi, N., Sprong, T., Matera, G., Liberto, M.C., Foca, A., van Deuren, M., Kullberg, B.J., et al. (2007). Bartonella quintana lipopolysaccharide is a natural antagonist of Toll-like receptor 4. Infect. Immun. *75*, 4831–4837. https://doi.org/10.1128/IAI.00237-07.

51. Wu, T.D., and Nacu, S. (2010). Fast and SNP-tolerant detection of complex variants and splicing in short reads. Bioinformatics *26*, 873–881. https://doi.org/10.1093/bioinformatics/btq057.

52. Langmead, B. (2010). Aligning short sequencing reads with Bowtie. Curr Protoc Bioinformatics *Chapter*. Curr. Protoc. Bioinformatics *Chapter 11*, Unit 11 17. https://doi.org/10.1002/0471250953.bi1107s32.

53. Turro, E., Su, S.Y., Gonçalves, Â., Coin, L.J.M., Richardson, S., and Lewin, A. (2011). Haplotype and isoform specific expression estimation using multi-mapping RNA-seq reads. Genome Biol. *12*, R13. https://doi.org/10.1186/gb-2011-12-2-r13.

54. Huang, D.W., Sherman, B.T., Tan, Q., Collins, J.R., Alvord, W.G., Roayaei, J., Stephens, R., Baseler, M.W., Lane, H.C., and Lempicki, R.A. (2007). The DAVID Gene Functional Classification Tool: a novel biological module-centric algorithm to functionally analyze large gene lists. Genome Biol. *8*, R183. https://doi.org/10.1186/gb-2007-8-9-r183.

55. Lachmandas, E., Boutens, L., Ratter, J.M., Hijmans, A., Hooiveld, G.J., Joosten, L.A.B., Rodenburg, R.J., Fransen, J.A.M., Houtkooper, R.H., van Crevel, R., et al. (2016). Microbial stimulation of different Toll-like receptor signalling pathways induces diverse metabolic programmes in human monocytes. Nat. Microbiol. *2*, 16246. https://doi.org/10.1038/nmicrobiol.2016.246.

56. Agorio, C., Schreiber, F., Sheppard, M., Mastroeni, P., Fernandez, M., Martinez, M.A., and Chabalgoity, J.A. (2007). Live attenuated Salmonella as a vector for oral cytokine gene therapy in melanoma. J. Gene Med. *9*, 416–423. https://doi.org/10.1002/jgm.1023.

57. Bascuas, T., Moreno, M., Grille, S., and Chabalgoity, J.A. (2018). Salmonella Immunotherapy Improves the Outcome of CHOP Chemotherapy in Non-Hodgkin Lymphoma-Bearing Mice. Front. Immunol. *9*, 7. https://doi.org/10.3389/fimmu.2018.00007.

58. Koeken, V.A., de Bree, L.C.J., Mourits, V.P., Moorlag, S.J., Walk, J., Cirovic, B., Arts, R.J., Jaeger, M., Dijkstra, H., Lemmers, H., et al. (2020). BCG vaccination in humans inhibits systemic inflammation in a sex-dependent manner. J. Clin. Invest. *130*, 5591–5602. https://doi.org/10.1172/JCI133935.

STAR★METHODS

KEY RESOURCES TABLE

REAGENT or RESOURCE	SOURCE	IDENTIFIER
Antibodies		
Rabbit polyclonal anti-H3K4me3	Diagenode	Cat#pab-003-050, C15410003-50; RRID: AB_2616052
anti-mouse Lineage Cocktail Pacific Blue	Biolegend	Cat#133310; RRID: AB_11150779
anti-mouse Lineage Cocktail APC	BD Biosciences	Cat#51-9003632
anti-mouse CD117 (ckit) PE	BD Biosciences	Cat#553355; RRID: AB_394806
anti-mouse Ly-6A/E (sca1) PE/Cy7	Biolegend	Cat#122514; RRID: AB_756199
anti-mouse CD34 FITC	eBioscience	Cat#11-0341-85; RRID: AB_465022
anti-mouse CD16/32 BV421	Biolegend	Cat#101332; RRID: AB_2650889
anti-mouse CD135 (FLT3) APC	Biolegend	Cat#135310; RRID: AB_2107050
anti-mouse CD150 PerCP/Py5.5	Biolegend	Cat#115922; RRID: AB_230363
anti-mouse CD48 APC/Cy7	Biolegend	Cat#103432; RRID: AB_1561919
anti-mouse CD45 PE	Biolegend	Cat#103106; RRID: AB_31271
anti-mouse CD11b FITC	Biolegend	Cat#101206; RRID: AB_ 312788
anti-mouse CD8 APC	Biolegend	Cat#100712; RRID: AB_312750
anti-mouse Ly6G BV510	Biolegend	Cat#127633; RRID: AB_2562937
anti-mouse F4/80 APC	Biolegend	Cat#157306; RRID: AB_2832548
biotin anti-PDL1	eBioscience	Cat#13598282; RRID: AB_466837
anti-human TLR2	Invivogen	Cat#maba2-htlr2-2; RRID: AB_11142484
Human Dectin-1/CLEC7A Allophycocyanin Mab	Bio-Techne/R&D	Cat#MAB1859; RRID: AB_2081791
Human Dectin-2/CLEC6A Antibody	Bio-Techne/R&D	Cat#MAB3114; RRID: AB_2081647
anti-hIntegrin beta2 - hIntegrin b2 Affinity Purified Goat IgG	Bio-Techne/R&D	Cat#AF1730; RRID: AB_354957
Normal Goat IgG Control	Bio-Techne/R&D	Cat#AB-108-C; RRID: AB_354267
DC-SIGN Monoclonal Antibody	Bio-Techne/R&D	Cat#MA1-25615; RRID: AB_779638
Mouse IgG2B Isotype Control	Bio-Techne/R&D	Cat#MAB004; RRID: AB_357346
IgG1 Isotype Control	Bio-Techne/R&D	Cat#MAB002; RRID: AB_357344
Human MMR/CD206 Antibody	Bio-Techne/R&D	Cat#AF2534; RRID: AB_2063019
Anti-hMincle-IgG	Invivogen	Cat#mabg-hmcl
InVivoMAb anti-mouse PD-1 (CD279)	BioXcell	Cat#BE0146; RRID: AB_10949053
InVivoMab rat IgG2a isotype control, anti-trinitrophenol	BioXcell	Cat#BE0089; RRID: 1107769
Chemicals, peptides, and recombinant proteins		
β−glucan (β1,3-(D)-glucan	Professor David Williams, College of Medicine, Johnson City, USA	N/A
Lipopolysaccharide	Sigma-Aldrich	Cat#L2880From E. coli serotype 055:B5,
Grace's insect medium	Gibco, Life Technologies	Cat#11595-030
Heat-inactivated fetal bovine serum (FBS)	Gibco, Life Technologies	Cat#10500064
Protease inhibitor cocktail	Sigma-Aldrich	Cat#P8465
Giemsa	Merck Millipore	Cat#1.09204.0100
Percoll	Sigma-Aldrich	Cat#P1644
Ficoll-Paque	GE Healthcare	Cat#17-1440-03
Roswell Park Memorial Institute medium (RPMI)	Invitrogen	Cat#22406031
TRIzol reagent	Life Technologies	Cat#15596018
16% Formaldehyde	Fisher Scientific	Cat#28908, 11835835

(*Continued on next page*)

Continued

REAGENT or RESOURCE	SOURCE	IDENTIFIER
Zymosan	Sigma-Aldrich	Cat#Z4250
Pam3Cys	EMC microcollections	Cat#L2000
Adenosine 5'-triphosphate (ATP) disodium salt hydrate	Merck	Cat#A1852-1VL
2-deoxy-D-glucose	Merck	Cat#D6134
Oligomycin A	Merck	Cat#75351-5MG
FCCP	Merck	Cat#C2920-10mg
Antimycin	Merck	Cat#A8674-25mg
Rotenone	Merck	Cat#R8875-1G
cytochalasin B	Merck	Cat#C6762
Ponatinib	Selleck	Cat#S1490
GW5074 Raf1 kinase inhibitor	Merck	Cat#G6416
SP600125 JNK Inhibitor	Invivogen	Cat#tlrl-sp60
Wortmannin	Invivogen	Cat#tlrl-u0126-5
Torin 1	Invivogen	Cat#inh-tor1
Rapamycin	LC laboratories	Cat#R-5000
R406	EMD Millipore	Cat#505819
luminol (5-amino-2,3, dihydro-1,4-phtalazinedione)	Merck	Cat#521-31-3
SYBR Green	Applied Biosciences	Cat#4368708
APC streptavidin	BD Biosciences	Cat#554067
Phenyl-Sepharose CL-4B	VWR	Cat#17-0810-01
Critical commercial assays		
Pierce BCA protein assay kit	ThermoFisher Scientific	Cat#23225
Human TNFα ELISA	R&D systems	Cat#DY210
Human IL-6 ELISA	R&D systems	Cat#DY206
Human IL-10 ELISA	R&D systems	Cat#DY217B
Human IL-1β ELISA	R&D systems	Cat#DY201
Human IL-1Ra ELISA	R&D systems	Cat#DY280
Lactate Fluorometric Assay kit	Biovision	Cat#K607
iScript cDNA Synthesis Kit	Bio-Rad	Cat#1708891
miRNeasy Micro Kit	QIAGEN	Cat#217084
MACS pan monocyte isolation kit	Milteney Biotec	Cat#130-096-537
QuantSeq 3′ mRNA-Seq Library Prep Kit FWD	Lexogen	Cat#191-196
MinElute PCR purification Kit	QIAGEN	Cat#28006
Max Deluxe set mouse TNFa ELISA	Biolegend	Cat # 430916
Max Deluxe set mouse TNFa ELISA IL6	Biolegend	Cat # 431315
Max Deluxe set mouse TNFa ELISA IL1b	Biolegend	Cat# 43261
Mouse Explanatory panel	Olink Proteomics	Cat#95380
Deposited data		
Raw and analyzed data	This paper	GSE211212
Experimental models: organisms/strains		
Leishmania Viannia braziliensis	Leisbank IPTSP/UFG	MHOM/BR/2003/IMG
Leishmania Viannia guyanensis	Leisbank IPTSP/UFG	MHOM/BR/2006/PLR6
Leishmania Leishmania amazonensis	Leisbank IPTSP/UFG	IFLA/BR/67/PH8
BALB/c	Dilave, Uruguay	N/A
C57Bl/6	Dilave, Uruguay	N/A
A20 cell line	ATCC	Cat#TIB-208
B16F10	ATCC	Cat#CRL-6475

(*Continued on next page*)

Continued

REAGENT or RESOURCE	SOURCE	IDENTIFIER
Software and algorithms		
GraphPad Prism	Graphpad Software	https://www.graphpad.com
R statistical programming	N/A	RRID:SCR_001905
DESeq2	N/A	RRID:SCR_015687
flowCore	N/A	RRID:SCR_002205
TopSpin 4.0.9	Bruker	https://www.bruker.com
Diva	BD FACSDiva Software v.6.1.3	Cat#643629

RESOURCE AVAILABILITY

Lead contact

Further information and requests for resources and reagents should be directed to and will be fulfilled by the lead contact, Leo Joosten (leo.joosten@radboudumc.nl). This study did not generate unique reagents. All data are available in the main text or the supplementary materials.

Materials availability

The materials generated in this study are available from the lead contact upon request.

Data and code availability

- RNA-sequencing data have been made available on the Gene Expression Omnibus (https://www.ncbi.nlm.nih.gov/geo), series number GSE211212, and are publicly available as of the date of publication.
- This paper does not report original code.
- Any additional information required to reanalyze the data reported in this paper is available from the lead contact upon request.

EXPERIMENTAL MODEL AND STUDY PARTICIPANT DETAILS

Human subjects

The study was approved by the Ethics Committee of Radboud University Nijmegen, the Netherlands (no. 42561.091.12). Experiments were conducted according to the principles expressed in the Declaration of Helsinki. All blood donors (Sanquin Blood Bank, Nijmegen, The Netherlands) gave written informed consent before donating the blood.

Animals

In vivo experiments were performed in 6–8 weeks old, female BALB/c or C57Bl/6 mice, which were housed on 12:12 h light/dark cycles and given food and water *ad libitum*. The experiments with animals were approved by the University's Ethical Committee for Animal Experimentation, Uruguay (Exp. no. 070153-000830-20, protocol title ''Evaluación de la inmunidad innata entrenada en cancer'', no. 1026).

Tumor cell lines

The A20 cell line (American Type Culture Collection, Manassas, USA) was routinely grown and maintained as previously described.[43] PD-L1 expression on A20 cells was performed using anti-PD-L1-biotin (clone MIH5), followed by streptavidin-APC (BD Bioscience). The B16F10 cell line (American Type Culture Collection, Manassas, USA) was routinely grown and maintained as suggested by the supplier.

Leishmania *parasites*

L. (*V*.) *braziliensis* (MHOM/BR/2003/IMG), *L*. (*V*.) *guyanensis* (MHOM/BR/2006/PLR6), both strains from *Leishbank* IPTSP/UFG (Goiás, Brazil), and *L*. *amazonensis* (IFLA/BR/67/PH8), a reference strain, were used. Promastigote forms were cultured in Grace's insect medium (Gibco, Life Technologies, USA) supplemented with 20% of heat-inactivated fetal bovine serum (FBS, Gibco, Life Technologies, USA) and 100 U/mL of penicillin/streptomycin (Sigma-Aldrich) at 26°C. Stationary-phase parasites were obtained on the 6th day of growth and washed three times with phosphate-buffered saline (PBS; 1000xg, 10 min 10°C). After, they were suspended in PBS and quantified by using hemocytometer after fixation with PBS/0.4% formaldehyde. Live parasites were used in macrophage infection experiments. In addition, parasite lysates were obtained by 5 freeze-thaw cycles of promastigotes in the presence of protease inhibitors (Protease inhibitor cocktail, Sigma-Aldrich) in liquid nitrogen followed by thawing in a water bath at 37°C. Protein quantification was performed by using Pierce BCA protein assay kit (ThermoFisher Scientific, USA). The extraction and purification of *L*. *braziliensis* lipophosphoglycan (LPG) were performed as described in.[44,45] Briefly, stationary-phase parasites were obtained on 6th day of growth and washed three times with PBS. The LPG extraction with solvent E (MilliQ/Ethanol/Diethylether/Pyridine/NH_4OH 25%; 15:15:5:1:0.017) over multiple centrifugation steps. For purification, the extract was dried under

N_2 evaporation, resuspended in 0.1 M acetic acid (AcOH or $C_2H_4O_2$)/0.1M sodium chloride (NaCl) in MilliQ over hydrophobic chromatography using a column of phenyl-Sepharose. The column was washed with 0.1 M acetic acid/0.1M NaCl, 0.1 M acetic acid and MiliQ, respectively. The purified LPG was eluted in solvent E and dried under N_2 evaporation.

METHOD DETAILS

NMR structural analysis of LPG derived from *L. braziliensis*

The crude LPG extract was passed through a Sephadex G-25 column and the molecule of interest was eluted in the void volume. The carbohydrate was identified and structurally characterized by NMR analysis as described by Lowman et al.[46] In summary, ^{1}H NMR spectra for the *Leishmania* fractions were collected on a Bruker Avance III 400 NMR spectrometer operating at 294 K (21°C) and 333 K (60°C) in 5-mm NMR tubes. LPG fractions (about 7 mg) were dissolved in about 600 μL D_2O (Cambridge Isotope Laboratories, 99.8+% deuterated). Chemical shift referencing was accomplished relative to TMSP at 0.0 ppm. 1D NMR spectra were collected as follows: 5000 scans, 65,536 data points, 20.69 ppm sweep width centered at 6.175 ppm, 1 s pulse delay and processed using exponential apodization with 1.0 Hz line broadening. 2D COSY spectra were collected as 2048 by 128, processed as 1024 by 1024, 16 pre-scans, 256 scans, sweep width 10 ppm centered at 4.5 ppm, and relaxation delay 1.49 s using sine apodization in both dimensions. Data processing was accomplished using TopSpin (version 4.0.9) on the MacBook Pro running macOS Catalina (version 10.15.7).

Peripheral blood mononuclear cells (PBMC), monocyte training and treatments

Human peripheral blood mononuclear cells (PBMCs) were isolated by dilution of blood in pyrogen-free PBS and differential density centrifugation over Ficoll-Paque (GE healthcare, UK) as previously described.[47] Percoll isolation of monocytes was performed as previously described.[48] Briefly, 150–200 × 10^6 PBMCs were layered on a hyper-osmotic Percoll solution (48.5% Percoll, 41.5% sterile water, 0.16 M NaCl) and centrifuged for 15 min at 580 g (4°C). The interphase layer was collected, and cells were washed with cold PBS. Cells were resuspended in RPMI 1640 culture medium (Roswell Park Memorial Institute medium; Invitrogen, USA) supplemented with 50 μg/mL gentamicin, 2 mM glutamax (Gibco, Life Technologies, USA), and 1 mM pyruvate (Gibco) and quantified. Adherent monocytes were trained as described previously (depicted in Figure 1).[49] Briefly, 100.000 cells were incubated either with culture medium containing 10% pooled human serum, referred to as complete medium, as a negative control, 5 μg/mL of β-glucan (β-1,3-(D)-glucan (kindly provided by Professor David Williams, College of Medicine, Johnson City, USA), lysates of *L. braziliensis* (50 μg/mL, 25 μg/mL, 10 or 1 μg/mL), lysates of *L. guyanensis* (25 μg/mL), or lysates of *L. amazonensis* (25 μg/mL). After 24 h (37°C), cells were washed once with 200 μL of warm PBS and incubated for 5 days with one change of complete medium. On day 6, cells were restimulated with either 200 μL RPMI, 10 ng/mL of lipopolysaccharide (LPS) derived from *E. coli* serotype O55:B5 (LPS - Sigma), or 10 μg/mL of Pam_3Cys (Sigma) for 24 h. To assess the ability of live forms of *L. braziliensis* in inducing TI, monocytes were also incubated with stationary-phase promastigotes (MOI 50:1, 10:1, 5:1, 2:1 parasite/cell) were also used for 24 h. For experiments of IL-1β secretion, on day 6, cells were restimulated with RPMI, 10 ng/mL of LPS, 50 μg/mL of *L. braziliensis* for 23 h followed by an additional 1 h incubation with 1.25 mM ATP (Sigma). Supernatants were collected and stored at −20°C.

In inhibition experiments, monocytes were pre-incubated with the inhibitors 1 h prior to adding the stimuli (lysates of *L. braziliensis*). The metabolic and epigenetic inhibitors used were 1 mM 2-deoxyglucose (2-DG, Sigma), 10 μM oligomycin (Sigma), 1 mM methylthioadenosine (MTA - Sigma), or 100 μM cyproheptadine (CHP - Sigma). For receptor blockade experiments, 10 μg/mL of antibodies anti-TLR2 (InvivoGen), dectin-1, dectin-2, mincle, mannose, complement receptor 3 (CR3), and DC-SIGN (R&D systems) with its respective isotype controls were used. *Bartonella quintana* LPS[50] (5 μg/mL) was used for inhibiting TLR4. 1 μg cytochalasin B (Sigma) and 100 nM Ponatinib (Selleckchem) were used for inhibiting endocytosis and RIP2 kinase, respectively. Spleen tyrosine kinase and serine-threonine kinase Raf-1 were inhibited by 50 nM of R406 (EMD Millipore) and 1 μM of GW5074 (Raf-Sigma), respectively. The c-Jun N-terminal kinase pathway was blocked by 10 μM of SP600125 (JNK-InvivoGen). Phosphatidylinositol 3-kinase (PI3K/AKT) and mTOR were blocked by 100 nM wortmannin (InvivoGen),10 nM rapamycin (LC laboratories), and 100 nM torin (InvivoGen), respectively. In all experiments, either RPMI or RPMI+DMSO (vehicle) were used as negative controls.

For experiments of oxygen consumption rate (OCR) and intracellular acidification rate (ECAR), 10 × 10^6 cells were trained *in vitro* in petri dishes (Corning, NY, USA) in 10 mL medium for 24 h as described above. On day 6, cells were detached from the plate with versine (Gibco) and counted. The analyses were performed as described below.

Cytokine and lactate measurements

Cytokine production was determined in supernatants using commercial ELISA kits (R&D Systems) for human TNF, IL-6, IL-10, IL-1β, and IL-1Ra. Total intracellular IL-1β was measured in cell-lysates collected in Triton X-100 0.5% (Sigma). Lactate concentration was measured in supernatants of human macrophages using Lactate Fluorometric Assay kit (Biovision, CA, USA).

Reactive oxygen species (ROS) assessment

Monocytes were isolated and trained with lysates of *L. braziliensis* (25 μg/mL) as described above. On day 6, ROS were measured by luminol (5-amino-2,3, dihydro-1,4-phtalazinedione - Sigma). A total of 1 × 10^5 cells were seeded in white-96 well assay plate (Corning) in a volume of 100 μL. Next, the cells were stimulated with 25 μg/mL of *L. braziliensis* or 1 mg/mL of serum-treated zymosan (Sigma), used as a control of ROS production. Immediately after adding the stimuli, 1 mM of luminol diluted in hanks balanced salt solution (HBSS - Gibco) containing 0.5% of bovine serum albumin (BSA- Sigma) was added to each well. Chemiluminescence was measured in BioTek Synergy HT reader. The reading was performed at 37°C for every minute for 1 h.

RNA sequencing and differential gene expression analysis

For obtaining the RNA, monocytes were isolated with magnetic activated cell sorting with MACS pan monocyte isolation (Miltenyi Biotec) and trained with *L. braziliensis* lysates (25 μg/mL) as described above. Cells were collected at the relevant time points and harvested in RLT buffer (Qiagen) before freezing at −80°C. RNA was isolated using RNeasy mini columns (Qiagen) according to the manufacturer's instructions. RNA sequencing library preparation was performed using the Quantseq 3′ mRNA-Seq Library Prep Kit-FWD from Lexogen (Lexogen, 015.96, Vienna, Austria) according to the manufacturer's instructions. Sequencing of the libraries was performed on a NextSeq 500 instrument (Illumina, San Diego, CA, USA). RNA-seq reads were mapped to the hg19 human reference genome using GSNAP.[51] To infer gene expression levels, RNA-seq reads were aligned to the Ensembl v68 human transcriptome using Bowtie.[52] Quantification of gene expression levels as RPKM was performed using MMSEQ.[53] Differential gene expression analysis was performed with DESeq2 v1.22.0, with a fold change of >2.5 for genes with >5 RPKM considered differentially expressed. An average expression value was generated by combining the three donors for each condition across each time point. We then performed Gene Ontology analysis on a dynamic list of genes using a Gene Functional Classification Tool (DAVID).[54] The DNA-binding motif analysis was performed as described by.[13]

Assessment of oxygen consumption and acidifications rates

Real-time analysis of ECAR and OCR on monocytes was performed using an XF-96 Extracellular Flux Analyzer (Seahorse Bioscience) as previously described.[55] Monocytes were isolated and trained with lysates of *L. braziliensis* (25 μg/mL) as described above. On day 6, 200.000 macrophages/well were seeded in quintuplicate in XF-96 cell culture plates in the presence of XF Base Medium (unbuffered DMEM with 5.5 mM glucose and 2 mM L-glutamine, pH adjusted to 7.4). The metabolic rates of monocytes were analyzed in four consecutive measurements. After three basal measurements, three consecutive measurements were taken following the addition of 1.5 μM oligomycin, 1 μM carbonyl cyanide-4-(tri-fluoromethoxy) phenylhydrazone (FCCP), and 2 μM antimycin together with 1 μM rotenone to determine basal and maximum OCR and ECAR. All compounds used during the Seahorse runs were acquired from Sigma.

Chromatin immunoprecipitation (ChIP)

Monocytes were isolated and trained with lysates of *L. braziliensis* (25 μg/mL) as described above. On day 6, cells were harvested and fixed in 1% methanol-free formaldehyde. Fixed cell preparations were sonicated using Diagenode Bioruptor Pico sonicator and immunoprecipitated using antibodies against H3K4me3 (Diagenode, Seraing, Belgium). A MinElute PCR purification Kit (QIAGEN) was used for DNA isolation. qPCR analysis was performed using an SYBR Green method, and samples were analyzed by a comparative Ct method. Myoglobin was used as negative control and H2B as a positive control according to the manufacturer's instructions. Primer sequences are described in.[11,20]

Evaluation of macrophage infection

Monocytes were trained with lysates of *L. braziliensis* as described above (25 μg/mL). 2×10^5 cells were added to 24-well plates on 12 mm coverslips (Corning), adhered for 1 h at 37°C, and infected with stationary-phase promastigotes of *L. braziliensis* at 1.0×10^6/well (MOI 5:1) in a final volume of 500 μL complete medium. Coverslips were collected after 2-, 24-, and 48-h incubation. The cells were fixed with methanol (Sigma) and stained by Giemsa (Merck Millipore). 300 cells were analyzed under a light microscope, and the percentage of infected cells and the mean number of intracellular parasites per infected cell (at least 50) were determined. Infection index = percentage of infected cells × mean number of parasites per infected cell.

In vivo L. *braziliensis*-induced trained immunity

Tumor inoculation and treatment regimen

The A20 and B16F10 cell lines were grown in culture and harvested in log phase. Then cells were washed and resuspended to a final concentration of 5×10^6 cells/mL and 2.5×10^6 cells/mL in PBS for A20 and B16F10, respectively. Balb/C or C57Bl/6 mice were injected subcutaneously (s.c.) into the right flank with 1×10^6 A20 cells in 0.2 mL of PBS or 2.5×10^5 B16F10 cells in 0.1 mL of PBS, respectively. Animals were divided in 2 groups (n = 12 per group): control (PBS) and lysate of *L. braziliensis* (L. braz) groups. On day 15 post-tumor implantation (p.t.i.) for A20 lymphoma model or 10 p.t.i. for B16F10 melanoma model, mice received a subcutaneous injection of 0.33 mg of lysate of *L. braziliensis* or PBS as control (in 100 μL). Afterward, as tumors become palpable, mice received a weekly intratumoral (i.t.) injection of 0.33 mg of lysate of *L. braziliensis* or PBS for two weeks (days 24 and 31 p.t.i. for A20 model or 17 and 24 p.t.i. for melanoma model). For experiments involving checkpoint inhibition therapy, 200 mg anti-PD-1 (clone, RMP1-14, BioXcell) or isotype control was injected intraperitoneally twice a week. The treatment started after the first injection of PBS or *L. braziliensis* lysates injection and continued until day 37 p.t.i. Tumors were measured every other day with a microcaliper, and tumor volumes were calculated as length × width × depth × π/6.[56] Euthanasia was carried out by cervical dislocation when tumors reached 4,000 mm^3 or earlier if animals showed signs of distress.

Bone marrow phenotyping and flow cytometry

To study the effect of *L. braziliensis* lysates on hematopoietic progenitor cells mice received a single or three subsequent subcutaneous injections of 0.33 mg of lysate of *L. braziliensis* or PBS as control (in 100 μL) (n = 5 per group); mice were euthanized 7 days after the last injection (day 7 and 21). In another experiment, mice were injected with A20 cells as described above, and after 14 days, the animals received one or three i.t. injections of 0.33 mg of lysate of *L. braziliensis* or PBS; mice were euthanized 21 and 35 days p.t.i. (e.i. 7 days after the first and third dose, respectively). The bone marrow (BM) was flushed from the femur using a 5% PBS-FBS solution. BM surface phenotype analysis was performed as described by.[30] Cell suspensions were incubated with several antibody

cocktails including a lineage cocktail (Lin) containing anti-CD3e (clone 145-2C11), anti-CD11b (clone M1/70), anti-Gr1 (clone RB6-8C5), anti-B220 (clone RA3-6B2), anti-TER119 (clone TER-119), anti-Sca1 (clone E13–161.7), anti-cKit (clone 2B8), anti-CD135 (clone A2F10), anti-CD48 (clone HM48-1), anti-CD150 (clone TC15-12F12.2), anti-CD16/CD32 (clone 93), and anti-CD34 (clone RAM34), and a lineage cocktail (Lin) containing anti-CD3 (clone 17A2), anti-CD11b (clone M1/70), anti-Gr1 (clone RB6-8C5), anti-CD45R/B220 (clone RA3-6B2), and anti-TER119 (clone TER-119). All data were acquired on FACSCanto II (BD Bioscience) and data analysis was performed using Diva software (BD Bioscience). On another experiment, 1×10^5 BM cells were stimulated with 10 ng of LPS from *E. coli* (Invivogen) for 24 h. Supernatant were collected and stored at −80°C until analyzed. Cytokine production was determined using commercial ELISA kits (R&D SystemsBiolegend) for mouse TNF, IL-1β and IL-6.

Tumor flow cytometry

To study the effect of *L. braziliensis* lysates on tumor infiltrating cells, A20-lymphoma bearing mice received a single or three subsequent subcutaneous injection of 0.33 mg of lysate of *L. braziliensis* or PBS as control (in 100 μL) (n = 5 per group) as described above. Mice were euthanized 7 or 21 days later, and tumors were removed and processed as previously described.[57] Cell suspensions were incubated with anti-CD45 (clone 30-F11), anti-CD11b (clone M1/70), anti-CD8 (clone 53–6.7), anti-Ly6G (clone 1AS) and anti-F4/80 (clone QA17A29). All data were acquired on FACSCanto II (BD Bioscience) and data analysis was performed using Diva software (BD Bioscience).

Ex vivo *cytokine production and cytotoxic capacity of splenocytes*

To study the effect of *L. braziliensis* lysates on induction of trained immunity on splenocytes, mice received a single or three subsequent subcutaneous injection of 0.33 mg of lysate of *L. braziliensis* or PBS as control (in 100 μL) (n = 5 per group); mice were euthanized 7 days after the last injection (day 7 and 21). In other experiment, mice were injected with A20 cells as described above and after 14 days, the animals received one or three i.t. injection of 0.33 mg of lysate of *L. braziliensis* or PBS; mice were euthanized 21 and 35 days p.t.i. (e.i. 7 days after the first and third dose, respectively) (n = 5 per group). Spleens were aseptically removed and splenocytes were purified and counted. 5×10^5 cells were stimulated with 100 ng of LPS from *E. coli* (Invivogen) for 24 h. Supernatant were collected and stored at −80°C until analyzed. Cytokine production was determined using commercial ELISA kits (R&D Systems) for mouse TNF, IL-1β and IL-6.

In another experiment, five A20 lymphoma-bearing mice treated with *Leishmania* lysates (L.braz-treated, n = 2, and PD1+L.braz treated, n = 3) and complete recovered were sacrificed at the end of the follow-up period. Five age-matched naive mice served as controls. Spleens were removed, and purified splenocytes were stimulated with 5 μg/mL of A20 cell lysate to recall anti-tumor activity. After 48 h of stimulation, cytotoxicity was assessed by flow cytometry. Briefly, unlabeled splenocytes were used as effectors (E) and A20 lymphoma cells served as targets (T). Tumor cells were labeled with CFSE (Sigma) and seeded into 48-well plates (Nunc) at 2.5×10^4 cells per well. Re-stimulated splenocytes were seeded in 200:1, 100:1 and 25:1 E:T ratios in supplemented RPMI. In parallel, target CFSE-labelled A20 cells were incubated alone to measure spontaneous cell death. Co-cultures were incubated for 18 h, and then cells were collected and stained with propidium iodide (Sigma) prior to analysis by flow cytometry. The percentage of tumor cell death (cytotoxicity) was calculated as: % Cytotoxicity = [(% target cell death - % spontaneous target cell death)/(100 - % spontaneous cell death)] x100.

In another experiment, eight A20 lymphoma-bearing mice treated with 3 doses of *L. braziliensis* lysates (39 days p.t.i.), eight control A20 lymphoma-bearing mice and two age-matched naive mice were sacrificed. Spleens were removed, and cytotoxic assay was performed as described above.

Serum proteomics

Serum was obtained from whole peripheral blood collected 35 days post tumor from the PBS- and *L. braziliensis*-treated groups. Targeted proteomics was performed by Proceek © Multiplex Proximity extension assay using the commercially available Olink Proteomics AB (Uppsala Sweden) Mouse Explanatory panel (92 proteins). Expression levels were calculated as described by Koeken et al.[58] assessing the fold change in between the two groups.

QUANTIFICATION AND STATISTICAL ANALYSIS

Differences were analyzed using Student's t test or Wilcoxon signed-rank test. For cytokine production before and after *Leishmania* training, the data are shown as fold increases or raw cytokine compared to the RPMI control. The statistical analyses were performed on these ratios. Analyses were performed using Prism software version 6.0 (GraphPad, San Diego, CA, USA) and R version 4.0.3 (RStudio, Boston, MA, USA). Significance was established as $p < 0.05$.

Cell Reports, Volume *43*

Supplemental information

Leishmania braziliensis enhances monocyte responses to promote anti-tumor activity

Jéssica Cristina dos Santos, María Moreno, Lisa U. Teufel, Sofía Chilibroste, Samuel T. Keating, Laszlo Groh, Jorge Domínguez-Andrés, David L. Williams, Zuchao Ma, Douglas W. Lowman, Harry E. Ensley, Boris Novakovic, Fátima Ribeiro-Dias, Mihai G. Netea, José A. Chabalgoity, and Leo A.B. Joosten

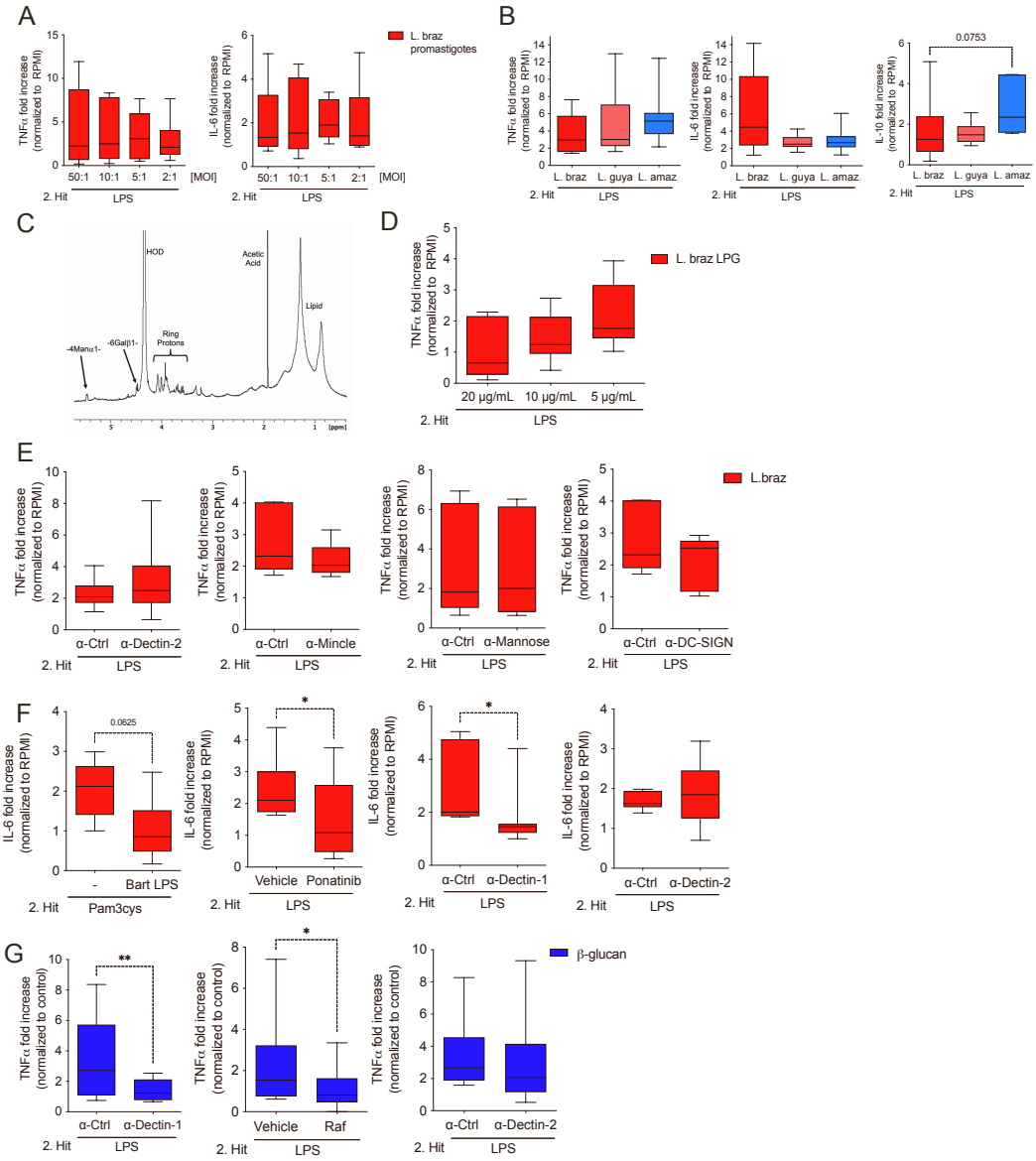


Figure S1. ***Leishmania spp.*** **induces trained immunity, Related to Figure 1.** (**A**) TNF and IL-6 release from monocytes trained with RPMI, or *L. braziliensis* live promastigotes (MOI 50, 10, 5 and 1) for 24 hours after LPS (10 ng/ml) restimulation at day 7, measured by ELISA. (**B**) TNF, IL-6 and IL-10 release from *L. braziliensis*. *L. guyanensis* and *L. amazonensis* lysates-trained macrophages (25 μg/mL) after restimulation with LPS (10 ng/mL) at day 7. (**C**) Characterization of lypophosphoglycan (LPG) fraction of *L. braziliensis* by 1D ^{1}H NMR analysis at 60^{o}C in D_2O. (**D**) TNF production after LPS restimulation at day 7 of *L. braziliensis*-LPG-trained (20 μg/mL, 10 μg/mL, 5 μg/mL) macrophages. (**E**) TNF production after LPS restimulation at day 7 of *L. braziliensis*-trained (25 μg/mL) macrophages ± anti-Dectin-2, anti-Mincle, anti-Mannose and anti-DC-SIGN. (**F**) IL-6 production after LPS or Pam3Cys restimulation at day 7 of *L. braziliensis*-trained (25 μg/mL) macrophages ± *B. quintana* LPS (Bart. LPS, TLR4 antagonist), the RIP2 kinase inhibitor ponatinib, anti-Dectin-1, anti-Dectin-2. (**G**) TNF production after LPS restimulation at day 7 of β-glucan-trained (5 μg/mL) macrophages ± anti-Dectin-1, Raf inhibitor GW5074, and anti-Dectin-2. *n*= 6 independent donors. Cytokine measurements are represented as fold increase normalized to RPMI

(non-trained cells). The data is shown in box and whiskers (Min to Max) plots from 2 independent experiments (*$p < 0.05$ by Wilcoxon test).

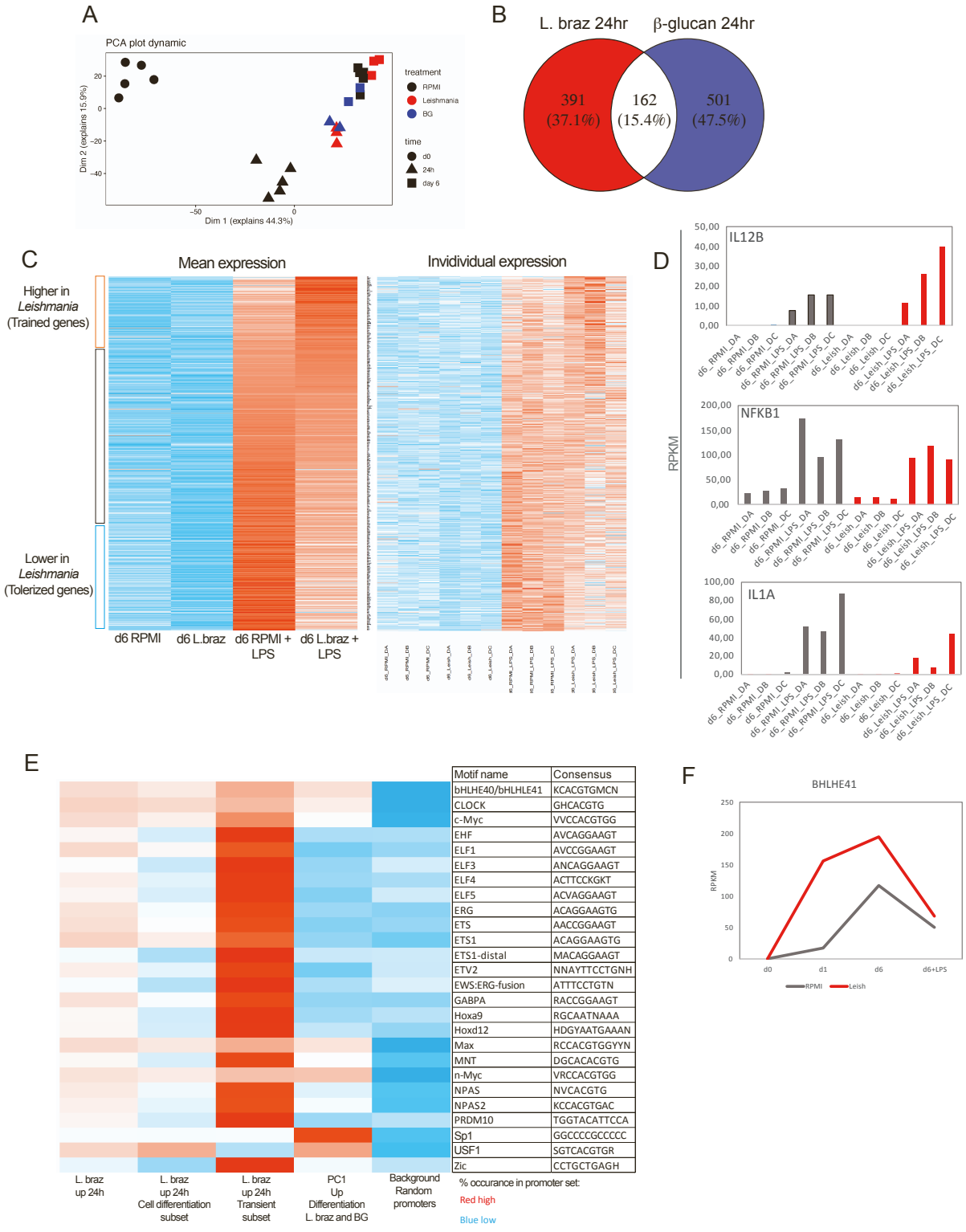


Figure S2. Transcriptional responses induced by *L. braziliensis* and β-glucan upon training, Related to figure 1. (**A**) Principal component plot (PCA) of gene expression dynamic across treatment and time

points (RPMI, black; *L. braziliensis* lysates, red; β-glucan, blue; day 0, circle; 24 hours, triangle; day 6, square). (**B**) Venn diagram representing the percentage of modulated genes which are *L. braziliensis*-, β-glucan-specific or common to both stimuli after 24-hours exposure. (**C**) Heatmap showing the mean and individual gene expression (upregulated, red; downregulated, blue) at the indicated time points (day 6) after RPMI or *L. braziliensis* lysates exposure (25 µg/mL) followed by LPS restimulation (10 ng/mL). (**D**) Example of genes which were either upregulated, equal, or downregulated in *L. braziliensis*-trained cells restimulated with LPS. (**E**) Transcription factors motif analysis performed in the subset of genes which were transient or associate with cell differentiation processes after 24 hours exposure with *L. braziliensis*. (**F**) Time-resolved median expression of *BHLHE41*, which is one of the TF associated with the transient subset of upregulated genes in *L. braziliensis*-exposed cells. *n*= 3 independent donors.

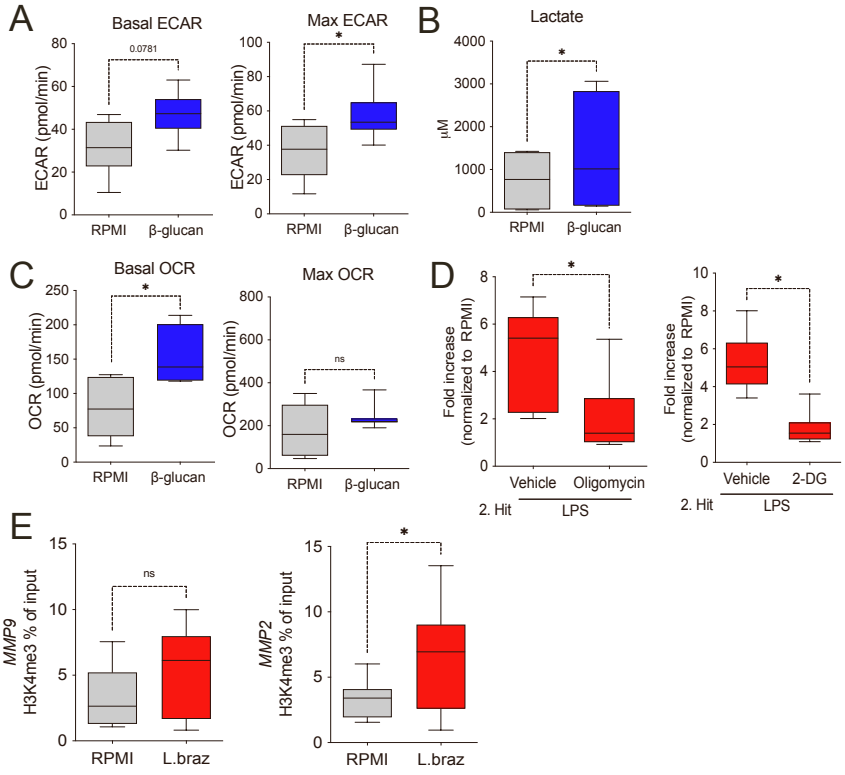


Figure S3. **Metabolic routes involved in trained immunity, Related of Figure 2.** (**A**) Basal and maximum extracellular acidification rates (ECAR) of RPMI- and β-glucan-trained macrophages at day 6, measured by seahorse. (**B**) Lactate production assessed in the supernatant of trained macrophages at day 6 by fluorometric assay. (**C**) Basal and maximum oxygen consumption rate (OCR) of RPMI- and β-glucan -trained macrophages at day 6, measured by seahorse. (**D**) TNF production after LPS restimulation at day 7 of *L. braziliensis*-trained (25 µg/mL) macrophages ± the OXPHOS and glycolysis inhibitors 2-DG and oligomycin, respectively. (**E**) Levels of H3K4me3 at *MMP9* and *MMP2* promoters of RPMI- and *L. braziliensis*-exposed macrophages assessed by ChiP-qPCR. *n*= 6 independent donors. Cytokine measurements are represented as fold increase normalized to RPMI (non-trained cells). The data is shown in box and whiskers (Min to Max) plots from 2 independent experiments (*p < 0.05 by Wilcoxon test; ns p > 0.05).

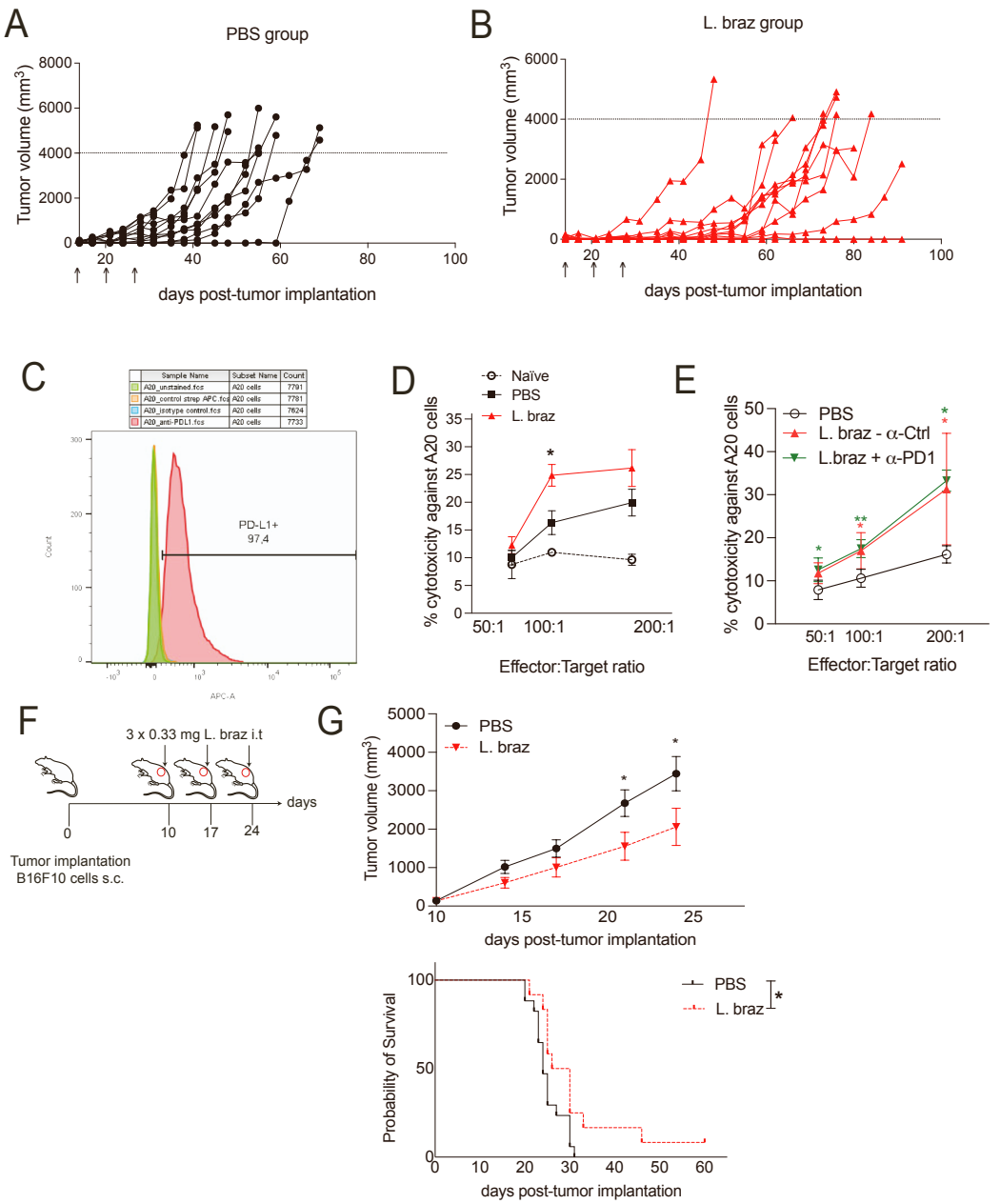


Figure S4. ***L. braziliensis*** **exerts anti-tumor activities *in vivo*, Related to Figure 4.** (**A-B**) *In vivo* tumor growth curves of showing the tumor volume of each BALB/c mouse individually. Mice were inoculated with 1×10^6 A20 tumor cells and submitted to a regimen consisted of three subcutaneously injections of PBS- or *L. braziliensis* lysates (0.33 mg/mL each injection). Overall survival was followed up for 100 days (n = 12). Significance was calculated in between the groups (*p < 0.05 by t-test). (**C**) PDL-1 expression in the A20 cells assessed by flow cytometry. (**D**) Cell-mediated cytotoxicity percentage at different ratios E:T performed in naïve, PBS, *L. braziliensis*-treated mice 39 days post-tumor implantation (n=8). (**E**) Cell-mediated cytotoxicity percentage at different ratios E:T performed in *L. braziliensis*-anti-PD1 and *L. braziliensis*-isotype control-treated mice which survived until the end of the follow up period (n = 12). Splenocytes were used as effector cells and A20 as target cells. (**F-G**) C57BL6 mice were inoculated with 2.5×10^5 B16F10 tumor cells and submitted to a regimen consisted of three intratumorally injections of PBS- or *L. braziliensis* lysates (0.33 mg/mL each injection). Tumor growth and survival was followed up for 60 days (n = 12). Significance was calculated in between the groups (*p < 0.05 by *t*-test).

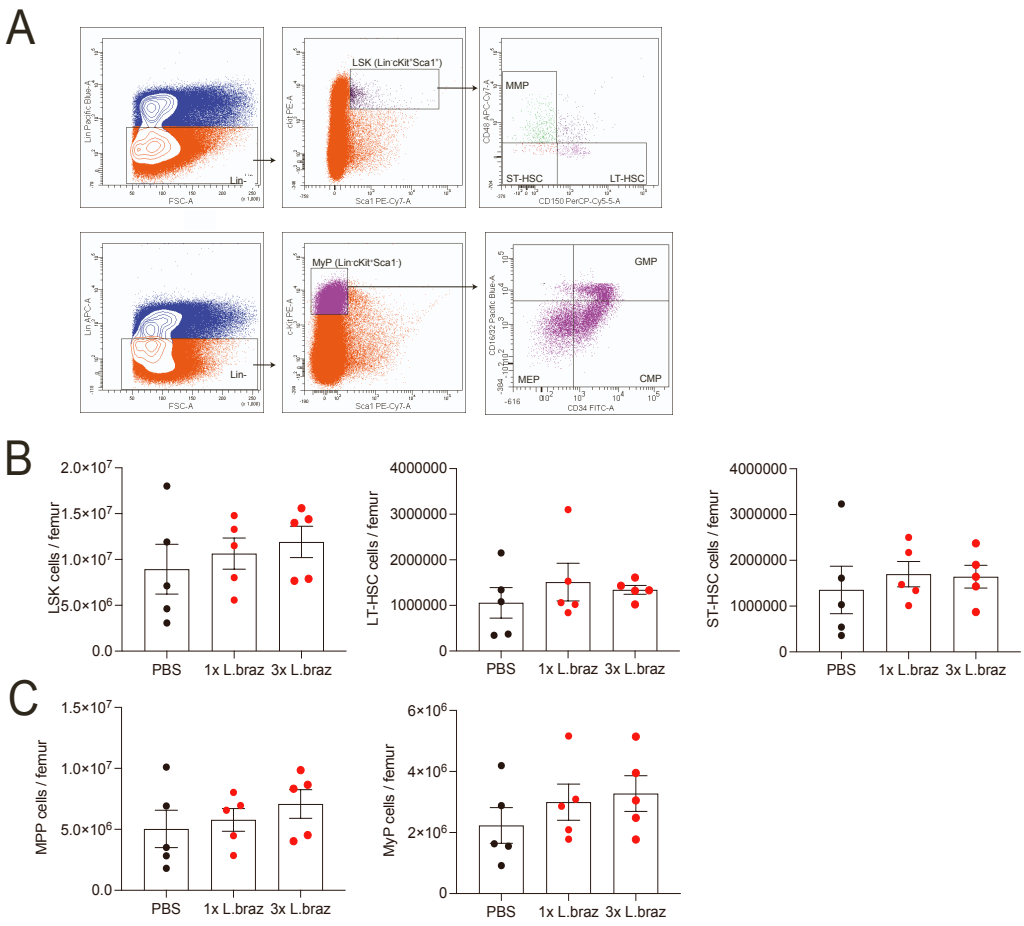


Figure S5. **Bone marrow effects induced by *L. braziliensis* exposure *in vivo*, Related to Figure 4.** (**A**) Representative flow cytometry plots of bone marrow phenotyping. Mice were injected with one single dose of *L. braziliensis* for 7 days or three doses of *L. braziliensis* or PBS every 7 days. Bone marrow cells were collected for *ex vivo* immunophenotyping analysis by flow cytometry. (**B**) Absolute numbers of LSKs, LT- and ST-HSCs, (**C**) MMPs, and MyPs in PBS- and *L. braziliensis*-treated mice (n=5). The data is shown in bar plots (Mean ± SD).

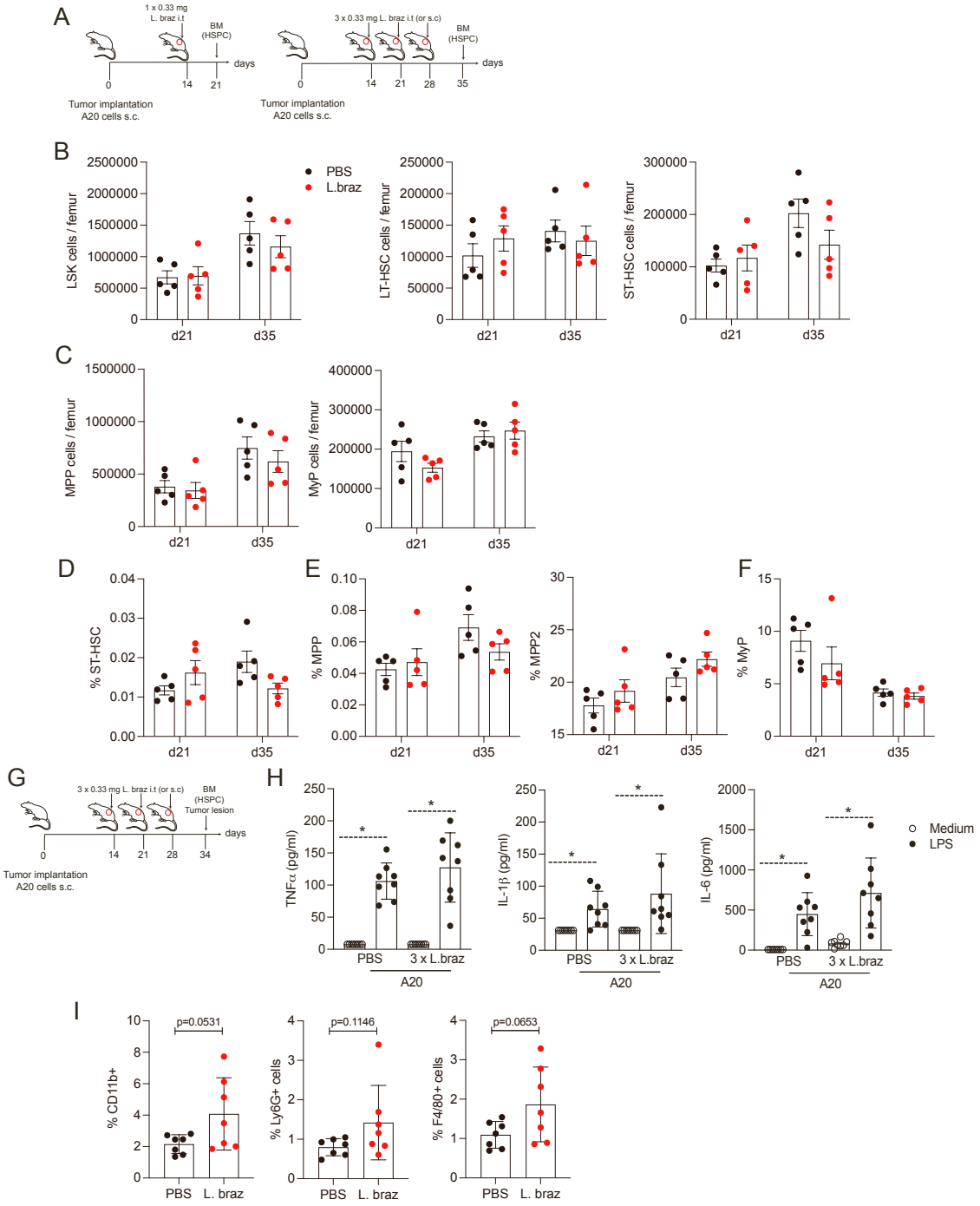


Figure S6. **Post-tumor effects induced by *L. braziliensis* at the bone marrow and at the tumor site, Related to Figure 5**. (**A**) Experimental setup. *Ex vivo* bone marrow phenotyping of tumor-bearing PBS- and *L. braziliensis*-treated (0.33 mg/mL) mice submitted to both single (day 21) and triple (day 35) doses regimen injected subcutaneously. (**B**) Absolute numbers of LSKs, LT- and ST-HSCs, (**C**) MMPs and MyPs, (**D**) percentages of ST-HSCs, (**E**) MMPs, MMP2 and (**F**) MyPs assessed by flow cytometry (n=5). (**G**) Cytokine production of bone marrow cells and innate immune cells infiltration of tumor-bearing PBS- and *L. braziliensis*-treated (0.33 mg/mL) mice submitted to triple (day 34) doses regimen injected subcutaneously. (**F**) 1×10^5 bone marrow cells were restimulated for 24 hours with LPS (10 ng/mL). (**H-I**)

TNF, IL-1β and IL-6 production was assessed in the supernatant by ELISA (n=8). Percentages $CD11b^+$, $Ly6G^+$ and $F4/80^+$ cells into the tumor lesion were assessed by flow cytometry (n=7). The data is shown in bar plots (Mean ± SD).

Current Research in Immunology 3 (2022) 159–166

Contents lists available at ScienceDirect

Current Research in Immunology

journal homepage: www.sciencedirect.com/journal/current-research-in-immunology

Salmonella-induced immune response reduces recurrence and tumor dissemination in preclinical melanoma model

Amy Mónaco [a,1], María C. Plata [a,1], Sofía Chilibroste [a], Magdalena Vola [b], Jose A. Chabalgoity [a], María Moreno [a,*]

[a] Departamento de Desarrollo Biotecnológico, Instituto de Higiene, Facultad de Medicina, Universidad de la República, Montevideo, Uruguay
[b] Cátedra de Dermatología, Hospital de Clínicas, Facultad de Medicina, Universidad de la República, Montevideo, Uruguay

ARTICLE INFO

Keywords:
Salmonella
Melanoma
Neoadjuvant therapies
Minimal residual disease
Memory immune response

ABSTRACT

Localized melanoma is easy to remove by surgery, resulting in a high five-year relative survival rate. However, when disseminated the disease management is challenging. The use of immunotherapies, such as anti-checkpoint monoclonal antibodies, has improved treatment options but still only a small percentage of patients responds to these expensive treatments. In this work, we apply a bacteria-based immunotherapy using LVR01, an attenuated *Salmonella enterica* serovar Typhimurium, as neoadjuvant therapy one week before surgery in a preclinical disseminated murine melanoma model. LVR01 administration resulted in tumor growth retardation prior to tumor resection, due to a rapid upregulation of inflammatory genes in the tumor microenvironment. As a consequence, cell infiltration increased, particularly neutrophils, macrophages and NK cells, being the latter involved in *Salmonella* anti-tumor activity. Besides, tumor-draining lymph node infiltration is characterized by reinvigorated $CD4^+$ and $CD8^+$ lymphocytes. Induced immune response could account for the prevention or delay of tumor recurrence and appearance of metastasis, resulting in a prolonged overall survival after surgery. Furthermore, upon rechallenge mice show partial protection, suggesting the existence of specific memory against melanoma. We propose that neoadjuvant LVR01 treatment could represent an interesting inexpensive alternative that may ease tumor resection, while preventing tumor recurrence in patients with melanoma.

1. Introduction

Melanoma is the most lethal type of skin cancer with an increasing incidence in young population worldwide (Matthews et al., 2018). The use of BRAF and MEK inhibitors has shown some benefit, but its use is restricted to approximately half of the patients who carry BRAF mutations (Chapman et al., 2011; Grimaldi et al., 2017). In the last years, new therapies have been approved for the management of advanced disease, as is the case of antibodies against immune checkpoints CTLA-4, PD-1 and PD-L1, alone or combined (Hodi et al., 2010; Robert et al., 2014; Gutzmer et al., 2020). However, these approaches present major side effects, induce resistance to treatment and exhibit escalating costs, making them available for a reduced number of patients, mainly from high income countries (reviewed in (Shah and Dronca, 2014)). The recent FDA approval of the first microbe-based therapy for advanced melanoma patients, Talimogene Laherparepvec (Andtbacka et al., 2015), while also expensive, has paved the road for new immunotherapies based on the use of live attenuated agents, as virus or bacteria.

New strategies promoting tumor cell death and/or inducing protective host antitumor immunity are of high priority. In this regard, *Salmonella*-based immunotherapies meet both conditions. *Salmonella* displays tumor tropism (Forbes et al., 2003), and once it reaches the tumor microenvironment, it can invade and replicate within tumor cells, leading to cell death (Mi et al., 2019). Besides, *Salmonella* triggers inflammation (reviewed in (Zhou et al., 2018)), promoting the development of antitumor immunity. Indeed, *Salmonella* has been shown to be an effective immunotherapy in many cancer models (Hernandez-Luna and Luria-Perez, 2018) and safe, even in oncologic patients (Cunningham and Nemunaitis, 2001; Toso et al., 2002).

We have previously developed LVR01, an attenuated *Salmonella enterica* serovar Typhimurium, that showed to be safe as vaccine vector in many animal models (Chabalgoity et al., 2000; Petavy et al., 2008; Goni et al., 2015; Grille et al., 2014; Kramer et al., 2015; Bascuas et al.,

* Corresponding author.
E-mail address: mmoreno@higiene.edu.uy (M. Moreno).
[1] Share first authorship.

https://doi.org/10.1016/j.crimmu.2022.08.001
Received 16 December 2021; Received in revised form 20 June 2022; Accepted 1 August 2022
2590-2555/© 2022 Published by Elsevier B.V. This is an open access article under the CC BY-NC-ND license (http://creativecommons.org/licenses/by-nc-nd/4.0/).

2018; Vola et al., 2018; Chilibroste et al., 2021; Mónaco et al., 2022). Besides, it holds great potential as a vaccine vector and tool for cancer immunotherapies (Chabalgoity et al., 2000). Using that strain, we demonstrated that administered intratumorally, it induces inflammasome activation in both tumor cells and infiltrating macrophages, and that this phenomenon is central for the exertion of the antitumor effect (Mónaco et al., 2022). Furthermore, intratumoral injection of LVR01 together with topical administration of the TLR7 agonist imiquimod retards tumor growth and dissemination and prolongs overall survival through the induction of the expression of pro-inflammatory Th1 cytokines and chemokines in the tumor microenvironment (TME), that resulted in a broad antitumor response in local and distant masses (Vola et al., 2018). Moreover, when using neoadjuvant *Salmonella* combined with intraperitoneal dacarbazine (DTIC) chemotherapy we found a strong synergistic anti-tumor effect, driven by combination of the DTIC-induced reduction of secondary lymphoid organ cellularity and the activation of cytotoxic cell compartments (Chilibroste et al., 2021). Analogously, lymphoma-bearing mice undergoing CHOP chemotherapy benefit from LVR01 administration, resulting in prolonged overall survival and an improved health status (Bascuas et al., 2018). These results highlight the potential of *Salmonella* as immunotherapy to control low tumor burden. In this work, we evaluated the benefit of LVR01 administration prior to surgery in melanoma-bearing mice and sought to explain the mechanisms involved in this prolonged antitumor effect.

2. Material and methods

2.1. Tumor cell lines

B16F1 and B16F10 melanoma cells were purchased from American Type Culture Collection (ATCC, CRL-6323 and CRL-6475, respectively) and maintained in Dulbecco's modified Eagle's medium (DMEM) supplemented with 10% fetal bovine serum at 37 °C in 5% CO_2 atmosphere.

2.2. Bacterial strain

Salmonella enterica serovar Typhimurium LVR01, an attenuated strain constructed by introducing a null deletion into the *aroC* gene of the parental canine *S.* Typhimurium isolate P228067 (Chabalgoity et al., 2000) was used in this study. Bacteria were grown at 37 °C in Luria-Bertani (LB) media shaking at 200 rpm ON and stored at −80 °C in 15% glycerol stocks until used. For *in vivo* experiments, bacteria were thawed and resuspended in saline solution to a final concentration of 1×10^7 CFU/ml. Bacterial inoculum was confirmed by serial dilution and plating in LB agar.

2.3. Animal experiments

Female C57BL/6 mice (Dilave, Uruguay), 6–8 weeks old, were used for *in vivo* experiments. Animals were housed on 12:12 h light/dark cycles with controlled temperature (22 ± 2 °C) and humidity (60%), with water and food *ad libitum*. All animal experimentation protocols were approved by the University's Ethical Committee for Animal Experimentation, Uruguay.

2.3.1. Neoadjuvant and adjuvant setting

Salmonella LVR01 neoadjuvant melanoma model was performed as previously described (Vola et al., 2018). Briefly, C57BL/6 mice were intradermically inoculated with 1×10^5 melanoma cells in the right flank, giving rise to only one primary tumor per mice. When tumors were palpable (day 11 post-tumor inoculation, pti), mice were divided into 2 groups: control (treated with 100 μl of saline solution) and LVR01. Animals were treated with one single dose of intratumoral (i.t.) LVR01 (1×10^6 CFU). Primary tumor resection was performed on day 18–19 pti, and relapse and/or occurrence of metastasis were followed up for 90–100 days pti. Affected lymph nodes and tumor relapse were measured with a caliper and volume was calculated as: (length x width x depth) x π/6. Mice were sacrificed by cervical dislocation when tumor volume exceeded 4000 mm^3 or before if they showed any sign of distress. Disease-free survival (DFS) corresponds to the day that tumor recurrence was detected for the first time, while overall survival (OS) corresponds to the day that mice died.

Rechallenge was performed on the opposite flank (left flank) of tumor-free surviving mice, no further treatment received. Animals were followed up as described above.

Salmonella LVR01 adjuvant melanoma model was performed as a modification of the above described neoadjuvant model. B16F1 melanoma was implanted on day 0 and primary tumor resection was performed on day 18–19 pti, without receiveing any previous treatment. Nine days after surgery, animals were divided into 2 groups, control and LVR01, and were treated with a weekly LVR01 injection (1×10^6 CFU) for the next 4 weeks within the tumor if it was palpable or otherwise subcutaneously in the same area. Affected lymph nodes and tumor relapse were measured with a caliper and sizes were calculated using the above-mentioned formula.

2.3.2. In vivo melanoma tumor models and treatment

C57BL/6 mice were subcutaneously inoculated with 2.5×10^5 B16F1 melanoma cells. Animals were divided into 2 or 3 groups: control, *Salmonella* LVR01 and *Salmonella* plus depletion when needed. At day 11 pti, *Salmonella* (1×10^6 CFU) were intratumorally injected. Mice were followed up every 2–3 days, and tumor sizes were calculated using the above-mentioned formula.

2.3.3. Depletion regimes

C57BL/6 mice were subcutaneously inoculated with 2.5×10^5 B16F1 melanoma cells as stated above. Animals were divided into 3 groups: control, LVR01 and depletion + LVR01. At day 11 pti, *Salmonella* (1×10^6 CFU) were intratumorally injected. Mice were followed up as described above. Rat α-CD8 (clone 2.43) and α-Gr1 (clone RB6-8C5), and mouse α-NK1.1 (clone PK136) antibodies were purified by affinity chromatography (Hi-trap G protein column) from hybridoma supernatants and amount of each was quantified using Bradford protein assay. All protocols were based on previous reports (Stern et al., 2015; Cook and Whitmire, 2013; Westphal et al., 2008) and adapted to our model. For CD8 depletion, a single dose of 100 μg of antibody was administered, for NK cell depletion two consecutive daily doses of 75 μg and for the depletion of neutrophils, three successive daily doses of 100 μg. In every case, the depletion was performed by intraperitoneal injection and started one day prior to LVR01 treatment. Depletions were followed up by flow cytometry using PBMC from blood samples taken overtime.

2.3.4. Gene expression analysis

In independent experiments, which did not include surgery, mice were sacrificed at day 3 or 8 post LVR01-treatment (days 14 or 19 pti) and tumors were removed, collected in TRIzol reagent (Invitrogen, Carlsbad, CA, USA) and stored at −80 °C until processed as previously described (Vola et al., 2018). Following retrotranscription, quantitative RT-PCR for *Ifng, Tnfa, Il6, Il12, Il18, Cxcl1, Cxcl2, Cxcl9, Cxcl10, Ccl2, Ccl3, Ccl4, Ccl5* and *Ccl2*0 mRNA were conducted using QuantiTect® SYBR® Green PCR Kit (Qiagen) in a Rotor-Gene 6000 (Corbett), primer sequences are available under request. This panel was based in our previous work, with modifications (Chilibroste et al., 2021). GAPDH encoding gene *Gapdh* was used as house-keeping gene. The relative mRNA amount in each sample was calculated using the $2^{-\Delta\Delta Ct}$ method as previously described (Livak and Schmittgen, 2001) where $\Delta Ct = Ct_{\text{gene of interest}} - Ct_{\text{gapdh}}$, and expressed as relative mRNA levels in the test groups compared to the control group.

2.3.5. Absolute numbers

In independent experiments, which did not include surgery, tumor-bearing mice were sacrificed at day 16 post LVR01-treatment (day 27

pti) and tumor draining lymph nodes (TDLN) were removed to prepare a single-cell suspension. Cell numbers were determined using Cellometer K2 automatic cell counter (Nexcelom Bioscience LLC, Lawrence, MA, USA).

2.3.6. Flow cytometry analysis

In independent experiments, which did not include surgery, mice were sacrificed at day 3, 8 or 16 post LVR01-treatment (days 14, 19 or 27 pti) and tumors or TDLN were removed and prepared to obtain single-cell suspensions. Cells were immunostained at 4 °C in the dark for 30 min with antibodies against B220, CD3, CD4, CD8, CD11b, CD11c, CD19, CD27, CD44, CD49b, CD62L, CD69, CD127, CD152 (CTLA-4), CD197 (CCR7), CD279 (PD-1), F4/80, Ly6G, MHCII, NK1.1 and NKG2D (all reagents from BD Pharmingen, San Diego, CA, USA). Absolute cell numbers were obtained using CountBright absolute counting beads (Invitrogen), according to manufacturer's instructions. Flow cytometry data were acquired on a FACS Canto II cytometer and analysed using FACS Diva software (BD Biosciences, Oxford, UK). Flow cytometry gating strategies are illustrated in Supplementary Fig. 1.

2.3.7. IFN-γ measurement

In independent experiments, which did not include surgery, tumor-bearing mice were sacrificed at day 16 post LVR01-treatment (day 27 pti). Spleens were collected and splenocytes purified by erythrocyte lysis. Cells were counted and seeded in 96-well plates along with B16F1 cells at a ratio of 100:1 (re-exposure). After 18 h, supernatants were collected and stored at −80 °C until analysed. IFN-γ determination was performed by ELISA using a commercial pair of antibodies (capture ab Cat. No. 551216; recombinant mouse IFN-γ protein Cat. No. 554587 as the standard and detection ab Cat. No. 554410, all from BD), according to the manufacturer's instructions.

2.4. Statistical analysis

The statistical significances of differences between groups were analysed using Student's t-test, 2-way ANOVA or Tukey's multiple comparisons test. A value of $p < 0.05$ was considered statistically significant. Differences in survival times were determined using Kaplan–Meier and log-rank test.

3. Results

3.1. Salmonella neoadjuvant treatment improves surgery outcome

As we had previously described, intratumoral *Salmonella* LVR01 monotherapy resulted in tumor growth retardation and prolonged survival in a melanoma-bearing mice model (Vola et al., 2018; Chilibroste et al., 2021Mónaco et al., 2022). In this work we studied the potential of *Salmonella* immunotherapy in a low burden tumor model, achieved by surgery to remove primary tumors. B16F1 melanoma-bearing mice were treated with one single dose of intratumoral *Salmonella* LVR01 a week before exeresis of primary tumor (Fig. 1a). Consistently with our previously reported results, a marked difference in tumor burden was found between *Salmonella*-treated and control (mock-treated) mice at the time of surgery ($p = 0.0013$, Student's T test) (Fig. 1b). Upon surgery, animals treated with LVR01 exhibited an improved outcome, determined by a prolonged disease-free survival ($p < 0.0001$, Log-rank test) (Fig. 1c) and overall survival ($p < 0.0001$, Log-rank test) (Fig. 1d). Bacteria-based neoadjuvant treatment helped to protect from disease recurrence or metastasis, and hence death, in approximately half of the animals (Fig. 1d). The observed effect could be due to tumor growth restriction and therefore impairment of metastasis occurrence, or to metastatic cell elimination by the immune response elicited by LVR01 treatment, which allows disease control. Of note, this effect is not only restricted to low metastatic potential cells, as similar results were observed using B16F10 highly metastatic cell line (Supplementary Fig. 2).

3.2. LVR01 treatment induces broad local and systemic immune responses

Thus, we analysed the immune response elicited by *Salmonella* immunotherapy which could be contributing to the elimination of residual cells. Firstly, we deepened into the kinetics of cytokines and chemokines expression over time upon treatment. *Salmonella* rapidly induced a strong proinflammatory tumor microenvironment, characterized by upregulated expression of many chemokine and cytokine mRNAs, including *Ifng*, *Tnfa*, *Il6*, *Il18*, *Cxcl1*, *Cxcl2*, *Cxcl9*, *Cxcl10*, *Ccl2*, *Ccl3* and *Ccl5*, which slowly dissipated by day 8 post-*Salmonella* administration (day 19 pti, day of surgery) (Fig. 2a). Besides, an increase in immune cell recruitment to the tumor, mainly neutrophils and macrophages but also natural killer (NK) soon after treatment ($p = 0.0292$, $p = 0.0277$ and $p = 0.0151$, respectively, Student T test) was found at an early time point (Fig. 2b, top). However, this rapid infiltration disappeared as soon as day 8 post-*Salmonella* administration, being NK the

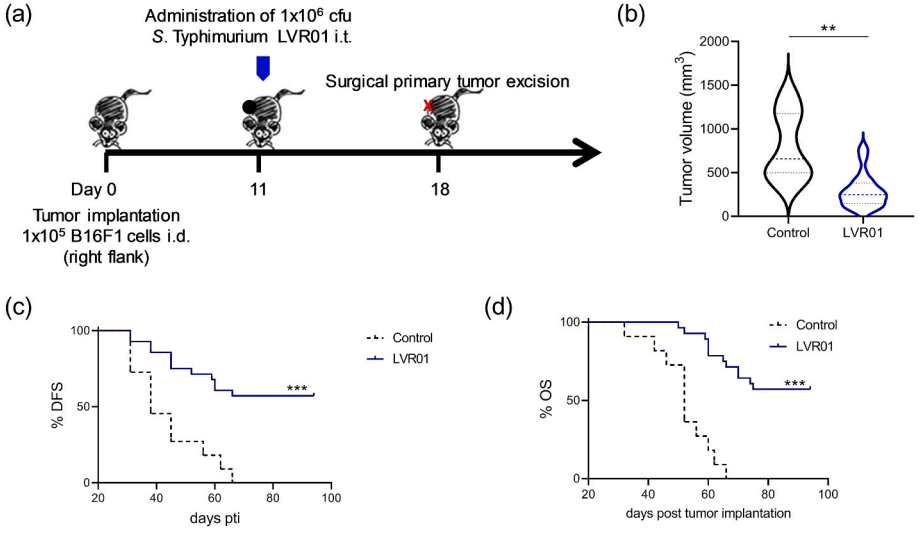


Fig. 1. Tumor size, free of disease and overall survival of B16F1 melanoma bearing mice treated with LVR01 prior to surgery. (a) Schematic representation of treatment schedule. Mice were treated with 1×10^6 cfu LVR01 i.t. as described in M&M. (b) Tumor size at day 18, prior to surgery. Volume was calculated as (LxWxD)xπ/6 and results are shown as median and quartiles. **p < 0.01 Student's T test. (c) Reemergence of the disease is plotted as disease-free survival (DFS) curve. Then tumor size was measured every 2–3 days. (d) Animal survival is plotted as overall survival (OS) curve. Survival was followed up for 100 days, ***p < 0.001, Log-rank Test (Control group n = 12, LVR01 group n = 30).

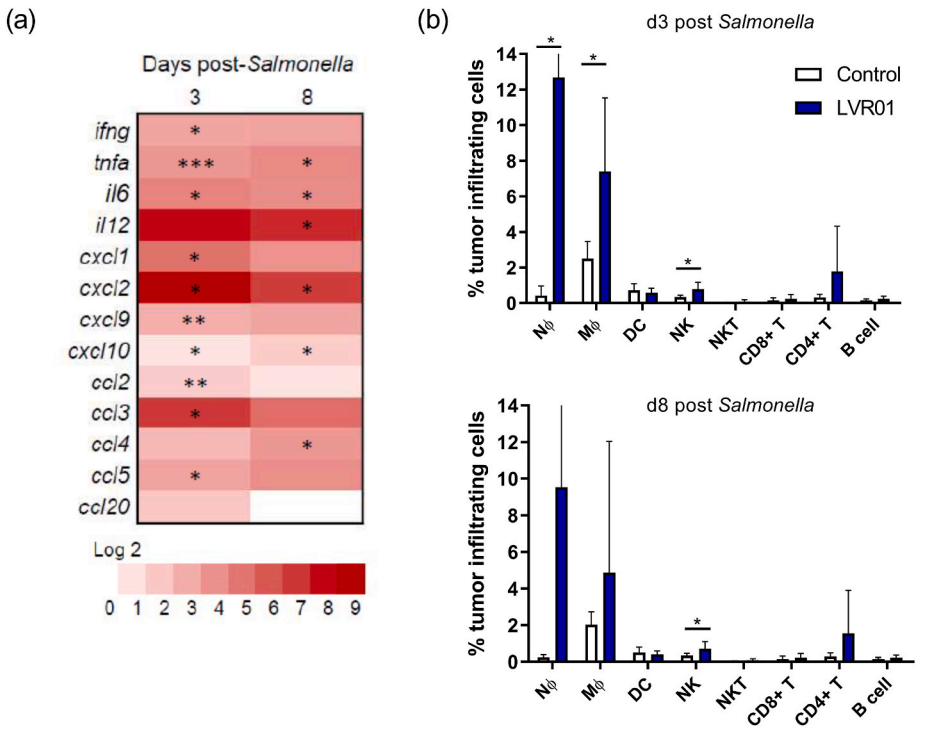


Fig. 2. Tumor setting at days 3 or 8 induced by LVR01 neoadjuvant intralesional administration in mice prior to surgery. (a) Cytokine/chemokine profile in LVR01-treated mice, normalized against control untreated mice, expressed as mean Log2 (n = 5–6) **(b)** Tumor immune cell phenotypification. Tumor homogenates were stained for detecting different tumor infiltrating populations of granulocytes and lymphocytes. Gating strategies are shown in Suppl. Fig. 1. All results are shown as mean ± SD (n = 5–11). Student's T test, $*p < 0.05$, $**p < 0.01$ and $***p < 0.001$.

only analysed cell population which remained higher in LVR01-treated mice at the time of surgery (p = 0.0151, Student's T test) (Fig. 2b, bottom). Noteworthy, this low, yet significant, percentage of NK cells is in accordance with previous reports (Bascuas et al., 2018).

As adaptive immune response takes longer time to develop, we studied it in lymphoid tissues at a later time point (16 days post-LVR01 treatment). For that, mice did not undergo surgery. LVR01-treated tumor draining lymph nodes (TDLN) exhibited a broad activation profile, characterized by expansion of lymphocytic populations. Significantly higher absolute numbers of NK, NKT, $CD4^+$ and $CD8^+$ T cells were counted ($p < 0.0001$ in all cases, Student T test) (Fig. 3a). Furthermore, a marked reduction in CTLA-4 expression on $CD4^+$ and $CD8^+$ T cells ($p = 0.0072$ and $p = 0.0047$ for $CD4^+$ and $CD8^+$ T cells, respectively, Student T test), as well as PD-1 expression reduction on $CD8^+$ T cells ($p = 0.0228$, Student T test) was observed (Fig. 3b), suggesting a reinvigoration in T cell function. Of note, this decrease is not due to higher naive or recently activated T cell recruitment, since the percentages of these cells remained unchanged (data not shown). In addition, LVR01 treatment expanded effector T cells ($p < 0.001$ in all cases, Student's T test) (Fig. 3c) and effector memory cell subpopulations within both $CD4^+$ and $CD8^+$ T cell population ($p < 0.001$ and $p = 0.0046$, respectively, Student's T test) (Fig. 3d). Moreover, splenocytes from LVR01-treated mice released higher levels of IFN-γ upon re-exposure to tumor cells ($p = 0.0305$, Student T test) (Fig. 3e).

3.3. NK cells participate in the antitumor effect exerted by Salmonella

Due to broad immune activation, we sought to evaluate the individual contribution of different cell types, namely neutrophils and cytotoxic NK and $CD8^+$ T lymphocytes, in *Salmonella*-mediated antitumor effect. Total $CD8^+$ T cell depletion did not alter the outcome of *Salmonella* treatment (Fig. 4a). Likewise, transient neutrophil depletion did not impact on tumor growth retardation upon LVR01 administration (Fig. 4b). Nonetheless, partial NK cell depletion abrogated early tumor growth control induced by LVR01 ($p = 0.0252$, Tukey's multiple comparisons test) (Fig. 4c), suggesting a role in *Salmonella*-mediated antitumor response.

3.4. Salmonella treatment induces tumor-specific memory response that contributes to tumor control upon rechallenge

In order to evaluate the potential of *Salmonella*-induced immune response to eliminate tumor cells, we rechallenged mice that survived to primary melanoma after *Salmonella* treatment followed by surgery (tumor-free mice from Fig. 1d). For that, we injected the same melanoma cell line in the opposite flank at day 76 post-primary tumor resection and compared disease development to that in naïve mice (Fig. 5a). Tumor growth was slower in mice that were previously treated with LVR01 compared to naïve mice ($p < 0.0001$, two-way ANOVA) (Fig. 5b) and, as a consequence, overall survival was extended ($p < 0.0001$, Log-rank test) (Fig. 5c). Noteworthy, a few animals did not develop tumors, suggesting the presence of a tumor-specific memory immune response capable of eliminating melanoma cells (Fig. 5c).

Salmonella LVR01 anti-tumor potential is not restricted to neoadjuvant application. We treated mice that underwent surgery for primary tumor removal with weekly LVR01 injection (Fig. 6a). Treatment resulted in tumor growth delay ($p < 0.0001$, Two-way ANOVA) (Fig. 6b), and subsequently prolonged overall survival ($p < 0.0001$, Log-rank test) (Fig. 6c). Yet, this approach did not provide complete protection, as all animals eventually developed disease.

4. Discussion

Microbe-based immunotherapies have been extensively studied for cancer treatment, and recently regained more attention (Forbes et al., 2018). However, to date only two of these therapies have been approved. Firstly, the use of BCG for superficial bladder cancer that is still in use and has many decades of significant results (reviewed in (Gontero et al., 2010)) and more recently, talimogene laherparepvec for advanced melanoma (Andtbacka et al., 2015). Due to *Salmonella* characteristics, i.e. tumor tropism, intrinsic antitumor activity and broad immune response induction, it is one of the most attractive bacteria to be used as a microbe-based cancer immunotherapy (reviewed in (Moreno et al., 2010)). To date, it has been evaluated in different tumor models, with optimistic results. Within TME, *Salmonella* elicits activation of

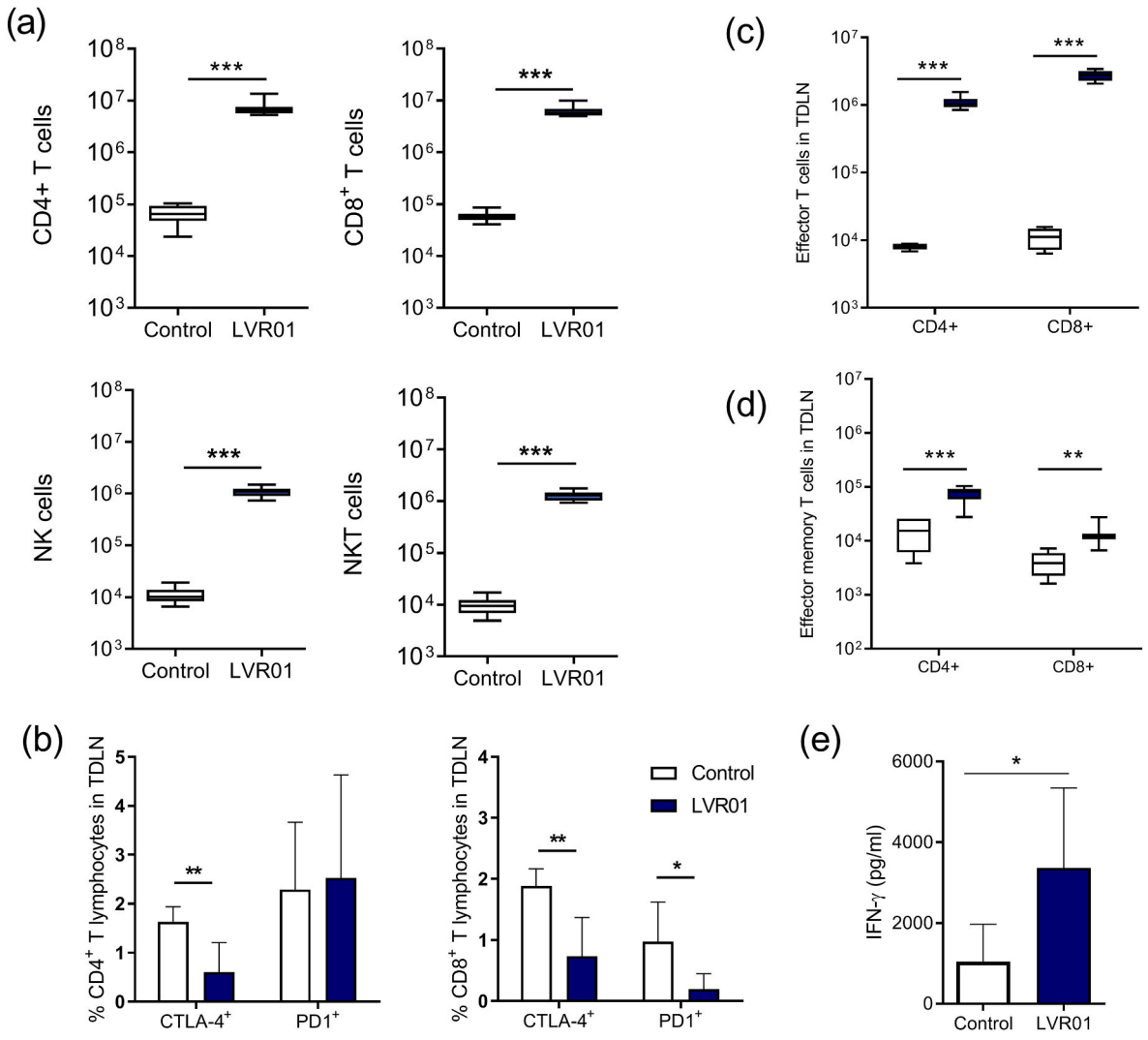


Fig. 3. Immune profile induced by LVR01 in secondary lymphoid organs at day 16 after *Salmonella* treatment. TDLN homogenates were stained for detecting different lymphocyte subpopulations. **(a)** Counts of lymphocytes are expressed as absolute numbers. **(b)** CTLA-4 and PD-1 expression on $CD4^+$ T and $CD8^+$ T cells. **(c)** Effector and **(d)** effector memory $CD4^+$ and $CD8^+$ T cell counts. **(e)** Secreted IFNγ levels by B16F1 re-stimulated splenocytes, measured by ELISA. All gating strategies are available in Suppl Fig. 1. Results in (a), (c) and (d) are shown as box and whiskers (min to max), while (b) and (e) are shown as mean ± SD (n = 5–6). Student's T test, $*p < 0.05$, $**p < 0.01$ and $***p < 0.001$.

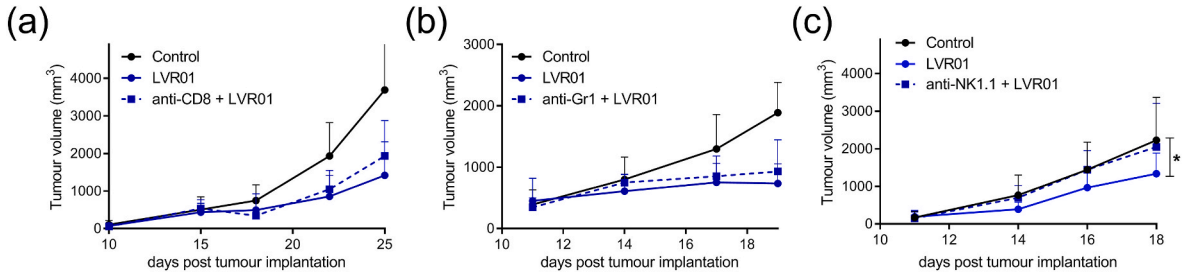


Fig. 4. Relevance of different cell types in tumor control induced by LVR01. Tumor growth after *Salmonella*-treated melanoma-bearing mice depleted of **(a)** $CD8^+$ T cells, **(b)** Neutrophils, and **(c)** NK cells. Gating strategies and depletion followup are shown in Suppl. Fig. 3. All results are shown as mean ± SD (n = 11–12). Student's T test, $*p < 0.05$.

immune responses through different mechanisms: by activation of macrophages -evidenced by the enhanced expression of soluble mediators (e.g. inducible nitric oxide synthase and IFN-γ)-, M2/M1 shift, inhibition of the expression of immunosuppressive factors (e.g. arginase-1, interleukin-4, transforming growth factor-β and vascular endothelial growth factor), and activation of different pathways of cell death, such as apoptosis, autophagy and pyroptosis (Mónaco et al., 2022; Kaimala et al., 2014; Ganai et al., 2011; Lee et al., 2014). Besides, released tumor antigens in this inflammatory setting are captured and presented by dendritic cells, triggering a specific antitumor response (Saccheri et al., 2010).

We have recently shown the potential of neoadjuvant *Salmonella*

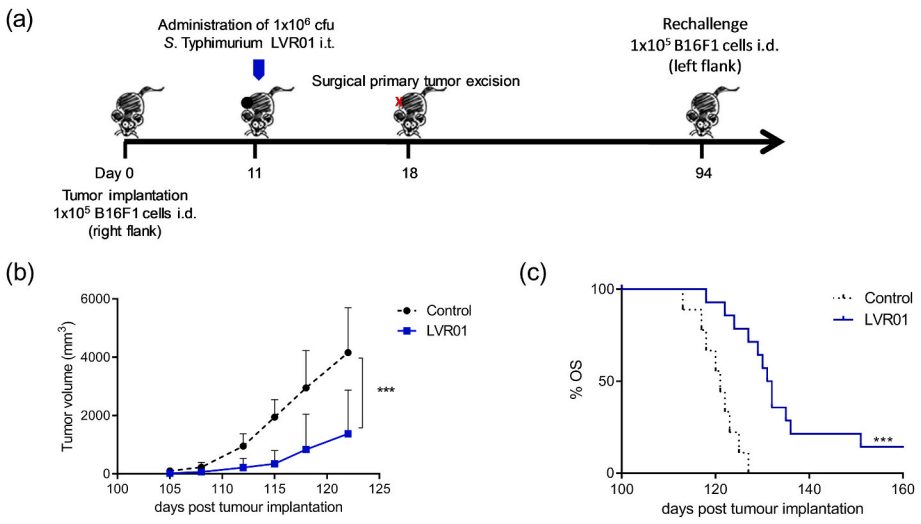


Fig. 5. Tumor size and overall survival of B16F1 melanoma bearing mice treated with neoadjuvant LVR01, after rechallenge. (a) Schematic representation of treatment schedule. Mice were treated with 1×10^6 cfu LVR01 i.t., tumors were excised a week later and 76 days later surviving mice were rechallenged subcutaneously in the opposite flank with 1×10^5 B16F1 cells. **(b)** Tumor growth curve, expressed as days post primary tumor implantation. Tumor size was measured every 2–3 days and volume was calculated as (LxWxD)xπ/6. Results are shown as mean ± SD (n = 12–16) ***$p < 0.001$, Student's T test. **(c)** Survival was followed up for 160 days ***$p < 0.001$, Log-rank Test.

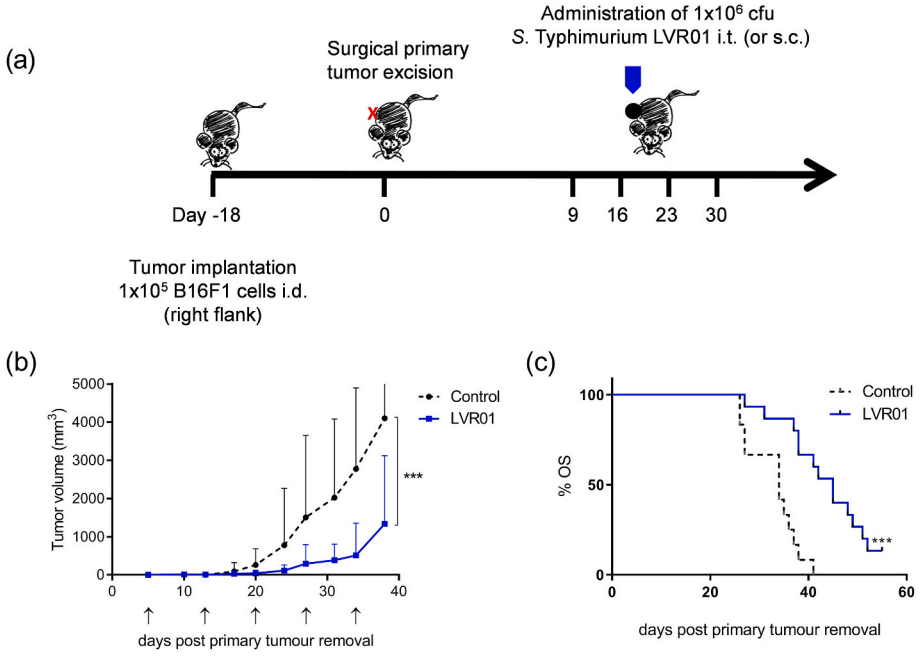


Fig. 6. Tumor size and overall survival of B16F1 melanoma bearing mice treated with LVR01 post surgery. (a) Schematic representation of treatment schedule. 18 days post tumor implantation, tumors were excised and starting 9 days later mice were treated weakly with 1×10^6 cfu LVR01 i.t., or s.c. when tumors were not palpable. **(b)** Tumor growth curve, expressed as days post primary tumor removal. Tumor size was measured every 2–3 days and volume was calculated as (LxWxD)xπ/6. Results are shown as mean ± SD (n = 12) ***p < 0.001, two-way ANOVA. **(c)** Survival was followed up for 60 days after primary tumor removal ***p < 0.001, Log-rank Test.

treatment in animals undergoing chemotherapy, highlighting the relevance of low tumor burden for *Salmonella* success (Bascuas et al., 2018; Chilibroste et al., 2021). In line with this, neoadjuvant LVR01 prolongs animal survival upon surgery to remove high tumor burden in a metastatic 4T1 breast cancer model (Kramer et al., 2015). In this work we assessed the potential of *Salmonella*-induced antitumor immune response in a minimal residual disease melanoma model to prevent tumor relapse and metastasis occurrence. This approach resulted in more than 50% complete recovery.

It is known that the immune system and cancer are intimately related, the immune system controls and shapes tumor cells immunogenicity, while tumor cells condition TME to impair anti-tumor immunity (Mittal et al., 2014). Immunotherapies can help to generate neoantigens, stimulate recruitment and activation of anti-tumor immune cells and override immunosuppression (Ward et al., 2016; Guerrouahen et al., 2020). Likewise, *Salmonella* induces local and systemic antitumor immunity as it mediates tumor cell death in a pro-inflammatory microenvironment, triggering a short-term immune cell tumor infiltration and an long-term adaptive immune response (reviewed in (Pangilinan and Lee, 2021)).

In the early stage of the disease, tumor growth is controlled by innate effectors, such as NK cells and macrophages, recruited to the TME upon *Salmonella* administration. We have previously shown that macrophages recruited to the tumor site, along with tumor cells, exhibit inflammasome activation upon LVR01 treatment. Besides, both macrophages and caspase-1/11 axis proved to be central to *Salmonella* antitumor effect (Mónaco et al., 2022). In addition Kupz *et al* have pinpointed the NLRC4 inflammasome essentiality to the *in vivo* IFN-γ secretion by NK cells in response to *Salmonella* (Kupz et al., 2014), providing a possible link between NK and macrophages in the context of *Salmonella*-based immunotherapy success.

We have shown that NK cells are important to control tumor growth at an early stage. In addition, we observed upregulation of *Ifng* gene expression in the TME, as well as IFN-γ increased secretion by LVR01-treated mice' splenocytes re-exposed to tumor cells. Our results also showed that both the neoadjuvant or adjuvant treatment improved

tumor outcome to surgery, which could be indicating that the immunotherapy is successful at suppressing metastasis development. This is in line with what Lin and collaborators have recently shown, that NK cells are the main cell type involved in *Salmonella*-elicited control of metastatic cells through the secretion of IFN-γ, which at the same time shapes NK cells to eliminate cancer cells, in a positive feedback loop (Lin et al., 2021).

We have also shown here by systemically depleting Gr1 cells that neutrophils are not essential for the antitumor effect exerted by immunotherapy. This is in accordance with our previous results in which besides inducing an increase of Th17-associated gene expression, *Salmonella* immunotherapy benefited both wild type and IL17a knock-out melanoma bearing mice (Chilibroste et al., 2021). It has also been shown that neutrophils are dispensable for preventing metastasis by *Salmonella* treatment in the 4T1 breast cancer model (Lin et al., 2021). However, a few works demonstrate different neutrophils-mediated pro-tumor mechanisms. Neutrophils represent a ring-barrier that contains *Salmonella* within the necrotic area, restraining its antitumor activity (Westphal et al., 2008). In addition, *Salmonell*a-induced neutrophil extracellular trap release facilitates tumor cell dissemination (Cools-Lartigue et al., 2013; Najmeh et al., 2017). Neutrophils are a very heterogeneous cell population (Fridlender et al., 2009) and actually some of them, namely N2 neutrophils, are indeed immunosuppressive and associated with cancer progression (Masucci et al., 2019). In addition, the depletion regime consisting of anti-Gr1 antibodies could also be depleting other Gr1+ cells, such as myeloid-derived suppressor cells (MDSC), which are also known for their pro-tumoral potential (Yang et al., 2010). Hence, Gr1+ cell-depletion of both N2 and MDSC could be masking the therapeutic efficacy of anti-tumor N1 neutrophils.

The role of $CD8^+$ T cells has shown to be non-essential in early stages of disease in our model. Nevertheless, as adaptive immunity takes time to develop, $CD8^+$ T cells could be relevant in latter stages. Upon LVR01 treatment, $CD8^+$ T cells reinvigorate, as demonstrated by expansion of effector subpopulations, and downregulation of CTLA-4, as well as PD-1 expression. Besides, $CD8^+$ T resident memory (Trm) cells, which are relevant in the skin scenario because they persist as alarm sensors long after initial threat, are not sensitive to depletion (Galvez-Cancino et al., 2018). In this way, Trm may remain to exert their antitumor potential. Melanoma-specific Trm cells may also act upon rechallenge, steadily killing tumor cells by the production of IFN-γ, TNF-α, granzyme B and proinflammatory cytokines (Cheuk et al., 2017; Ariotti et al., 2014). However, in our hands LVR01 administration does not induce Trm (data not shown), but instead triggers T effector memory cell expansion in TDLN, which remains after surgery. This subpopulation could turn into T central memory cells (Martin and Badovinac, 2018) that may rapidly differentiate to Trm following tumor challenge (Enamorado et al., 2017).

It has been reported that *Salmonella*-mediated downregulation of tumor PD-L1 contributes to the reactivation of tumor-specific T cells (Chen et al., 2019). We have shown that LVR01 induces downregulation of PD-1 expression in $CD8^+$ T lymphocytes. In this way, *Salmonella* controls both sides of the immune synapse, releasing the brakes that allow an increased cytotoxic response.

In addition to *Salmonella*-induced T cell reinvigoration, we observed the generation of memory cells upon LVR01 treatment At this time, tumor escapes immune-mediated control, and tumor mass is no longer manageable by the immune system. Surgery provides for a window of time of action that allows the adapted immune system to eliminate minimal residual cells. Indeed, LVR01 treatment before surgery induces a tumor-specific immune response that controls tumor establishment and growth as evidenced by tumor rechallenge long after surgery.

To sum up, intratumoral *Salmonella* administration prior to surgery represents an interesting strategy for the treatment of melanoma. Primary lesion injection helps to control tumor growth that allows a better resection outcome and besides, the induction of systemic tumor-specific immunity constrains distant metastasis. Of note, intralesional approach is already used in the clinic with Talimogene laherparepvec for advanced melanoma patients.

5. Conclusions

LVR01-induced immune response impacts tumor control in two levels. Firstly, LVR01 generates a proinflammatory tumor microenvironment characterized by immune cell recruitment, which restrains tumor growth and impairs the occurrence of metastasis. Secondly, LVR01 induces a tumor-specific immune response that helps to clear residual tumor cells, partially preventing relapse.

In conclusion, neoadjuvant LVR01 administration could be considered as a promising alternative treatment for advanced melanoma patients, by diminishing the occurrence of tumor metastasis upon primary surgery.

Institutional review board statement

The study was conducted according to the guidelines approved by the Comisión Honoraria de Experimentación Animal (CHEA), the Ethics Committee of Universidad de la República (protocol approval file Nº 070153-000446-18, approved on August 29, 2018).

CRediT authorship contribution statement

Amy Mónaco: Conceptualization, Formal analysis, Investigation, Methodology, Visualization, Writing – original draft, Preparation, Writing – review & editing. **María C. Plata:** Formal analysis, Investigation, Methodology, Writing – original draft, Preparation, Writing – review & editing. **Sofía Chilibroste:** Formal analysis, Investigation, Methodology. **Magdalena Vola:** Funding acquisition, Methodology. **Jose A. Chabalgoity:** Formal analysis, Funding acquisition, Writing – review & editing. **María Moreno:** Conceptualization, Formal analysis, Funding acquisition, Investigation, Methodology, Supervision, Visualization, Writing – original draft, Preparation, Writing – review & editing.

Declaration of competing interest

The authors declare that they have no known competing financial interests or personal relationships that could have appeared to influence the work reported in this paper.

Acknowledgments

The authors would like to thank La Foundation La Roche-Posay, Agencia Nacional de Investigación e Innovación (ANII, Uruguay), Comisión Sectorial de Investigación Científica (CSIC, Uruguay), and Programa de Desarrollo de las Ciencias Básicas (PEDECIBA, Uruguay) fo their support.

Appendix A. Supplementary data

Supplementary data to this article can be found online at https://doi.org/10.1016/j.crimmu.2022.08.001.

References

Andtbacka, R.H., et al., 2015. Talimogene laherparepvec improves durable response rate in patients with advanced melanoma. J. Clin. Oncol. 33 (25), 2780–2788.
Ariotti, S., et al., 2014. T cell memory. Skin-resident memory CD8(+) T cells trigger a state of tissue-wide pathogen alert. Science 346 (6205), 101–105.
Bascuas, T., et al., 2018. Salmonella immunotherapy improves the outcome of CHOP chemotherapy in non-hodgkin lymphoma-bearing mice. Front. Immunol. 9, 7.
Chabalgoity, J.A., et al., 2000. Salmonella typhimurium as a basis for a live oral Echinococcus granulosus vaccine. Vaccine 19 (4–5), 460–469.
Chapman, P.B., et al., 2011. Improved survival with vemurafenib in melanoma with BRAF V600E mutation. N. Engl. J. Med. 364 (26), 2507–2516.

Chen, M.C., Pangilinan, C.R., Lee, C.H., 2019. Salmonella breaks tumor immune tolerance by downregulating tumor programmed death-ligand 1 expression. Cancers 12 (1).
Cheuk, S., et al., 2017. CD49a expression defines tissue-resident CD8(+) T cells poised for cytotoxic function in human skin. Immunity 46 (2), 287–300.
Chilibroste, S., et al., 2021. Preclinical evaluation of LVR01 attenuated Salmonella as neoadjuvant intralesional therapy in combination with chemotherapy for melanoma treatment. J. Invest. Dermatol. 142 (5), 1435–1443.
Cook, K.D., Whitmire, J.K., 2013. The depletion of NK cells prevents T cell exhaustion to efficiently control disseminating virus infection. J. Immunol. 190 (2), 641–649.
Cools-Lartigue, J., et al., 2013. Neutrophil extracellular traps sequester circulating tumor cells and promote metastasis. J. Clin. Invest. 123 (8), 3446–3458.
Cunningham, C., Nemunaitis, J., 2001. A phase I trial of genetically modified Salmonella typhimurium expressing cytosine deaminase (TAPET-CD, VNP20029) administered by intratumoral injection in combination with 5-fluorocytosine for patients with advanced or metastatic cancer. Protocol no: CL-017. Version: april 9, 2001. Hum. Gene Ther. 12 (12), 1594–1596.
Enamorado, M., et al., 2017. Enhanced anti-tumour immunity requires the interplay between resident and circulating memory CD8(+) T cells. Nat. Commun. 8, 16073.
Forbes, N.S., et al., 2003. Sparse initial entrapment of systemically injected Salmonella typhimurium leads to heterogeneous accumulation within tumors. Cancer Res. 63 (17), 5188–5193.
Forbes, N.S., et al., 2018. White paper on microbial anti-cancer therapy and prevention. J Immunother Cancer 6 (1), 78.
Fridlender, Z.G., et al., 2009. Polarization of tumor-associated neutrophil phenotype by TGF-beta: "N1" versus "N2" TAN. Cancer Cell 16 (3), 183–194.
Galvez-Cancino, F., et al., 2018. Vaccination-induced skin-resident memory CD8(+) T cells mediate strong protection against cutaneous melanoma. OncoImmunology 7 (7), e1442163.
Ganai, S., et al., 2011. In tumors Salmonella migrate away from vasculature toward the transition zone and induce apoptosis. Cancer Gene Ther. 18 (7), 457–466.
Goni, F., et al., 2015. Mucosal immunization with an attenuated Salmonella vaccine partially protects white-tailed deer from chronic wasting disease. Vaccine 33 (5), 726–733.
Gontero, P., et al., 2010. The role of bacillus Calmette-Guerin in the treatment of non-muscle-invasive bladder cancer. Eur. Urol. 57 (3), 410–429.
Grille, S., et al., 2014. Salmonella Enterica serovar Typhimurium immunotherapy for B-Cell Lymphoma induces broad antitumor immunity with therapeutic effect. Immunology 143 (3), 428–437.
Grimaldi, A.M., et al., 2017. MEK inhibitors in the treatment of metastatic melanoma and solid tumors. Am. J. Clin. Dermatol. 18 (6), 745–754.
Guerrouahen, B.S., et al., 2020. Reverting immune suppression to enhance cancer immunotherapy. Front. Oncol. 9, 1554.
Gutzmer, R., et al., 2020. Atezolizumab, vemurafenib, and cobimetinib as first-line treatment for unresectable advanced BRAF(V600) mutation-positive melanoma (IMspire150): primary analysis of the randomised, double-blind, placebo-controlled, phase 3 trial. Lancet 395 (10240), 1835–1844.
Hernandez-Luna, M.A., Luria-Perez, R., 2018. Cancer immunotherapy: priming the host immune response with live attenuated Salmonella enterica, 2018 J Immunol Res, 2984247.
Hodi, F.S., et al., 2010. Improved survival with ipilimumab in patients with metastatic melanoma. N. Engl. J. Med. 363 (8), 711–723.
Kaimala, S., et al., 2014. Salmonella-mediated tumor regression involves targeting of tumor myeloid suppressor cells causing a shift to M1-like phenotype and reduction in suppressive capacity. Cancer Immunol. Immunother. 63 (6), 587–599.
Kramer, M.G., et al., 2015. Neoadjuvant administration of Semliki Forest virus expressing interleukin-12 combined with attenuated Salmonella eradicates breast cancer metastasis and achieves long-term survival in immunocompetent mice. BMC Cancer 15, 620.
Kupz, A., et al., 2014. In vivo IFN-gamma secretion by NK cells in response to Salmonella typhimurium requires NLRC4 inflammasomes. PLoS One 9 (5), e97418.
Lee, C.H., et al., 2014. Salmonella induce autophagy in melanoma by the downregulation of AKT/mTOR pathway. Gene Ther. 21 (3), 309–316.
Lin, Q., et al., 2021. IFN-gamma-dependent NK cell activation is essential to metastasis suppression by engineered Salmonella. Nat. Commun. 12 (1), 2537.
Livak, K.J., Schmittgen, T.D., 2001. Analysis of relative gene expression data using real-time quantitative PCR and the 2(-Delta Delta C(T)) Method. Methods 25 (4), 402–408.
Martin, M.D., Badovinac, V.P., 2018. Defining memory CD8 T cell. Front. Immunol. 9, 2692.
Masucci, M.T., Minopoli, M., Carriero, M.V., 2019. Tumor associated neutrophils. Their role in tumorigenesis, metastasis, prognosis and therapy. Front. Oncol. 9, 1146.
Matthews, N.H., et al., 2018. Epidemiology of Melanoma.
Mi, Z., et al., 2019. Salmonella-mediated cancer therapy: an innovative therapeutic strategy. J. Cancer 10 (20), 4765–4776.
Mittal, D., et al., 2014. New insights into cancer immunoediting and its three component phases–elimination, equilibrium and escape. Curr. Opin. Immunol. 27, 16–25.
Mónaco, A., et al., 2022. Inflammasome Activation, NLRP3 Engagement and Macrophage Recruitment to Tumor Microenvironment Are All Required for Salmonella Antitumor Effect. Cancer Immunol. Immunother.
Moreno, M., et al., 2010. Salmonella as live trojan horse for vaccine development and cancer gene therapy. Curr. Gene Ther. 10 (1), 56–76.
Najmeh, S., et al., 2017. Neutrophil extracellular traps sequester circulating tumor cells via beta1-integrin mediated interactions. Int. J. Cancer 140 (10), 2321–2330.
Pangilinan, C.R., Lee, C.H., 2021. Highlights of immunomodulation in salmonella-based cancer therapy. Biomedicines 9 (11).
Petavy, A.F., et al., 2008. An oral recombinant vaccine in dogs against Echinococcus granulosus, the causative agent of human hydatid disease: a pilot study. PLoS Neglected Trop. Dis. 2 (1), e125.
Robert, C., et al., 2014. Anti-programmed-death-receptor-1 treatment with pembrolizumab in ipilimumab-refractory advanced melanoma: a randomised dose-comparison cohort of a phase 1 trial. Lancet 384 (9948), 1109–1117.
Saccheri, F., et al., 2010. Bacteria-induced gap junctions in tumors favor antigen cross-presentation and antitumor immunity. Sci. Transl. Med. 2 (44), 44ra57.
Shah, D.J., Dronca, R.S., 2014. Latest advances in chemotherapeutic, targeted, and immune approaches in the treatment of metastatic melanoma. Mayo Clin. Proc. 89 (4), 504–519.
Stern, C., et al., 2015. Induction of CD4(+) and CD8(+) anti-tumor effector T cell responses by bacteria mediated tumor therapy. Int. J. Cancer 137 (8), 2019–2028.
Toso, J.F., et al., 2002. Phase I study of the intravenous administration of attenuated Salmonella typhimurium to patients with metastatic melanoma. J. Clin. Oncol. 20 (1), 142–152.
Vola, M., et al., 2018. TLR7 agonist in combination with Salmonella as an effective antimelanoma immunotherapy. Immunotherapy 10 (8), 665–679.
Ward, J.P., Gubin, M.M., Schreiber, R.D., 2016. The role of neoantigens in naturally occurring and therapeutically induced immune responses to cancer. Adv. Immunol. 130, 25–74.
Westphal, K., et al., 2008. Containment of tumor-colonizing bacteria by host neutrophils. Cancer Res. 68 (8), 2952–2960.
Yang, L., Edwards, C.M., Mundy, G.R., 2010. Gr-1+CD11b+ myeloid-derived suppressor cells: formidable partners in tumor metastasis. J. Bone Miner. Res. 25 (8), 1701–1706.
Zhou, S., et al., 2018. Tumour-targeting bacteria engineered to fight cancer. Nat. Rev. Cancer 18 (12), 727–743.